CR 137746

(NASA-CR-137746) MODELS FOR ESTIMATING RUNWAY LANDING CAPACITY WITH MICROWAVE LANDING SYSTEM (MLS) (California Univ.) 204 p HC $7.25 CSCL 01E

N75-32084

Unclas
G3/04 41379

MODELS FOR ESTIMATING RUNWAY LANDING CAPACITY WITH MICROWAVE LANDING SYSTEM (MLS)

Prepared by

Vojin Tošić and Robert Horonjeff

September 1975

This report has been prepared for the Aeronautical Systems Office, Ames Research Center, National Aeronautics and Space Administration, under Contract No. NSG-2046. The contents of this report reflect the views of the contractor, who is responsible for the facts and the accuracy of the data presented herein, and do not necessarily reflect the official views or policy of the National Aeronautics and Space Administration.

Institute of Transportation and Traffic Engineering
University of California
Berkeley, California

ACKNOWLEDGMENT

The authors are grateful to Professors A. Kanafani and Sheldon Ross and Dr. Stephen Hockaday for reviewing this report and making helpful suggestions. Thanks are also extended to Mr. Tom Ellison of United Air Lines for contributing input data for the study and to the staff of the Federal Aviation Administration TRACON facility at the Oakland Airport for the use of their facilities. Mr. George Kenyon and Mr. Mark Waters of the Ames Research Center were most helpful in providing data for the study. Finally, the authors are most appreciative of the efforts of John O'Shea of the staff of the Institute of Transportation and Traffic Engineering for editing the manuscript.

ABSTRACT

When using the Instrument Landing System (ILS) all aircraft must follow a single straight line approach path before landing. The Microwave Landing System (MLS) will allow use of differing approach paths and they need not be on a straight line.

The objective of this research is to find out whether the introduction of MLS with its multiple approach path capability can bring an increase in runway landing capacity compared with conventional ILS.

A model is developed which is capable of computing the ultimate landing runway capacity, under ILS and MLS conditions, when aircraft population characteristics and Air Traffic Control separation rules are given. This model can be applied in situations when only a horizontal separation between aircraft approaching a runway is allowed, as well as when both vertical and horizontal separations are possible. It is assumed that the system is free of errors, that is that aircraft arrive at specified points along the prescribed flight path precisely when the controllers intend for them to arrive at these points. Although in the real world there is no such thing as an error-free system,the assumption is adequate for a qualitative comparison of MLS with ILS.

Results suggest that an increase in runway landing capacity, caused by introducing the MLS multiple approach paths, is to be expected only when an aircraft population consists of aircraft with significantly differing approach speeds and particularly in situations when vertical separation can be applied. Vertical separation can only be applied if one of the types of aircraft in the mix has a very steep descent angle

(i.e. 7.5 degrees) such as an STOL vehicle. When approaching aircraft are separated only horizontally, examples considered in this research show a modest capacity increase of 10 to 15 percent. When both vertical and horizontal separations are applied, capacity improvement can be greater depending on the proportion of steep descent aircraft in the mix.

It was also found that the angles of entry to the extended runway centerline have a significant effect on landing capacity, and they should be optimized.

TABLE OF CONTENTS

1. Introduction

Improved navigational aids for approach and landing at airports have been under development for many years. One such aid is the Microwave Landing System (MLS) which provides multiple flight paths to the runway rather than a single path defined by the current Instrument Landing System (ILS).

There are a number of advantages cited for the MLS. Among these are (1) curved path approaches can reduce flight over noise sensitive areas, (2) the system is less sensitive to interference from terrain and man made objects, (3) since the system extends much farther from the runway than the current ILS, aircraft have precise guidance over their intended flight paths for a longer period of time before landing, and (4) flexibility in flight paths might increase the landing capacity of a runway.

This research deals with item 4, landing capacity. Models for capacity are developed to reflect the multipath capability of MLS. The models are then applied to hypothetical situations, and the capacities obtainable with MLS and ILS are compared to determine if there are any significant differences.

In this research it is assumed that both the ILS and MLS are free of any errors; that is, that aircraft arrive at points in space when the controllers intend them to be there (e.g., at the entry gate to ILS). Therefore, no buffer is added to interarrival times. It is recognized, however, that in the real world there is no such thing as an error free system.

The objective of this research is, then, to compare in a qualitative manner the ILS and MLS systems to see if there is a significant

difference in their respective capacities, and if so under what conditions.

The term capacity as used in this research refers to the maximum number of landings that a runway can accept when there is a continuous demand for service and a certain specified set of conditions (i.e., aircraft mix, air traffic control (ATC) rules, etc.). These conditions can significantly effect runway landing capacity.

This research focuses on one of the factors that influence capacity: flight path geometry, particularly that geometry which ensures maximum landing capacity for a specified set of the other factors that influence capacity, i.e., aircraft population and mix, length of common approach path, ATC rules.

1.1. Characteristics of ILS

The existing ILS is essentially a straight line in three-dimensional space (see Fig. 1*). This line ends on the runway. Aircraft follow the line and land on the runway. There are three pieces of information that the pilot obtains about the position of his aircraft, with respect to the line leading to the runway and the distance from threshold:

1. position of the aircraft with respect to the alignment of the runway; namely, whether the aircraft is left or right of the centerline of the runway;
2. position of the aircraft with respect to the required height above the runway, referred to as the glide path; namely, whether the aircraft is above or below the glide path;

---

*All figures are placed in Chapter 7.

3. distance of the aircraft from the runway threshold. Distance information is provided by markers (two or three): one at the beginning of the ILS approach and the other (or two others) nearer to the runway threshold.

With the current ILS (see Fig. 1), landing aircraft follow each other on a common path, ET (E being the "entry gate" and T the runway threshold). Normally there are two markers installed on the common approach path, except for ILS Category II (or lower) weather conditions when a third marker is added. The marker furthest from the runway (about 5 nm) is the "outer marker" (OM); the marker generally closest to the runway (about 0.6 nm) is the "middle marker" (MM); and the sometimes used third marker (about 0.2 nm) is known as the "inner marker" (IM).

1.2. Characteristics of MLS

The MLS provides glide path information up to about 15 degrees elevation and alignment information as much as 130 degrees relative to the runway (65 degrees each side of the center line of the runway). In lieu of markers, continuous information on distance to the runway will be incorporated into the MLS. The MLS is shown in Fig. 2.

MLS gives information on the position of the aircraft relative to the runway in three-dimensional space. The area of coverage can be described as a quasi-pyramid with the runway threshold as the apex (see Fig. 3). The three-dimensional information is continuous and provides a means of describing different paths for aircraft to follow in the space covered by MLS. However, even if the information on the position of aircraft is accurate and the equipment is available to program any type of trajectory inside the pyramid, all described paths cannot

be followed by an aircraft. Several assumptions need then to be made about possible restrictions on the types of trajectories, as follows.

1. It is assumed that aircraft need to fly along the prolongation of the centerline of the runway before landing ($E_{i=1,2,3}$ to T , Fig. 3). E_i is the "entry gate" for this straight portion of the final approach for aircraft of type i .
2. It is assumed that there are some restrictions to the curved paths because of the minimum turning radius of an aircraft.
3. It is assumed that there are restrictions to the maximum angle of descent.
4. It is assumed that there are sufficient exit taxiways on the runway so that runway occupancy time is always less than the threshold interarrival time which ensures the ATC-required separation of aircraft in the air.

These restrictions, together with air traffic control (ATC) separation rules, limit the number of usefully considered approach paths. As section 2.2 indicates, within these limits rather simple flight paths are chosen, these representing the most desirable paths from the standpoint of runway capacity.

1.3. Existing ATC Separation Rules

According to ATC rules, aircraft can be separated vertically and horizontally. Horizontal separation can be expressed in time or distance. It is here assumed that radar coverage is available, and therefore separations are in terms of distance rather than time. Two aircraft approaching the runway should, then, never to closer to each other than the minimum horizontal distance prescribed by ATC.

Another important safety regulation, one that could influence the capacity of a runway, is that two aircraft can not be on the runway at the same time; the first aircraft has to clear the runway before the second crosses the threshold. (It is assumed that runway occupancy time is always less than that threshold interarrival time, which ensures the ATC required separation of airborne aircraft; therefore, runway occupancy time is not a constraint.)

1.4. Runway Landing Capacity Model Basic Structure

Basic landing capacity models using the current ILS were developed by Dr. Richard Harris of Mitre Corporation[1] and refined and expanded by Peat, Marwick, Mitchell and Co.[2] The landing capacity of a runway is defined as that maximum number of landing operations that can take place on a runway in a unit of time (usually one hour) during which aircraft continually wish to land. This concept of capacity is often referred to as "ultimate" or "saturation" capacity. The maximum number of landing operations on the runway depends on a number of conditions, as follows:

1. minimum separation rules specified by ATC;
2. aircraft mix (i.e., the proportion of different types of aircraft using a runway in a given period of time);
3. location and type of exit taxiways (i.e., if there are an insufficient number of taxiways, the runway occupancy time rather than air separation might be critical);
4. geometry of the approach paths associated with the runway (i.e., multiple paths are available with MLS).

To compute capacity, each of these conditions must be specified.

Runway landing capacity is actually the capacity of a system, consisting of a runway and the airspace adjacent to the runway. The runway is that part of the system where the flow of all aircraft operations converge; consequently, the landing capacity can also be defined as that number of operations in unit time which pass through a point which all aircraft have to pass. In this analysis this point is taken as the runway threshold. To find the capacity it is then necessary to determine t_{ij}, it being defined as follows: t_{ij} = interarrival time at the threshold between aircraft type i (lead aircraft) and aircraft type j (trailing aircraft); t_{ij} should then be such that:

a. aircraft i and aircraft j will not occupy the runway at the same time (i.e., when j passes the threshold i should have cleared the runway);

b. in the air, aircraft i and aircraft j are never closer than the minimum separation specified by ATC rules, then,

$t_{ij} = \min({}_{a}t_{ij}, {}_{r}t_{ij})$ where

${}_{a}t_{ij}$ = interarrival time at the threshold, dictated by ATC minimum separation rules for airborne aircraft,

${}_{r}t_{ij}$ = interarrival time at the threshold, dictated by ATC runway occupancy rule: only one aircraft can occupy the runway during any interval time.

Existing models of capacity assume independence, that is, the type of trailing aircraft j is not dependent on the type of leading aircraft i. The proportion of aircraft in the mix over the unit of time being considered (usually one hour) has, however, to be preserved. This

implies the following:

$p_{ij} = p_i p_j$, where

p_{ij} = probability of the sequence ij ,

p_i, p_j = proportions of aircraft i and j in the mix.

When t_{ij} and p_{ij} are found for all i and j , the expected interarrival time at the threshold can be computed as:

$$\bar{t} = \sum_{ij} t_{ij} p_{ij} \quad .$$

The capacity, assuming independence in the sequence of aircraft but with the restriction that the aircraft mix will remain constant during the unit of time selected ($p_k = 1$, where p_k = proportion of aircraft of type k), is

$$\lambda = \frac{1}{\bar{t}}$$

where λ = landing capacity

$\bar{t}$ = expected interarrival time between aircraft over the runway threshold.

1.5. Factors Affecting Runway Landing Capacity

If it is desired to maximize λ , it is necessary to minimize $\bar{t}$ (i.e., $\min \sum_{ij} t_{ij} p_{ij}$). If sequencing is not applied to the stream of the landing aircraft, with given p_k , all p_{ij} are fixed. Conse-

quently, the term that requires analysis is t_{ij} .

As noted, it is assumed that air separation rather than the runway occupancy rule is critical in all landing cases, so that $t_{ij} = {}_a t_{ij}$. Two more assumptions are made in the following analysis.

1. All aircraft have uniform velocities when they are on the final approach to the runway.
2. All aircraft of the same type use the same path for approach to the runway.

These two assumptions are critical to an analysis of capacity. Consider simple case, only two aircraft types, "fast" and "slow." We see immediately that there are four interarrival times:

t_{FS} = interarrival time between "fast" followed by "slow"
t_{SF} = " "slow" " "fast"
t_{FF} = " "fast" " "fast"
t_{SS} = " "slow" " "slow"

Cases t_{FF} and t_{SS} are simpler than the other two, because the landing trajectory is the same for both aircraft and the distance between the two aircraft measured along the trajectory is constant. The distance has, however, to be such that during the entire approach the two aircraft never come closer to each other, measured on a straight line in the horizontal plane, than the minimum specified by ATC rules.

The situation for t_{FS} and t_{SF} is more complex. First, the two aircraft might not have a common trajectory, in which case the separation can not be measured along the trajectory but rather by horizontal, vertical or diagonal separation. Second, if part of the trajectory is common to both aircraft (see aircraft 1 and 3 in Fig. 3),

the distance between them measured on the common path is not constant; it depends on the relative speeds of the two aircraft. The distance and corresponding time will increase for $v_j < v_i$ (aircraft type i followed by aircraft j) and decrease for $v_j > v_i$.

As noted, there are capacity models available for computation of ultimate capacity. These models are, however, primarily applicable to a single trajectory corresponding to current ILS procedures. The structure of these models was briefly described in paragraph 1.4. The method for computing t_{ij} in these models is shown in Fig. 4.[1,2] This figure represents a time-space diagram in the horizontal plane. Time is the abscissa and distance is the ordinate.

Several remarks concerning the procedure for computation of t_{ij} are in order to develop a better understanding of the assumptions.

Figure 4 shows that all aircraft are fed into the entry gate (E) from the same path, an extension of the current single ILS alignment path which is, in turn, an extension of the center of the runway. An important point is that the state of the system is considered only when $t > 0$ (i.e., only for that time after the instant, $t = 0$, when the leading aircraft passes through the entry gate).

In the case of sequence FS (fast followed by slow), shown in Fig. 4a, it can be seen that the horizontal distance between the two aircraft, $d(t)$, is equal to the ATC minimum required horizontal separation, δ, when $t = 0$ and increases thereafter. It can also be seen that the horizontal separation constraint, $d(t) > \delta$, is violated prior to $t = 0$. (See dotted lines in Fig. 4.)

There are three possible explanations how one could have a slow aircraft only δ behind a fast aircraft when the fast aircraft is at

the entry gate, E .

The first is to have the approach path unchanged in the horizontal projection and assume that the velocities of an individual aircraft are not uniform during the approach. Velocities of the two aircraft should be at least equal ($v_S \geq v_F$) for $t < 0$. As it is not likely that v_F will be smaller when $t < 0$ than when $t > 0$, v_S has to be increased until it at least equals v_F (see Fig. 5). This increase in speed is not very practical, especially in the case where two approach speeds are very different.

The sequence FS is of particular interest since the interarrival time, t_{FS} , is critical from a capacity point of view since the time gap between F and S opens as they approach the runway along the common path (see Fig. 4a). In addition, if it is assumed that an increase in speed of the slow aircraft (v_S) is possible, the problem of the two aircraft being separated exactly δ when $t = 0$ remains only partially solved; i.e., it is still assumed that both aircraft are on the straight line (a prolongation of the runway centerline) when $t < 0$ and are coming from infinity on this line, continually separated by at least δ . This assumption does not of course fully consider the real world since one of the following events must have occurred before $t = 0$.

1. Aircraft F has overtaken aircraft S (observed in the horizontal projection) on the straight line, indicating that vertical separation was imposed (the fast aircraft went either under or above the slow).
2. Aircraft S joins the straight line path (observed in the horizontal projection) after aircraft F has passed through

the point E_S , this point being where the slow aircraft joins the common path.

A second possibility is that two aircraft can be separated vertically in the approach air space before $t = 0$. Fig. 6 shows how this separation might look using distances which are appropriate to current ATC rules and procedures. It is assumed that when $t = 0$, vertical separation is imposed in such a way that the slow aircraft is above the fast and both are flying level. Two conditions are necessary to ensure the vertical separation shown in Fig. 6.

1. $h \geq \chi$

   where h is vertical distance between the two aircraft and χ is the minimum permissible vertical separation. At present ATC rules specify χ as 1,000 ft (305 m).

2. The fast aircraft should be able to perform straight level approach at an altitude equal to threshold elevation plus H , a distance of $2\ {}_{E}d_{c}$ (see Fig. 5), before intercepting the glide path at the entry gate, E .

In Fig. 7 another possible vertical separation for aircraft approaching the entry gate, E , is shown, when the fast aircraft is at E , and the slow one is a distance of δ behind and χ below the fast. Two conditions are necessary to ensure this vertical separation.

1. $(H - \chi)/\sin\theta$ has to be greater than the distance necessary for the slow aircraft to stabilize on the glide path. If this condition is not satisfied, the resulting problem could theoretically be solved by the slow aircraft climbing to intercept the glide path after $t = 0$. The slow aircraft climbs--or climbs and levels--until it intercepts the glide path (see Fig. 7).

2. The second condition is similar to the second condition of the previous vertical separation case (a slow aircraft above a fast); but it is far more difficult to satisfy: the slow aircraft is required to perform straight level approach at an altitude equal to threshold elevation plus $H - \chi$, for a distance of $2\ {}_{E}d_{c} - \delta$ before reaching point F. Considering the values of H (shown in Fig. 6) this condition is almost impossible to satisfy since χ is 1,000 ft, i.e., slow aircraft would be required to fly level at a height above the terrain of only 500 to 1500 ft which is not acceptable (see Fig. 7).

The third possibility of having the slow aircraft only δ behind the fast one, when the fast one is at E, is briefly discussed below.

Does, for example, a path leading to E exist, such that, if the slow aircraft is behind the fast on this path separated by distance δ (measured along the path) when the fast passes E ($t = 0$), the distance between the two aircraft (measured as a straight line in the horizontal plane) is never (when $t < 0$ and when $t > 0$) less than δ ? (See Fig. 8a.)

To satisfy the condition $d(t) \geq \delta$, $d(t)$ being the distance between the slow and fast aircraft measured along a straight horizontal line, for all values of t, it is also necessary to satisfy this condition when $t = 0$. Obviously, this condition can only be satisfied if the path of the slow aircraft to E is on a straight line leading to E for at least length δ before E is reached. This implies that at the moment when $t = 0$ the slow aircraft should be somewhere on the circle of radius δ which has its center at E (see Fig. 8b).

However, strictly speaking, though the slow aircraft is on this circle when $t = 0$, the distance that the slow aircraft has to fly along the path to E does not equal δ; in fact, this distance is more than δ, with the exception of position 1 (see Fig. 8b) for the following reason. The distance that the slow aircraft must fly to reach E is greater than δ because of a change in heading which is required for positions 2, 3, and 4. This change can only be made on a curved path; so the sum of the straight and curved path will always be greater than the radius of the circle. However, even if the slow aircraft is at point 1 when $t = 0$, it will violate the condition $d(t) \geq \delta$ when $t = -\Delta t$ (see Fig. 4). So we can conclude that strictly speaking the path we were looking for does not exist.

In spite of the shortcomings which have been discussed in this section, existing runway capacity models can be used to find potential sources for an increase in landing runway capacity. Fig. 4 allows us to examine interarrival times, t_{FS}, t_{SF}, t_{FF} and t_{SS}, and attempt to decrease them, as a way of decreasing mean interarrival time, $\bar{t}$, and consequently increasing landing capacity, λ. For ease of computation, v_S can be expressed as $v_S = \mu v_F$, $0 \leq \mu \leq 1$.

From Fig. 4

$$t_{SF} = \frac{\delta}{v_F} ,$$

$$t_{FF} = \frac{\delta}{v_F} ,$$

$$t_{SS} = \frac{\delta}{\mu v_F} , \text{ and}$$

$$t_{FS} = \frac{1}{v_F}\left(\frac{\delta + \gamma}{\mu} - \gamma\right) = \frac{1}{v_F}\,\frac{\delta + \gamma(1 - \mu)}{\mu} = \frac{\delta + \gamma(1 - \mu)}{\mu v_F} \quad .$$

Possible ways to decrease t_{ij} are then as follows.

1. The most efficient would be to decrease δ, thus simultaneously decreasing all t_{ij}'s.
2. Increase both v_S and v_F, thus ensuring a higher velocity of aircraft stream at the runway threshold which results in a higher flow.
3. Increase μ only, keeping v_F constant. (This can be achieved by requesting slow aircraft to maintain cruise speed as long as possible.)
4. Decrease γ, the common part of final approach.

The implementation of MLS could reduce δ (case 1) and γ (case 4).

In summary, then, this research is concerned with whether the approaches along the curved paths described by MLS will improve the landing capacity of a runway, and, if the answer to this question is positive, what is the value of this increase over that capacity obtained with ILS?

The following analysis of capacity will begin with the assumption that vertical separation within the operating area of MLS is not permitted, i.e., horizontal separation is crucial. The situations governed by this assumption are examined in Chapters 2 and 3. The assumption that vertical separation may be permitted (either horizontal or vertical separation could therefore be employed) governs the situations examined in Chapters 4 and 5.

2. Analysis of Capacity with Horizontal Separation Only

2.1. Introduction

In this chapter the influence of multiple flight approach paths on the landing capacity of a runway is analyzed. It is assumed that all approaching aircraft are on the same horizontal plane, that is, no vertical separation exists.

The procedure for the current ILS is shown in Fig. 9. All aircraft landing in IFR have to pass through a point E (entry gate), located distance γ (common approach path length) from the landing threshold, T , along the extended runway centerline, and remain on the centerline until they reach the threshold. As shown in Fig. 10, with MLS there is no need for aircraft to use a common approach path of length γ . Similarly, all aircraft do not need to pass through the common entry gate, E . Multiple paths are possible. Each path intersects the prolongation of the runway centerline at E_i , and, as noted in Chapter 1, Section 1.5, this path is used only by aircraft of type i . Each intersection of the runway centerline, E_i , is located γ_i from the runway threshold. Each intersection, E_i , can be considered as the entry gate for type i aircraft.

The objective of the analysis is to develop a model to describe multiple rather than common entry path geometry. The model should represent the two approach path situations (ILS and MLS) shown in Figs. 9 and 10 and determine the ultimate capacities of the two (under given conditions). The model should also be able to determine a geometry (i.e., set of approach paths) which maximizes ultimate capacity for either the ILS or MLS situation. Once the maximum ultimate capacity for each of the two situations has been determined the effect of MLS on

runway landing capacity can be obtained by comparing the two capacities.

Analysis of the effect of geometry on the ultimate capacity, either with ILS or MLS, will concentrate on an aircraft pair consisting of two aircraft types, a fast aircraft, F, and a slow aircraft, S. When analyses of cases involving more than two aircraft types in a population are necessary they can be treated in pairs. These pairs in all cases consist of fast and slow aircraft. This approach of breaking down an aircraft population in couples and dealing with four general case interarrival times, t_{FF}, t_{FS}, t_{SF}, and t_{SS} (i.e., t_{FS} = interarrival time at threshold for a fast aircraft followed by a slow one, etc.) will be used throughout the analysis since any of the interarrival times, t_{ij}, can be represented by one of these four times.

From Fig. 4 we can draw some rough conclusions about aircraft operations with ILS. In conventional ILS all aircraft pass through an entry gate, E, and travel on a common approach path through a distance of γ to the runway threshold. As Fig. 4a illustrates, in the case of a slow aircraft following a fast one, the interarrival time over the threshold, t_{FS}, increases as γ is increased. Similarly, in the case of MLS for a situation involving a fast aircraft followed by a slow, γ_{FS}, the common path for the two aircraft should be considered rather than the single common path, γ, where

$$\gamma_{FS} = \min(\gamma_F, \gamma_S) \quad .$$

A new assumption is therefore introduced; it will be used in further analysis; it is

$$\gamma_F \geq \gamma_S \quad .$$

This assumption requires that an aircraft with a higher approach speed will need at least as long a final straight approach along the extended runway centerline as an aircraft with a lower approach speed. That is,

$$\gamma_{FS} = \gamma_S$$

i.e., the common approach path is equal to the length of the final straight approach for slower aircraft.

Therefore, if $\gamma_S < \gamma$, t_{FS} is decreased. However, even if $\gamma_S = 0$ (i.e., that a slow aircraft does not need any portion of straight level wing approach before landing) the interarrival time, t_{FS}, remains equal to δ/v_S (see Fig. 4a).

Fig. 4 also illustrates that if γ is reduced the only possible reduction in interarrival times that can be made is a reduction of t_{FS}. The other three times, t_{FF}, t_{SF}, and t_{SS}, will remain unchanged.

Intuitively, it can be expected that an increase in landing capacity will be small if a decrease in t_{FS} is the only reduction of interarrival time possible. For example, consider the case where an aircraft population is equally divided between fast and slow aircraft, that is, $p_F = 0.5$ and $p_S = 0.5$. If the sequence of the arrivals is considered as random, then the fraction of slow aircraft following fast aircraft will be 0.25, which is the result of $p_F \times p_S$. Seventy-five percent of the arrivals will constitute pairs of aircraft with interarrival times, t_{FF}, t_{SF}, and t_{SS}. These times cannot be changed. Therefore, a significant reduction in the mean interarrival time, $\bar{t}$, and consequently, an increase in landing capacity, λ, cannot be expected.

This conclusion will be examined in detail in the following sections of this chapter.

As noted in Chapter 1, Section 1.5, in order to decrease t_{FS} a slow aircraft must be brought as close as possible to the threshold when a fast one is over the threshold. Minimum horizontal separation rules must not, however, be violated.

The following examination of the effect of MLS on runway capacity will involve analysis of changes of interarrival times over the threshold, t_{ij}. The first step in this analysis is to see how these changes respond to certain variables.

The variables that affect t_{ij} are as follows:

v_F = velocity of the fast aircraft

v_S = velocity of the slow aircraft

μ = v_S/v_F

γ_F = length of the approach on extended runway centerline of the fast aircraft

γ_S = length of the approach on extended runway centerline of the slow aircraft

δ = minimum horizontal separation required between the two aircraft measured in the horizontal plane.

If the values for all of these variables are given, then the effect on capacity of various possible aircraft paths, herein referred to as trajectories, is necessarily the subject of the following analysis.

2.2. Types of Trajectories to Be Considered

The following assumptions and examples will indicate that family of trajectories that will be considered in the later analysis of capacity.

It is assumed that there are no obstacles in the approach area, nor are there any constraints due to noise; therefore, there are no restrictions as to the type of approach paths.

The case of a fast aircraft followed by a slow aircraft will be initially considered since, as noted in Section 2.1, this is the critical sequence.

Assume that a turning radius of an aircraft is zero, that is, its heading can be changed instantaneously. Further, assume that a fast aircraft is at E_S, the entry gate for slow aircraft, where $t = 0$ (as shown in Fig. 11). A useful question is: where should the slow aircraft be to ensure that the interarrival time t_{FS} is as small as possible? Obviously, the two aircraft should be separated at a minimum distance of δ (i.e., the slow aircraft should be somewhere on the circle of radius δ with center in E_S), but the condition of minimum separation has to be maintained until and after the moment the fast aircraft reaches E_S. Assuming that a slow aircraft is always flying toward E_S, Fig. 11 shows that to maintain a minimum separation, δ, its location at $t = 0$ has to be somewhere on the portion of the circle marked with a heavy line (e.g., point A). For any position of a slow aircraft on the light line portion of the circle, the condition $d(t) \geq \delta$ will not be satisfied for $t > 0$, where $d(t)$ is equal to the horizontal distance between two aircraft. The conclusion is, then, that a slow aircraft should approach the point E_S anywhere from the heavy

line portion of the circle; in other words, from the right side of the line, perpendicular to the extended runway centerline passing through the point E_S .

Consider a slow aircraft at point M and a fast one at E_S (when t = 0), as shown in Fig. 12. What kind of a path should the slow aircraft follow between M and E_S ? If a slow aircraft must reach E_S as quickly as possible, the desirable path is the straight line ME_S . On the other hand, if it is necessary for some reason to increase the time that the slow aircraft takes to reach E_S , a curved path between M and E_S is one alternative. Another alternative is to require the slow aircraft at $t = 0$, to be at a position, N , this position being further away than M on the same straight line; and then to have the slow aircraft continue on the straight line to E_S . Consequently, it can be concluded that straight line entries to E_S are at least as good as any other family of trajectories. The straight line entries because of their simplicity will be exclusively used in further analysis. A general straight line approach path configuration is shown in Fig. 13.

Before proceeding with analysis of this configuration it is necessary to establish arbitrarily that the index of aircraft type increases with approach speed, i.e., if $i > j$ then $v_i \geq v_j$, where i and j are indices of aircraft types. As noted in Section 2.1, that $\gamma_F > \gamma_S$, it follows that $\gamma_1 \leq \gamma_2 \cdots \leq \gamma_n$, where the subscript 1 refers to that aircraft type which needs the shortest straight-line part of the final approach, i.e., that aircraft type that can intersect the extension of the runway centerline closest to the runway threshold.

A useful question, then, in terms of understanding the character-

istics of the family of trajectories that is being considered is, what should be the angles α_1 , α_2 , $\cdots$ α_n ?

It has been shown earlier in this section that $|\alpha_i| \leq 90^o$ for any i , α_i being positive when measured counterclockwise from the extended runway centerline and negative when measured clockwise.

All approaches are assumed to be in a horizontal plane. Therefore, to assure that the two approach paths will not intersect, the following conditions must be met:

$\alpha_i < \alpha_j$ for all i and j such that $i > j$, $\alpha_i > 0$ and $\alpha_j > 0$

$\alpha_i > \alpha_j$ for all i and j such that $i > j$, $\alpha_i < 0$ and $\alpha_j < 0$.

These conditions state that if i and j are a pair of aircraft such that $v_i > v_j$, then when both α_i and α_j are positive, α_i has to be less than α_j . However, if α_i and α_j are both negative, then α_i must be greater than α_j (i.e., the absolute value of α_i is smaller than that of α_j).

The above conditions enable us to use any possible combination of paths and compute t_{ij} , where i can be F or S and j can be F or S , thereby preventing any two paths to intersect before they merge on the extended runway centerline.

If the case of only two aircraft types, fast and slow, is considered, then the necessary geometry of approach paths is shown in Fig. 14. This geometry requires that the following conditions have to be satisfied.

$$0 < \alpha_S < 90^o$$

$$-90^o < \alpha_F < \alpha_S \quad .$$

At the beginning of this section an assumption, "zero turning radii," was introduced. If this assumption were not made the geometry of the approach paths would follow that shown in Fig. 15, rather than that shown in Fig. 14. We will now determine whether the geometry shown in Fig. 14 is a close enough approximation of the geometry shown in Fig. 15.

For the purpose of this determination, even for very unusual conditions (high approach speed, high angle of interception of extended runway centerline, and low rate of change of heading) the straight line paths shown in Fig. 14 give a good approximation of the circular arc paths shown in Fig. 15. For example, if the approach speed of an aircraft is 160 kts and the rate of change of heading is 3^o per second, the difference in the length of the approach path measured along the straight line paths and the circular arc is 0.09 nm, if the angle of interception $\alpha = 60^o$, and only 0.02 nm if the angle of interception $\alpha = 30^o$. These differences in the length of the approach paths are for the purposes of this study negligible.

The conclusion, then, is that the geometry of approach paths that should be considered in further analysis of capacity is that shown in Fig. 14 for the case of two aircraft types, or that shown in Fig. 13 for the more general case.

2.3. Objective of the Horizontal Separation Model

Consider the case of the two aircraft shown in Fig. 16. The threshold interarrival time,

$$t_{ij} = \frac{\gamma_{ij} + \hat{d}_{ij_o}}{v_j} - \frac{\gamma_{ij}}{v_i} ,$$

where t_{ij} is increasing with initial separation $_{ij}\hat{d}_o$. Initial separation $_{ij}\hat{d}_o$ is the distance between two aircraft i and j at the time $t = 0$ (leading aircraft i enters the common path on the extended runway centerline), measured along the trajectory of trailing aircraft j. If for the given situation (aircraft types i and j and a given approach path geometry) one wants to minimize t_{ij}, then the problem could be stated as follows:

$$\min \; {}_{ij}\hat{d}_o$$

$$\text{subject to} \quad d_{ij}(t) \geq \delta_{ij} \quad \text{for} \quad t \leq \frac{\gamma_{ij}}{v_i}$$

where

$d_{ij}(t)$ = distance between aircraft i and j measured on a straight line in the horizontal plane

δ_{ij} = minimum horizontal separation for aircraft i followed by aircraft j, given by ATC rules.

Condition $t \leq \frac{\gamma_{ij}}{v_i}$ states that the ATC horizontal separation, δ_{ij}, is required only while both aircraft i and j are airborne. This condition can be released after leading aircraft, i, crosses the runway threshold, at $t = \frac{\gamma_{ij}}{v_i}$. However, the overall objective function of the horizontal separation model is much more complex; it can be stated as follows:

$$\min \bar{t} = \sum_{ij} t_{ij} p_{ij}$$

$$\text{subject to} \quad d_{ij}(t) \geq \delta_{ij}, \quad \text{for} \quad t < \frac{\gamma_{ij}}{v_i}, \quad \text{for all } i \text{ and } j.$$

In this situation the geometry is not given, as it was in the previous very simple example. The problem becomes, then, one of finding a geometry which for a given aircraft population and given ATC rules will provide the highest landing capacity.

The next step is to study how the distance between two successively landing aircraft changes with time.

2.4. Equations for Distance between Two Aircraft in a Plane

If the selected geometry of approach paths is that shown in Fig. 14, and if two types of aircraft, fast F and slow S, are considered, there are four possible approach sequences to be studied: FF, SS, FS and SF (where FS refers to fast followed by slow, etc.). It has been noted in Section 2.3 that for the sequence of any two aircraft ij, $t = 0$ is the instant in time when the leading aircraft, i, enters the first point of the common path on the extended runway centerline.

All four sequences mentioned above are shown in Fig. 17 at the point when $t = 0$. As can be seen, for the sequence SF there are two cases: at the point when $t = 0$ and the aircraft S is at E_S, aircraft F could already be on the extended runway centerline, i.e., aircraft F could have passed through point E_F (case a) or it could still be on that part of the approach path leading towards E_F (case b).

The important point here is that in all cases $\hat{d}_{o_{ij}}$ is the distance between two aircraft when $t = 0$, measured along the path of the trailing aircraft, j.

The next step is to analyze interarrival times by studying the distance between two aircraft measured along a straight line in a

horizontal plane, as a function of time. This distance will be denoted by $d_{ij}(t)$ and will be studied for the four sequences mentioned above. However, as Fig. 17 illustrates, cases 1 and 2 (SS and FF sequences) represent essentially similar cases; they will therefore be studied as one case.

2.4.1. The case of fast aircraft followed by a fast aircraft, or slow aircraft followed by a slow aircraft

From Fig. 18 it can be seen that the function $d(t)$, the horizontal distance between two aircraft, is a piecewise function of t. Therefore,

1. for $t < 0$ (neither of the two aircraft is on the extended centerline yet)

$$d(t) = {}_1d(t) = \hat{d}_o ;$$

2. for $0 < t < \frac{\hat{d}_o}{v}$ (only the leading aircraft is on the extended runway centerline)

$$d^2(t) = {}_2d^2(t) = \{vt + (\hat{d}_o - vt)\cos\alpha\}^2 + \{(d_o - vt)\sin\alpha\}^2$$

$$= 2v^2t^2(1 - \cos\alpha) - 2\hat{d}_o vt(1 - \cos\alpha) + \hat{d}_o^2 ; \qquad (1)^*$$

3. for $t > \frac{\hat{d}_o}{v}$ (both aircraft are on the extended runway centerline)

$$d(t) = {}_3d(t) = \hat{d}_o .$$

*Only equations which are referred to later are enumerated.

2.4.2. The case of fast aircraft followed by slow aircraft

From Fig. 19 it can be seen that the function $d_{FS}(t)$, the horizontal distance between two aircraft (fast followed by slow), is also a piecewise function of t. Therefore,

1. for $t < -\frac{\beta}{v_F}$ (neither of the two aircraft is on the extended runway centerline yet)

$$d_{FS}^2(t) = {}_1d_{FS}^2(t)$$

$$= \{({}_{FS}\hat{d}_o - \mu v_F t)\cos\alpha_S - \beta + (v_F t + \beta)\cos\alpha_F\}^2$$

$$+ \{({}_{FS}\hat{d}_o - \mu v_F t)\sin\alpha_S + (v_F t + \beta)\sin\alpha_F\}^2$$

$$= t^2 v_F^2\{\mu^2 - 2\cos(\alpha_S - \alpha_F) + 1\}$$

$$+ t2v_F\{\beta\{(1 - \cos\alpha_F) - \mu(\cos(\alpha_S - \alpha_F) - \cos\alpha_S)\}$$

$$+ {}_{FS}\hat{d}_o\{\cos(\alpha_S - \alpha_F) - \mu\}\} + {}_{FS}\hat{d}_o^2$$

$$+ 2\beta_{FS}\hat{d}_o\{\cos(\alpha_S - \alpha_F) - \cos\alpha_S\} + 2\beta^2(1 - \cos\alpha_F) \quad ; \tag{2}$$

2. For $-\frac{\beta}{v_F} < t < \frac{{}_{FS}d_o}{v_F}$ (only the leading aircraft is on the extended runway centerline)

$$d_{FS}^2(t) = {}_2d_{FS}^2(t)$$

$$= [({}_{FS}\hat{d}_o - \mu v_F t)\cos\alpha_S + v_F t]^2 + [({}_{FS}\hat{d}_o - \mu v_F t)\sin\alpha_S]^2$$

$$= t^2 v_F^2(\mu^2 - 2\mu\cos\alpha_S + 1)$$

$$+ t2_{FS}\hat{d}_o v_F(\cos\alpha_S - \mu)$$

$$+ {}_{FS}\hat{d}_o^2 \quad ; \qquad (3)$$

3. For $t > \dfrac{{}_{FS}\hat{d}_o}{\mu\, v_F}$ (both aircraft are on the extended runway centerline)

$$d_{FS}(t) = {}_3d_{FS}(t)$$

$$= {}_{FS}\hat{d}_o + v_F(1 - \mu)\, t \quad . \qquad (4)$$

2.4.3. The case of slow aircraft followed by fast aircraft

Here two cases can be distinguished:

a. at $t = 0$ trailing aircraft is already on the extended runway centerline, as shown in Fig. 20a (${}_{SF}d_o < \beta$);

b. at $t = 0$ trailing aircraft is not yet on the extended runway centerline, as shown in Fig. 20b (${}_{SF}d_o > \beta$).

In both cases, $d_{SF}(t)$ is the horizontal distance between the two aircraft and is a piecewise function of t. The two cases will be treated separately.

Case a. (See Fig. 20a, $_{SF}\hat{d}_o < \beta$.)

1. For $t < \dfrac{{}_{SF}\hat{d}_o - \beta}{v_F}$ (neither of the two aircraft is on the extended runway centerline yet)

$$d_{SF}^2(t) = {}_1d_{SF}^2(t)$$

$$= [v_F t(\mu\cos\alpha_S - \cos\alpha_F) + ({}_{SF}\hat{d}_o - \beta)\cos\alpha_F + \beta]^2$$

$$+ [v_F t(\mu\sin\alpha_S - \sin\alpha_F) + ({}_{SF}\hat{d}_o - \beta)\sin\alpha_F]^2$$

$$= t^2 v_F^2[\mu^2 - 2\mu\cos(\alpha_S - \alpha_F) + 1]$$

$$+ t2v_F\{\beta[(1 - \cos\alpha_F) - \mu(\cos(\alpha_S - \alpha_F) - \cos\alpha_S)]$$

$$+ {}_{SF}\hat{d}_o[\mu\cos(\alpha_S - \alpha_F) - 1]\} + {}_{SF}\hat{d}_o^2$$

$$- 2\beta\,{}_{SF}\hat{d}_o(1 - \cos\alpha_F) + 2\beta^2(1 - \cos\alpha_F) \quad . \qquad (5)$$

2. For $\dfrac{{}_{SF}\hat{d}_o - \beta}{v_F} < t < 0$ (only the trailing aircraft is on the extended runway centerline)

$$d_{SF}^2(t) = {}_2d_{SF}^2(t)$$

$$= [v_F t(\mu\cos\alpha - 1) + {}_{SF}\hat{d}_o]^2 + [\mu v_F t\sin\alpha_S]^2$$

$$= t^2 v_F^2(\mu^2 - 2\mu\cos\alpha_S + 1) + t2v_F\,{}_{SF}\hat{d}_o(1 - \mu\cos\alpha_S) + {}_{SF}\hat{d}_o^2 \quad .$$

(6)

3. For $t > 0$ (both aircraft are on the extended runway centerline)

$$d_{SF}(t) = {}_3d_{SF}(t)$$

$$= {}_{SF}\hat{d}_o - v_F(1 - \mu)t \ . \qquad (7)$$

Case b. (See Fig. 20b, ${}_{SF}\hat{d}_o > \beta$.)

1. For $t < 0$ (neither of the two aircraft is on the extended runway centerline yet)

$$d_{SF}^2(t) = {}_1d_{SF}^2(t)$$

$$= [v_F t(\mu\cos\alpha_S - \cos\alpha_F) + ({}_{SF}\hat{d}_o - \beta)\cos\alpha_F + \beta]^2$$

$$+ [v_F t(\mu\sin\alpha_S - \sin\alpha_F) + ({}_{SF}\hat{d}_o - \beta)\sin\alpha_F]^2$$

$$= t^2v_F^2[\mu^2 - 2\mu\cos(\alpha_S - \alpha_F) + 1] +$$

$$+ t2v_F\{\beta[(1 - \cos\alpha_F) - \mu(\cos(\alpha_S - \alpha_F) - \cos\alpha_S)]$$

$$+ {}_{SF}\hat{d}_o[\mu\cos(\alpha_S - \alpha_F) - 1]\} + {}_{SF}\hat{d}_o^2$$

$$- 2\beta\,{}_{SF}\hat{d}_o(1 - \cos\alpha_F) + 2\beta^2(1 - \cos\alpha_F) \ . \qquad (8)$$

Note that this ${}_1d_{SF}(t)$ is the same as in the previous case a.

2. For $0 < t < \dfrac{{}_{SF}\hat{d}_o - \beta}{v_F}$ (only the leading aircraft is on the extended runway centerline)

$$d_{SF}^2(t) = {}_2d_{SF}^2(t)$$

$$= [v_F t(\mu - \cos\alpha_F) + ({}_{SF}\hat{d}_o - \beta)\cos\alpha_F + \beta]^2$$

$$+ [-v_F t \sin\alpha_F + ({}_{SF}\hat{d}_o - \beta)\sin\alpha_F]^2$$

$$= t^2 v_F^2[\mu^2 - 2\mu\cos\alpha_F + 1]$$

$$+ t\, 2v_F[{}_{SF}\hat{d}_o(1 - \mu\cos\alpha_F) - \beta(1 - \cos\alpha_F)(1 + \mu)]$$

$$+ {}_{SF}\hat{d}_o^2 - 2{}_{SF}\hat{d}_o\beta(1 - \cos\alpha_F) + 2\beta^2(1 - \cos\alpha_F) \quad . \quad (9)$$

3. For $t > \dfrac{{}_{SF}\hat{d}_o - \beta}{v_F}$ (both aircraft are on the extended runway centerline)

$$d_{SF}(t) = {}_3d_{SF}(t)$$

$$= {}_{SF}\hat{d}_o - v_F(1 - \mu)\, t \quad . \quad (10)$$

2.5. Initial Separation

This section will describe procedures for determining those optimal initial separations which satisfy model requirements.

Initial separation here refers to that distance between two runway approaching aircraft, measured along the trajectory of the trailing aircraft, that exists when the first aircraft intersects the common approach path (see Fig. 16).

Section 2.3 notes that the threshold interarrival time is an increasing function of initial separation. This section also notes that the objective of the model is to minimize initial separation subject to constraints imposed by ATC rules on the required horizontal distance between two approaching aircraft.

As noted in Section 2.4 the horizontal distance between two aircraft is a function of many variables rather than simply a function of time. The function could be written as follows.

$$d_{ij}(t) = d_{ij}(v_i, v_j, \gamma_i, \gamma_j, \alpha_i, \alpha_j, t, {}_{ij}\hat{d}_o) .$$

However, v_i , v_j , γ_i and γ_j can be considered as fixed parameters rather than variables, so

$$d_{ij}(t) = d_{ij}(\alpha_i, \alpha_j, t, {}_{ij}\hat{d}_o) .$$

To maximize the capacity for a given geometry (i.e., α_i , α_j , γ_i and γ_j are fixed) one wants ${}_{ij}d_o$ to be as short as possible but still such that the ATC rule, $d_{ij}(t) \geq \delta_{ij}$, is not violated for any $t < \frac{\gamma_{ij}}{v_i}$. For this condition and for ${}_{ij}\hat{d}_o$ to be minimized, the two aircraft have to be separated exactly δ_{ij} when they are closest to each other.

Using a partial derivative of d_{ij} with respect to t, the moment of minimal separation t^* can be obtained, as follows.

$$\frac{\partial d_{ij}}{\partial t} = 0 \rightarrow t^* = \phi(\alpha_i, \alpha_j, {}_{ij}\hat{d}_o) .$$

At the t^* moment the two aircraft should be separated by horizontal separation δ_{ij}, i.e.,

$$d_{ij}(t)\Big|_{t=t^*} = \delta_{ij}$$

$$d_{ij}(t)\Big|_{t=t^*} = \xi(\alpha_i, \alpha_j, {}_{ij}\hat{d}_o) = \delta_{ij} .$$

The initial separation ${}_{ij}\hat{d}_o$ is then found:

$${}_{ij}\hat{d}_o = \xi^{-1}(\alpha_i, \alpha_j, \delta_{ij}) .$$

Note that δ_{ij} can also be taken for a parameter with a fixed value; initial separation could then be written:

$${}_{ij}\hat{d}_o = \xi^{-1}(\alpha_i, \alpha_j) .$$

As noted, the threshold interarrival time, t_{ij}, is a function of initial separation, ${}_{ij}\hat{d}_o$; this function will vary depending on the particular pair of aircraft types to be considered, so that

$$t_{ij} = \begin{cases} f(\alpha_i, \alpha_j) & \text{for } i = j \text{ (two aircraft of same type)} \\ f_{FS}(\alpha_i, \alpha_j) & \text{for } i > j \text{ (fast followed by slow)} \\ f_{SF}(\alpha_i, \alpha_j) & \text{for } i < j \text{ (slow followed by fast)} . \end{cases}$$

The functions t_{ij} are included in the objective function of the model, which is

$$\min \Sigma\ t_{ij}\ p_{ij} \qquad (p_{ij} \text{ are given})$$

$$\text{s.t.}\quad d_{ij}(t) > \delta_{ij} \qquad \text{for } t \leq \frac{\gamma_{ij}}{v_i}$$

$$\text{for all } i \text{ and } j\ .$$

The objective function, $\Sigma t_{ij}p_{ij}$, becomes very complex for the following reasons.

a. Summation $\Sigma t_{ij}p_{ij}$ has n^2 members, when n represents number of aircraft types in airport population.

b. Members are nonlinear functions of α_i and α_j.

c. Each member belongs to one of the three types of functions mentioned above

$$f(\alpha_i,\alpha_j) \qquad \text{for } i = j$$

$$f_{FS}(\alpha_i,\alpha_j) \qquad \text{for } i > j$$

$$f_{SF}(\alpha_i,\alpha_j) \qquad \text{for } i < j\ .$$

However, function f can take two different forms, function f_{FS} four and function f_{SF} even five different forms, depending on the values of input parameters v_i, v_j, γ_i, γ_j and δ_{ij}, as well as on the values of variables α_i and α_j themselves. The several possible forms of the three functions are the result of the fact that $\delta_{ij}(t)$, being a piecewise function of t, could have a global minimum in more

than one of its segments. For example, the two aircraft could be minimally separated with neither being on the extended runway centerline, or minimal separation could occur when the first aircraft has already entered the extended runway centerline, or, when both aircraft are on the extended runway centerline.

Because, as noted, the objective function is complex and because the constraints are non-linear, it was found necessary to compute initial separations and, consequently, interarrival times and runway landing capacity for fixed α_i and α_j. This computation involves the development of computer programs capable of determining capacities for different discrete values of these intercept angles.

2.5.1. The case of fast aircraft followed by a fast aircraft, or slow aircraft followed by a slow aircraft

This case is shown in Fig. 18 and distance equations are given in Section 2.4.1.

From equations for ${}_1d(t)$, ${}_2d(t)$ and ${}_3d(t)$ it can be seen that the min d(t), i.e., the minimum separation between two aircraft, will occur for $0 < t < \hat{d}_o/v$, i.e., the minimum will be somewhere on the segment ${}_2d(t)$ of function d(t). Range $(0, \hat{d}_o/v)$ for variable t represents that time when the leading aircraft is already on the extended runway centerline and when the trailing aircraft is still approaching it.

From equation (1) and for

$$\frac{\partial_2 d^2(t)}{\partial t} = 0 \quad ,$$

the time when minimum separation occurs can be found by

$$t_2^* = \frac{\hat{d}_o}{2v} \quad .$$

At that time when they are minimally separated the two aircraft have to be separated distance δ ,

$$2d^2(t)\Big|_{t=t_2^*} = \delta^2 \quad ,$$

i.e., if t_2^* is substituted for t in equation (1) and the distance is δ , the following result is obtained:

$$\hat{d}_{02} = \frac{\delta}{\left|\sqrt{\frac{1}{2}(1 + \cos\ )}\right|} \quad .$$

Subscript 02 indicates that the initial separation is computed for the case when $\min d(t)$ occurs on the second segment, $_2d(t)$, of function $d(t)$.

The graph of function $d(t)$ is shown in Fig. 21. As can be seen, the initial gap (horizontal separation) between the two aircraft begins to close when $t > 0$ and reaches its minimum, which is equal to δ , when $t = t_2^*$. The two aircraft are, therefore, always separated more than is required, except at the moment t_2^* . It is possible, however, for the first aircraft to land (e.g., very short γ) before $t = t_2^*$ (see Fig. 22); in this case, the separation of the two aircraft should be distance δ at the moment when the first aircraft lands, if the conditions $d_{ij}(t) \geq \delta_{ij}$ is to be satisfied for that period when both aircraft are airborne, i.e.,

$$ {}_2d^2(t)\Big|_{t=\frac{\gamma}{v}} = \delta^2 \quad . $$

Therefore, from (1) the following quadratic equation is obtained

$$ A\,\hat{d}_{05}^2 + B\,\hat{d}_{05} + C = 0 $$

where

$$ A = 1 $$

$$ B = -2\gamma(1 - \cos\alpha) $$

$$ C = 2\gamma^2(1 - \cos\alpha) - \delta^2 \quad . $$

Consequently, the necessary initial separation is

$$ \hat{d}_{05} = \frac{-B + \sqrt{B^2 - 4C}}{2} \quad . $$

Finally, the necessary initial separation, $\hat{d}_o$, for two aircraft of the same type, depending on which of the two cases shown in Fig. 21 and Fig. 22 one deals with, must be either $\hat{d}_{02}$ or $\hat{d}_{05}$.

Subroutines SDOFF and SDOSS of the program compute values for ${}_{FF}\hat{d}_o$ and ${}_{SS}\hat{d}_o$. These subroutines are given in Appendix B.2.

2.5.2. The case of fast aircraft followed by slow aircraft

The above case is shown in Fig. 19, its distance equations are given in Section 2.4.2. From these distance equations it can be seen that the first two segments of the functions $d_{FS}(t)$, ${}_1d_{FS}(t)$ and ${}_2d_{FS}(t)$ are square roots of a parabola and, being distances, they are positive square roots of a parabola. The third segment of $d_{FS}(t)$--${}_3d_{FS}(t)$--is a linear increasing function of t. It can be shown

further that the slope of ${}_2d_{FS}(t)$ for $t = {}_{FS}d_o/\mu v_F$ is always greater than the slope of ${}_3d_{FS}(t)$. A conclusion can therefore be drawn: the function $d_{FS}(t)$ could resemble any of the various shapes shown in Fig. 23a; the following table lists all of the possible shapes of this function.

${}_1d_{FS}(t)$	${}_2d_{FS}(t)$	min $d_{FS}(t)$ at point
a	c	A
a	d	A
a	e	C
b	c	B
b	e	C

Whichever of the above forms of the function $d_{FS}(t)$ is encountered the same approach is taken, that is, when the two aircraft are separated by a minimum distance, that distance should be equal to the minimum horizontal separation required by ATC rules. This minimum separation condition is therefore used to find the necessary initial separation.

However, there is another case to be considered in addition to those shown in the above table: the case presented in Fig. 23b. If the minimum distance between two aircraft occurs during the second segment of $d_{FS}(t)$, i.e., at ${}_2d_{FS}(t)$, and if the leading aircraft lands before the gap between two aircraft reaches its minimum, i.e.,

$$\frac{\gamma_S}{v_F} < {}_{FS}t_2^* ,$$

then, as the argument in Section 2.5.1 suggests, the minimum horizontal separation δ_{FS} should be imposed when $t = \gamma_S/v_F$. In short, the function $d_{FS}(t)$ reaches its minimum at the upper limit of its domain.

Following are solutions of initial separation derived for the cases when $\min d_{FS}(t)$ appears in one of the four points, A, B, C, or D shown in Fig. 23.

Case A: $\min d_{FS}(t)$ at segment ${}_1d_{FS}(t)$, i.e., for $t < -\beta/v_F$

From equation (2) and for

$$\frac{\partial {}_1d_{FS}^2(t)}{\partial t} = 0 \quad ,$$

the time when the minimum separation appears, ${}_{FS}t_1^*$, can be found:

$${}_{FS}t_1^* = - \frac{{}_{FS}\hat{d}_o[\cos(\alpha_S-\alpha_F) - \mu] + \beta\{(1 - \cos\alpha_F) - \mu[\cos(\alpha_S-\alpha_F) - \cos\alpha_S]\}}{\{\mu^2 - 2\mu\cos(\alpha_S - \alpha_F) + 1\}\, v_F}$$

Using the condition that the minimal distance between two aircraft is exactly equal to the minimum required by ATC rules, i.e.,

$${}_1d_{FS}(t)\Big|_{t={}_{FS}t_1^*} = \delta_{FS} \quad ,$$

from equation (2) the following is found

$${}_{FS1}A\ {}_{FS}\hat{d}_{01}^2 + {}_{FS1}B\ {}_{FS}\hat{d}_{01} + {}_{FS1}C = 0 \quad ,$$

where

$${}_{FS1}A = 1 - \frac{[\cos(\alpha_S - \alpha_F) - \mu]^2}{\mu^2 - 2\mu\cos(\alpha_S - \alpha_F) + 1} \quad ,$$

$$_{FS1}B = 2\beta\{[\cos(\alpha_s - \alpha_F) - \cos\alpha_S] - \frac{[\cos(\alpha_S-\alpha_F) - \mu][(1 - \cos\alpha_F) - \mu(\cos(\alpha_S-\alpha_F) - \cos\alpha_S)]}{\mu^2 - 2\mu\cos(\alpha_S-\alpha_F) + 1}\},$$

and

$$_{FS1}C = \beta^2\{2(1 - \cos\alpha_F) - \frac{[(1 - \cos\alpha_F) - \mu(\cos(\alpha_S-\alpha_F) - \cos\alpha_S)]^2}{\mu^2 - 2\mu\cos(\alpha_S-\alpha_F) + 1}\} - \delta_{FS}^2 .$$

The necessary initial separation for the A case is therefore,

$$_{FS}\hat{d}_{01} = \frac{-_{FS1}B + \sqrt{_{FS1}B^2 - 4_{FS1}A_{FS1}C}}{2_{FS1}A} .$$

Case B: min $d_{FS}(t)$ at the limit of segments $_1d_{FS}(t)$ and $_2d_{FS}(t)$, i.e., for $t = -\beta/v_F$

From equations (2) or (3) and for

$$_1d_{FS}(t)\Big|_{t= -\beta/v_F} = {}_2d_{FS}(t)\Big|_{t= -\beta/v_F} = \delta_{FS}$$

the following is found

$$_{FS4}A\ _{FS4}\hat{d}_{04}^2 + {}_{FS4}B\ _{FS4}\hat{d}_{04} + {}_{FS4}C = 0$$

where

$$_{FS4}A = 1$$

$$_{FS4}B = -2\beta(\cos\alpha_S - \mu)$$

$$_{FS4}C = \beta^2(\mu^2 - 2\mu\cos\alpha_S + 1) - \delta_{FS}^2 .$$

The necessary initial separation for Case B is therefore,

$$_{FS}\hat{d}_{04} = \frac{-_{FS4}B + \sqrt{_{FS4}B^2 - 4\ _{FS4}C}}{2} .$$

Case C: min $d_{FS}(t)$ at segment $_2d_{FS}(t)$, i.e., for $\frac{-\beta}{v_F} < t < \frac{_{FS}\hat{d}_o}{\mu\ v_F}$

From equation (3) and for

$$\frac{\partial_2 d_{FS}^2(t)}{\partial t} = 0$$

the time when minimum separation appears, $_{FS}t_2^*$, can be found:

$$_{FS}t_2^* = -\frac{_{FS}\hat{d}_o(\cos\alpha_S - \mu)}{(\mu^2 - 2\mu\cos\alpha_S + 1)\ v_F} .$$

Using again the same condition as in Case A, i.e.,

$$_2d_{FS}(t)\Big|_{t=_{FS}t_2^*} = \delta_{FS}$$

and equation (3), it is found that the necessary initial separation for Case C is:

$$\hat{d}_{FS02} = \frac{\delta_{FS}}{\left| \sqrt{1 - \frac{(\cos \alpha_S - \mu)^2}{\mu^2 - 2 \cos \alpha_S + 1}} \right|} \quad .$$

Case D: min $d_{FS}(t)$ at the segment ${}_2d_{FS}(t)$ but when $t = \gamma_S/v_F$, i.e., when leading aircraft is landing.

From equation (3) and for

$${}_2d_{FS}(t)\Big|_{t=\gamma_S/v_F} = \delta_{FS}$$

it follows that

$${}_{FS5}A \; {}_{FS5}d_{05}^2 + {}_{FS5}B \; {}_{FS5}\hat{d}_{05} + {}_{FS5}C = 0$$

where

$${}_{FS5}A = 1$$

$${}_{FS5}B = 2 \gamma_S (\cos \alpha_S - \mu)$$

$${}_{FS5}C = \gamma_S^2 (\mu^2 - 2 \mu \cos \alpha_S + 1) - \delta_{FS}^2 \quad .$$

The necessary initial separation for Case D is therefore,

$$\hat{d}_{FS05} = \frac{- {}_{FS5}B + \sqrt{{}_{FS5}B^2 - 4 \; {}_{FS5}C}}{2} \quad .$$

The above solutions to cases A, B, C, and D illustrate how to compute

$\hat{d}_{FS01}$, $\hat{d}_{FS02}$, $\hat{d}_{FS04}$ and $\hat{d}_{FS05}$. The question now is which of these four values represents $\hat{d}_{FSo}$.

The rule governing this choice will be as follows:

$$\hat{d}_{FSo} = \min_{k} \hat{d}_{FSok} ,$$

such that

$$d_{FS}(t) \geq \delta_{FS} \quad \text{for all} \quad t \quad \text{and}$$

$$d_{FS}(t)\Big|_{t={}_{FS}t^{k*}} = \delta_{FS} .$$

Algorithm for $\hat{d}_{FSo}$ is given in Appendix A.1 . Subroutine SDOFS which computes $\hat{d}_{FSo}$ is given in Appendix B.2.

2.5.3. The case of slow aircraft followed by fast aircraft

This case is shown in Figs. 20a and 20b, and corresponding distance equations are given in Section 2.4.3. From the distance equations it can be seen that the first two segments of $d_{SF}(t)$, ${}_1d_{SF}(t)$ and ${}_2d_{SF}(t)$ are positive square roots of a parabola and that the third segment, ${}_3d_{SF}(t)$, is an increasing linear function of t .

As noted in Section 2.4.3, this SF (slow followed by fast) sequence consists of cases a and b ; they will be treated here separately.

Case a: $\hat{d}_{SFo} < \beta$ (See Fig. 20a and Fig. 24a.)

From equation (6) and for

$$\frac{\partial_2 d^2{}_{SF}(t)}{\partial t} = 0 ;$$

the time of minimum separation on second segment, ${}_{SF}t_2^*$, is found to be

$$ {}_{SF}t_2^* = \frac{{}_{SF}\hat{d}_o\,(1 - \mu\cos\alpha_S)}{(\mu^2 - 2\mu\cos\alpha_S + 1)v_F} \quad . $$

It can be seen that ${}_{SF}t_2^* > 0$; the second segment of $d_{SF}(t)$ is therefore a decreasing function of t over its entire range (see Fig. 24a).

On the other hand, the third segment of $d_{SF}(t)$ is a decreasing linear function of t . It can also be shown that the slope of ${}_2d_{SF}(t)$ when $t = 0$ ($t = 0$ being the limit between ${}_2d_{SF}(t)$ and ${}_3d_{SF}(t)$) is steeper than the slope of ${}_3d_{SF}(t)$.

The above characteristics of the function $d_{SF}(t)$ can then be said to support the following conclusion: the shape of function $d_{SF}(t)$ could correspond to one of the alternatives shown in Fig. 24a.

The following table lists all of the possible shapes of function $d_{SF}(t)$, see also Fig. 24a.

${}_1d_{SF}(t)$	${}_2d_{SF}(t)$	min $d_{SF}(t)$ at point
a	d	A
b	d	D
c	d	D

Using, then, the argument developed in Section 2.5.2, the solutions for initial separations are derived for the cases when min $d_{SF}(t)$ occurs at points A or D (Fig. 24a).

Case A: min $d_{SF}(t)$ at segment $_1d_{SF}(t)$, i.e., for $t < \frac{{}_{SF}d_o - \beta}{v_F}$

From equation (5) and for

$$\frac{\partial_1 d_{SF}^2(t)}{\partial t} = 0 \quad .$$

The time when the minimum separation appears, $_{SF}t_1^*$, is then found to be

$${}_{SF}t_1^* = - \frac{{}_{SF}\hat{d}_o[\mu\cos(\alpha_S - \alpha_F) - 1] + \beta[(1 - \cos\alpha_F) - \mu(\cos(\alpha_S - \alpha_F) - \cos\alpha_S)]}{\{\mu^2 - 2\mu\cos(\alpha_S - \alpha_F) + 1\}v_F}$$

Further, from condition

$$ {}_1d_{SF}(t)\Big|_{t={}_{SF}t_1^*} = \delta_{SF}$$

and from equation (5), the following is found

$${}_{SF1}A \; {}_{SF}\hat{d}_{01}^2 + {}_{SF1}B \; {}_{SF}\hat{d}_{01} + {}_{SF1}C = 0$$

where

$${}_{SF1}A = 1 - \frac{[\mu\cos(\alpha_S - \alpha_F) - 1]^2}{\mu^2 - 2\mu\cos(\alpha_S - \alpha_F) + 1}$$

$${}_{SF1}B = -2\beta\{(1-\cos\alpha_F) + \frac{[\mu\cos(\alpha_S-\alpha_F)-1][(1-\cos\alpha_F)-\mu(\cos(\alpha_S-\alpha_F)-\cos\alpha_S)]}{\mu^2 - 2\mu\cos(\alpha_S - \alpha_F) + 1}\}$$

$$_{SF1}C = \beta^2\{2(1-\cos\alpha_F) - \frac{(1 - \cos\alpha_F) - \mu(\cos(\alpha_S-\alpha_F) - \cos\alpha_S)^2}{\mu^2 - 2\,\mu\,\cos(\alpha_S - \alpha_F) + 1}\}\ \delta^2_{SF} .$$

The necessary initial separation for Case A is therefore,

$$\hat{}_{SF}d_{01} = \frac{-\ _{SF1}B + \sqrt{_{SF1}B^2 - 4\ _{SF1}A\ _{SF1}C}}{2\ _{SF1}A} .$$

Case D: min $d_{SF}(t)$ at the upper limit of the range of segment $_3d_{SF}(t)$, i.e., for $t = t_5 = \frac{\gamma_S}{\mu v_F}$ (the time when leading aircraft is landing)

From equation (7) and for

$$t = t_5 = {}_{SF}t^*_3 = \frac{\gamma_S}{\mu v_F}$$

and using the condition

$$_3d_{SF}(t)\Big|_{t=t_5={}_{SF}t^*_3} = \delta_{SF}$$

it follows that the necessary initial separation for case D is:

$$\hat{}_{SF}d_{03} = \hat{}_{SF}d_{05} = \delta + (1 - \mu)\frac{\gamma_S}{\mu} .$$

Case b. $_{SF}\hat{d}_o > \beta$ (See Fig. 20b and Fig. 24b, c, and d.)

The only general conclusion about function $d_{SF}(t)$ is that in case b the third segment, $_3d_{SF}(t)$, is a decreasing linear function of t.

The possible alternatives for the shape of $d_{SF}(t)$ and the locations of the min $d_{SF}(t)$ are shown in Figs. 24b, c and d; these alternatives are presented in the following table.

$_1d_{SF}(t)$	$_2d_{SF}(t)$	$_3d_{SF}(t)$	min $d_{SF}(t)$ at point	Fig.
a	e	f or g	A	24b
b	e	g	D	"
c	e	g	D	"
c	e	f	C	"
d	e	f	C	"
d	e	g	D	"
a	h	g	A	24c
b	h	g	D	"
d	h	g	D	"
a	i	f	A	24d
a	i	g	D	"
d	i	f	B	"
d	i	g	D	"

Comparing equations (5) and (7) or (8) and (10) it can be seen that they are identical, but the ranges of functions are different. However, the initial separations found for the cases when min $d_{SF}(t)$

occurs at points A or D are the same, for both the a and b cases. Therefore, only the initial separations for the situations when $\min d_{SF}(t)$ occurs at points B or C have to be found.

Case B: $\min d_{SF}(t)$ at the limit of segments ${}_1d_{SF}(t)$ and ${}_2d_{SF}(t)$, i.e., when $t = 0$

From equations (8) and (9) and for

$$ {}_1d_{SF}(t)\Big|_{t=0} = {}_2d_{SF}(t)\Big|_{t=0} = \delta_{SF} $$

the following is found

$$ {}_{SF}{}_4{}^A \; {}_{SF}\hat{d}_{04}^2 + {}_{SF}{}_4{}^B \; {}_{SF}d_{04} + {}_{SF}{}_4{}^C = 0 , $$

where

$$ {}_{SF}{}_4{}^A = 1 $$

$$ {}_{SF}{}_4{}^B = -2\beta(1 - \cos\alpha_F) $$

$$ {}_{SF}{}_4{}^C = 2\beta^2(1 - \cos\alpha_F) - \delta_{SF}^2 . $$

The necessary initial separation for case B is therefore,

$$ {}_{SF}\hat{d}_{04} = \frac{- {}_{SF}{}_4{}^B + \sqrt{{}_{SF}{}_4{}^{B^2} - 4 \; {}_{SF}{}_4{}^C}}{2} . $$

Case C: min $d_{SF}(t)$ at segment $_2d_{SF}(t)$, i.e., when $0 < t < \frac{\hat{SFd}_o - \beta}{v_F}$

From equation (9) and for

$$\frac{\partial_2 d^2_{SF}(t)}{\partial t} = 0$$

the time when minimum separation appears, $_{SF}t^*_2$, can be found, as follows

$$_{SF}t^*_2 = \frac{\hat{SFd}_o(1 - \mu\cos\alpha_F) - \beta(1 - \cos\alpha_F)(1 + \mu)}{(\mu^2 - 2\mu\cos\alpha_F + 1)\, v_F} .$$

Therefore from equation (9) and for

$$_2d_{SF}(t)\Big|_{t=_{SF}t^*_2} = \delta_{SF}$$

the following is found

$$_{SF2}A\ \hat{_{SF}d^2_{02}} + {_{SF2}B}\ \hat{_{SF}d_{02}} + {_{SF2}C} = 0 ,$$

where

$$_{SF2}A = 1 - \frac{(1 - \mu\cos\alpha_F)^2}{\mu^2 - 2\mu\cos\alpha_F + 1}$$

$$_{SF2}B = -2\beta\{(1 - \cos\alpha_F) - \frac{(1 - \mu\cos\alpha_F)(1 - \cos\alpha_F)(1 + \mu)}{\mu^2 - 2\mu\cos\alpha_F + 1}\}$$

$$SF2^C = \beta^2\{2(1 - \cos\alpha_F) - \frac{(1 - \cos\alpha_F)^2(1 + \mu)^2}{\mu^2 - 2\mu\cos\alpha_F + 1}\} - \delta_{SF}^2 \quad .$$

The necessary initial separation for case C is therefore,

$$\hat{SF}d_{02} = \frac{-SF2^B + \sqrt{SF2^{B^2} - 4\,SF2^A\,SF2^C}}{2\,SF2^A} \quad .$$

The above solutions to cases A , B , C , and D illustrate how to compute $\hat{SF}d_{01}$, $\hat{SF}d_{02}$, $\hat{SF}d_{04}$ and $\hat{SF}d_{05}$. The question now is which of these four values represents $\hat{SF}d_o$.

The rule governing this choice will be as follows.

$$\hat{SF}d_o = \min_k \hat{SF}d_{ok} \quad ,$$

such that

$$d_{SF}(t) \geq \delta_{SF} \quad \text{for all } t$$

and

$$d_{SF}(t)\Big|_{t=SFt^{k*}} = \delta_{SF} \quad .$$

The algorithm to find $\hat{SF}d_o$ is shown in a flowchart in Appendix A.2. Subroutine SDOSF which computes $\hat{SF}d_o$ is given in Appendix B.2.

2.6. Equations for Interarrival Time at Threshold

When all initial separations for the four sequences (FF, SS, FS and SF) are found, the threshold interarrival times for the same sequences should be computed.

Using the expression for t_{ij} given in section 2.3,

$$t_{ij} = \frac{\gamma_{ij} + {}_{ij}\hat{d}_o}{v_j} - \frac{\gamma_{ij}}{v_i} ,$$

and the definition of γ_{ij} from Section 2.1,

$$\gamma_{ij} = \min(\gamma_i, \gamma_j) ,$$

The interarrival times at the threshold for the four above sequences will be

$$t_{FF} = \frac{{}_{FF}\hat{d}_o}{v_F}$$

$$t_{SS} = \frac{{}_{SS}\hat{d}_o}{v_S}$$

$$t_{FS} = \frac{\gamma_S + {}_{FS}\hat{d}_o}{v_S} - \frac{\gamma_S}{v_F}$$

$$t_{SF} = \frac{\gamma_S + {}_{SF}\hat{d}_o}{v_F} - \frac{\gamma_S}{v_S} .$$

Subroutine SDOT given in Appendix B.2 computes the values of interarrival times.

In the case when there are more than two aircraft types in a population, the matrix of the interarrival times should be computed in such a way that the aircraft population is considered pair by pair; each pair always consists of a fast and a slow aircraft.

2.7. Model for Arrival Runway Capacity When Aircraft Mix Consists of Two Aircraft Types

As noted in Section 2.5, it was decided to compute capacity for the discrete values of angles α_i . The model will then consist of the following steps:

1. Generate angles α_S and α_F ;
2. Compute initial separation ${}_{FF}\hat{d}_o$, ${}_{SS}\hat{d}_o$, ${}_{SF}\hat{d}_o$ and ${}_{FS}\hat{d}_o$;
3. Compute interarrival times at threshold t_{FF} , t_{SS} , t_{SF} and t_{FS} ;
4. Compute mean interarrival times $\bar{t}$;

$$\bar{t} = \Sigma t_{ij} p_i p_j = t_{FF} p_F p_F + t_{SF} p_S p_F + t_{FS} p_F p_S + t_{SS} p_S p_S \ .$$

5. Compute landing capacity ,

$$\lambda = \frac{1}{\bar{t}} \ ;$$

6. Go to 1.

The restrictions for model input parameters as well as the ranges for variables α_S and α_F are given in Fig. 25.

Program computing capacity for the case of only two aircraft types, CAPSF, is given in Appendix B.3.

For the following input:

-- aircraft approach velocities: v_F and v_S

-- necessary straight approach lengths: γ_F and γ_S

-- proportion of aircraft types in the mix: p_F and p_S

-- matrix of horizontal separation rules: $\delta_{ij} = \{\delta_{FF}, \delta_{FS}, \delta_{SF}, \delta_{SS}\}$,

the following output is obtained:

-- matrix of capacities $\lambda(\alpha_S,\alpha_F)$

-- matrices of initial separations $_{SF}\hat{d}_o(\alpha_S,\alpha_F)$

$_{FS}\hat{d}_o(\alpha_S,\alpha_F)$

$_{FF}\hat{d}_o(\alpha_S,\alpha_F)$

$_{SS}\hat{d}_o(\alpha_S,\alpha_F)$

-- matrices of indices showing the shape of function $d_{ij}(t)$ and location of minimum separation (see Appendix A)

$INDXSF(\alpha_S,\alpha_F)$

$INDXFS(\alpha_S,\alpha_F)$

$INDXFF(\alpha_S,\alpha_F)$

$INDXSS(\alpha_S,\alpha_F)$.

An example of this output is given in Appendix C.1.

2.8. Model for Arrival Runway Capacity When Aircraft Mix Consists of Three or Four Aircraft Types

A procedure similar to that discussed in Section 2.7 is used to compute capacity for these two cases, a difference being that instead of preserving the values of capacity for all combinations of angles generated, the highest N values for capacity are stored during the computation and then printed, together with the values of the angles which provide those N maximum capacities. For the purpose of comparison the lowest N values are preserved and printed as well.

The procedure to determine N maximum and N minimum capacities for the case of three aircraft consists of the following steps.*

*Note that the case when a population consists of four aircraft types is not illustrated, since this case is essentially similar to that following three aircraft.

1. Generate angles α_1 , α_2 and α_3 .
2. Group the aircraft types in couples, i.e.,

   1 and 2

   1 and 3

   2 and 3 ,

   and treat each of these couples as a pair of slow and fast, S and F .
3. For each of the couples compute initial separations, thus obtaining a matrix of initial separations,

$$_{ij}\hat{d}_o \ .$$

4. From the matrix of initial separation, $_{ij}\hat{d}_o$, compute the matrix of threshold interarrival times, t_{ij} .
5. Compute mean interarrival time,

$$\bar{t} = \Sigma \ t_{ij} \ p_i \ p_j \ .$$

6. Compute landing capacity,

$$\lambda = \frac{1}{\bar{t}} \ .$$

7. If the capacity found belongs to the set of N highest or N lowest capacity values, store it along with the corresponding angles. If the capacity does not belong to either of these sets, storage is unnecessary.
8. Go to 1.

The restrictions for model input parameters and the ranges of

variables α_i are given in Figs. 26 and 27, for the populations of three and four aircraft types.

Programs computing capacities for the two populations, CAP3 and CAP4 , are given in Appendices B.4 and B.5.

For the following input,

-- aircraft velocities v_i for i = 1, 2, 3 or i = 1, 2, 3, 4

-- necessary straight approach lengths γ_i " "

-- proportion of aircraft types in the mix p_i " "

-- matrix of horizontal separation rules d_{ij} for i = 1, 2, 3 or i = 1, 2, 3, 4 and j = 1, 2, 3 or j = 1, 2, 3, 4,

the following output is obtained:

- N maximum values of capacity λ and corresponding angles α_i for i = 1, 2, 3, or i = 1, 2, 3, 4
- N minimum values of capacity λ and corresponding angles α_i for i = 1, 2, 3 or i = 1, 2, 3, 4.

An example of output from program CAP4 is given in Appendix C.3. Value N is arbitrarily set at 40.

3. Application of Capacity Models with Horizontal Separation Only

3.1. Input Data

Data for inputs into the models were obtained from: several references given in the reference list[2,3,4], particularly those concerned with approach speeds and the minimum length of straight final approach; consultation with airlines and aircraft manufacturers; and approach speed studies at the TRACON facility at the Oakland International Airport.

A review of these three data sources indicated that the following tabled inputs will usefully demonstrate the application of the proposed models.

Aircraft Classification

Aircraft Type i	Description	Approach Velocity v_i (kts)
1	Propeller Driven 1	100
2	Propeller Driven 2	120
3	Nonheavy Jet	140
4	Heavy Jet	150

Minimum Length of Straight Final Approach (γ)

Aircraft Type i	γ_i (nm)
1	2
2	2
3	4
4	4

Minimum horizontal separation rules for aircraft i followed by aircraft j

a. δ_{ij} = 5 nm when the leading aircraft is aircraft type 4 (i = 4) and trailing aircraft is either type 1, 2, or 3 (j = 1, 2, 3)

δ_{ij} = 4 nm when the leading aircraft is aircraft type 4 (i = 4) and trailing aircraft is aircraft type 4 (j = 4)

δ_{ij} = 3 nm when the leading aircraft is either aircraft type 1, 2, or 3 (i = 1, 2, 3)

b. δ_{ij} = 3 nm for all aircraft types

c. δ_{ij} = 2 nm for all aircraft types

Aircraft Mix

Aircraft Type i	percentage of aircraft type i in mix						
	a	b	c	d	e	f	g
1					30	20	10
2					30	20	10
3	80	60	40	20	20	40	60
4	20	40	60	80	20	20	20

Using ILS, all aircraft have to pass through a common entry gate; therefore, the length of approach along the extended runway centerline is the same for all aircraft types; that is, $\gamma_i = \gamma = 6$ nm (6 nm is assumed to be the average distance from the entry gate to the runway threshold).

Using MLS, each aircraft of type i enters the extended runway centerline at its own entry gate, E_i, at distance γ_i from the runway threshold (see the table on the previous page).

For both ILS and MLS, the angles of entry to the common approach

path are optimized to provide maximum capacities. These capacities are then compared.

As stated in Chapter 1, this comparison is made assuming that both systems are free of errors: aircraft precisely maintain assigned flight paths and arrive at points in space precisely when they are expected to be there.

3.2. Analysis of Results

The first case involves aircraft mixes that contain only two aircraft types (mixes a, b, c and d), namely, heavy and nonheavy jet airplanes. The results are shown in Fig. 28, and the output tables for Points A and B are given in Appendices C.1 and C.2.

The curves in Fig. 28 correspond to the optimum values of the angles of intersection of the entry path with the final approach path, α_F and α_S. For point A, $\alpha_S = 10^o$ and $\alpha_F = -10^o$ (see table CAPSF, Appendix C.2). The analysis also shows that α_S and α_F can vary considerably and yet provide about the same capacity as long as the geometry of the flight paths is similar.

There are several points that can be made about the angles α_S and α_F which are important when landing capacity is considered (see Fig. 29). One is the value of the relative angle α_R (the angle between the two paths before they enter the extended runway centerline).

$$\alpha_R = |\alpha_S - \alpha_F| .$$

This relative angle is important when the two aircraft have a common entry gate, as in ILS (Fig. 29c and d) or when they have different entry gates, as in MLS (Fig. 29a and b). The optimum range of α_R

depends on the ratio of approach speeds of two aircraft, $\mu = \frac{v_S}{v_F}$. The greater is μ the smaller is α_R. From table CAPSF, in Appendix C.2, it can be seen that when v_S = 140 kts and when v_F = 150 kts, i.e., for a high value of μ, the optimum range for α_R is 10-40°.

Another point about path configuration is how well centered α_R is relative to the extended centerline of the runway. The configurations in which the approach paths are more or less symmetrical relative to the extended runway centerline, as shown in Figs. 29a and 29c, result in larger capacities than those when α_R is not symmetrical with the extended runway centerline (Figs. 29b and d). This point can be seen in the CAPSF table, Appendix C.2. (The optimal range of angles for α_S and α_F is circled in that table.)

Returning to Fig. 28, it can be seen that there is no essential difference in landing capacity between MLS and ILS when the mix consists of aircraft types with similar approach speeds. There is a slight increase in capacity as the proportion of faster aircraft in the mix is increased, when the minimum separation rules for all aircraft types are δ = 2 nm and δ = 3 nm. This slight increase is to be expected because the average speed of the stream of aircraft increases. When, however, the current δ = 3, 4, 5 nm, separation rules are applied; the capacity decreases as the proportion of fast aircraft increases. This decrease occurs for the following reasons: because the fast aircraft are also the heaviest, therefore, when a heavy aircraft is followed by a light one the pair must be minimally separated a distance of 5 nm; the minimum separation must be 4 nm when a heavy aircraft is followed by another heavy aircraft. In short, the average spacing between approaching aircraft increases when the minimum separation rule

δ = 3, 4, 5 nm is applied, and this has more influence on the capacity than the mentioned increase of average speed of the aircraft stream.

Fig. 30 shows the importance of optimizing entry angles. (The CAPSF tables in Appendices C.1 and C.2 should be consulted for a more detailed treatment of this subject.) Note that the figure's curves were plotted not only for the optimal angles of $\pm 10^{o}$ (see also Fig. 28 but also for values of α_S and α_F of $\pm 40^{o}$, $\pm 60^{o}$, and $\pm 80^{o}$. Decreases in landing capacity of 4%, 11% and 21% were found relative to the optimal configuration. Similar results could be shown for cases when the minimum separation rules are δ = 2 nm or δ = 3, 4, or 5 nm. This implies (compare Fig. 28 and Fig. 30) that under the assumptions of the model and for the aircraft types considered, runway landing capacity is more sensitive to changes in entry angles than to other parameters, such as, for example, the proportion of fast and slow aircraft, or the length of the common approach along the extended runway centerline. As shown in Fig. 28, shortening of the common approach length from 6 nm to 4 nm does not result in any significant increase of landing capacity even for the optimal angles of entry, because the difference in approach speed of the two aircraft is relatively small.

A second case which demonstrates the application of the model involves four aircraft types in a mix (mixes e, f and g from Section 3.1). The results are shown in Fig. 31. (Example output for point C in Fig. 31 is given in Appendix C.3.) From this figure it can be seen that the use of MLS increases landing capacity, and for the given example the increase is about 6-10% when minimum horizontal separation is δ = 3, 4, 5 nm, 7-11% when δ = 3 nm, and 10-16% when δ = 2 nm.

Note that the increase of capacity is greater when the aircraft

mix consists of approximately half fast and half slow aircraft (e.g., $p_1 = p_2 = .3$, $p_3 = p_4 = .2$) than in the case when one type of aircraft prevails (e.g., $p_1 = p_2 = .1$, $p_3 = .6$, $p_4 = .2$ which is a mix with 80% of fast aircraft). This point agrees with the conclusion made earlier in this section that the increase of capacity obtainable with MLS is rather small when a population consists of aircraft types with similar approach speeds. This point also agrees with the discussion of expected capacity increase given in Section 2.1.

The capacity increase obtained in the second case (four aircraft types) is significantly greater than that obtained in the first (two aircraft types), for two reasons: first, the differences between the velocities of the aircraft types are much greater in the second case than in the first; second, the decrease of the common path length is greater in the second case (on the average), and particularly because the slow aircraft types enter the entended runway centerline only 2 nm from the runway threshold.

As the model computes capacity for discrete values of angles α_i , it should be noted again (as in the case when there are two aircraft types in the mix) that, for all practical purposes, a group of solutions (rather than a single solution) ensure maximum capacity. This can be seen from the output example for CAP4, Appendix C.3.

Some of the solutions are presented graphically in Fig. 32; all result in about the same capacity. Differences between solutions are the result of: slight changes in some of the entry angles; an interchange of the given trajectories for two similar aircraft types; or a combination of both. It should, however, also be noted that the flight path configurations shown on Fig. 32 are not radically different.

If entry angles radically different from those shown on Fig. 32 are used, the capacity could be reduced by as much as 20% (see the Minimum Capacity table in Appendix C.3).

Some additional examples indicate that further decrease of the length of common straight approach (e.g., γ_1 = 1 nm, γ_2 = 2 nm, γ_3 = 3 nm and γ_4 = 4 nm) will not bring any significant increase in runway landing capacity (see Fig. 31).

4. Analysis of Capacity Models with Horizontal and Vertical Separation

4.1. Introduction

Chapters 2 and 3 have considered a landing capacity model which is governed by the assumption that in accordance with current ATC rules only horizontal separation between aircraft is allowed during approach.

In this (and the next) chapter, runway landing capacity will be analyzed. It will be here assumed that horizontal and vertical separation between aircraft approaching a runway is possible. Landing capacity will be computed using, for each particular aircraft pair, the more efficient of the two possible aircraft separations.

Some preparatory remarks should be made before proceeding. First, no two-segment approach paths will be considered. Second, as the feasible angles of descent under IFR conditions vary from 2.5^{o} to $8\text{-}10^{o}$, this span of about 7^{o} does not allow for more than two "useful" paths in the vertical plane, useful referring to those paths which provide vertical separations that are more suitable from a capacity point of view than the corresponding horizontal ones; consequently, there is no point in dividing all aircraft types into more than two categories, these categories being determined by the descent angle capabilities of the aircraft type.

These two categories will be: (1) aircraft capable of performing steep descent (STOL aircraft) and (2) the remaining aircraft population (CTOL aircraft). Second category aircraft are assumed to be in the same horizontal plane and are separated by horizontal separation rules. If a vertical separation of only 1000 ft (305 m) were applied (for descent angles of 2.5^{o} or 3^{o}) the resulting horizontal spacings are either greater than the prescribed minimum given by the horizontal

separation rules or are infeasible because of wake vortex separations. The argument in chapters 2 and 3 will apply to the situation when both groups of aircraft appear in the mix. Vertical separation will be examined only for the cases when at least one of the two consecutive landings is performed by an aircraft with steep descent capability.

4.2. Vertical Separation

If a pair of aircraft land one after the other and one of them is capable of performing steep descent, it is assumed that two distinct approach paths in the vertical plane are followed. (This situation is presented in Fig. 33.) These paths are denoted as higher approach, H , and lower approach, L . Similar notations will be used for all aircraft utilizing these paths. It is assumed further than the aircraft using the higher path will have lower approach speeds than those using the lower path, i.e.,

$$v_H < v_L \quad .$$

This assumption implies that if only horizontal separation is employed, the aircraft pair landing sequence low followed by high (LH) will be critical from a capacity point of view because it actually represents the fast followed by slow aircraft sequence (FS). This sequence is shown in Fig. 34 at the moment when the landing aircraft, L , crosses the threshold. If the vertical separation, χ , between the two aircraft produces $_H\ell_\chi$, the horizontal spacing between the two aircraft at that moment--which is less than the spacing required under ATC horizontal separation rules, some gains in capacity can be expected. However, to assure that a vertical separation between the two aircraft of

at least χ is continually preserved before the leading aircraft, L, lands, the following condition has to be satisfied:

$$v_H \sin \theta_H \geq v_L \sin \theta_L ,$$

i.e., the vertical component of the speed of aircraft H has to be equal to or higher than that of aircraft L . If this condition is satisfied, the vertical gap between the two aircraft continually closes during approach until it reaches χ , the minimum required vertical separation, when the leading aircraft lands.

This condition can also be:

$$v_H \geq \frac{v_L \sin \theta_L}{\sin \theta_H} .$$

This variation of the condition suggests, since angles θ_L and θ_H are small, that if the angle θ_H is three times as big as angle θ_L , then v_H has to be greater than one third of v_L . This is an approximation, but it shows that when θ_H is large enough the condition is always satisfied.

An exact solution for the minimum speed of an aircraft on the upper approach path, when $v_L = 150$ kts, $\theta_L = 3^o$ and $\theta_H = 7.5^o$, is that $v_H \geq 60$ kts. This condition will be satisfied because the aircraft capable of steep descent have expected minimum approach speeds of 70 to 80 kts.

When the necessary vertical separation condition is satisfied the separation between the two aircraft in sequence LH , at the moment when leading aircraft lands, will be

$$ {}_{H}^{\ell}\chi = \frac{\chi}{\tan \theta_H} . $$

When $\theta_H = 7.5^o$, ${}_{H}^{\ell}\chi$ has the following values.

χ (ft)	χ (m)	${}_{H}^{\ell}\chi$ (nm)
1000	305	1.25
1500	457	1.87
2000	610	2.50

The table indicates that vertical separation causes some capacity improvement, since the horizontal spacings of vertically separated aircraft are shorter than the minimum required horizontal separations, except when $\delta_{ij} = 2$ nm and $\chi = 2000$ ft (610 m).

The sequence under consideration has been LH , an aircraft on a lower path followed by an aircraft on a higher one. However, there are three other possible same pair sequences: HH , HL , and LL .

Sequence HH will require a vertical separation χ when the leading aircraft lands, at which moment (see Fig. 34) the horizontal spacing will be ${}_{H}^{\ell}\chi$.

For sequence HL , horizontal separation will be such that when the leading aircraft, H , lands, the trailing aircraft, which has, as noted, a higher approach speed, will be distance δ from the threshold.

Sequence LL requires horizontal separation only. The model described in Chapter 2 will be used to compute threshold interarrival time as it relates to horizontal separation.

The requirements for each of the above four approach sequences suggest that the threshold interarrival times for a pair of aircraft using different descent paths are

$$t_{LH} = t_{HH} = \frac{H^{\ell}X}{v_H} \quad ,$$

$$t_{HL} = \frac{\delta}{v_L} \quad .$$

t_{LL} = to be found using the model for horizontal separation only.

The next section will describe how these interarrival times can be combined and runway landing capacity will be computed.

4.3. Model for Arrival Runway Capacity

The following description of this simple model will consider four differing aircraft types using the same runway. The types are denoted as 1, 2, 3 and 4; speeds ascend from type 1, the slowest, to type 4, the fastest. Only type 1 aircraft are capable of performing steep descent, i.e., they are type H ; all other types are type L (see Section 4.2.). The following model parameters are

v_i	=	aircraft approach speed	$i = 1, 2, 3, 4,$
γ_i	=	min straight final approach lengths	$i = 1, 2, 3, 4$
p_i	=	proportion of aircraft type,	$i = 1, 2, 3, 4$
δ_{ij}	=	min horizontal separation matrix	$i = 1, 2, 3, 4; j = 1,2,3,4$

θ_i = angle of descent $\qquad \theta_1 > \theta_2 = \theta_3 = \theta_4$

χ = minimum vertical separation.

To find runway capacity when aircraft type 1 use a steeper angle of descent than the other types, and when vertical separation between aircraft type 1 and the others is applied, the following steps should be made.

1. Check whether the necessary condition for vertical separation (given in Section 4.2) is satisfied, i.e.,

$$v_H \geq \frac{v_L \sin \theta_L}{\sin \theta_H} ,$$

in this case it should read:

$$v_1 \geq \frac{v_4 \sin \theta_4}{\sin \theta_1} ,$$

and $v_4 \geq v_3 \geq v_2$ and $\theta_2 = \theta_3 = \theta_4$.

If the condition is satisfied vertical separation can be applied.

2. Form the matrix of interarrival times, as follows.

		Trailing aircraft			
		1	2	3	4
Leading aircraft	1	$t_{1,1}$	$t_{1,2}$	$t_{1,3}$	$t_{1,4}$
	2	$t_{2,1}$		$t_{L,L}$	
	3	$t_{3,1}$			
	4	$t_{4,1}$			

$$t_{1,1} = t_{2,1} = t_{3,1} = t_{4,1} = t_{HH} = \frac{H^{\ell}\chi}{v_H} = \frac{\chi}{v_H \tan \theta_H} = \frac{\chi}{v_1 \tan \theta_1}$$

$$t_{1,2} = \frac{\delta_{1,2}}{v_2}$$

$$t_{1,3} = \frac{\delta_{1,3}}{v_3}$$

$$t_{1,4} = \frac{\delta_{1,4}}{v_4}$$

t_{LL} is computed as the mean interarrival time when the population consists of three aircraft types; computation involves use of a model which assumes horizontal separation only (Program CAP3). All the input values of this model are the same as detailed earlier in this section, except that the proportion of aircraft in the mix is modified in such a way that $\sum_{i=2,3,4} p_i' = 1$, where p_i' are new proportions and the relation between p_2', p_3', and p_4' is the same as it was between p_2, p_3 and p_4, namely,

$$p_i' = \frac{p_i}{\sum_{i=2,3,4} p_i} .$$

It should be noted that when obtaining t_{LL} the optimal horizontal path geometry for aircraft types 2, 3 and 4 will be found.

3. Find the mean threshold interarrival time, $\bar{t}$.

$$\bar{t} = \sum_{\substack{i=1 \\ j=1,4}} t_{ij}p_{ij} + \sum_{\substack{i=2,4 \\ j=1}} t_{ij}p_{ij} + t_{LL} \sum_{\substack{i=2,4 \\ j=2,4}} p_{ij}$$

4. Compute runway landing capacity, which is

$$\lambda = \frac{1}{\bar{t}} .$$

5. Application of Capacity Model with Horizontal and Vertical Separation

5.1. Input Data

The second of the two examples given in Chapter 3 will be here modified so that the influence of vertical separation on capacity can be determined.

The example's classification of aircraft types is the same as that given in Section 3.1, page 55, excepting that type 1 aircraft are considered capable of performing steep descent. A corresponding set of descending angles are assumed as follows.

A/C type i	Angle of descent θ_i
1	7.5^o
2	3^o
3	3^o
4	3^o

Another exception is that if type 1 aircraft perform a descent where $\theta_1 = 7.5^o$ they will have lower approach speeds, so that $v_1 =$ 80 kts when vertical separation is applied. Speeds for aircraft types 2, 3, and 4 are the same as those listed in Section 3.1, page 55.

The remaining inputs for the capacity model with horizontal and vertical separation are as follows.

-- Minimum lengths of straight final approach for all four aircraft types are the same as those given in Section 3.1, page 55.

-- Minimum horizontal separation rules are as given in Section 3.1, page 56.

-- Minimum vertical separation rules are assumed to be the same as given in Section 4.2: χ = 1000, 1500 and 2000 ft (305, 457 and 610 m).

-- Aircraft mixes used in this example are the mixes e , f and g given in Section 3.1, page 56.

In summary, modification of the selected example involves the following assumptions: an aircraft type 1 performs descent at a 7.5^{o} angle with an approach speed of 80 kts; type 1 aircraft are separated vertically; type 1 aircraft are also separated from other aircraft types by vertical separation; a vertical separation between any two aircraft types can be either 1000, 1500 or 2000 ft. Aircraft types 2, 3 and 4 are separated horizontally.

Using the model described in Section 4.3, the results plotted in Figs. 35, 36 and 37 were obtained. Note that in these figures, plots for only horizontal separation are actually those given earlier in Fig. 31.

5.2. Analysis of Results

In Section 4.2, it was noted that for a steep angle of descent, $\theta_H = 7.5^{o}$; minimum vertical separations of χ are 1000, 1500 and 2000 ft (305, 457 and 610 m); horizontal spacings between two aircraft are 1.25, 1.87 and 2.50 nm, respectively, at that moment when the leading aircraft lands and trailing aircraft is on a steep descent path. These spacings are much shorter than the horizontal spacings between two aircraft at the moment when the leading aircraft lands if current ATC horizontal separation rules are applied. Consequently, significant improvements in landing capacity should be expected. An exception is

the case when required horizontal separation is only two nautical miles and vertical separation is either 1500 or 2000 ft; this exception applies particularly when vertical separation of 2000 ft is required and when $\theta_H = 7.5^o$; the resulting horizontal spacing, $_H\ell_\chi$, equals 2.5 nm; this horizontal spacing is larger than that required by minimum horizontal separation rules; therefore, the use of vertical separation in this case would decrease rather than increase capacity. The greatest improvement should be expected in the case when minimal horizontal separations are in their high range, e.g., 3, 4, 5 nm separation.

Figs. 35, 36, and 37 shows runway landing capacities for ILS and MLS procedures, the latter involving the use of: only horizontal separation, and horizontal and vertical separation. Input values for these capacities are those listed in the previous section

The single difference in the capacities shown in Figs. 35, 36, and 37 is a result of differing minimum horizontal separation rules.

The minimum horizontal separation rules used in computation of the capacities shown in Fig. 35 require that δ = 3, 4, or 5 nm. As this figure indicates, MLS procedures can produce a capacity increase of as much as 40 to 50% when compared under the same aircraft mix conditions with ILS procedures.

Fig. 36 shows the capacities obtained when the horizontal separation rules require that δ = 3 nm. The increase in capacity when MLS rather than ILS procedures are used can be as much as 30 to 40%.

The capacities shown in Figs. 35 and 36 indicate that when any of the three vertical separations (χ = 1000, 1500, or 2000 ft) are applied higher capacity increases, compared with capacities obtainable when MLS procedures with only horizontal separations are applied, are

obtained. However, when the horizontal separation rules are from a capacity point of view improved, i.e., minimum horizontal separations are shorter, the additional gain in capacity, if any, is, as noted, smaller, see for example Fig. 37. This figure shows that a vertical separation of 1500 ft produces about the same result as a horizontal separation of 2 nm, i.e., the increase in capacity obtainable in both MLS cases (with and without vertical separation) is about 15%, when compared with the capacity obtainable with ILS. The figure also shows that a vertical separation of 1000 ft produces a capacity improvement of 30%, when compared with that obtainable with ILS. In contrast, the figure shows that if type 1 aircraft are separated vertically, from themselves and from other aircraft, by 2000 ft, rather than horizontally, by 2 nm, the effect of vertical separation on the capacity is negative.

Note that the highest obtainable increase in landing capacity when using MLS procedures occurs when the aircraft population consists of roughly equal divisions of fast and slow aircraft. (This point is discussed in Section 3.2.)

In Section 4.3 it was noted that when the capacity model (which responds to both horizontal and vertical separation rules) is applied, it produces optimal horizontal path geometry for aircraft types 2, 3, and 4. Further, in Section 3.2 it was noted that when horizontal separation rules are applied (to either MLS or ILS procedures) more than one optimal configuration results. Fig. 38 illustrates one of these approach paths configurations; this configuration maximizes landing capacity and produces the results shown in Figs. 35, 36 and 37. The paths are as follows.

-- Aircraft type 1 approaches on a glide slope of 7.5^{o}, performing

either a straight (as shown in Fig. 38) or curved approach.

-- Aircraft types 2, 3 and 4 all approach on a 3^{o} glide slope.

-- Aircraft type 4 approach directly along the extended runway centerline.

-- Aircraft type 3 intercept the extended runway centerline from its left side, at an angle of 20^{o}, 4 nm from the threshold.

-- Aircraft type 4 intercept the extended runway centerline from its right side, at an angle of 30^{o}, 2 nm from the threshold.

6. Conclusions

MLS allows the use of multiple approach path geometry in the final stage of approach, whereas ILS requires use of a common approach path. This research has considered runway landing capacity increases obtainable when MLS rather than ILS procedures are employed. Conclusions are as follows.

1. The approach path configuration shown in Fig. 13 is at least as suitable from a capacity point of view as any other possible configuration, when only horizontal separation is allowed (see Section 2.2).
2. The angles of entry, α_i , to the extended runway centerline have a significant effect on landing capacity; they should be optimized (see Section 3.2).
3. When only horizontal separation is allowed and when an aircraft population consists of aircraft with similar approach speeds, MLS procedures (differing final straight approach path) do not produce any improvement in landing capacity, when compared with capacities obtainable with ILS procedures (a common final approach path). (See Section 3.3.)
4. When only horizontal separation is allowed and an aircraft population consists of aircraft with considerably differing approach speeds, and for mixes of roughly half fast and half slow aircraft landing capacity improvements of 10-15% can be expected, when MLS rather than ILS procedures are employed (see Section 3.2).
5. If both vertical and horizontal separations are allowed during the approach phase, depending highly on the aircraft mix and

the applied minimum vertical separation rules, very significant improvements in landing capacity, as much as 50%, can be achieved, when MLS rather than ILS procedures are employed (see Section 5.2). These improvements are due to the vertical separation.

7. Figures

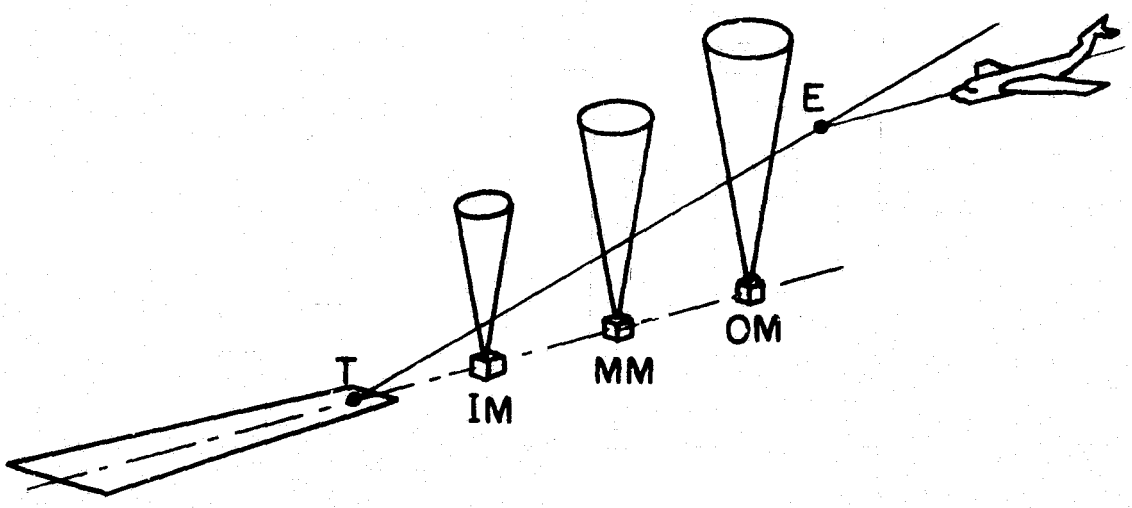

E Entry Gate

T Runway Threshold

OM Outer Marker

MM Middle Marker

IM Inner Marker

Figure 1

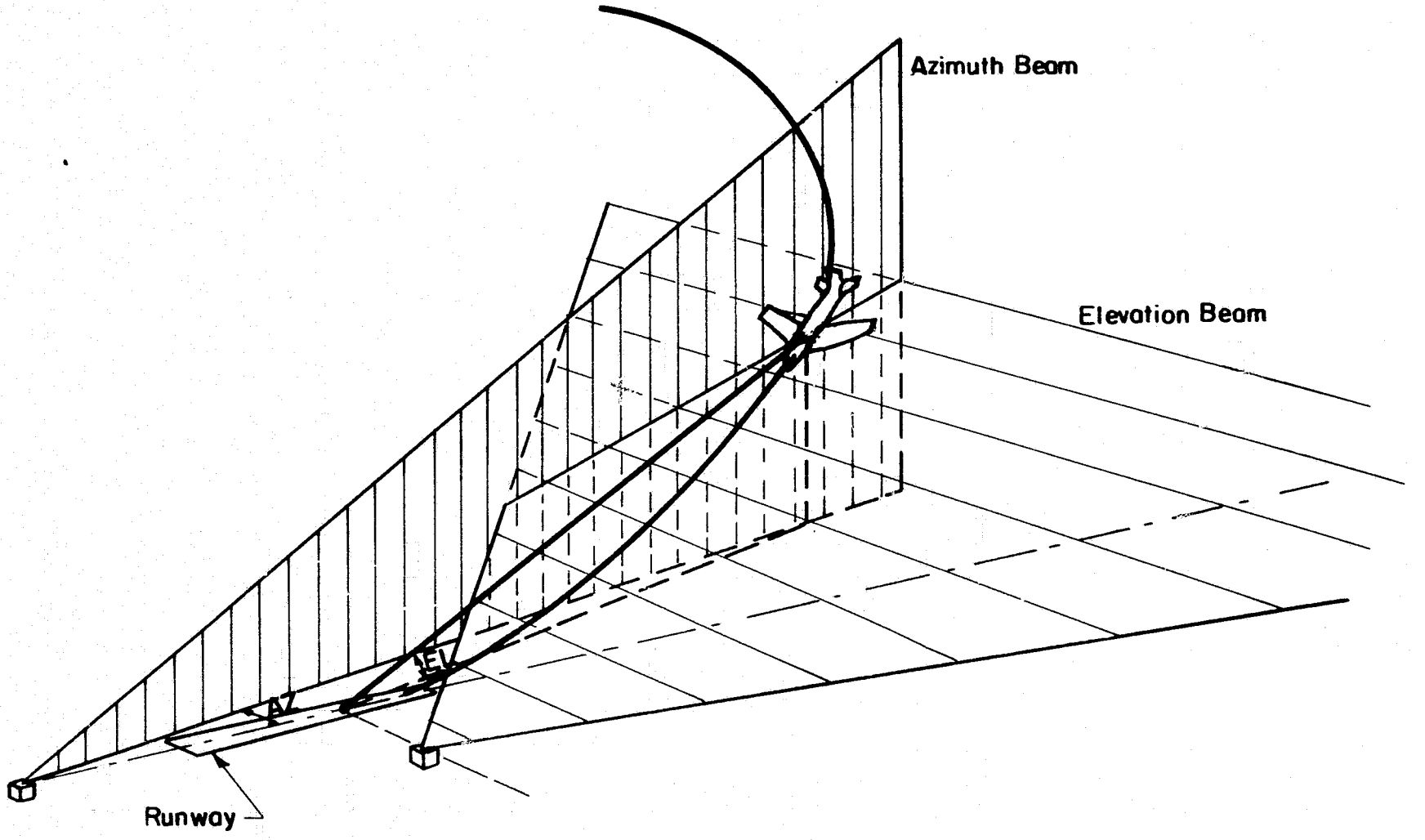

Figure 2

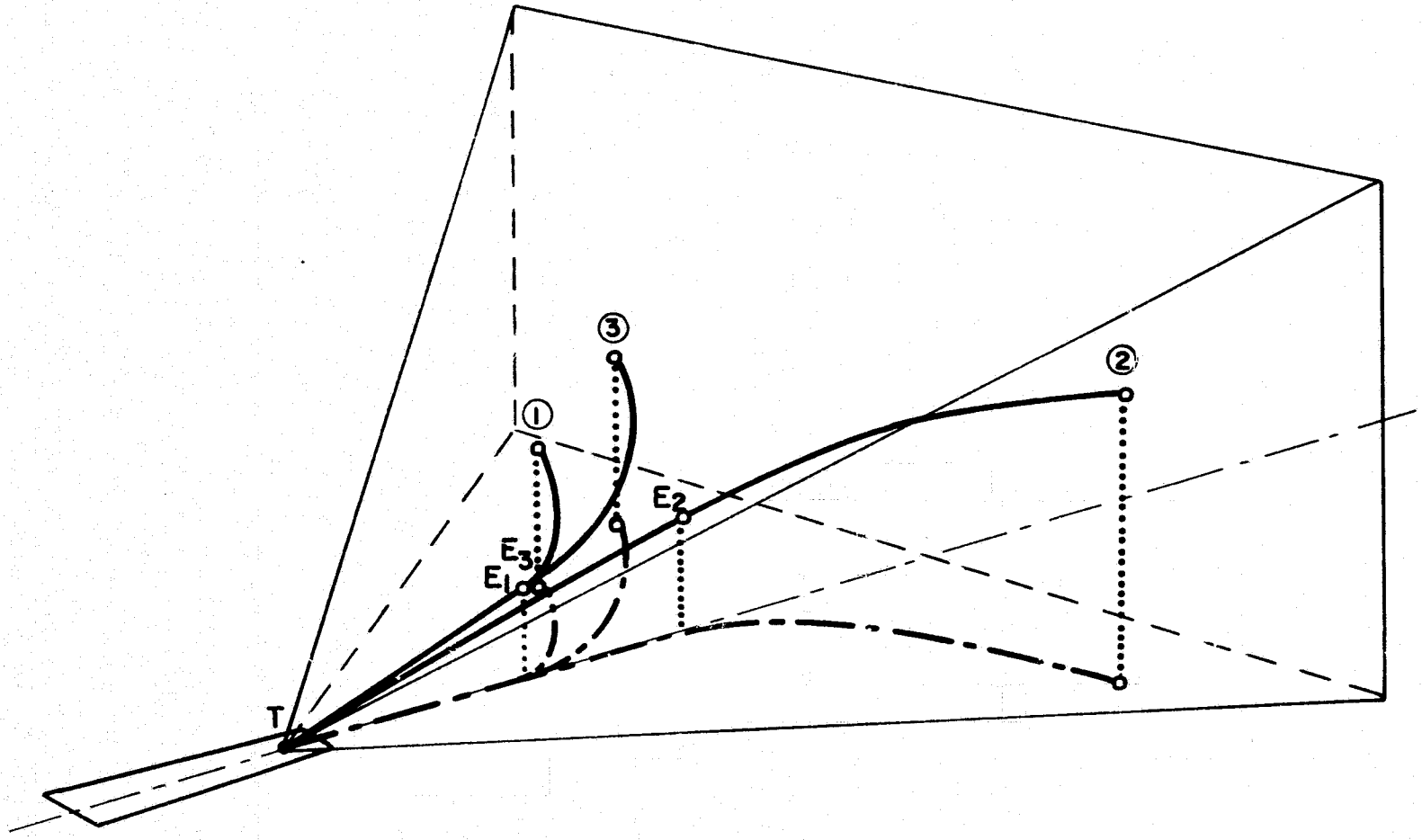

Figure 3

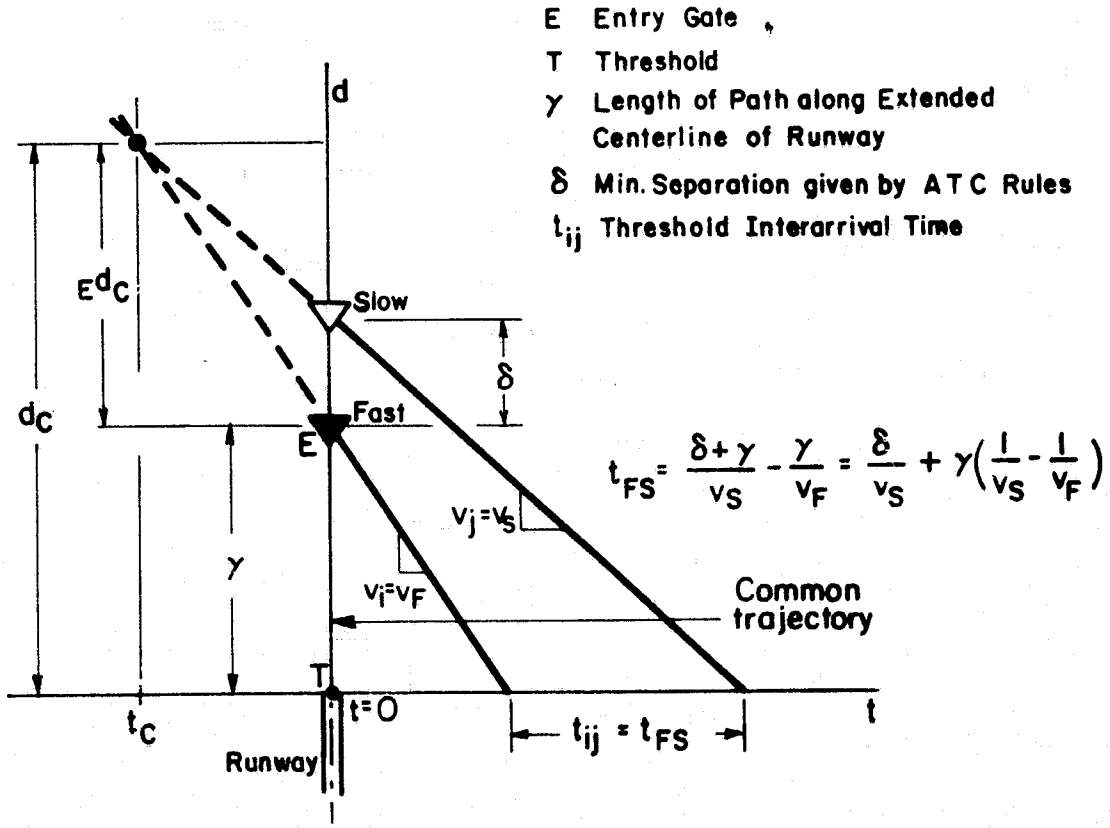

a. Fast aircraft followed by slow one. $V_i > V_j$

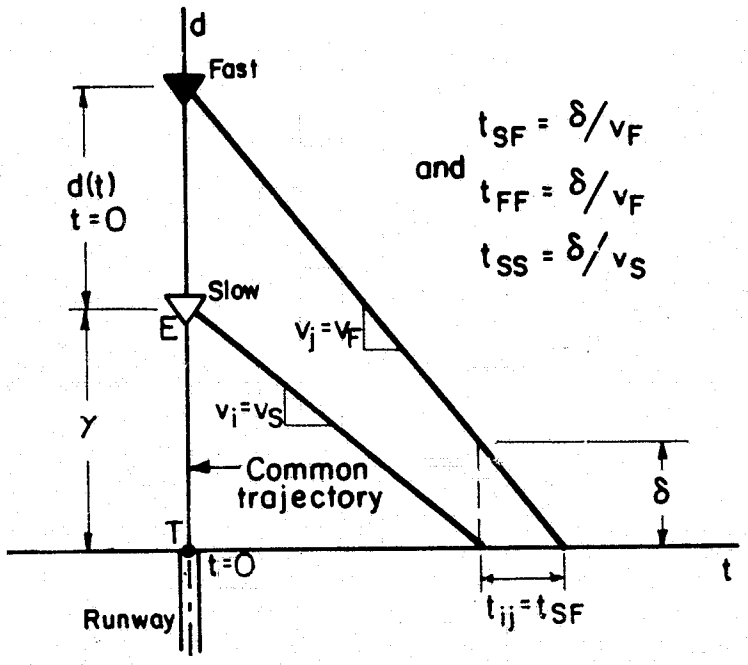

b. Slow aircraft followed by fast one. $V_i < V_j$

Figure 4

$$_E d_C = \delta \frac{V_F}{V_F - V_S}$$

d_C = Distance from the threshold where the two aircraft would "collide"

$_E d_C$ = Distance from the entry gate where the two aircraft would "collide"

t_C = Time of collision

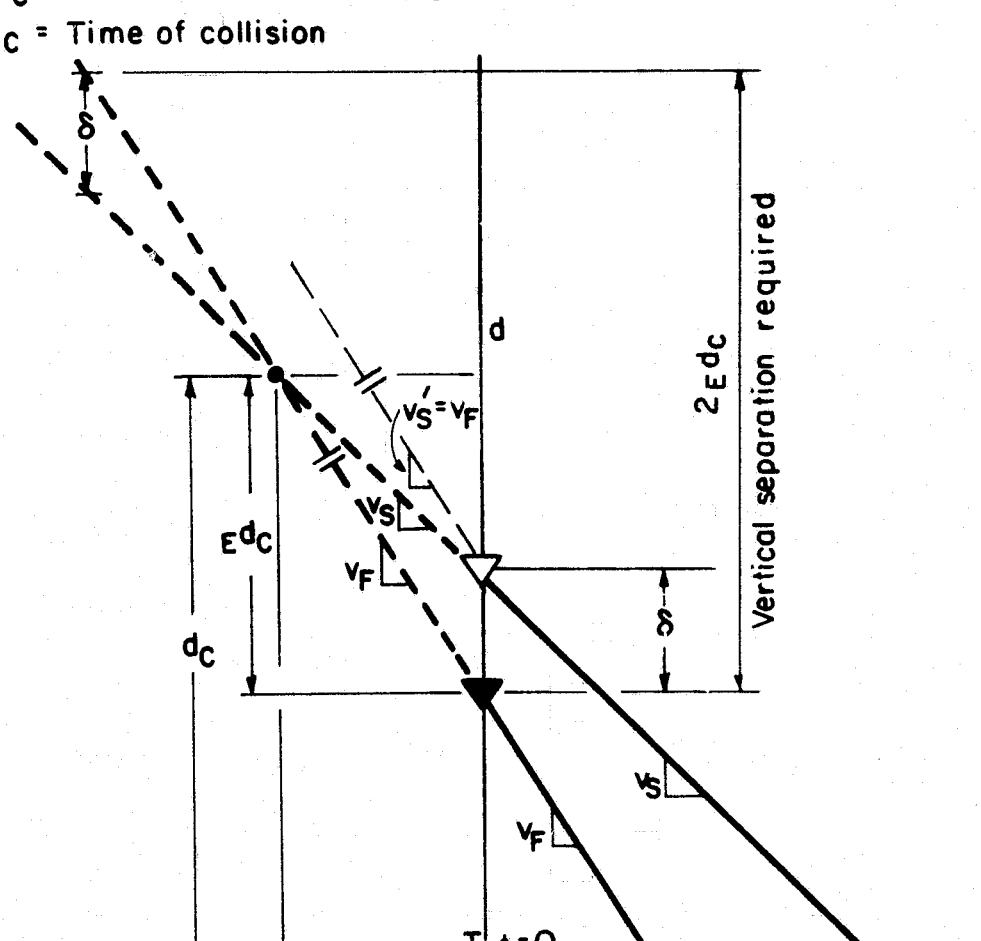

Figure 5

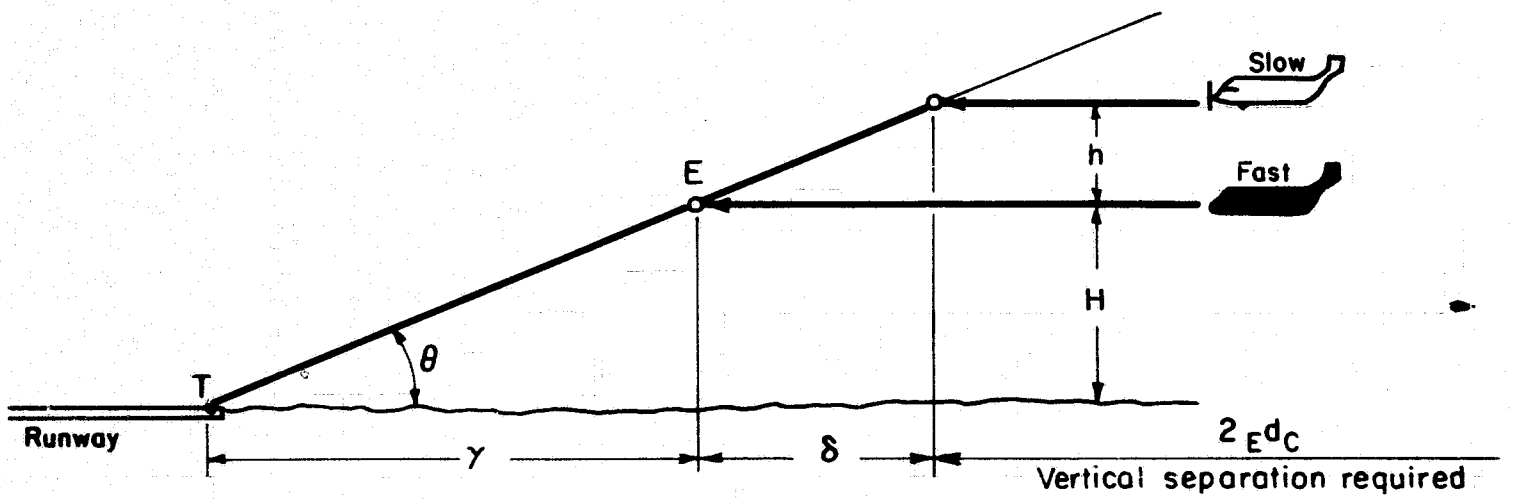

h

δ / θ	3 nm 18,240'	4 nm 24,320'	5 nm 30,400'
2.5	796'	1062'	1327'
3.0	955'	1274'	1593'

H

γ / θ	6 nm 36,480'	7 nm 42,560'	8 nm 48,640'
2.5	1593'	1858'	2124'
3.0	1912'	2230'	2549'

Figure 6

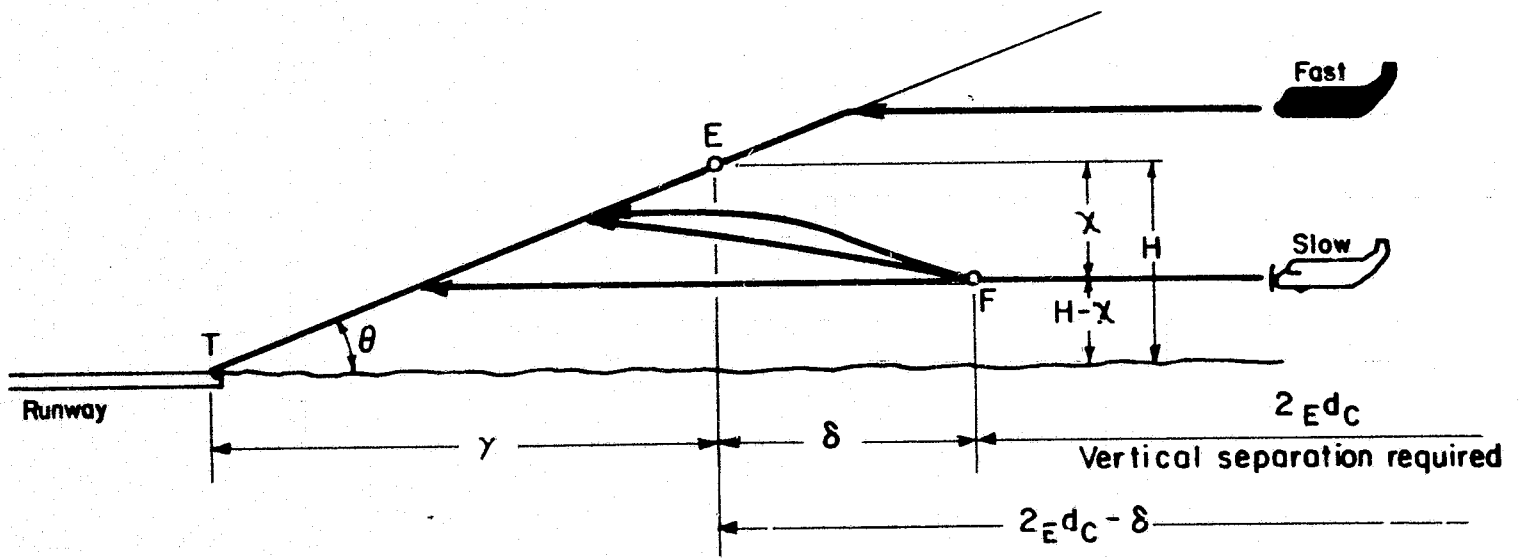
Fast
E
χ
H
Slow
F
H-χ
T
θ
Runway
2 E d C
γ
δ
Vertical separation required
2 E d C - δ

Figure 7

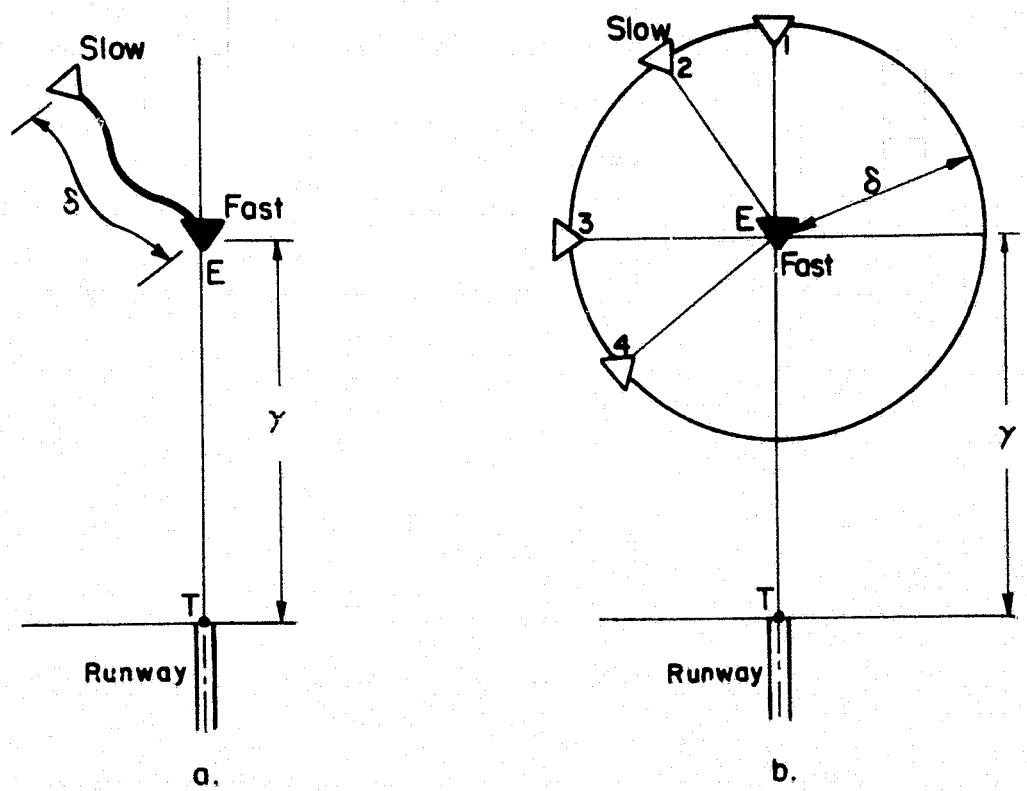

Figure 8

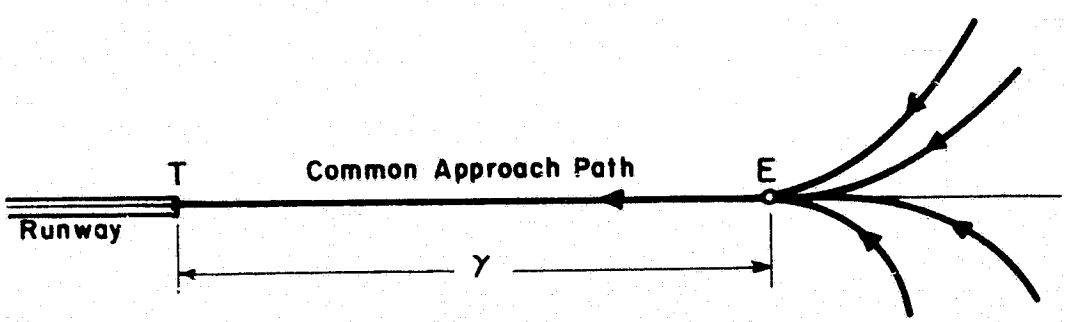

Figure 9

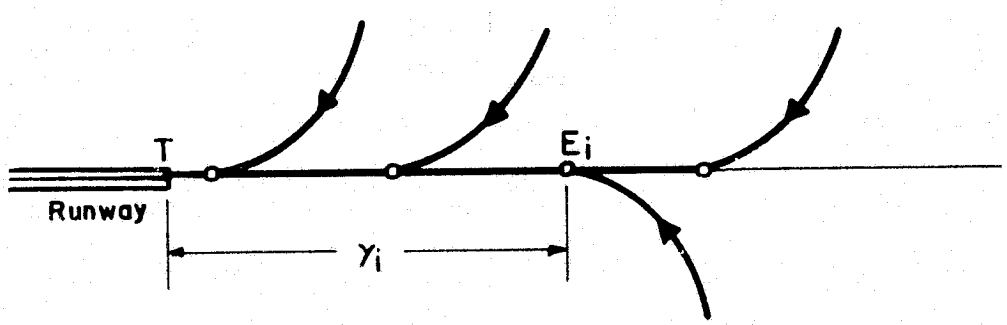

Figure 10

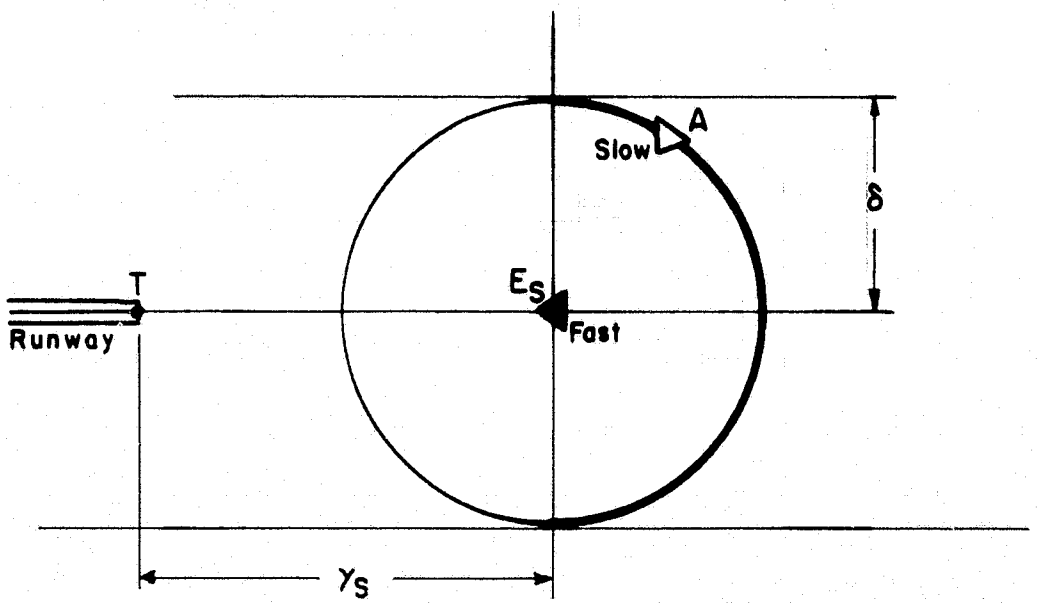

Figure 11

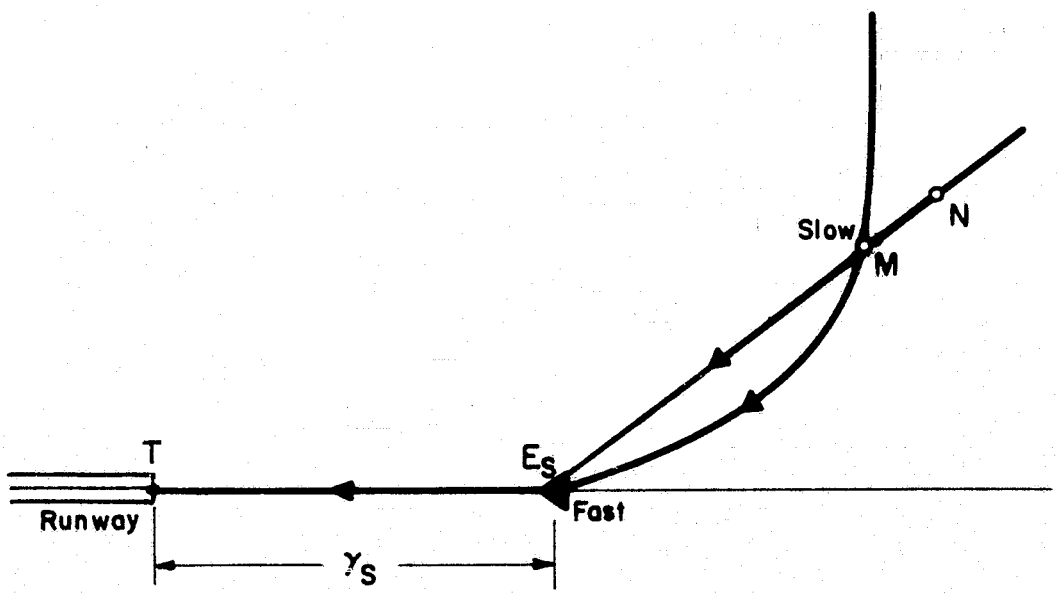

Figure 12

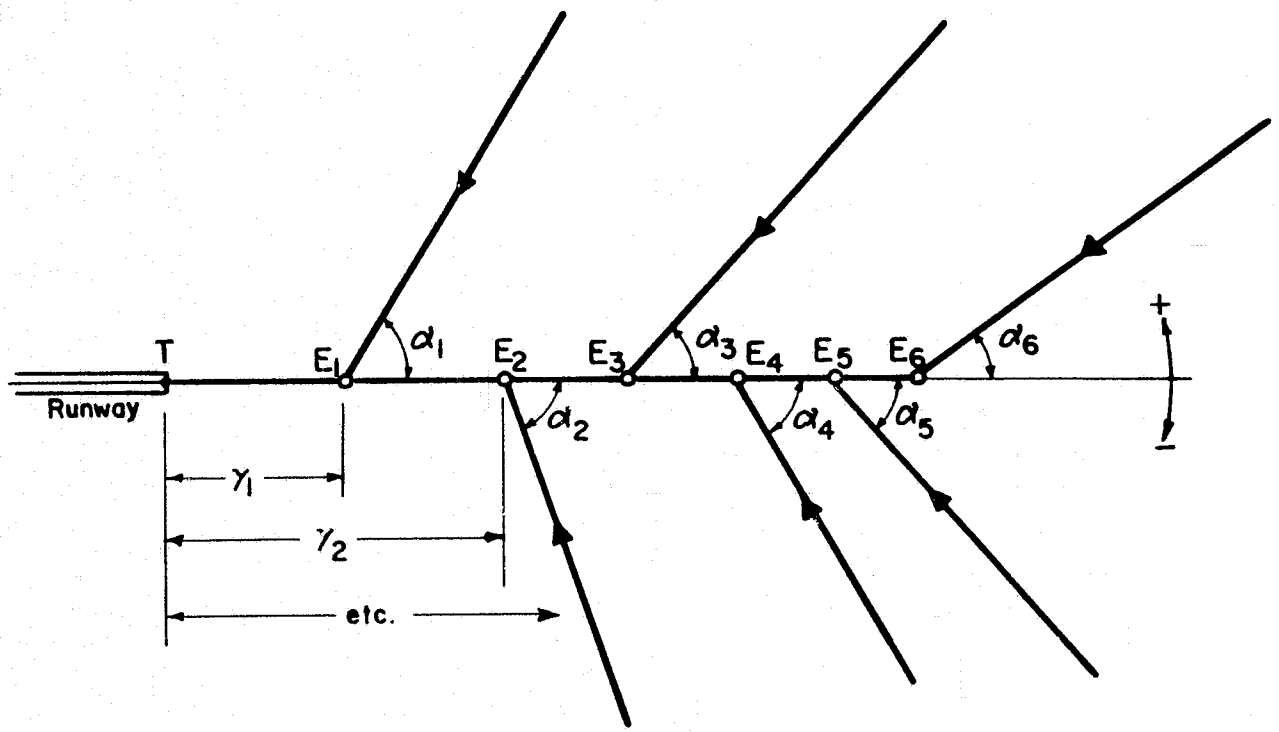

Figure 13

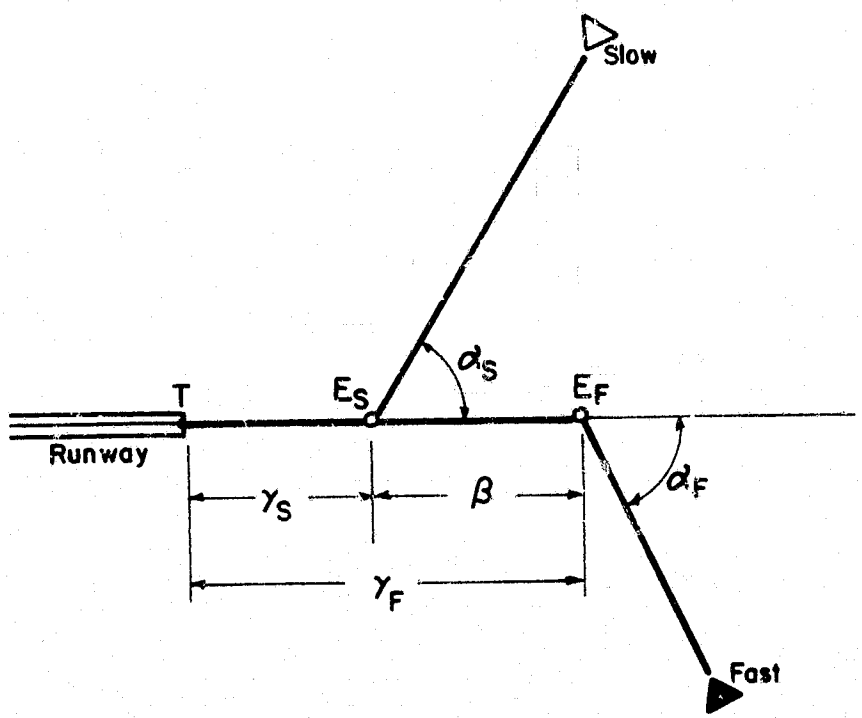

Figure 14

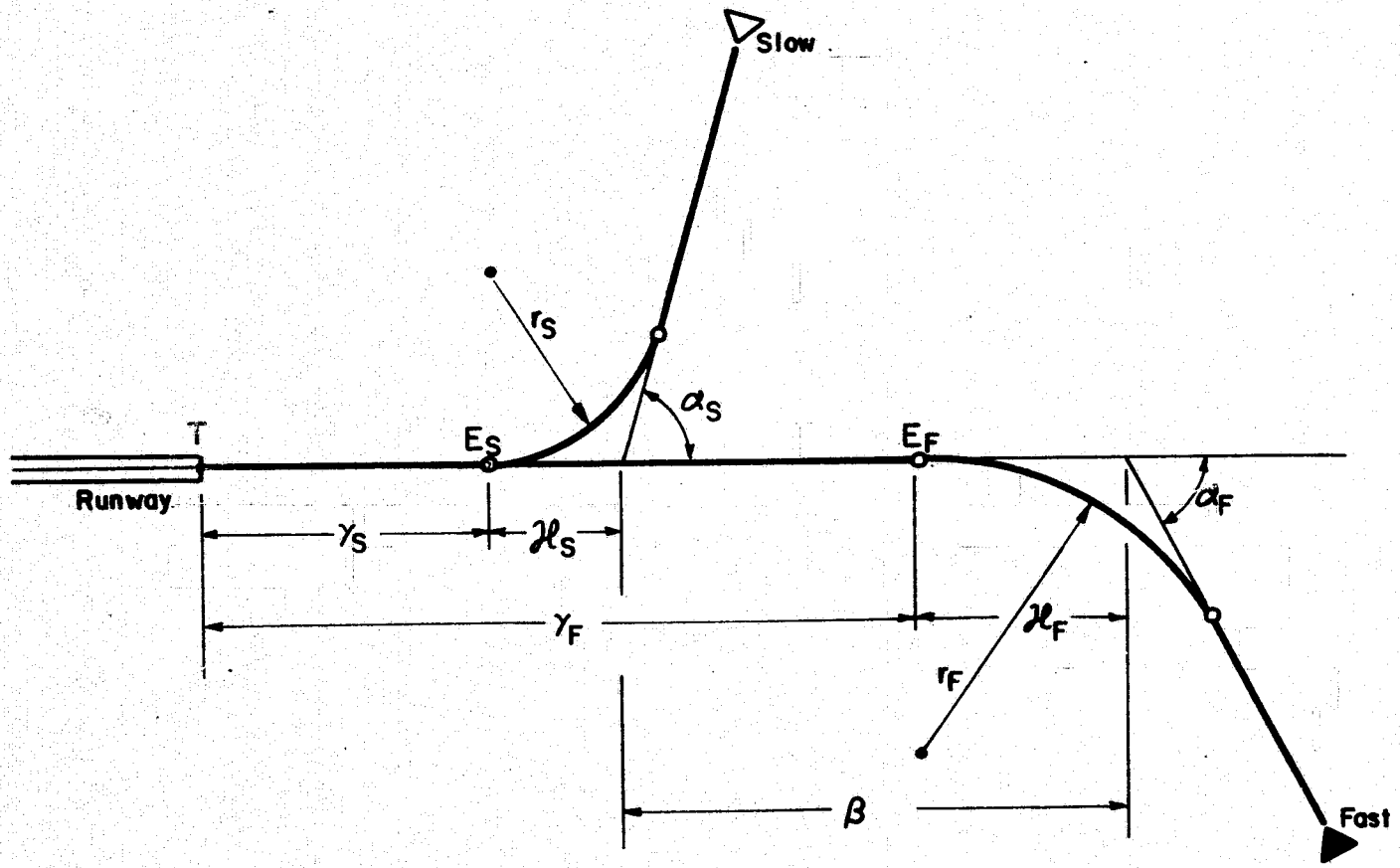
Slow
r_S
α_S
T
E_S
E_F
Runway
γ_S
$\mathcal{H}_S$
α_F
γ_F
$\mathcal{H}_F$
r_F
β
Fast

Figure 15

$$t_{ij} = \frac{\gamma_{ij} + {}_{ij}\hat{d}_o}{v_j} - \frac{\gamma_{ij}}{v_i}$$

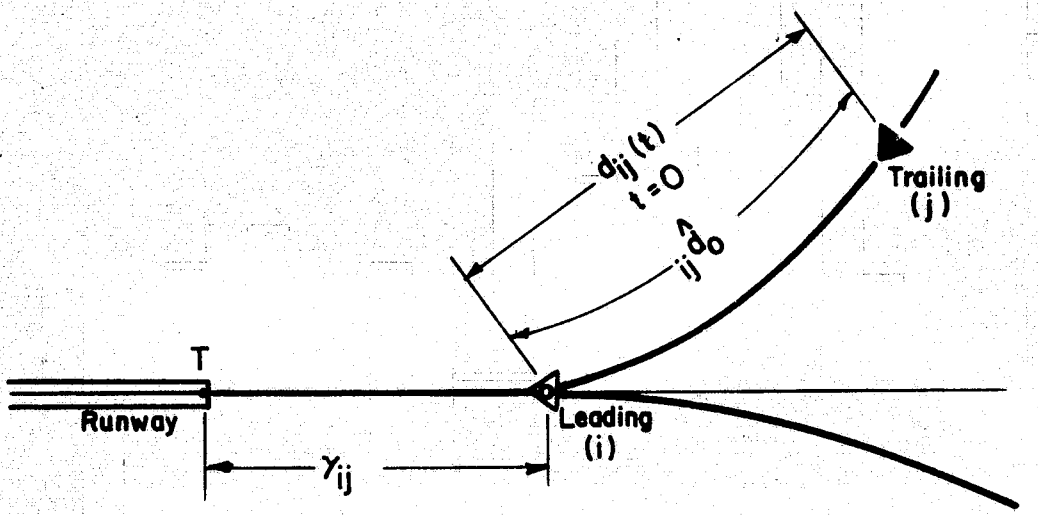

γ_{ij} = Length of common path along extended runway centerline

t_{ij} = Threshold interarrival time

${}_{ij}\hat{d}_o$ = Initial separation distance between aircraft i and j at t=0 measured along the path of aircraft j

Figure 16

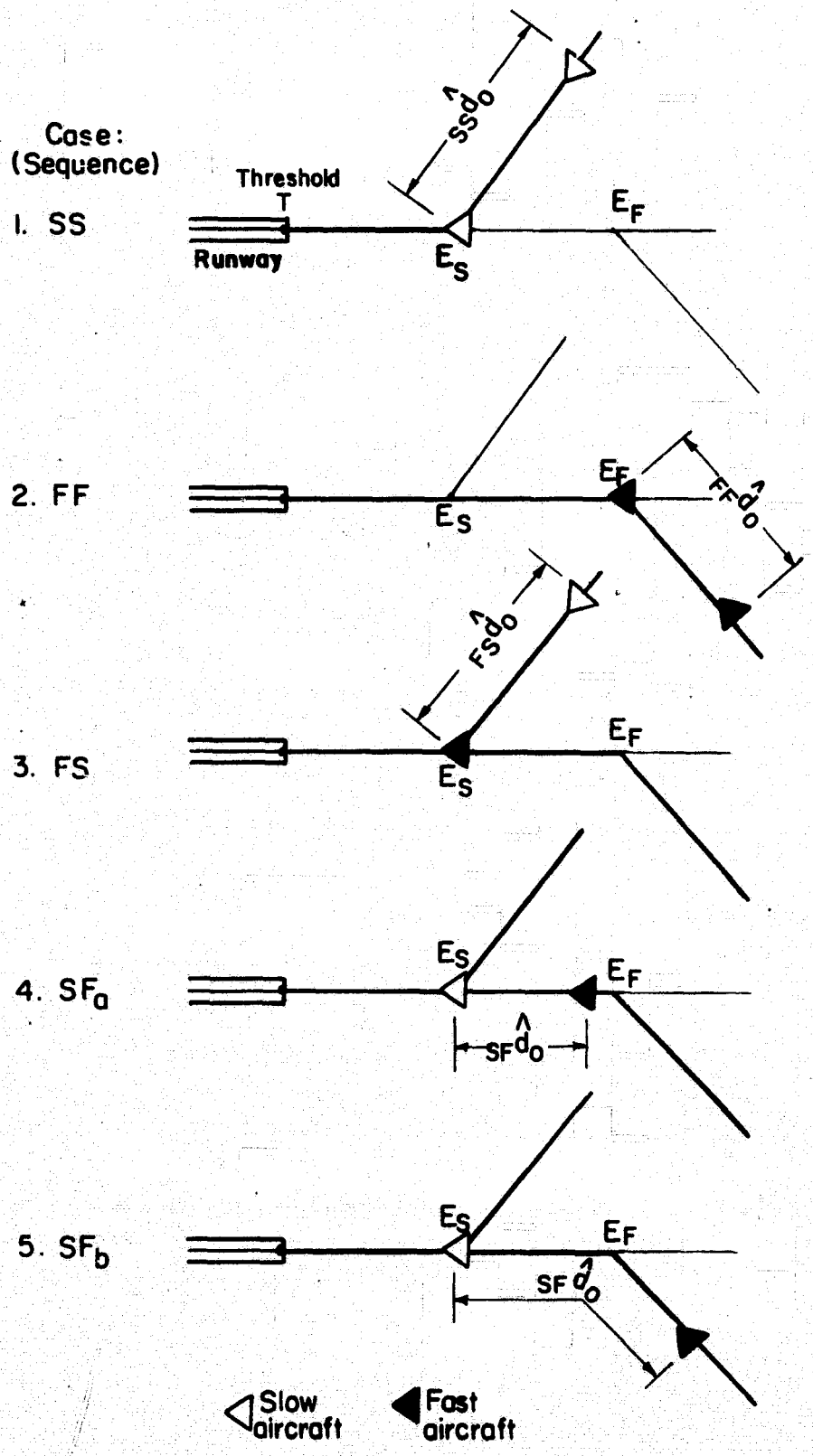
Case:
(Sequence)
1. SS
Threshold
T
Runway
E_S
E_F
$\hat{d}_{SS_o}$
2. FF
E_S
E_F
$\hat{d}_{FF_o}$
3. FS
E_S
E_F
$\hat{d}_{FS_o}$
4. SF_a
E_S
E_F
$\hat{d}_{SF_o}$
5. SF_b
E_S
E_F
$\hat{d}_{SF_o}$
Slow aircraft
Fast aircraft

Figure 17

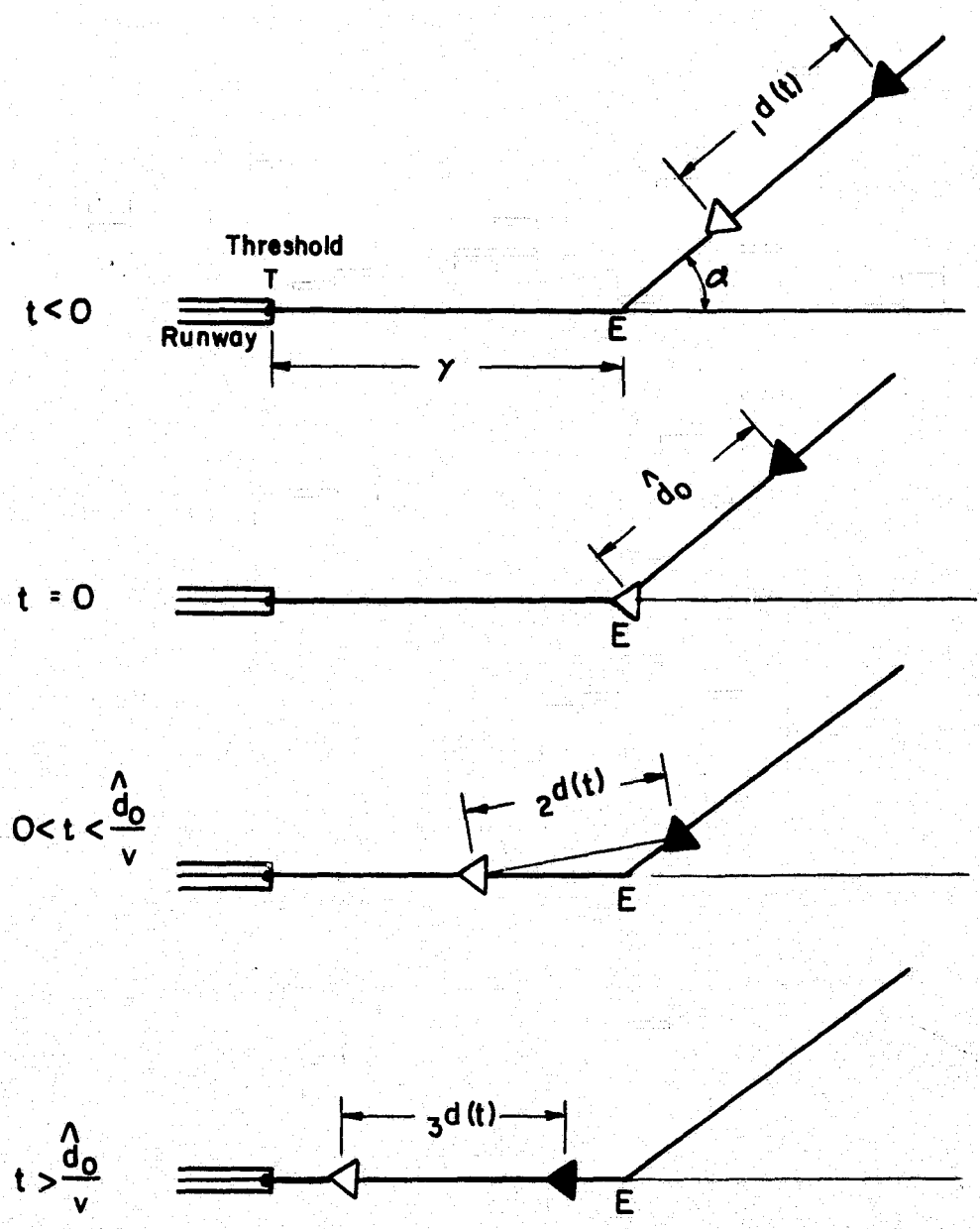

$$d(t) = d_{SS}(t) \text{ or } d_{FF}(t)$$

$$v = v_F \text{ or } v_S$$

$$\alpha = \alpha_F \text{ or } \alpha_S$$

$$\gamma = \gamma_F \text{ or } \gamma_S$$

$$\hat{d}_0 = {}_{FF}\hat{d}_0 \text{ or } {}_{SS}\hat{d}_0$$

Figure 18

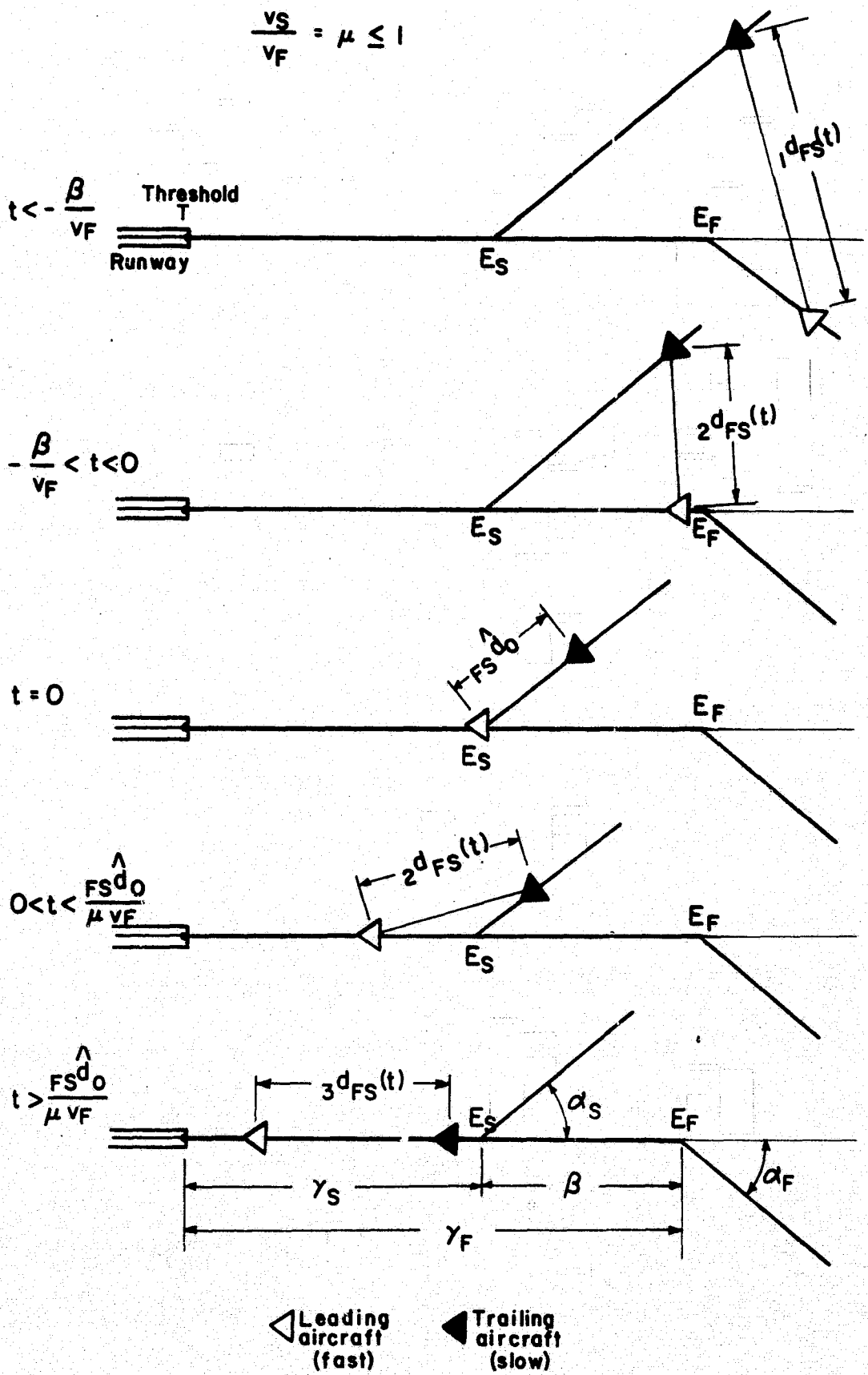
$\frac{v_S}{v_F} = \mu \leq 1$
$t < -\frac{\beta}{v_F}$
Threshold
T
Runway
E_S
E_F
$1^{d_{FS}(t)}$
$-\frac{\beta}{v_F} < t < 0$
$2^{d_{FS}(t)}$
$t = 0$
$\hat{d}_{FS_0}$
$0 < t < \frac{\hat{d}_{FS_0}}{\mu v_F}$
$t > \frac{\hat{d}_{FS_0}}{\mu v_F}$
$3^{d_{FS}(t)}$
α_S
α_F
γ_S
β
γ_F
Leading aircraft (fast)
Trailing aircraft (slow)

Figure 19

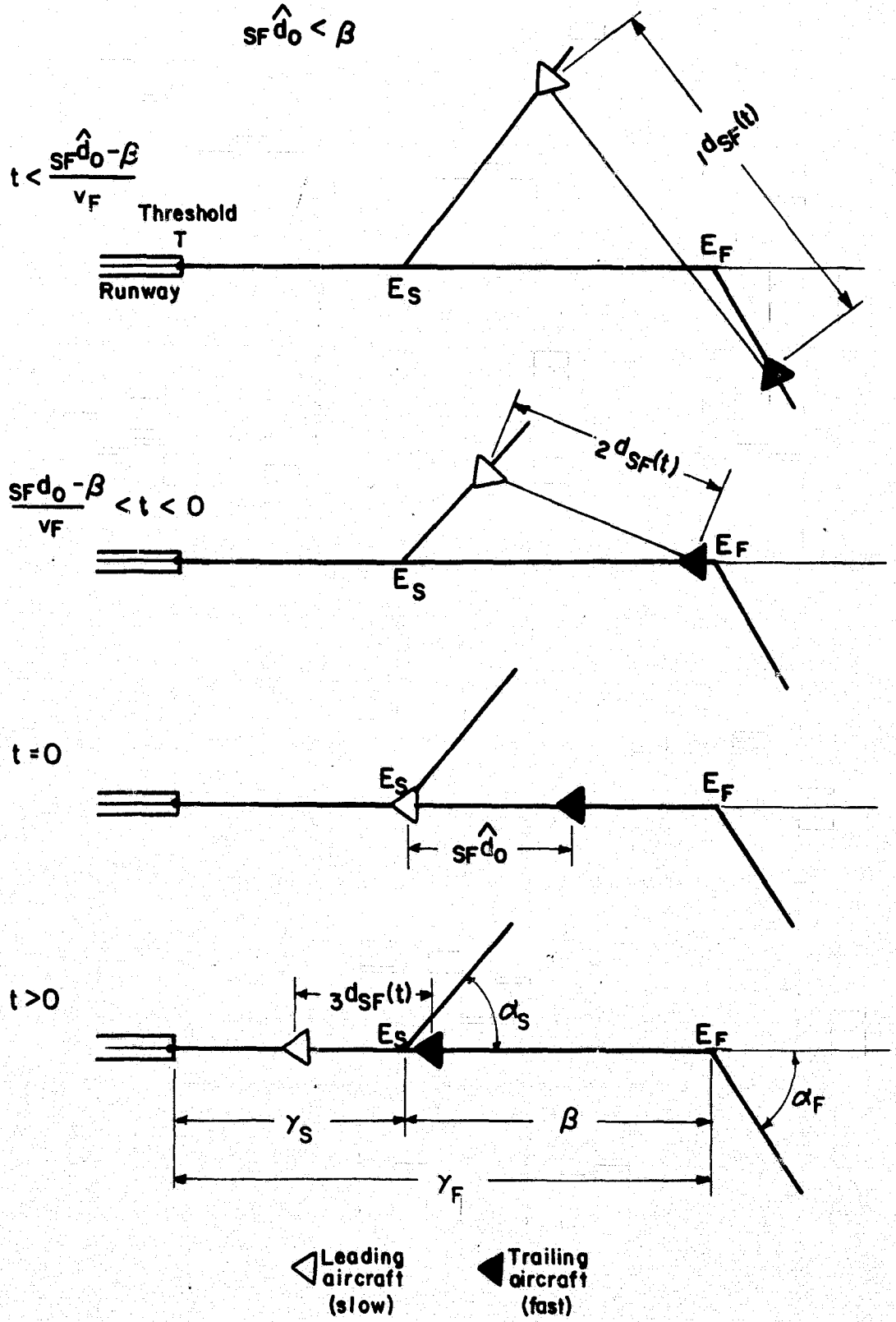
$_{SF}\hat{d}_0 < \beta$
$t < \frac{_{SF}\hat{d}_0 - \beta}{v_F}$
Threshold
T
Runway
E_S
E_F
$_1d_{SF}(t)$
$\frac{_{SF}d_0 - \beta}{v_F} < t < 0$
$_2d_{SF}(t)$
E_S
E_F
$t = 0$
E_S
E_F
$_{SF}\hat{d}_0$
$t > 0$
$_3d_{SF}(t)$
E_S
E_F
α_S
α_F
γ_S
β
γ_F
Leading aircraft (slow)
Trailing aircraft (fast)

Figure 20a

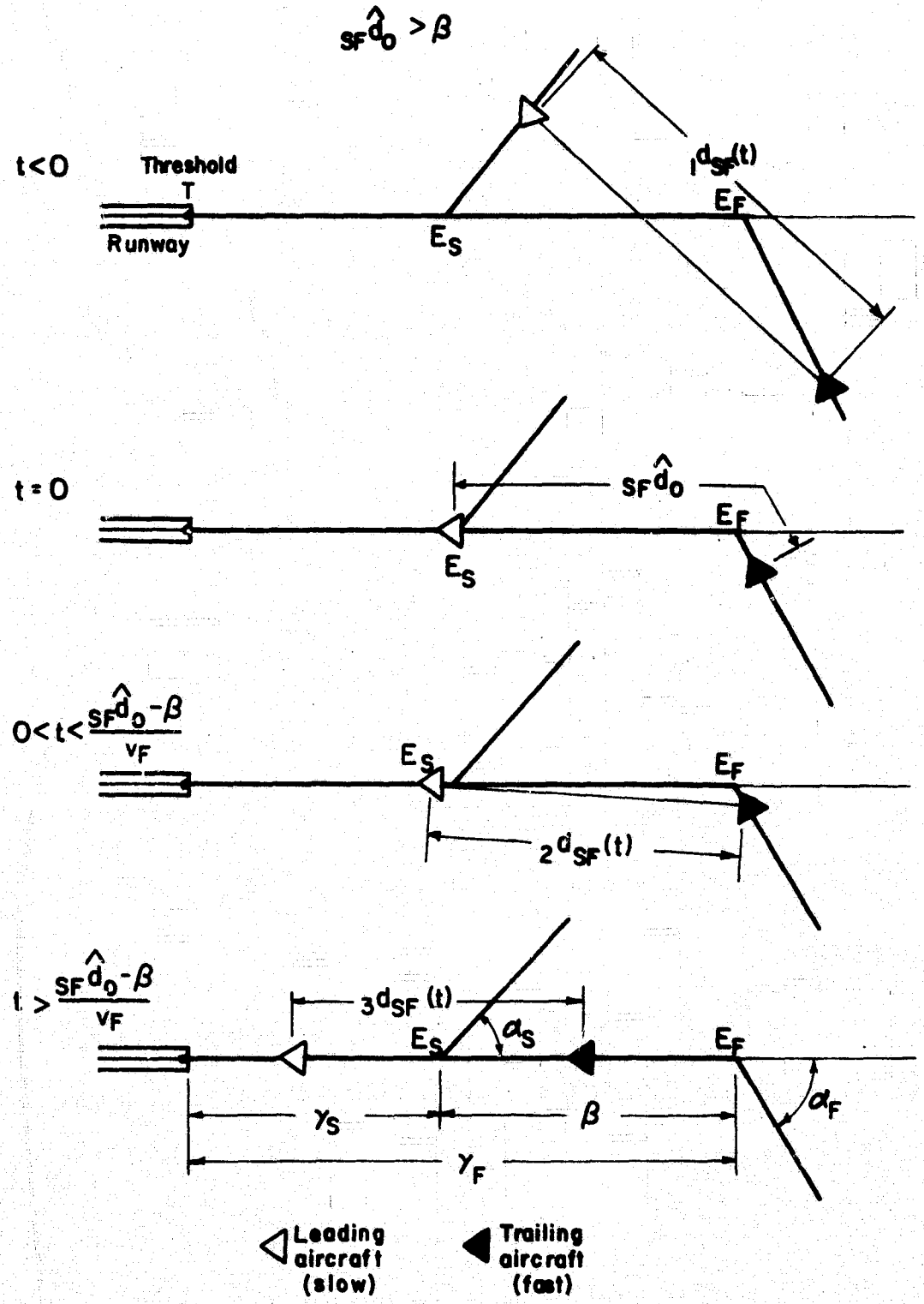
$_{SF}\hat{d}_0 > \beta$
t<0
Threshold
T
Runway
E_S
$_1d_{SF}(t)$
E_F
t = 0
$_{SF}\hat{d}_0$
E_F
E_S
$0<t<\frac{_{SF}\hat{d}_0-\beta}{v_F}$
E_S
E_F
$_2d_{SF}(t)$
$t>\frac{_{SF}\hat{d}_0-\beta}{v_F}$
$_3d_{SF}(t)$
E_S
α_S
E_F
α_F
γ_S
β
γ_F
Leading aircraft (slow)
Trailing aircraft (fast)

Figure 20b

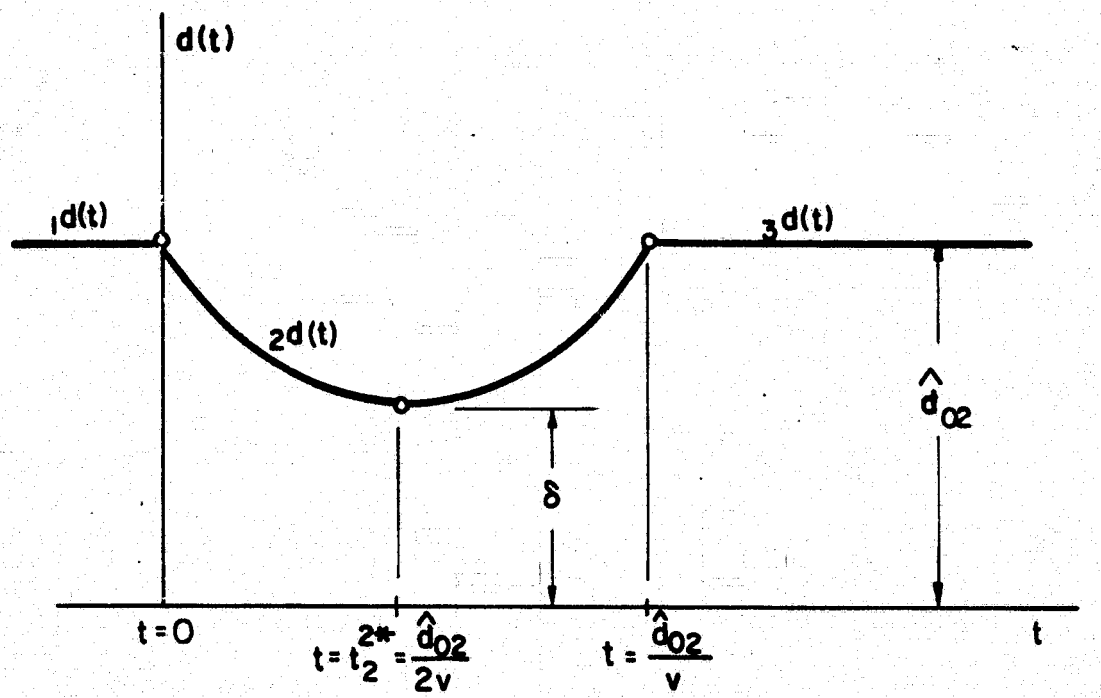

Figure 21

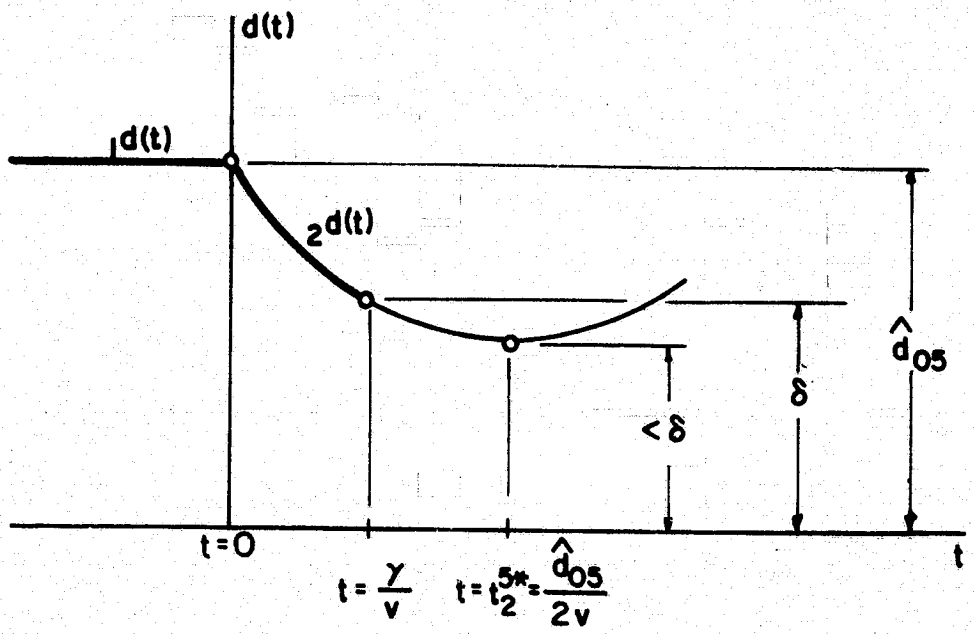

Figure 22

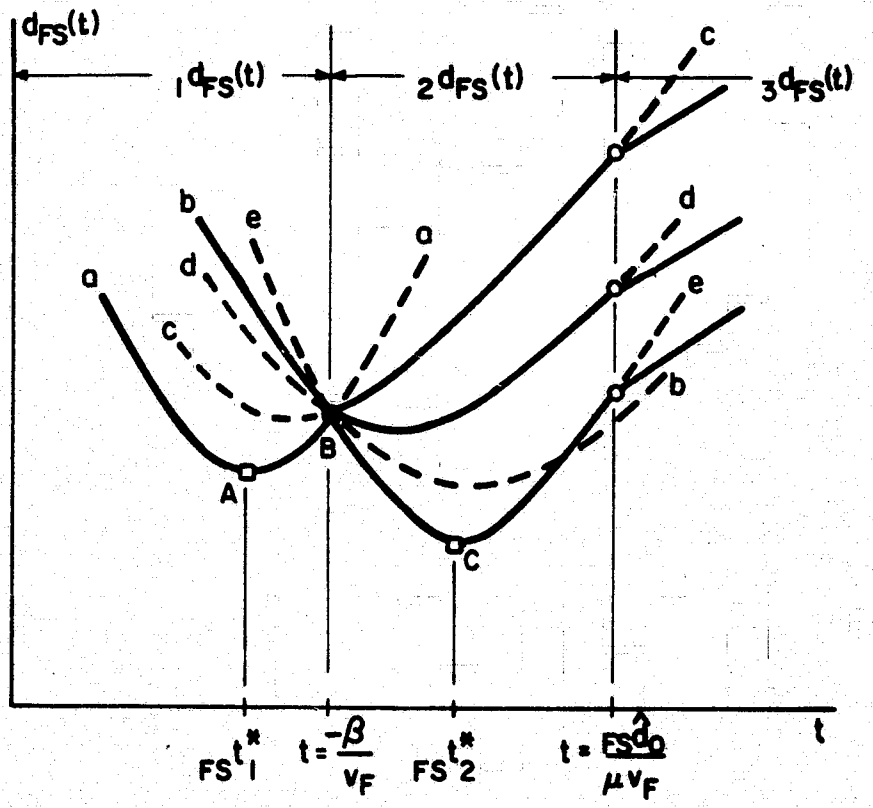
$d_{FS}(t)$
$_1d_{FS}(t)$
$_2d_{FS}(t)$
$_3d_{FS}(t)$
a
b
c
d
e
A
B
C
$_{FS}t_1^*$
$t=\frac{-\beta}{v_F}$
$_{FS}t_2^*$
$t=\frac{\hat{d}_0}{\mu v_F}$
t

a.

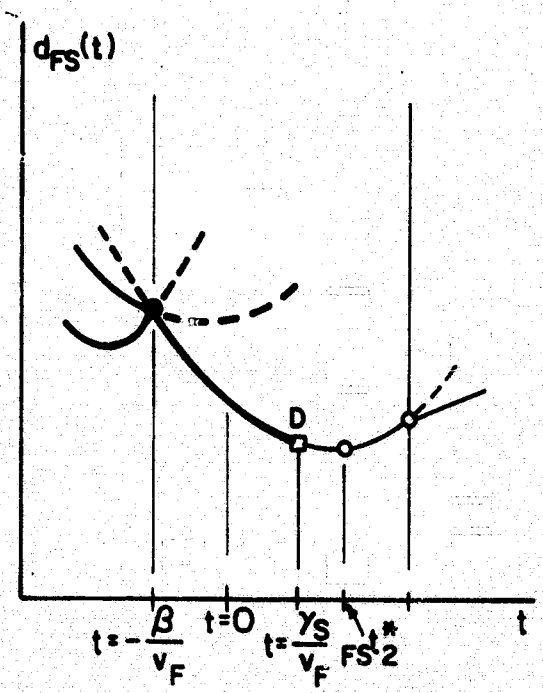
$d_{FS}(t)$
D
$t=-\frac{\beta}{v_F}$
t=0
$t=\frac{\gamma_S}{v_F}$
$_{FS}t_2^*$
t

b.

Figure 23

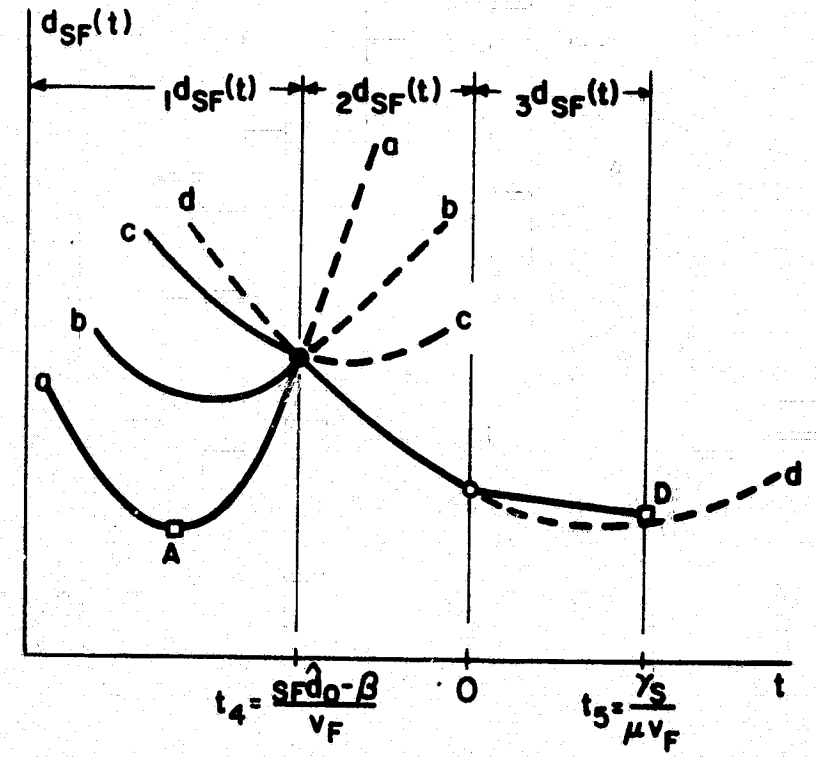

a.

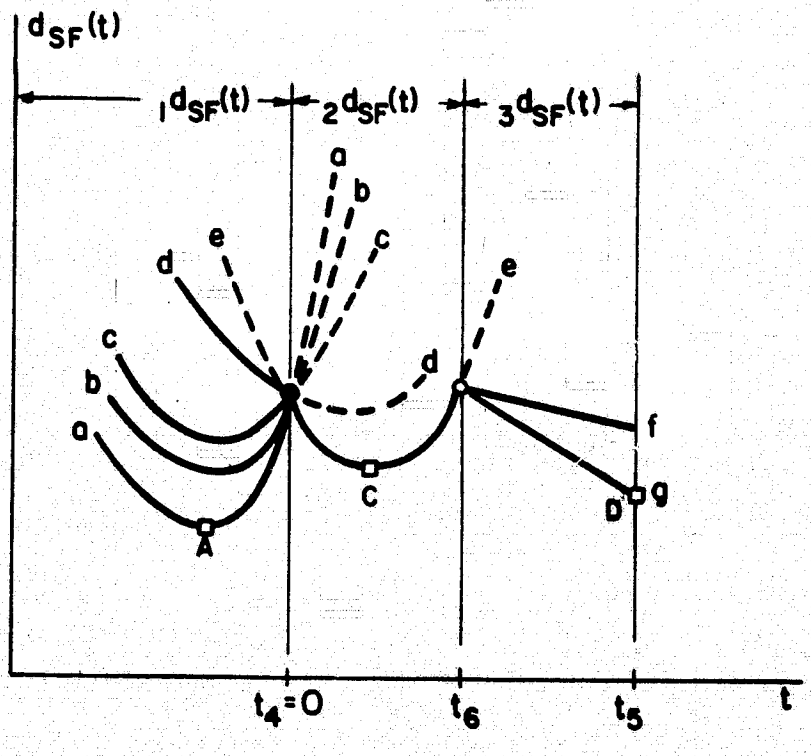

b.

Figures 24a and b

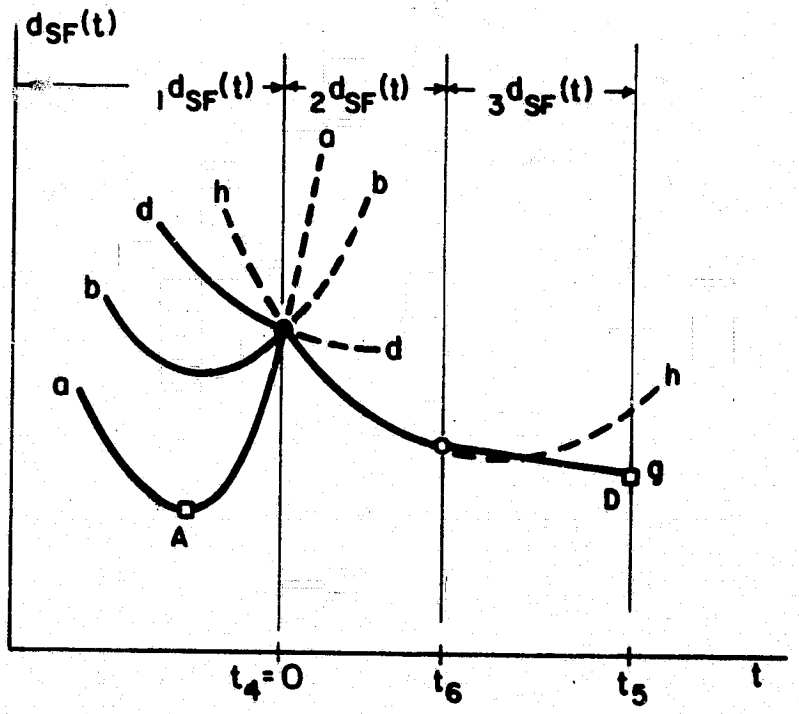

c.

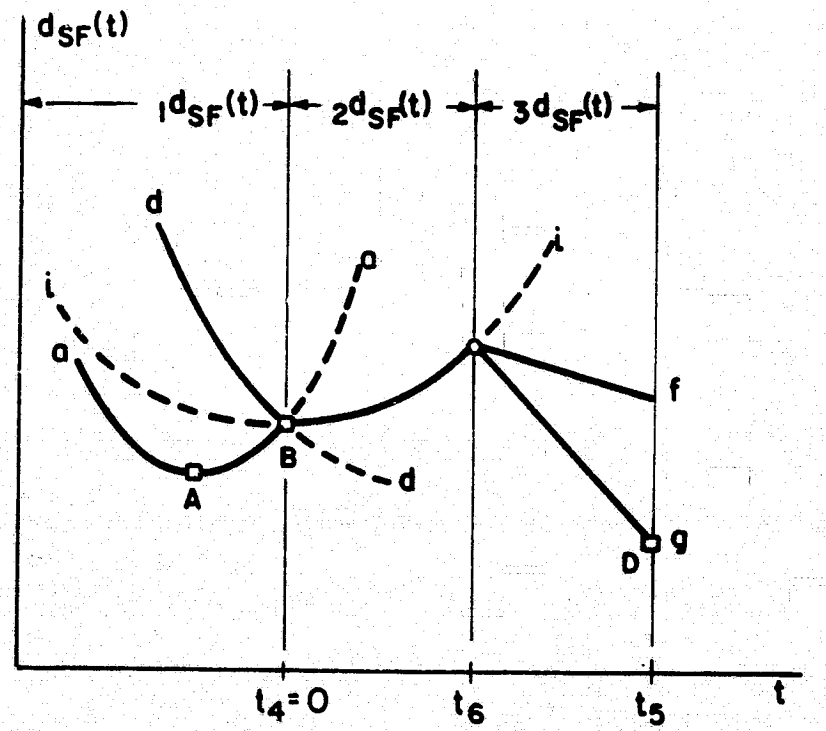

d.

Figures 24c and d

1. $0 \leq \gamma_S \leq \gamma_F$
2. $v_S \leq v_F$
3. $p_F + p_S = 1;\ p_F \geq 0;\ p_S \geq 0$
4. Angle increments 10° except when $\alpha_S \approx \alpha_F$ then $\alpha_S - \alpha_F = 5^\circ$

e.g.
$\alpha_S = 90^\circ \quad \alpha_F = 85^\circ$
$\alpha_S = 90^\circ \quad \alpha_F = 80^\circ$
$\alpha_S = 90^\circ \quad \alpha_F = 70^\circ$
etc.

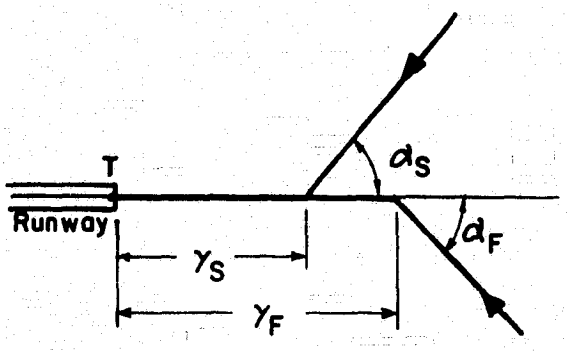

$0 \leq \alpha_S \leq 90^\circ$
$-90^\circ \leq \alpha_F \leq \alpha_S - 5^\circ$

Figure 25

1. $0 \le \gamma_1 \le \gamma_2 \le \gamma_3$
2. $v_1 \le v_2 \le v_3$
3. $p_i \ge 0;\ \Sigma p_i = 1$
4. Angle increments 10°

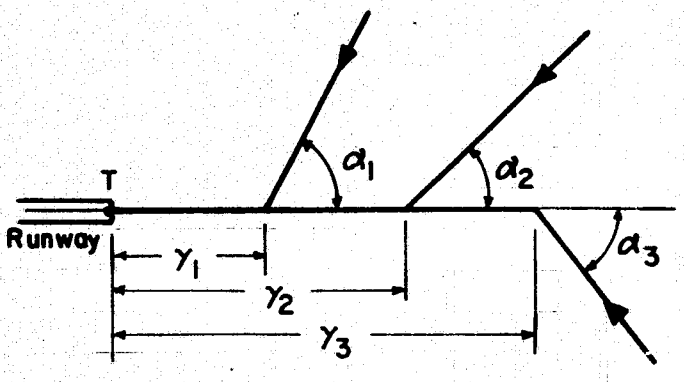

a.

$20° \le \alpha_1 \le 90°$

$10° \le \alpha_2 \le \alpha_1 - 10°$

$-90° \le \alpha_3 \le \alpha_2 - 10°$

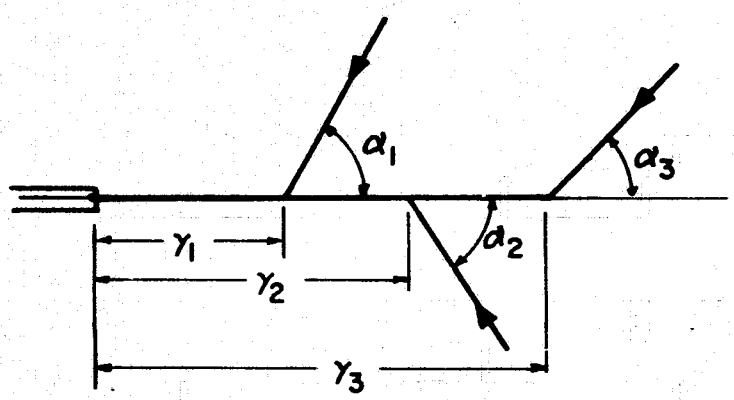

b.

$10° \le \alpha_1 \le 90°$

$-90° \le \alpha_2 \le -10°$

$\alpha_2 + 10° \le \alpha_3 \le \alpha_1 - 10°$

Figure 26

1. $0 \leq \gamma_1 \leq \gamma_2 \leq \gamma_3 \leq \gamma_4$
2. $v_1 \leq v_2 \leq v_3 \leq v_4$
3. $p_i \geq 0$; $\Sigma p_i = 1$
4. Angle increments 10°

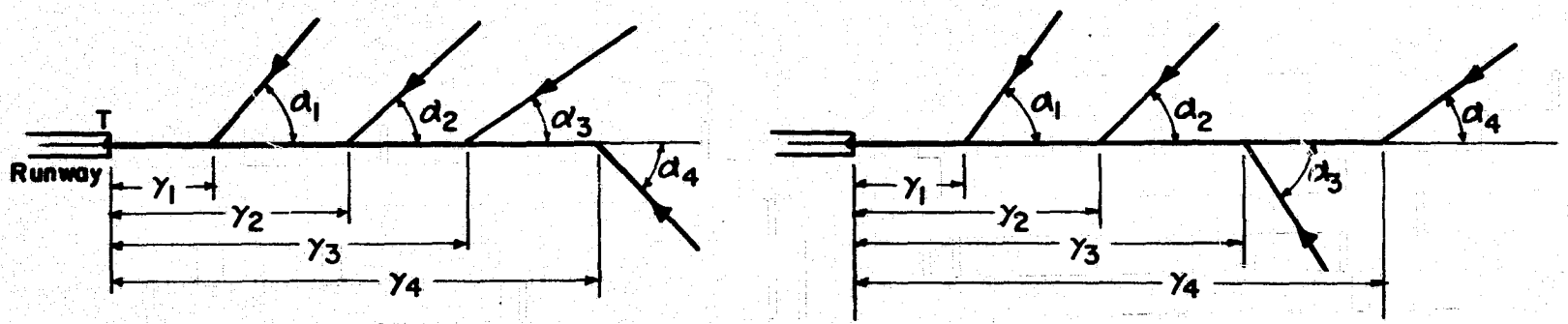

a.

$30^\circ \leq \alpha_1 \leq 90^\circ$

$20^\circ \leq \alpha_2 \leq \alpha_1 - 10^\circ$

$10^\circ \leq \alpha_3 \leq \alpha_2 - 10^\circ$

$-90^\circ \leq \alpha_4 \leq \alpha_3 - 10^\circ$

b.

$20^\circ \leq \alpha_1 \leq 90^\circ$

$10^\circ \leq \alpha_2 \leq \alpha_1 - 10^\circ$

$-90^\circ \leq \alpha_3 \leq -10^\circ$

$\alpha_3 + 10^\circ \leq \alpha_4 \leq \alpha_2 - 10^\circ$

Figure 27a

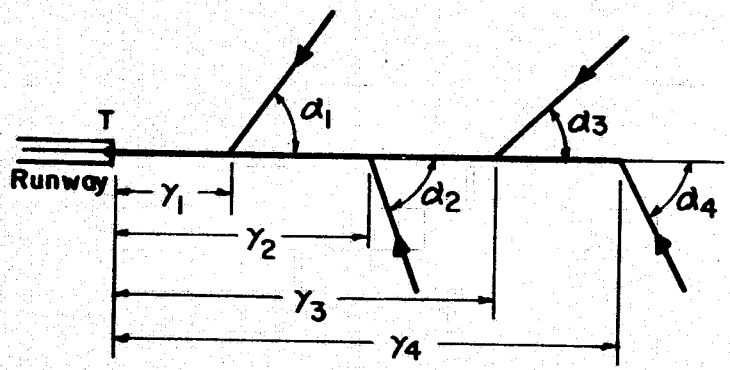

c.

$$20^\circ \leq \alpha_1 \leq 90^\circ$$
$$-90^\circ \leq \alpha_2 \leq -10^\circ$$
$$10^\circ \leq \alpha_3 \leq \alpha_1 - 10^\circ$$
$$\alpha_2 + 10^\circ \leq \alpha_4 \leq \alpha_3 - 10^\circ$$

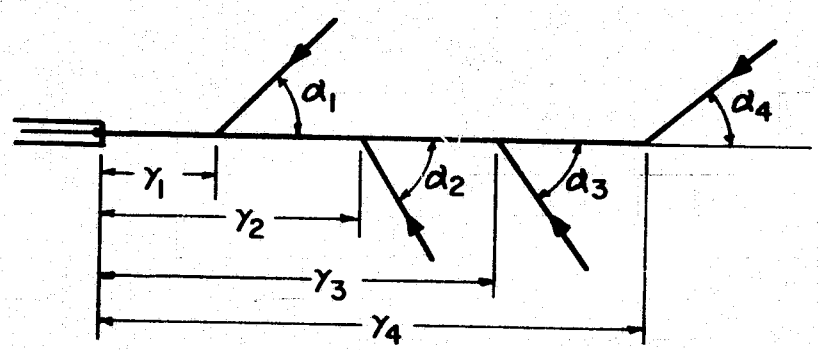

d.

$$10^\circ \leq \alpha_1 \leq 90^\circ$$
$$-90^\circ \leq \alpha_2 \leq -20^\circ$$
$$\alpha_2 + 10^\circ \leq \alpha_3 \leq -10^\circ$$
$$\alpha_1 - 10^\circ \leq \alpha_4 \leq \alpha_3 + 10^\circ$$

Figure 27b

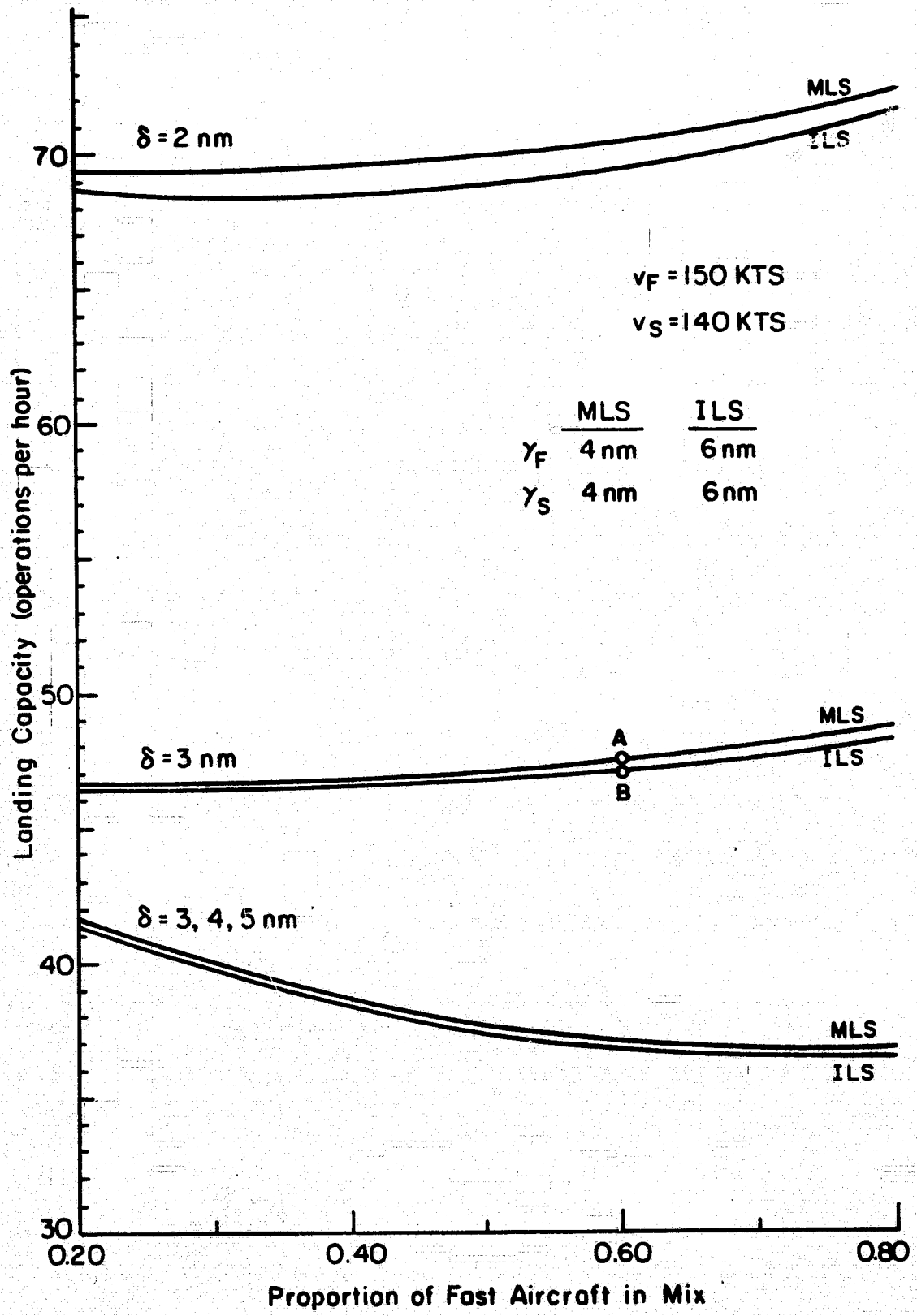
MLS
ILS
δ = 2 nm
70
v_F = 150 KTS
v_S = 140 KTS
MLS ILS
γ_F 4 nm 6 nm
γ_S 4 nm 6 nm
60
50
MLS
ILS
A
B
δ = 3 nm
δ = 3, 4, 5 nm
40
MLS
ILS
30
0.20
0.40
0.60
0.80
Landing Capacity (operations per hour)
Proportion of Fast Aircraft in Mix

Figure 28

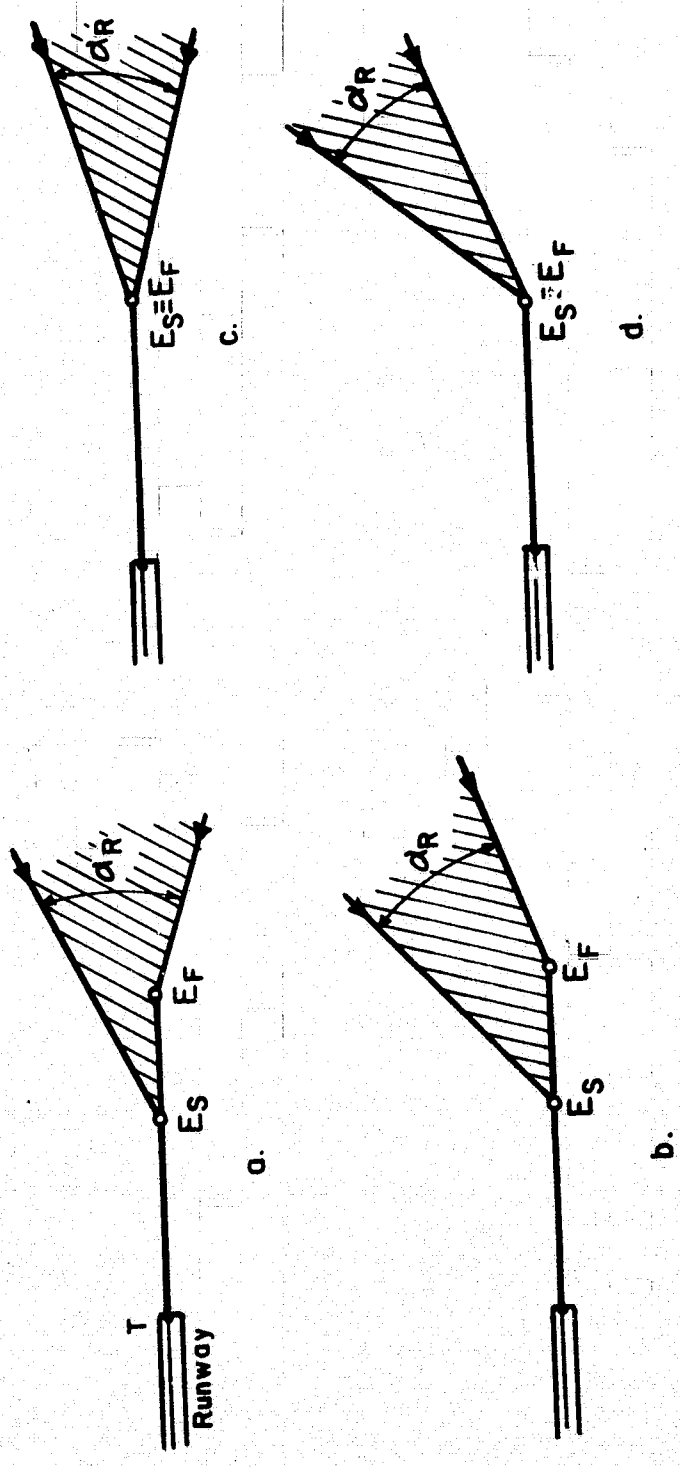

Figure 29

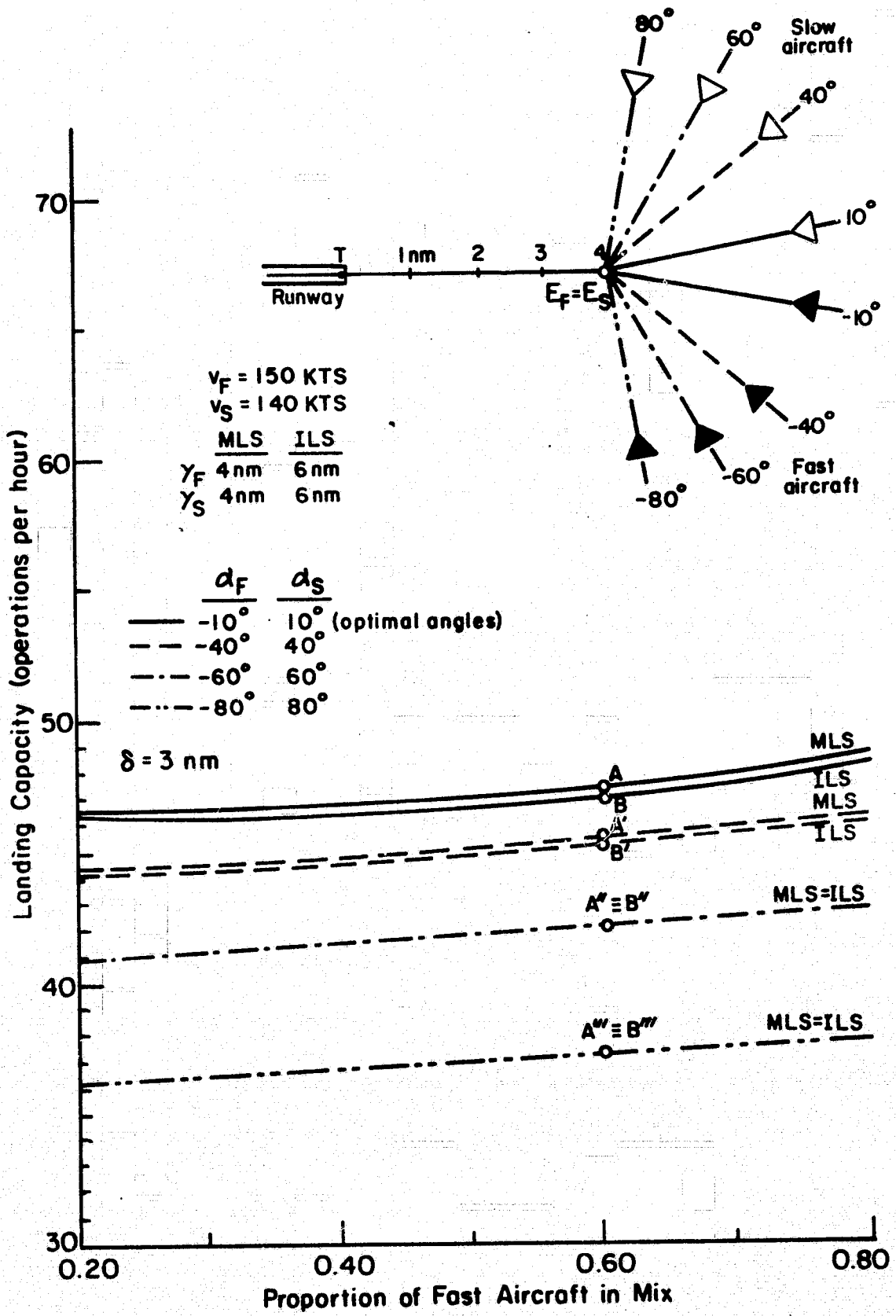
80°
60°
Slow aircraft
40°
10°
-10°
-40°
-60°
Fast aircraft
-80°
T
1nm
2
3
4
Runway
$E_F = E_S$
v_F = 150 KTS
v_S = 140 KTS
MLS ILS
γ_F 4nm 6nm
γ_S 4nm 6nm
d_F d_S
-10° 10° (optimal angles)
-40° 40°
-60° 60°
-80° 80°
δ = 3 nm
A
B
A'
B'
MLS
ILS
MLS
ILS
$A'' \equiv B''$
MLS=ILS
$A''' \equiv B'''$
MLS=ILS
Landing Capacity (operations per hour)
70
60
50
40
30
0.20
0.40
0.60
0.80
Proportion of Fast Aircraft in Mix

Figure 30

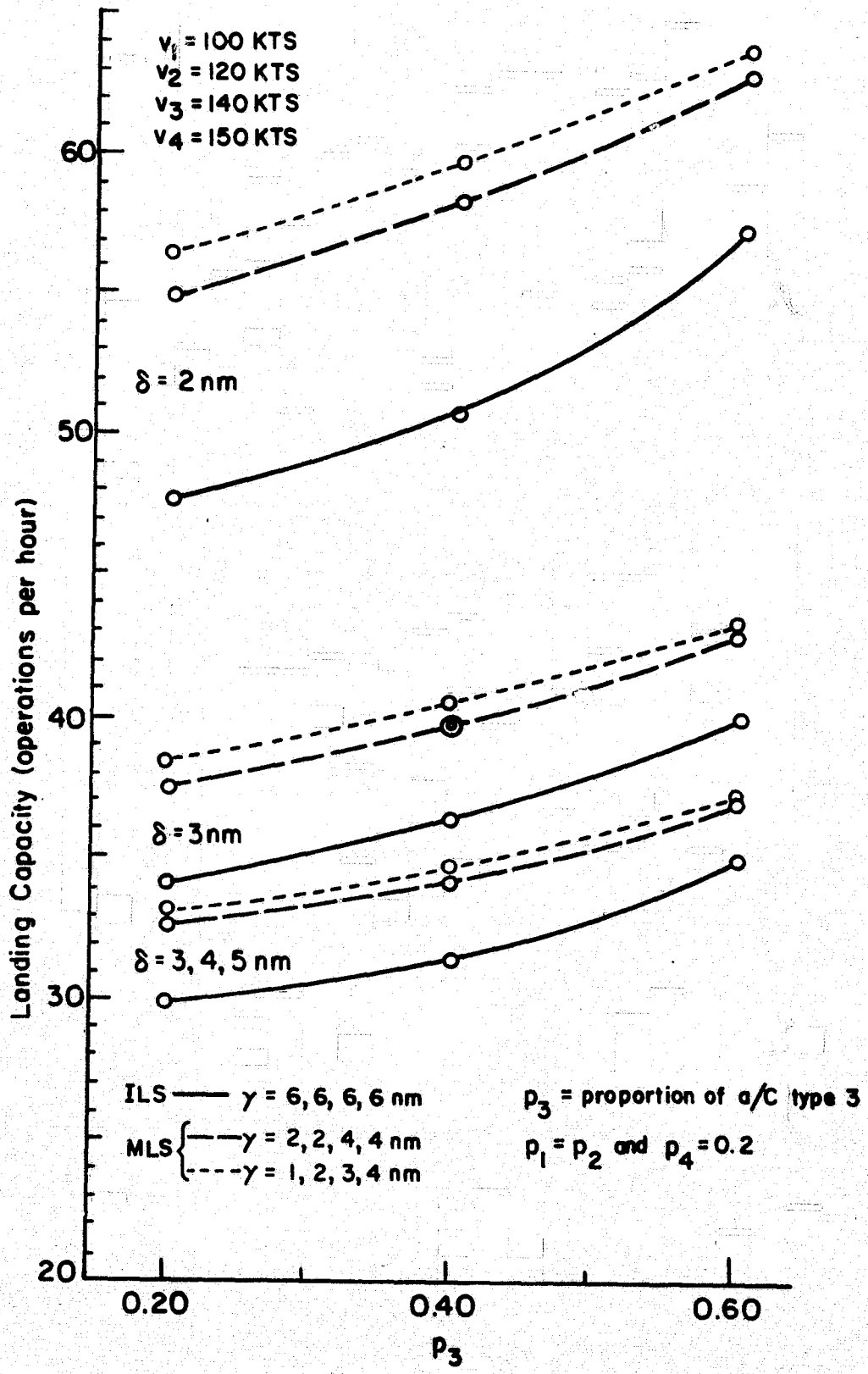
v_1 = 100 KTS
v_2 = 120 KTS
v_3 = 140 KTS
v_4 = 150 KTS
δ = 2 nm
δ = 3 nm
δ = 3, 4, 5 nm
Landing Capacity (operations per hour)
60
50
40
30
20
0.20
0.40
0.60
p_3
ILS —— γ = 6, 6, 6, 6 nm
MLS —— γ = 2, 2, 4, 4 nm
---- γ = 1, 2, 3, 4 nm
p_3 = proportion of a/C type 3
$p_1 = p_2$ and $p_4 = 0.2$

Figure 31

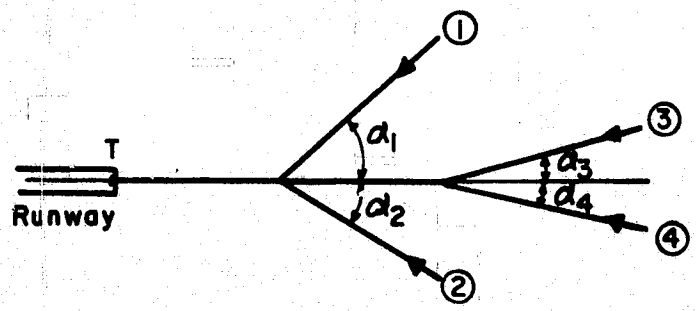

α_1	α_2	α_3	α_4	λ
40	-30	10	-10	39.887

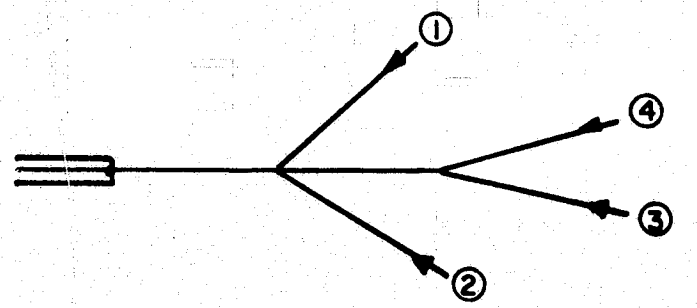

40 -30 -10 10 39.887

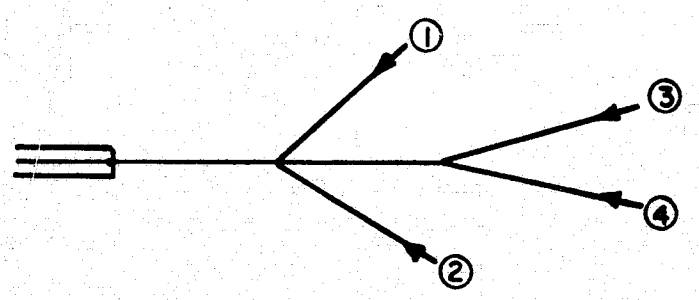

40 -30 20 -10 39.824

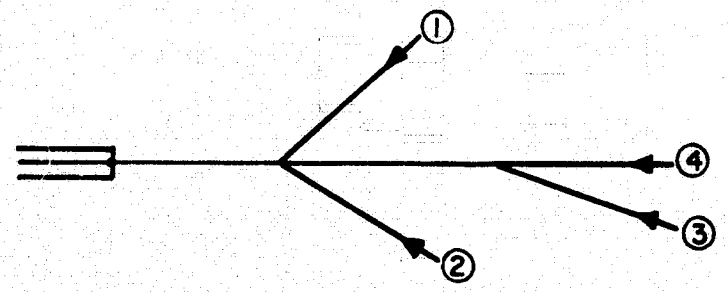

40 -30 -20 0 39.822

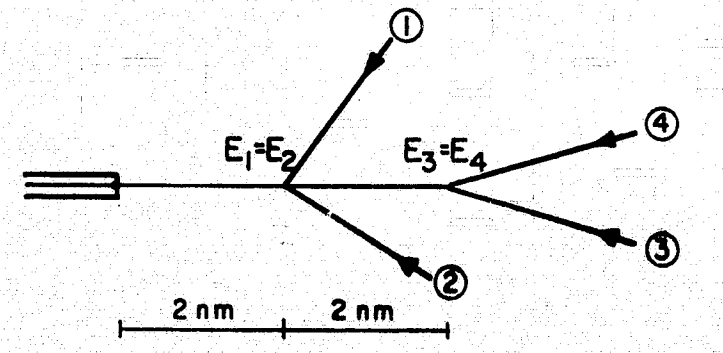

50 -30 -10 10 39.782

Figure 32

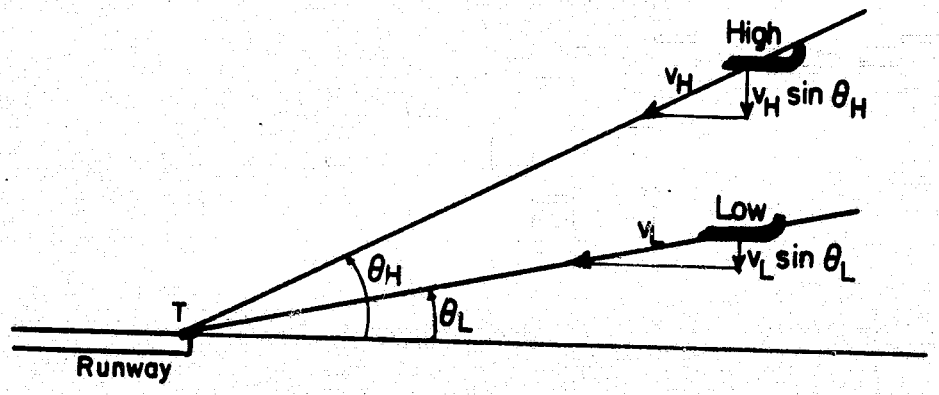
High
v_H
$v_H \sin \theta_H$
Low
v_L
$v_L \sin \theta_L$
θ_H
θ_L
T
Runway

Figure 33

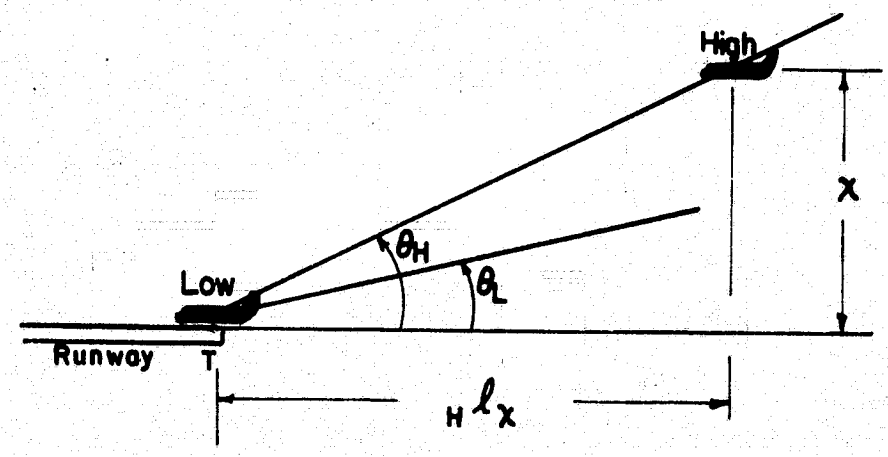

Figure 34

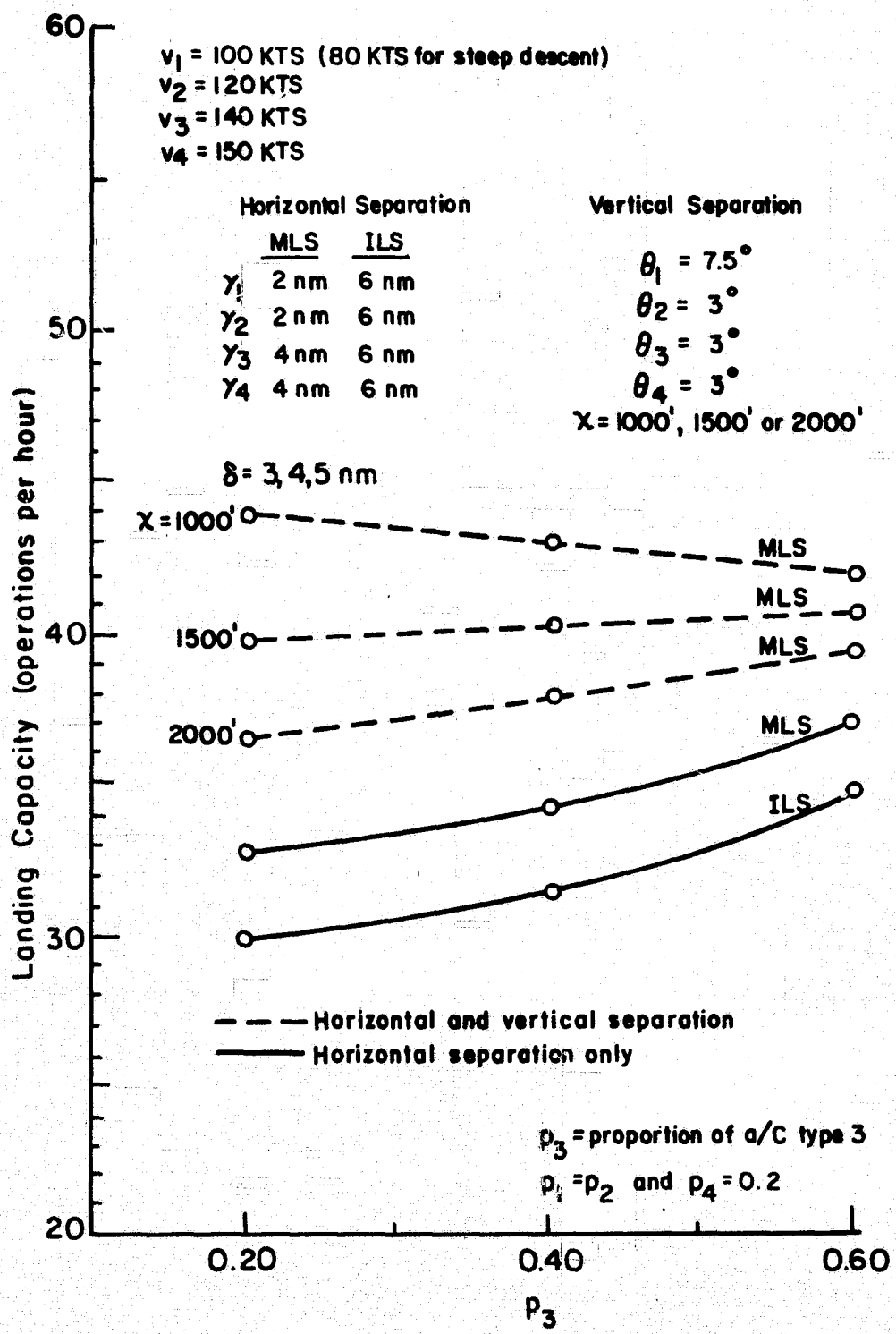
60
50
40
30
20
Landing Capacity (operations per hour)
v_1 = 100 KTS (80 KTS for steep descent)
v_2 = 120 KTS
v_3 = 140 KTS
v_4 = 150 KTS
Horizontal Separation
MLS ILS
γ_1 2 nm 6 nm
γ_2 2 nm 6 nm
γ_3 4 nm 6 nm
γ_4 4 nm 6 nm
Vertical Separation
θ_1 = 7.5°
θ_2 = 3°
θ_3 = 3°
θ_4 = 3°
χ = 1000', 1500' or 2000'
δ = 3, 4, 5 nm
χ = 1000'
1500'
2000'
MLS
MLS
MLS
MLS
ILS
Horizontal and vertical separation
Horizontal separation only
p_3 = proportion of a/C type 3
p_1 = p_2 and p_4 = 0.2
0.20
0.40
0.60
p_3

Figure 35

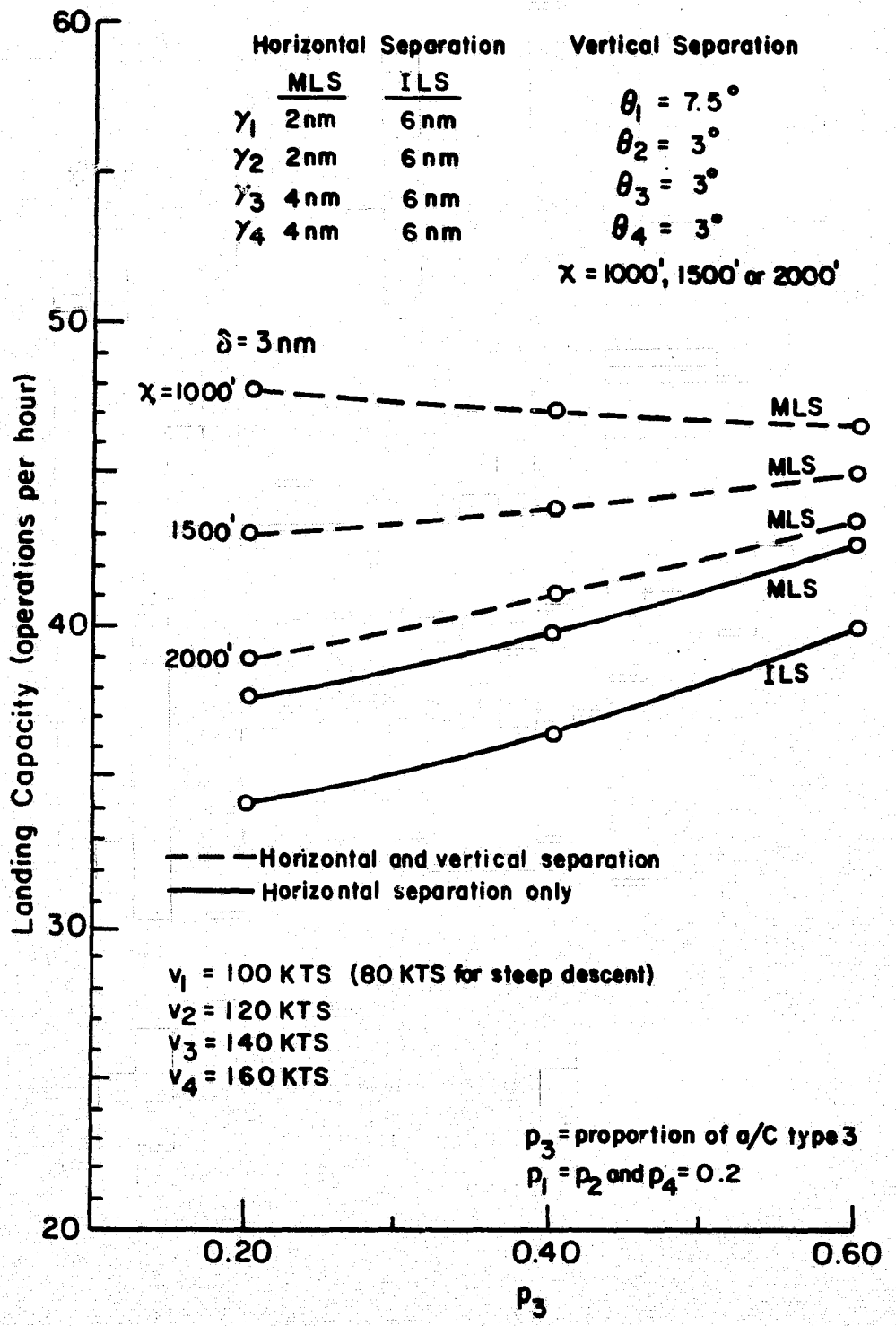
Horizontal Separation
MLS ILS
γ1 2nm 6nm
γ2 2nm 6nm
γ3 4nm 6nm
γ4 4nm 6nm
Vertical Separation
θ1 = 7.5°
θ2 = 3°
θ3 = 3°
θ4 = 3°
χ = 1000', 1500' or 2000'
δ = 3nm
χ=1000'
1500'
2000'
MLS
MLS
MLS
MLS
ILS
Horizontal and vertical separation
Horizontal separation only
v1 = 100 KTS (80 KTS for steep descent)
v2 = 120 KTS
v3 = 140 KTS
v4 = 160 KTS
p3 = proportion of a/C type 3
p1 = p2 and p4 = 0.2
Landing Capacity (operations per hour)
60
50
40
30
20
0.20
0.40
0.60
p3

Figure 36

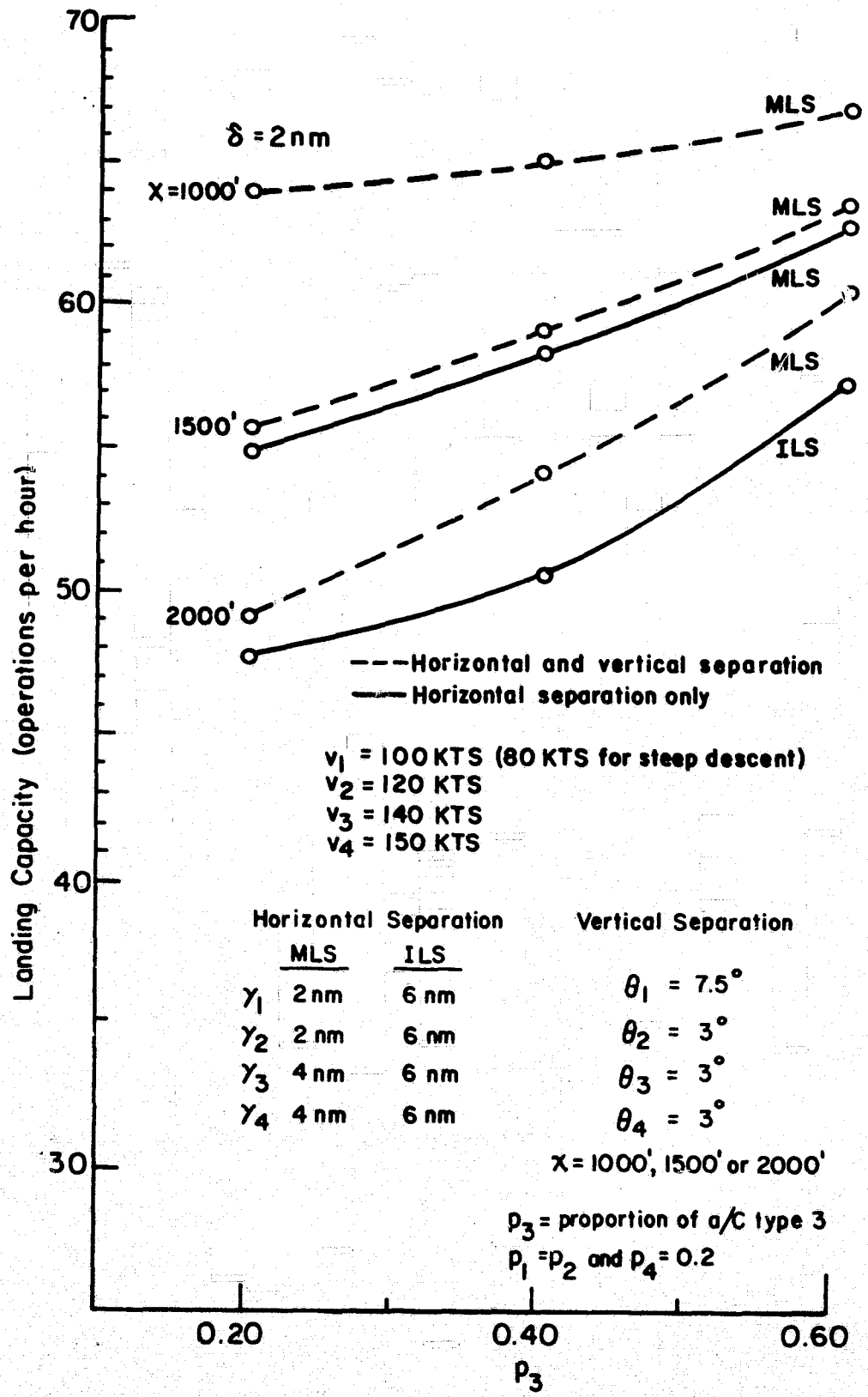
70
60
50
40
30
Landing Capacity (operations per hour)
δ = 2nm
X=1000'
1500'
2000'
MLS
MLS
MLS
MLS
ILS
---Horizontal and vertical separation
——Horizontal separation only
v1 = 100 KTS (80 KTS for steep descent)
v2 = 120 KTS
v3 = 140 KTS
v4 = 150 KTS
Horizontal Separation
MLS ILS
γ1 2nm 6 nm
γ2 2 nm 6 nm
γ3 4 nm 6 nm
γ4 4 nm 6 nm
Vertical Separation
θ1 = 7.5°
θ2 = 3°
θ3 = 3°
θ4 = 3°
X = 1000', 1500' or 2000'
p3 = proportion of a/C type 3
p1 = p2 and p4 = 0.2
0.20
0.40
0.60
p3

Figure 37

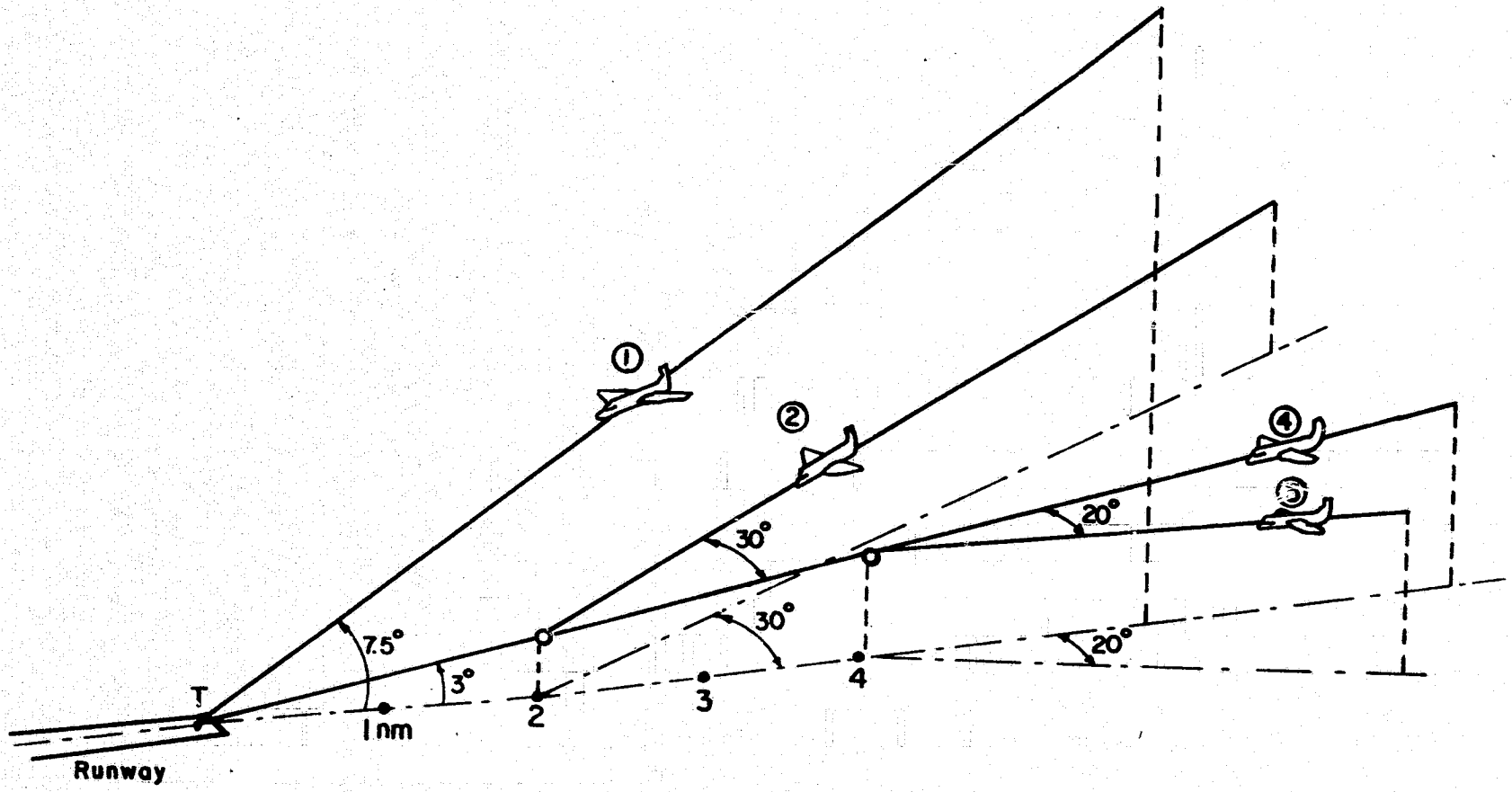

Figure 38

8. Glossary

Subscripts

i - aircraft type. This subscript can take numerical values 1, 2, ..., n, where 1 is the aircraft with the lowest approach speed. It can also take values F or S, denoting fast or slow aircraft in the case of only two aircraft types in the population.

ij - aircraft pair, consisting of two aircraft landing one after the other. i is the leading aircraft type; j is the trailing aircraft type. j can take all values that i takes (see the preceding paragraph).

Capital Letters

E - entry gate, point at which aircraft joins final straight approach path before landing.

E_i - entry gate, for aircraft of type i in the case of multiple approach paths.

T - runway threshold.

Small Letters

d(t) - distance between two aircraft measured on a straight line in horizontal plane. This distance is a function of time.

$d_{ij}(t)$ - distance d(t), for a pair of consecutively landing aircraft (i is the leading aircraft type and j is the trailing aircraft type).

$_1d_{ij}(t)$ - first segment of function $d_{ij}(t)$.

$_2d_{ij}(t)$ - second segment of function $d_{ij}(t)$.

${}^{3}d_{ij}(t)$ - third segment of function $d_{ij}(t)$.

${}_{ij}d_{o}$ - initial separation between aircraft i and j. This is the separation between the two aircraft at time, t = 0 (the moment when leading aircraft i reaches the beginning of the common straight approach path), measured along the path of trailing aircraft.

${}_{ij}\hat{d}_{om}$ - initial separation between aircraft i and j computed under the condition that the minimum of function $d_{ij}(t)$ is located as indicated by subscript m

m = 1 min $d_{ij}(t)$ occurs at the first segment of the function. ${}_{ij}\hat{d}_{01}$ is found from

$$ {}^{1}d_{ij}(t)\Big|_{t={}_{ij}t_1^*} = \delta_{ij} $$

m = 2 min $d_{ij}(t)$ occurs at the second segment of the function. ${}_{ij}\hat{d}_{02}$ is found from

$$ {}^{2}d_{ij}(t)\Big|_{t={}_{ij}t_2^*} = \delta_{ij} $$

m = 3 min $d_{ij}(t)$ occurs at the third segment of the function. ${}_{ij}\hat{d}_{03}$ is found from

$$ {}^{3}d_{ij}(t)\Big|_{t={}_{ij}t_3^*} = \delta_{ij} $$

m = 4 min $d_{ij}(t)$ occurs at the limit between the first and second segment of the function. ${}_{ij}\hat{d}_{04}$ is found from

$$ {}^{1}d_{ij}(t)\Big|_{t={}_{ij}t_4} = {}^{2}d_{ij}(t)\Big|_{t={}_{ij}t_4} = \delta_{ij} $$

m = 5 $\min d_{ij}(t)$ occurs at the upper limit of the domain of the function for $t = {}_{ij}t_5$ (i.e., leading aircraft i lands) ${}_{ij}\hat{d}_{05}$ is found, therefore, from

$$d_{ij}(t)\Big|_{t={}_{ij}t_5} = \delta_{ij}$$

p_i - proportion of aircraft type i in the population.

p_{ij} - probability of the pair ij aircraft occurring in the vehicle stream, i.e., aircraft type j landing after aircraft type i .

t - time

Note: t = 0 indicates for any pair of consecutively landing aircraft the time when leading aircraft reaches the first point on the common straight approach path (on the extended runway centerline).

t_{ij} - interarrival time at the runway threshold (time separation over the threshold) between leading aircraft of type i and trailing aircraft of type j.

$a^t{}_{ij}$ - time separation over the threshold dictated by the minimum separation rules in the air.

$r^t{}_{ij}$ - time separation over the threshold dictated by the runway occupancy time.

$\bar{t}$ - expected interarrival time at the threshold.

${}_{ij}t^*_1$ - time at which ${}_1d_{ij}(t)$ reaches minimum.

${}_{ij}t^*_2$ - time at which ${}_2d_{ij}(t)$ reaches minimum.

${}_{ij}t^*_3$ - time at which ${}_3d_{ij}(t)$ reaches minimum.

$_{ij}t_1^{1*}$ - time at which $_1d_{ij}(t)$ reaches minimum, computed for $_{ij}\hat{d}_o = {}_{ij}\hat{d}_{01}$.

$_{ij}t_1^{2*}$ - time at which $_1d_{ij}(t)$ reaches minimum, computed for $_{ij}\hat{d}_o = {}_{ij}\hat{d}_{02}$.

etc.

$_{ij}t_3^{5*}$ - time at which $_3d_{ij}(t)$ reaches minimum, computed for $_{ij}\hat{d}_o = {}_{ij}\hat{d}_{05}$.

in general

$_{ij}t^{k*}$ - time at which $d_{ij}(t)$ reaches minimum, computed for $_{ij}\hat{d}_0 = {}_{ij}\hat{d}_{ok}$.

$_{ij}t_4$ - time limit between the first and the second segment ($_1d_{ij}(t)$ and $_2d_{ij}(t)$) of function $d_{ij}(t)$.

$_{ij}t_5$ - time at which first of two aircraft in an aircraft pair lands

$$t_{ij} = \frac{\gamma_{ij}}{v_i}$$

$_{ij}t_6$ - time limit between the second and the third segment ($_2d_{ij}(t)$ and $_3d_{ij}(t)$) of function $d_{ij}(t)$.

v_i - approach speed of aircraft of type i.

Greek Letters

α_i - angle of entry of the aircraft of type i to the extended runway centerline measured relative to that line. Positive anti-clockwise, negative clockwise.

α_R - relative angle of entry for two aircraft of different types

$$\alpha_R = |\alpha_i - \alpha_j| \qquad i \neq j$$

e.g.,

$$\alpha_R = |\alpha_S - \alpha_F|$$

β - difference in the necessary lengths of straight final approaches along the extended runway centerline for fast (F) and slow (S) aircraft

$$\beta = \gamma_F - \gamma_S$$

γ - length of the straight common final approach along the extended runway centerline, for ILS case.

γ_i - necessary length of straight final approach for aircraft type i.

γ_{ij} - length of the common straight final approach for aircraft type i and type j, for MLS case

$$\gamma_{ij} = \min(\gamma_i, \gamma_j)$$

δ_{ij} - minimum horizontal separation between aircraft type i followed by aircraft type j, required by ATC rules.

θ_i - angle of descent in the final approach of aircraft of type i.

λ - runway landing capacity.

μ - ratio of approach speeds of slow (S) and fast (F) aircraft.

$$\mu = \frac{v_S}{v_F} \leq 1$$

χ - minimum vertical separation between two consecutively landing aircraft.

9. References

1. Harris Richard M. Models for Runway Capacity Analysis. Springfield, Va.: NTIS, December 1972. 140 p. (AD 760 637) (Report No. FAA-EM-73-5) (MITRE Corp. MTR 4102 Rev. 2)

2. Douglas Aircraft Company, Peat, Marwick, Mitchell & Co., et al. Procedures for Determination of Airport Capacity (Volumes I and II). Springfield, Va.: NTIS, April 1973. 184 p. (Report No. FAA-RD-73-11I)

3. Burrows C. et al. Preliminary Assessment of the Microwave Landing System Requirements for STOL Operations. Moffett Field, California: NASA, Ames Research Center, October 1973. 151 p. (NASA TM X-62.310)

4. Tonkin A.J. "Canadian Experience with Short Haul Air Transport". Paper presented at International Air Transportation Conference of American Society of Civil Engineers held in San Francisco, 24-26 March 1975. 5 p.

10. Bibliography

1. Adams G.D. Evaluation of STOL Instrument Landing System (TALAR IV). Atlantic City, New Jersey: NAFEC, April 1972. 32 p. (Report No. FAA-RD-72-15)

2. Adams G.D. Evaluation of STOL Modular Instrument Landing System (MODILS). Atlantic City, New Jersey: NAFEC, May 1972. 53 p. (Report No. FAA-RD-72-4)

3. Baran G. et al. Airspace/Airport Capacity Increase Potential. Renton, Wash.: Boeing Co. Commercial Airplane Division, 1969. 66 p.

4. Barr A.J. The Effect of Microwave Instrument Landing Systems on Airport Runway Capacity. Berkeley: The Institute of Transportation and Traffic Engineering, University of California, August 1973. 20 p. (Graduate Report)

5. Blake C.L. and Clark J.E. "Potential and Prospects of Increasing Capacity with New Aids to Navigation and Air Traffic Control Procedures". Paper presented at International Air Transportation Conference of American Society of Civil Engineers, held in San Francisco, 24-26 March 1975. 7 p.

6. Blumstein A. An Analytical Investigation of Airport Capacity. Buffalo, New York: Cornell Aeronautical Laboratory, Inc., June 1960 (Report No. TA-1358-8-1)

7. Brown D.A. "MLS May Extend Commuter Schedules", Aviation Week and Space Technology, V 98, No. 10, March 5, 1975, pp 42-46

8. Brown R. "Battle for the New Airport Landing Aid", New Scientist, V 60, No. 866, October 1973

9. Burrows C. et al. Preliminary Assessment of the Microwave Landing System Requirements for STOL Operations. Moffett Field, California: NASA, Ames Research Center, October 1973. 151 p. (NASA TM X-62.310)

10. Cherry G.W., MacKinnon D. and DeWolf B. A New Approach and Landing System: Help for Our Troubled Terminal Areas. Cambridge, Massachusetts: Charles Stark Draper Laboratory, MIT, 1970. 16 p. (Report R-654)

11. Crane H.L., Yenni K.R. and Fisher B.D. Flight Investigation of VFR and IFR Landing Approach Characteristics and Terminal Area Airspace Requirements for Light STOL Airplane. Hampton, Va.: NASA, Langley Research Center, June 1974. 38 p. (Report No. NASA TM X-3008)

12. Douglas Aircraft Company, Peat, Marwick, Mitchell & Co., et al. Procedures for Determination of Airport Capacity (Volumes I and II). Springfield, Va.: NTIS, April 1973. 184 p. (Report No. FAA-RD-73-11I)

13. Duning K.E., Hemesath N.B., Hickok C.W., Lammers D.G. and Goemaat M.L. Curved Approach Path Study. Cedar Rapids, Iowa: Collins Radio Company, Avioniscs Division, March 1973. 127 p. (Report No. FAA-RD-72-143)

14. Farrington F.D. A Simulation of a Linear Optimal Digital Autopilot Controlling an STOL Aircraft. Ph.D. Thesis, Indiana: Purdue University, June 1972. 170 p.

15. Harris Richard M. Models for Runway Capacity Analysis. Washington D.C.: The MITRE Corporation, October 1969. 125 p. (Technical Report MTR 4102)

16. Harris Richard M. Models for Runway Capacity Analysis. Springfield, Va.: NTIS, December 1972. 140 p. (AD 760 637) (Report No. FAA-EM-73-5) (MITRE Corp. MTR 4102 Rev. 2)

17. Hart E.D. "A Family of Scanning-Beam Approach/Landing Systems is Proposed for Maximum Operational Flexibility", ICAO Bulletin, V 29, No. 3, March 1974. pp 17-19

18. Hauer E. "Runway Capacity". Readings in Airport Planning. Chapter 5. pp 111-157. Center for Urban and Community Studies, Department of Civil Engineering, University of Toronto, 1972

19. Hockaday Stephen L.M. and Kanafani A.K. "Developments in Airport Capacity Analysis", Transportation Research, V 8, No. 3, August 1974, pp 171-180

20. Hughes N.H. "The Influence of the Future Landing Guidance System on Integration of Short Take-Off and Landing and Conventional Air Traffic at a Major Airport". Paper presented at the 14th Meeting of the Guidance and Control Panel of AGARD held in Edinburgh, Scotland, 26-29 June 1972. 17 p. (AGARD Conference Proceedings No. 105)

21. International Civil Aviation Organization. "ICAO Panel Appraises New Non-Visual Approach/Landing System Concepts", ICAO Bulletin, V 29, No. 3, March 1974. pp 14-16

22. McLean J.D. and Tobias L. "An Interactive Real Time Simulation for Scheduling and Monitoring of STOL Aircraft in the Terminal Area", Journal of Aircraft, V 10, No. 6, June 1973. pp 372-378

23. The MITRE Corporation. An Extension of the Throughput Runway Capacity Methodology to Include Multiple Glide Path Heights and Angles. Springfield, Virginia: NTIS, May 1973. 58 p. (AD 763 142) (Report No. FAA-Q5-73-3, V) (MITRE Corp. MTR 6338)

24. Noll R.B., Zvara J. and Simpson R.W. "Analysis of Terminal ATC Systems Operations". Paper presented at the 14th meeting of the Guidance and Control Panel of AGARD held in Edinburgh, Scotland, 26-29 June 1972. 15 p. (AGARD Conference Proceedings No. 105)

25. Odoni A.R. Analytical Models for Air Traffic Control, Cambridge: Flight Transportation Laboratory, MIT, March 1972. 49 p. (Course Notes)

26. Odoni A.R. "Modeling for Air Traffic Control Systems". Paper prepared for ORSA Conference in Dallas, May 1971. 26 p.

27. Park S.K., Straeter T.A. and Hogge J.E. "An Analytic Study of Near Terminal Area Optimal Sequencing and Flow Control Techniques". Paper presented at the 14th meeting of the Guidance and Control Panel of AGARD held in Edinburgh, Scotland, 26-29 June 1972. 18 p. (AGARD Conference Proceedings No. 105)

28. Rouse W. An Appraisal of the Problems of the Air Traffic Control System. Cambridge, Mass.: Air Traffic Control Systems, MIT, 1970. 54 p. Distributed by NTIS, Springfield, Va. N70-35713

29. Schmidt D.K. Optimal Multiple Aircraft Control for Terminal Area Approach. Ph.D. Thesis, Indiana: Purdue University, December 1972. 163 p.

30. Tonkin A.J. "Canadian Experience with Short Haul Air Transport". Paper presented at International Air Transportation Conference of American Society of Civil Engineers held in San Francisco, 24-26 March 1975. 5 p.

31. U.S. Air Force. Institute of Technology. Microwave Landing System Integration Study. Wright-Patterson Air Force Base, Ohio, March 1974. 3 vols.

32. U.S. Federal Aviation Administration. FAA Report on Airport Capacity. Volumes I and II. Washington D.C.: January 1974. 96 + 293 p. (Report No. FAA-EM-74-5, I and II)

33. U.S. Federal Aviation Administration. International Microwave Landing System (MLS) Symposium (Proceedings). Washington D.C., Nov. 30, Dec. 3-4, 1973. 471 p. (FAA-RD-74-65)

34. U.S. Federal Aviation Administration. Terminal Air Traffic Control. Washington D.C., January 1973. 259 p. (FAA Handbook 7110.8C)

35. U.S. Federal Aviation Administration. United States Standard for Terminal Instrument Procedures (TERPS). Washington D.C., February 1970 (FAA Handbook 8260.3A)

36. Welp D.W., Brown R.A., Ullman D.G. and Kuhner M.B. Effectiveness Evaluation of STOL Transport Operations. Columbus, Ohio: Battelle Columbus Laboratories, February 1974. 195 p.

37. Wheeldon Ronald and Fourbonne P. "MLS: The Next Generation Landing Aid", ICAO Bulletin, Vol. 27, No. 3, March 1972. pp 20-23

38. White J.S. Landing Rates for Mixed STOL and CTOL Traffic. Moffett Field, California, NASA, Ames Research Center, April 1974. 76 p.

39. Wilhelm W.E. and Schmidt J.W. "A View of Air Traffic Control in Future Terminal Areas", Journal of Aircraft, V 10, No. 6, June 1973. pp 366-372

Appendix

A. Flow Charts

A.1 Algorithm for $_{FS}\hat{d}_o$

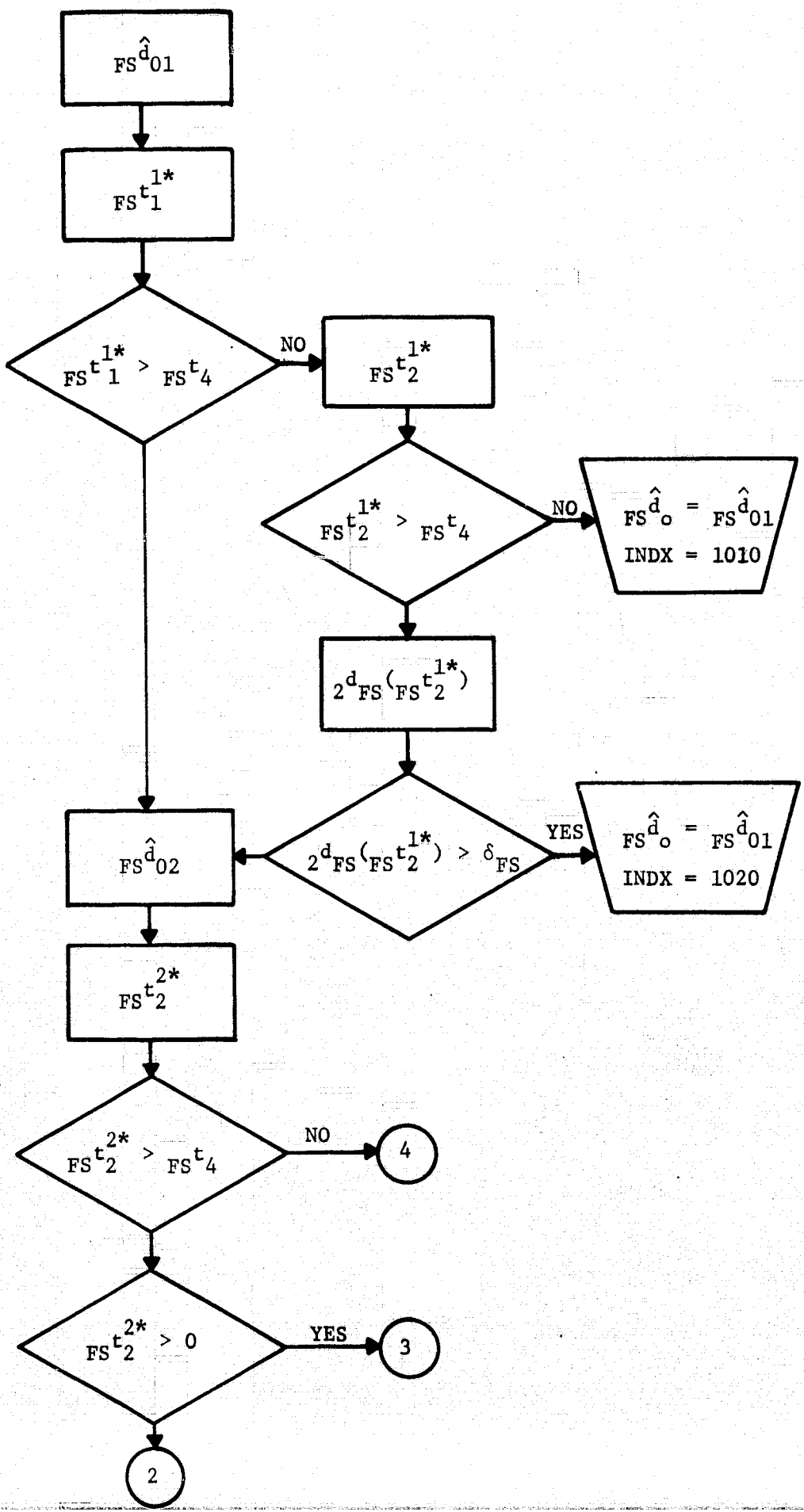
$FS\hat{d}_{01}$
$FS t_1^{1*}$
$FS t_1^{1*} > FS t_4$
NO
$FS t_2^{1*}$
$FS t_2^{1*} > FS t_4$
NO
$FS\hat{d}_o = FS\hat{d}_{01}$
INDX = 1010
$2^{d_{FS}(FS t_2^{1*})}$
$2^{d_{FS}(FS t_2^{1*})} > \delta_{FS}$
YES
$FS\hat{d}_o = FS\hat{d}_{01}$
INDX = 1020
$FS\hat{d}_{02}$
$FS t_2^{2*}$
$FS t_2^{2*} > FS t_4$
NO
4
$FS t_2^{2*} > 0$
YES
3
2

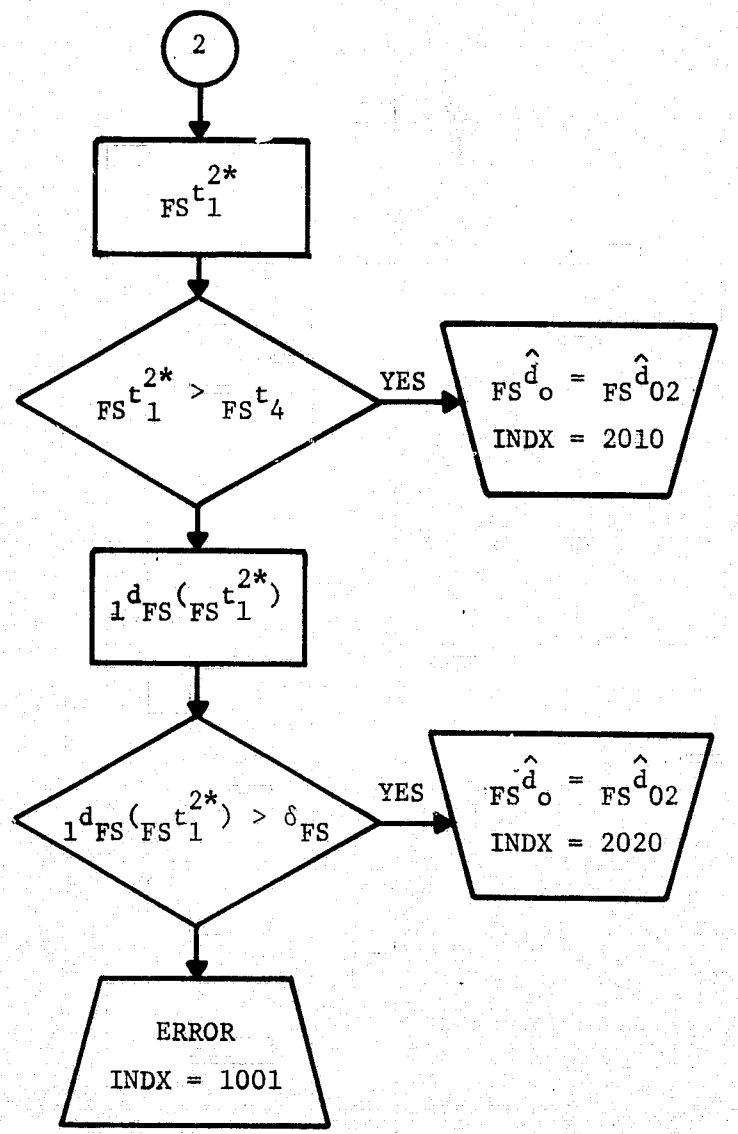
2
$FS^{t}_{1}^{2*}$
$FS^{t}_{1}^{2*} > FS^{t}_{4}$
YES
$FS\hat{d}_o = FS\hat{d}_{02}$
INDX = 2010
$1^{d}_{FS}(FS^{t}_{1}^{2*})$
$1^{d}_{FS}(FS^{t}_{1}^{2*}) > \delta_{FS}$
YES
$FS\hat{d}_o = FS\hat{d}_{02}$
INDX = 2020
ERROR
INDX = 1001

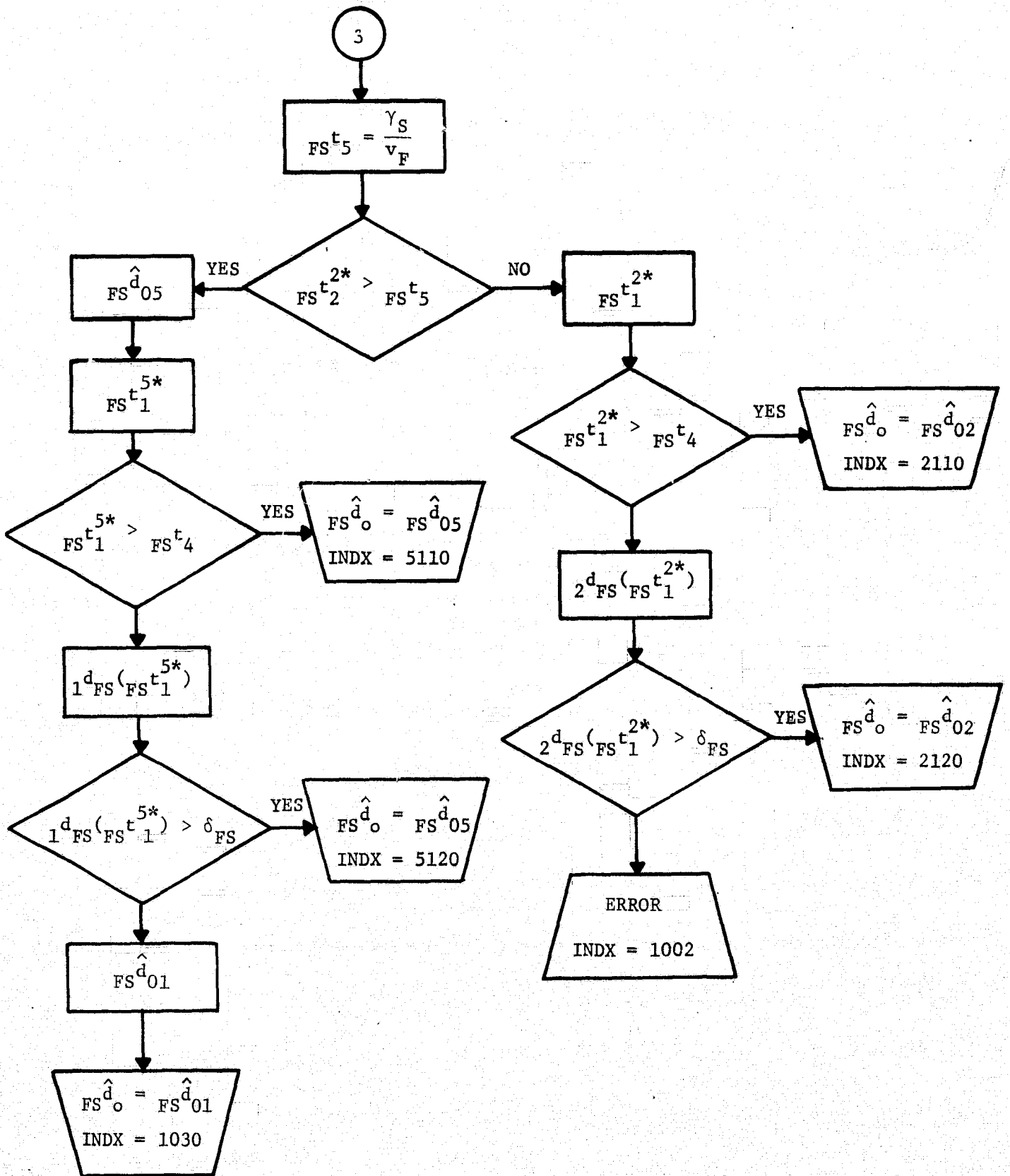
3
$FS^{t}5 = \frac{\gamma_S}{v_F}$
$FS^{t}2^{2*} > FS^{t}5$
YES
NO
$FS^{\hat{d}}05$
$FS^{t}1^{5*}$
$FS^{t}1^{5*} > FS^{t}4$
YES
$FS^{\hat{d}}o = FS^{\hat{d}}05$
INDX = 5110
$1^{d}FS(FS^{t}1^{5*})$
$1^{d}FS(FS^{t}1^{5*}) > \delta_{FS}$
YES
$FS^{\hat{d}}o = FS^{\hat{d}}05$
INDX = 5120
$FS^{\hat{d}}01$
$FS^{\hat{d}}o = FS^{\hat{d}}01$
INDX = 1030
$FS^{t}1^{2*}$
$FS^{t}1^{2*} > FS^{t}4$
YES
$FS^{\hat{d}}o = FS^{\hat{d}}02$
INDX = 2110
$2^{d}FS(FS^{t}1^{2*})$
$2^{d}FS(FS^{t}1^{2*}) > \delta_{FS}$
YES
$FS^{\hat{d}}o = FS^{\hat{d}}02$
INDX = 2120
ERROR
INDX = 1002

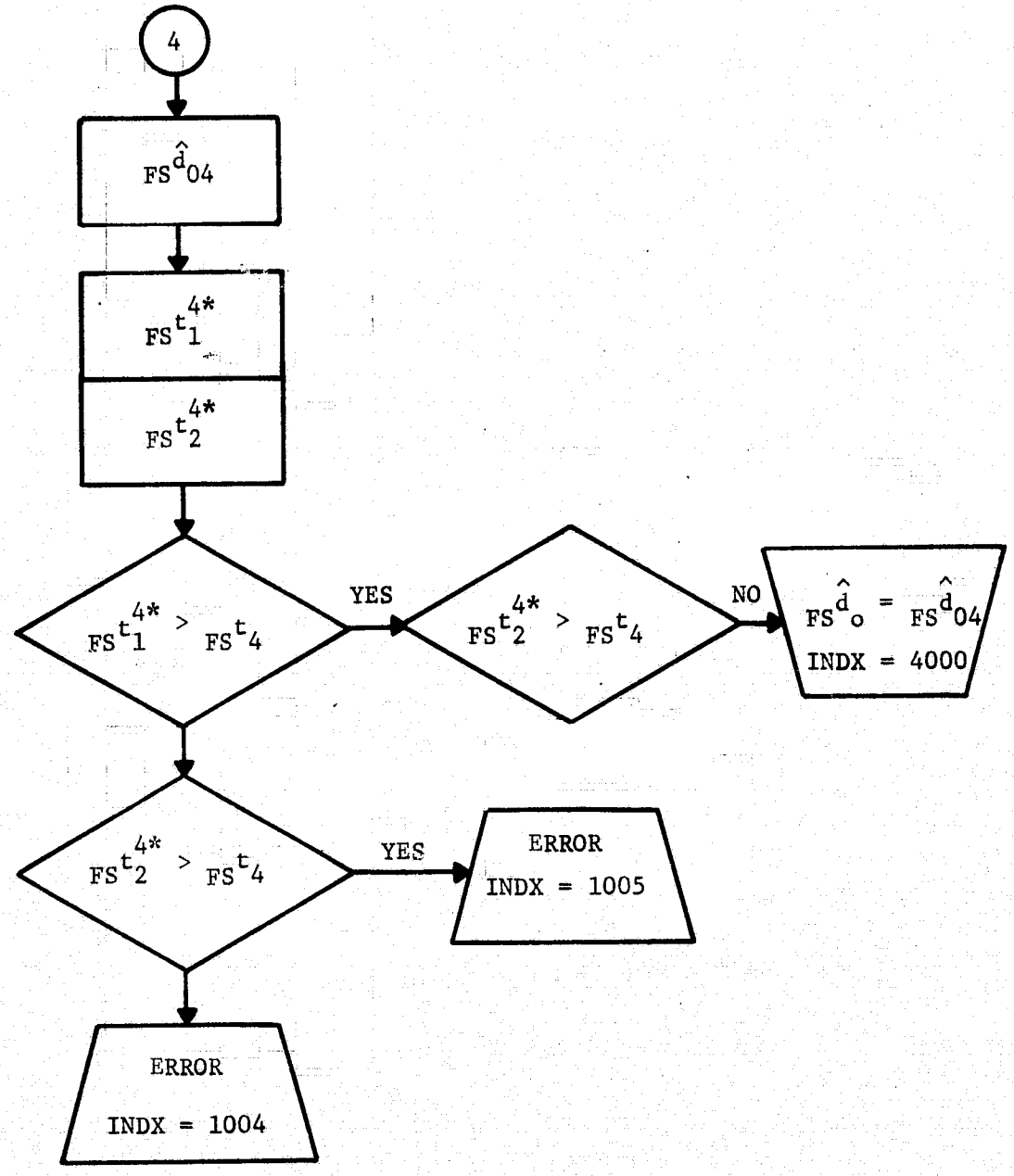
4
$FS\hat{d}_{04}$
$FS^{t}_{1}{}^{4*}$
$FS^{t}_{2}{}^{4*}$
$FS^{t}_{1}{}^{4*} > FS^{t}_{4}$
YES
$FS^{t}_{2}{}^{4*} > FS^{t}_{4}$
NO
$FS\hat{d}_{o} = FS\hat{d}_{04}$
INDX = 4000
$FS^{t}_{2}{}^{4*} > FS^{t}_{4}$
YES
ERROR
INDX = 1005
ERROR
INDX = 1004

Notes

1. It can be shown by geometrical proofs that all of the exits from the algorithm shown as "ERROR" cannot occur, if the input values of the variables and parameters are correct. However, such exits are preserved in the programs to facilitate location of eventual errors in programming or errors in the input data.
2. Index "INDX" describes the shape of the function $d_{FS}(t)$ and shows the range of this function where minimum separation between the two aircraft occurs. The key to values of "INDX" is given in the two following figures.

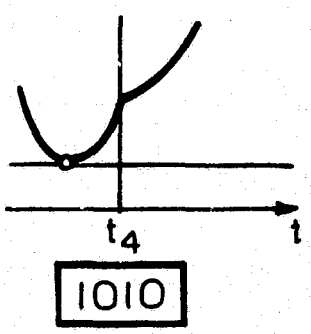

1010

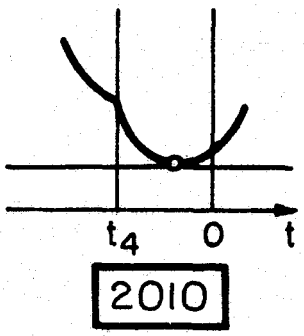

2010

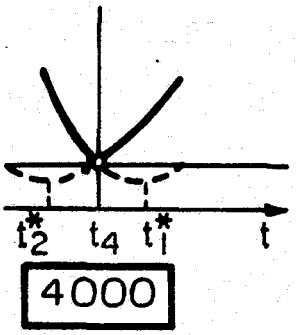

4000

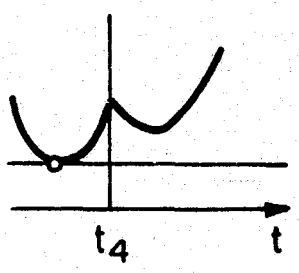

1020

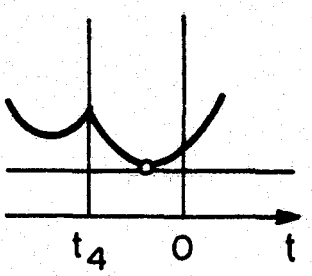

2020

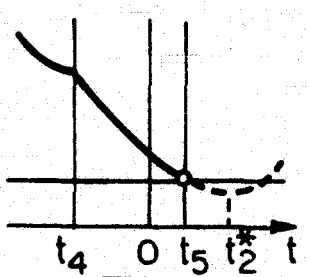

5110

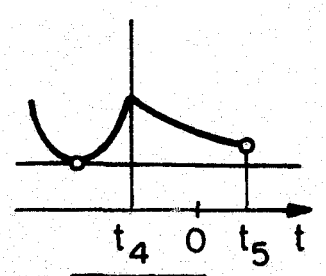

1030

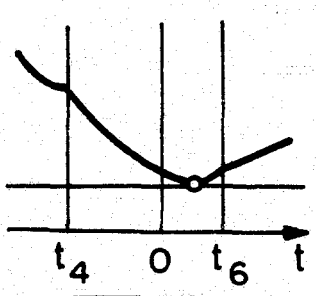

2110

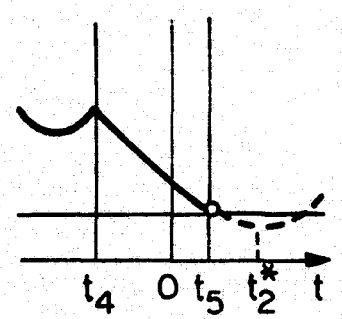

5120

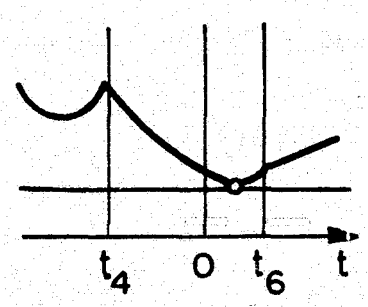

2120

Function $d_{FS}(t)$

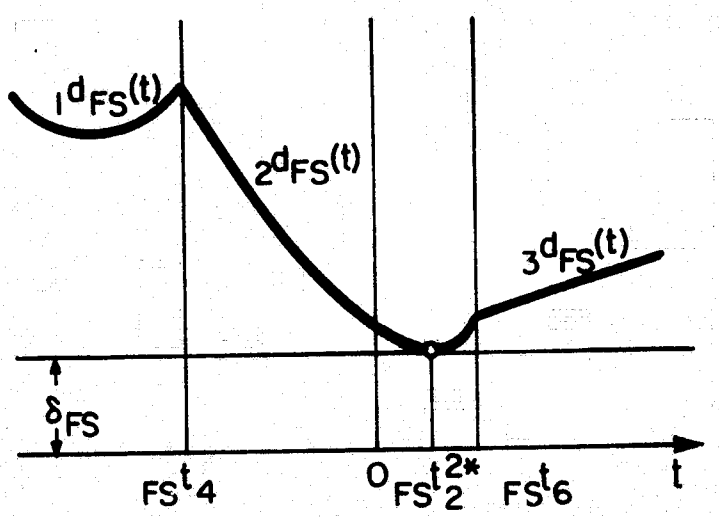

Detail of $d_{FS}(t)$ -- 2120

A.2 Algorithm for $_{SF}\hat{d}_o$

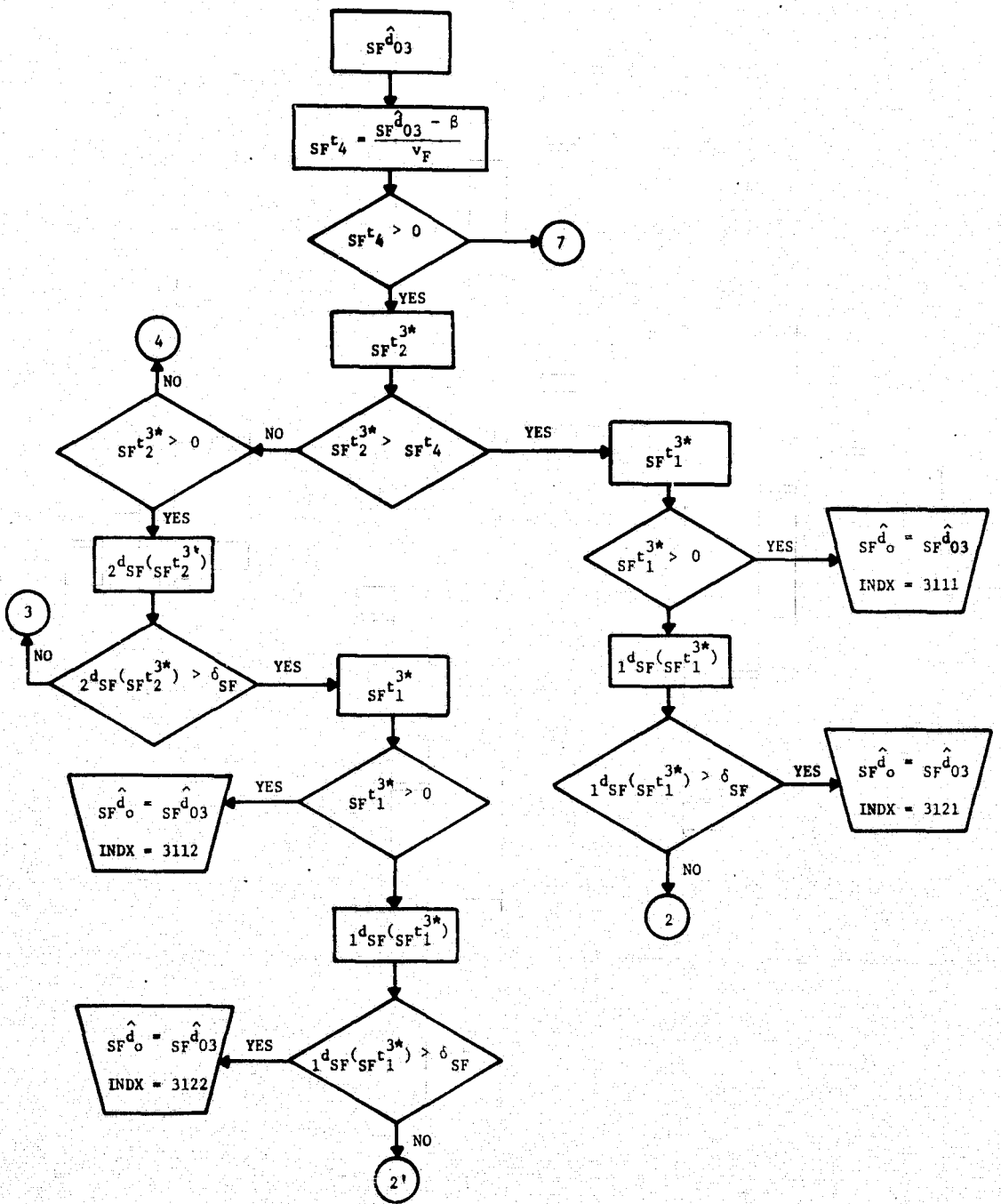
$SF\hat{d}_{03}$
$SF^{t}_{4} = \frac{SF\hat{d}_{03} - \beta}{v_F}$
$SF^{t}_{4} > 0$
7
YES
$SF^{t}_{2}{}^{3*}$
4
NO
$SF^{t}_{2}{}^{3*} > 0$
NO
$SF^{t}_{2}{}^{3*} > SF^{t}_{4}$
YES
$SF^{t}_{1}{}^{3*}$
YES
$2^{d}_{SF}(SF^{t}_{2}{}^{3*})$
3
NO
$2^{d}_{SF}(SF^{t}_{2}{}^{3*}) > \delta_{SF}$
YES
$SF^{t}_{1}{}^{3*}$
$SF^{t}_{1}{}^{3*} > 0$
YES
$SF\hat{d}_{o} = SF\hat{d}_{03}$
INDX = 3112
$1^{d}_{SF}(SF^{t}_{1}{}^{3*})$
$SF^{t}_{1}{}^{3*} > 0$
YES
$SF\hat{d}_{o} = SF\hat{d}_{03}$
INDX = 3111
$1^{d}_{SF}(SF^{t}_{1}{}^{3*})$
$1^{d}_{SF}(SF^{t}_{1}{}^{3*}) > \delta_{SF}$
YES
$SF\hat{d}_{o} = SF\hat{d}_{03}$
INDX = 3121
NO
2
$1^{d}_{SF}(SF^{t}_{1}{}^{3*})$
$SF\hat{d}_{o} = SF\hat{d}_{03}$
INDX = 3122
YES
$1^{d}_{SF}(SF^{t}_{1}{}^{3*}) > \delta_{SF}$
NO
2'

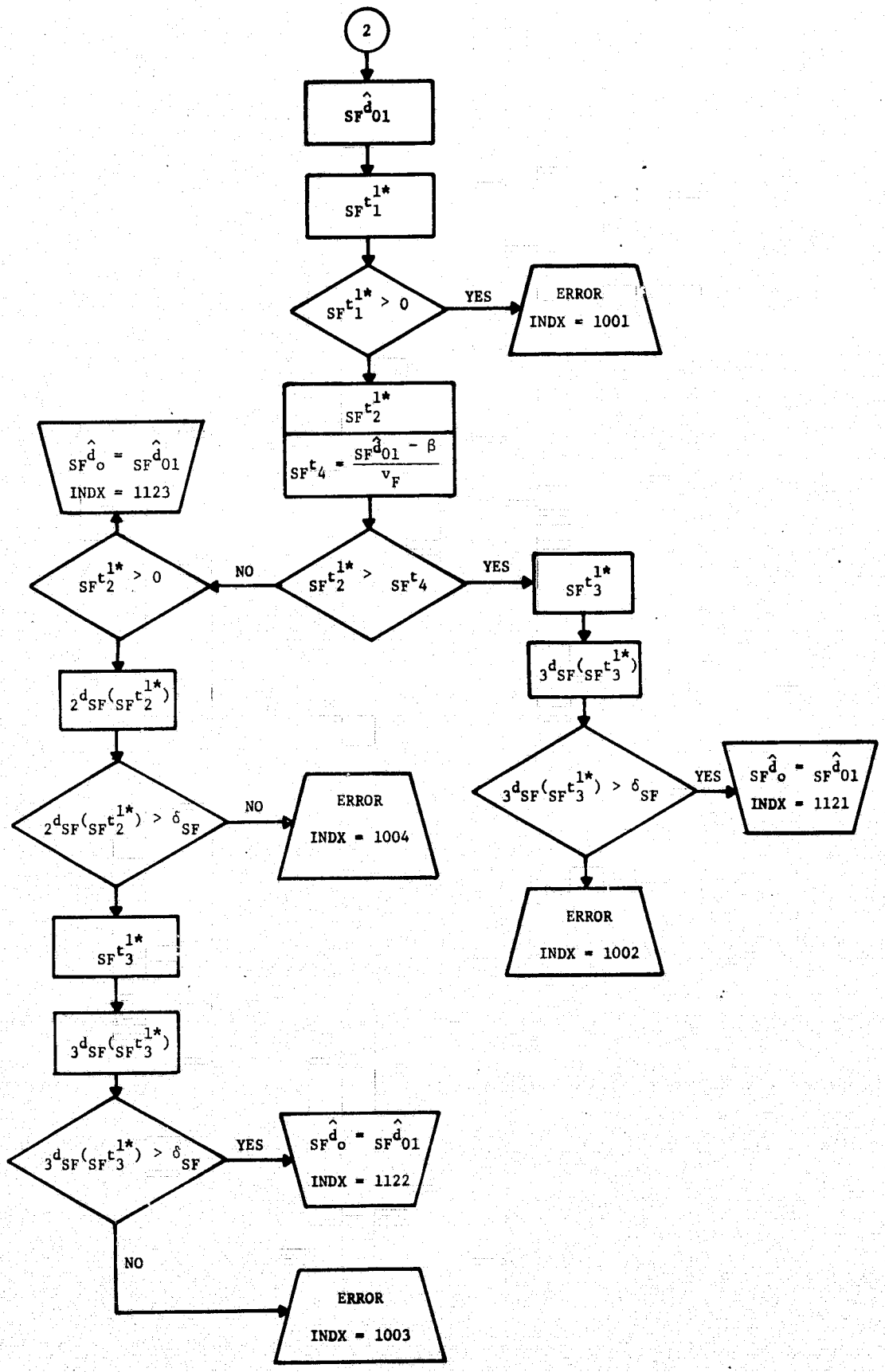
2
$SF\hat{d}_{01}$
$SF t_1^{1*}$
$SF t_1^{1*} > 0$
YES
ERROR
INDX = 1001
$SF t_2^{1*}$
$SF t_4 = \frac{SF\hat{d}_{01} - \beta}{v_F}$
$SF t_2^{1*} > SF t_4$
YES
NO
$SF t_3^{1*}$
$3^d SF(SF t_3^{1*})$
$SF\hat{d}_o = SF\hat{d}_{01}$
INDX = 1123
$SF t_2^{1*} > 0$
$2^d SF(SF t_2^{1*})$
$2^d SF(SF t_2^{1*}) > \delta_{SF}$
NO
ERROR
INDX = 1004
$3^d SF(SF t_3^{1*}) > \delta_{SF}$
YES
$SF\hat{d}_o = SF\hat{d}_{01}$
INDX = 1121
ERROR
INDX = 1002
$SF t_3^{1*}$
$3^d SF(SF t_3^{1*})$
$3^d SF(SF t_3^{1*}) > \delta_{SF}$
YES
$SF\hat{d}_o = SF\hat{d}_{01}$
INDX = 1122
NO
ERROR
INDX = 1003

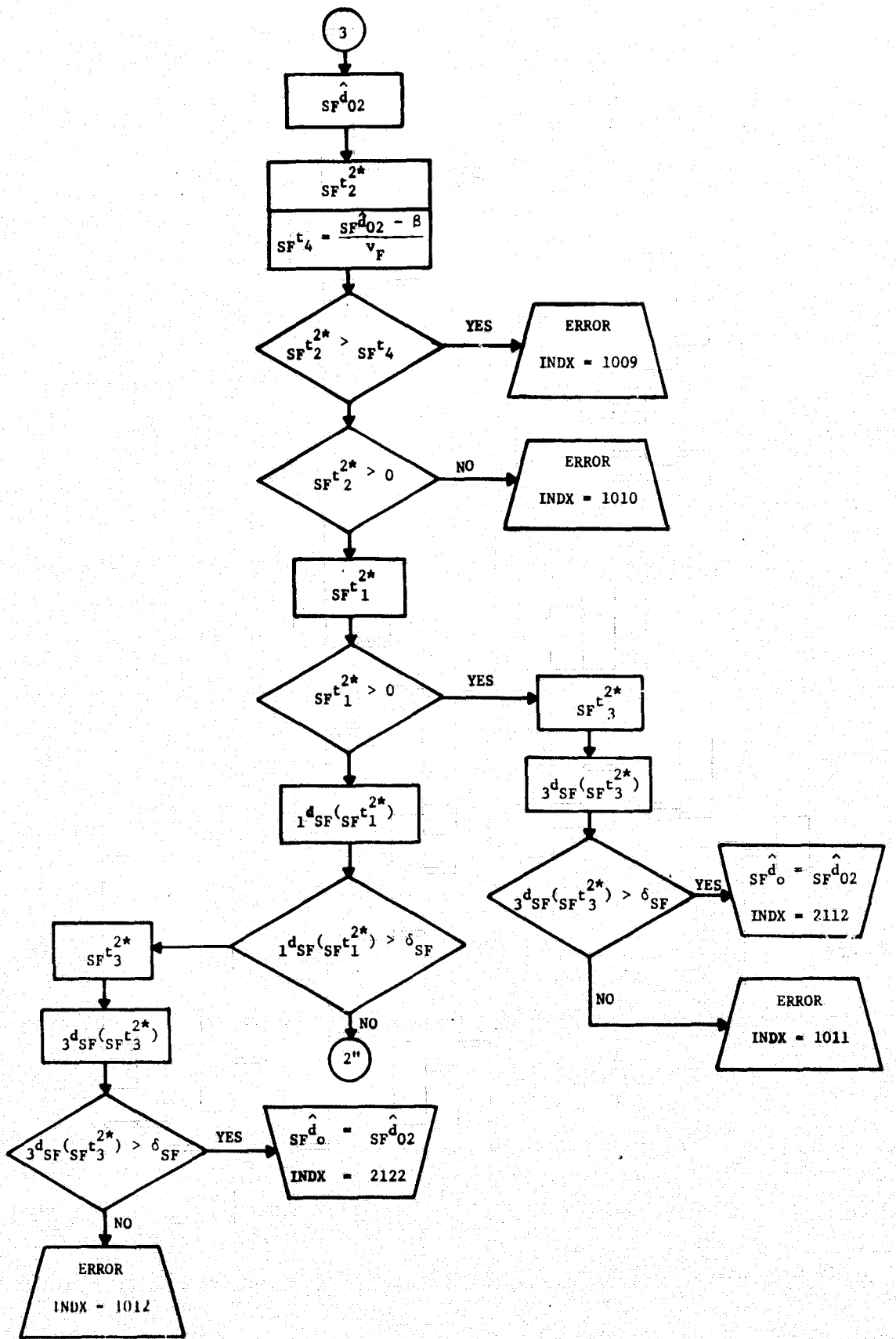
3
$SF\hat{d}_{02}$
$SF t_2^{2*}$
$SF t_4 = \frac{SF\hat{d}_{02} - \beta}{v_F}$
$SF t_2^{2*} > SF t_4$
YES
ERROR
INDX = 1009
$SF t_2^{2*} > 0$
NO
ERROR
INDX = 1010
$SF t_1^{2*}$
$SF t_1^{2*} > 0$
YES
$SF t_3^{2*}$
$1^{d}SF(SF t_1^{2*})$
$3^{d}SF(SF t_3^{2*})$
$1^{d}SF(SF t_1^{2*}) > \delta_{SF}$
$3^{d}SF(SF t_3^{2*}) > \delta_{SF}$
YES
$SF\hat{d}_o = SF\hat{d}_{02}$
INDX = 2112
NO
ERROR
INDX = 1011
NO
2"
$SF t_3^{2*}$
$3^{d}SF(SF t_3^{2*})$
$3^{d}SF(SF t_3^{2*}) > \delta_{SF}$
YES
$SF\hat{d}_o = SF\hat{d}_{02}$
INDX = 2122
NO
ERROR
INDX = 1012

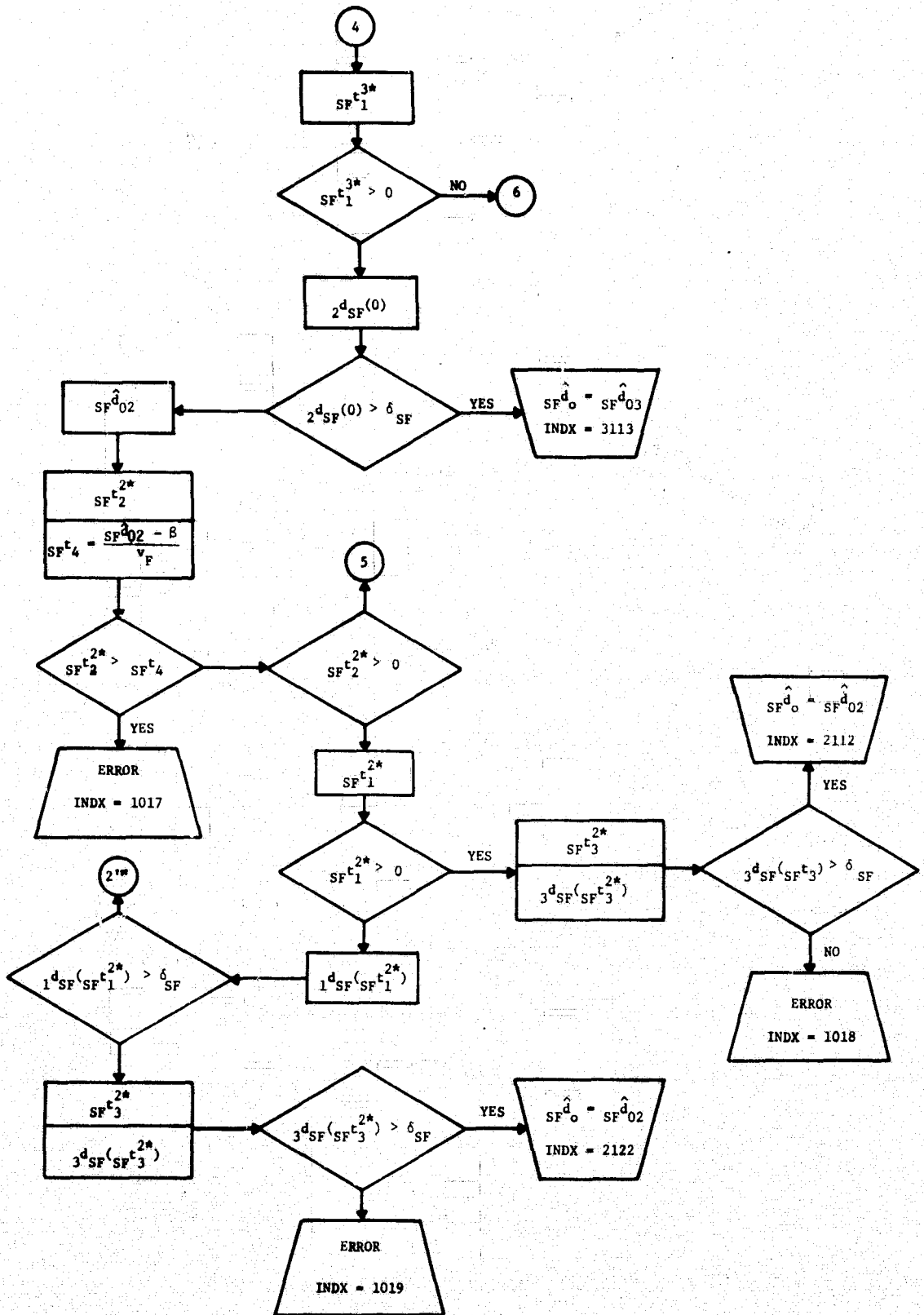
4
$SF^{t_1^{3*}}$
$SF^{t_1^{3*}} > 0$
NO
6
$2^{d_{SF}(0)}$
$2^{d_{SF}(0)} > \delta_{SF}$
YES
$SF^{\hat{d}_o} = SF^{\hat{d}_{03}}$
INDX = 3113
$SF^{\hat{d}_{02}}$
$SF^{t_2^{2*}}$
$SF^{t_4} = \frac{SF^{\hat{d}_{02}} - \beta}{v_F}$
5
$SF^{t_2^{2*}} > SF^{t_4}$
$SF^{t_2^{2*}} > 0$
YES
ERROR
INDX = 1017
$SF^{t_1^{2*}}$
$SF^{t_1^{2*}} > 0$
YES
$SF^{t_3^{2*}}$
$3^{d_{SF}(SF^{t_3^{2*}})}$
$3^{d_{SF}(SF^{t_3}) > \delta_{SF}}$
YES
$SF^{\hat{d}_o} = SF^{\hat{d}_{02}}$
INDX = 2112
NO
ERROR
INDX = 1018
2^{nd}
$1^{d_{SF}(SF^{t_1^{2*}}) > \delta_{SF}}$
$1^{d_{SF}(SF^{t_1^{2*}})}$
$SF^{t_3^{2*}}$
$3^{d_{SF}(SF^{t_3^{2*}})}$
$3^{d_{SF}(SF^{t_3^{2*}}) > \delta_{SF}}$
YES
$SF^{\hat{d}_o} = SF^{\hat{d}_{02}}$
INDX = 2122
ERROR
INDX = 1019

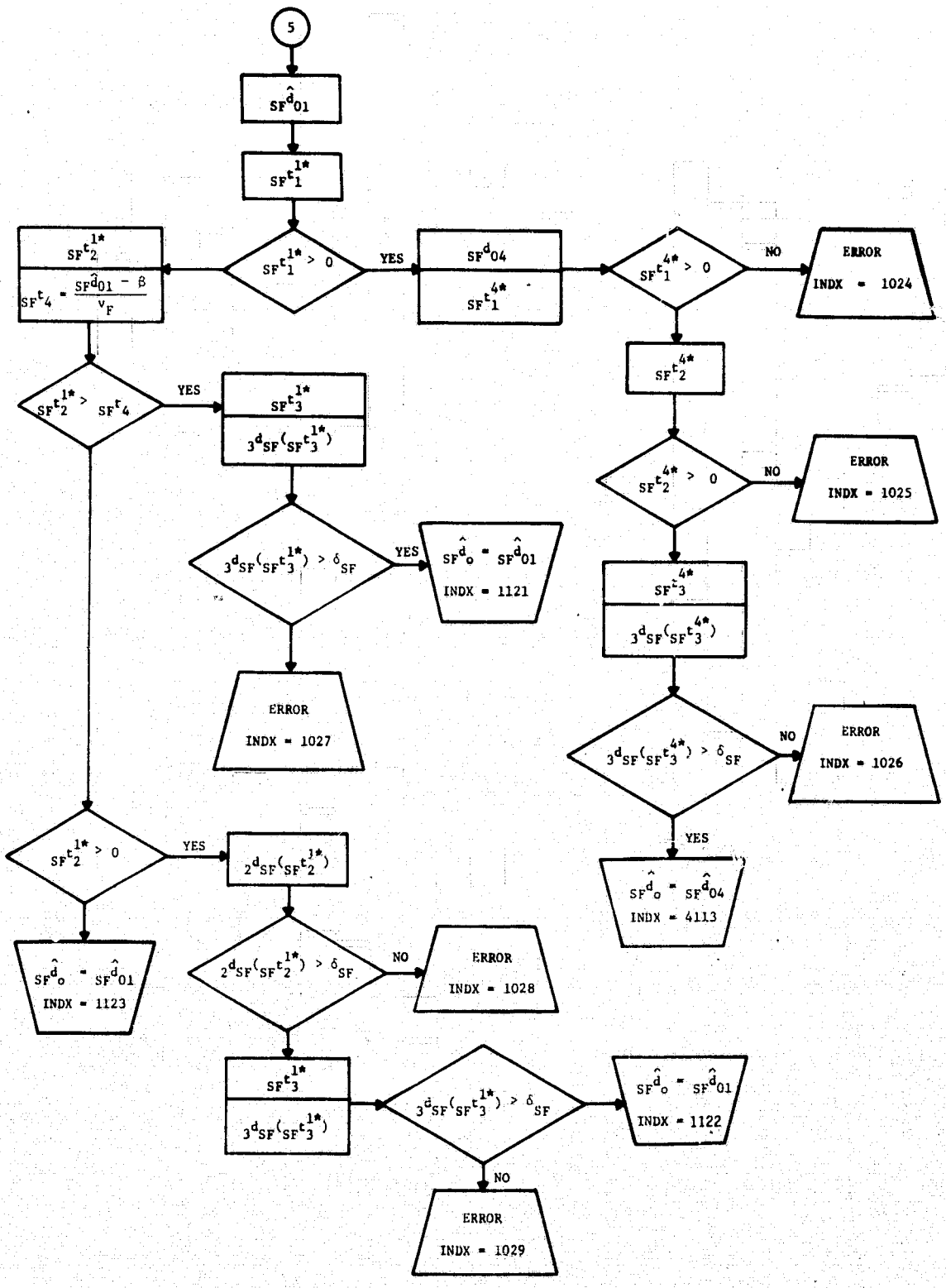
5
$SF\hat{d}_{01}$
$SF t_1^{1*}$
$SF t_1^{1*} > 0$
YES
$SF d_{04}$
$SF t_1^{4*}$
$SF t_1^{4*} > 0$
NO
ERROR
INDX = 1024
$SF t_2^{1*}$
$SF t_4 = \frac{SF\hat{d}_{01} - \beta}{v_F}$
$SF t_2^{1*} > SF t_4$
YES
$SF t_3^{1*}$
$3^d SF(SF t_3^{1*})$
$3^d SF(SF t_3^{1*}) > \delta_{SF}$
YES
$SF\hat{d}_o = SF\hat{d}_{01}$
INDX = 1121
ERROR
INDX = 1027
$SF t_2^{4*}$
$SF t_2^{4*} > 0$
NO
ERROR
INDX = 1025
$SF t_3^{4*}$
$3^d SF(SF t_3^{4*})$
$3^d SF(SF t_3^{4*}) > \delta_{SF}$
NO
ERROR
INDX = 1026
YES
$SF\hat{d}_o = SF\hat{d}_{04}$
INDX = 4113
$SF t_2^{1*} > 0$
YES
$2^d SF(SF t_2^{1*})$
$SF\hat{d}_o = SF\hat{d}_{01}$
INDX = 1123
$2^d SF(SF t_2^{1*}) > \delta_{SF}$
NO
ERROR
INDX = 1028
$SF t_3^{1*}$
$3^d SF(SF t_3^{1*})$
$3^d SF(SF t_3^{1*}) > \delta_{SF}$
$SF\hat{d}_o = SF\hat{d}_{01}$
INDX = 1122
NO
ERROR
INDX = 1029

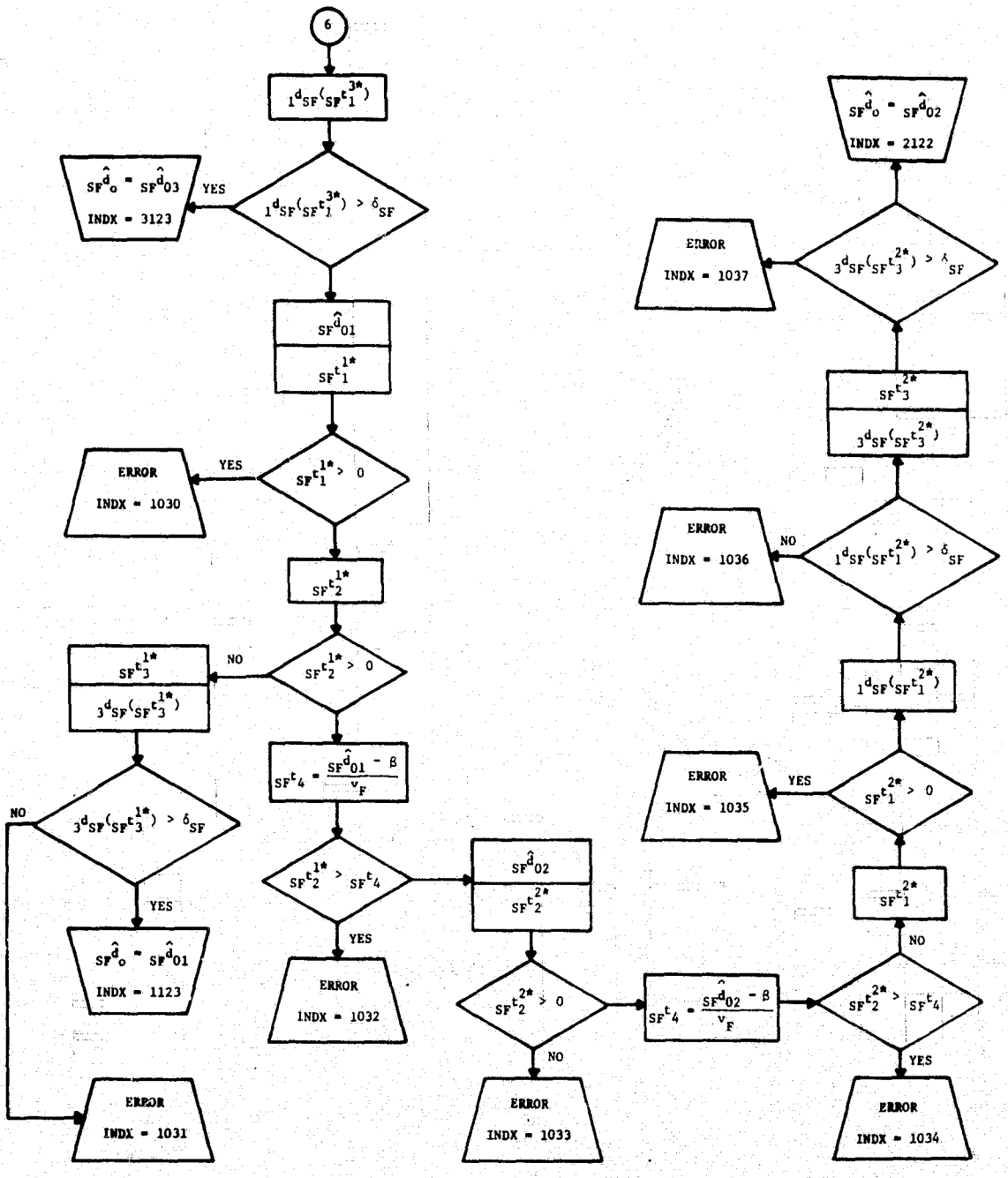
6
$1^{d}_{SF}(SF^{t}_{1}{}^{3*})$
$SF^{\hat{d}}_{o} = SF^{\hat{d}}_{03}$
INDX = 3123
YES
$1^{d}_{SF}(SF^{t}_{1}{}^{3*}) > \delta_{SF}$
$SF^{\hat{d}}_{01}$
$SF^{t}_{1}{}^{1*}$
ERROR
INDX = 1030
YES
$SF^{t}_{1}{}^{1*} > 0$
$SF^{t}_{2}{}^{1*}$
$SF^{t}_{3}{}^{1*}$
$3^{d}_{SF}(SF^{t}_{3}{}^{1*})$
NO
$SF^{t}_{2}{}^{1*} > 0$
$SF^{t}_{4} = \frac{SF^{\hat{d}}_{01} - \beta}{v_F}$
NO
$3^{d}_{SF}(SF^{t}_{3}{}^{1*}) > \delta_{SF}$
YES
$SF^{\hat{d}}_{o} = SF^{\hat{d}}_{01}$
INDX = 1123
ERROR
INDX = 1031
$SF^{t}_{2}{}^{1*} > SF^{t}_{4}$
YES
ERROR
INDX = 1032
$SF^{\hat{d}}_{02}$
$SF^{t}_{2}{}^{2*}$
$SF^{t}_{2}{}^{2*} > 0$
NO
ERROR
INDX = 1033
$SF^{t}_{4} = \frac{SF^{\hat{d}}_{02} - \beta}{v_F}$
$SF^{t}_{2}{}^{2*} > SF^{t}_{4}$
NO
YES
ERROR
INDX = 1034
$SF^{t}_{1}{}^{2*}$
YES
$SF^{t}_{1}{}^{2*} > 0$
ERROR
INDX = 1035
$1^{d}_{SF}(SF^{t}_{1}{}^{2*})$
NO
$1^{d}_{SF}(SF^{t}_{1}{}^{2*}) > \delta_{SF}$
ERROR
INDX = 1036
$SF^{t}_{3}{}^{2*}$
$3^{d}_{SF}(SF^{t}_{3}{}^{2*})$
$3^{d}_{SF}(SF^{t}_{3}{}^{2*}) > \delta_{SF}$
ERROR
INDX = 1037
$SF^{\hat{d}}_{o} = SF^{\hat{d}}_{02}$
INDX = 2122

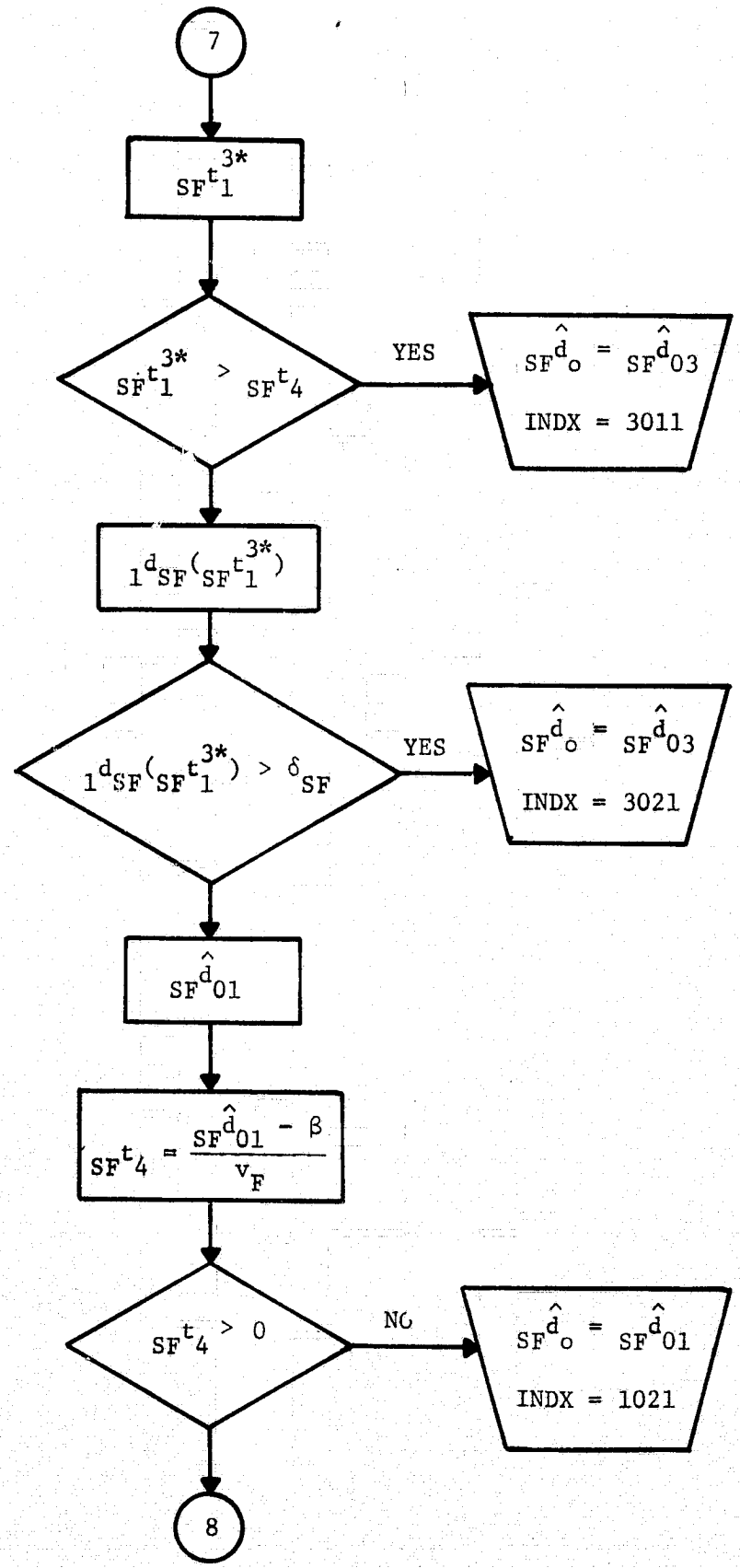
7
$SF^{t}_{1}{}^{3*}$
$SF^{t}_{1}{}^{3*} > SF^{t}_{4}$
YES
$SF^{\hat{d}}_{o} = SF^{\hat{d}}_{03}$
INDX = 3011
$1^{d}SF(SF^{t}_{1}{}^{3*})$
$1^{d}SF(SF^{t}_{1}{}^{3*}) > \delta_{SF}$
YES
$SF^{\hat{d}}_{o} = SF^{\hat{d}}_{03}$
INDX = 3021
$SF^{\hat{d}}_{01}$
$SF^{t}_{4} = \frac{SF^{\hat{d}}_{01} - \beta}{v_F}$
$SF^{t}_{4} > 0$
NO
$SF^{\hat{d}}_{o} = SF^{\hat{d}}_{01}$
INDX = 1021
8

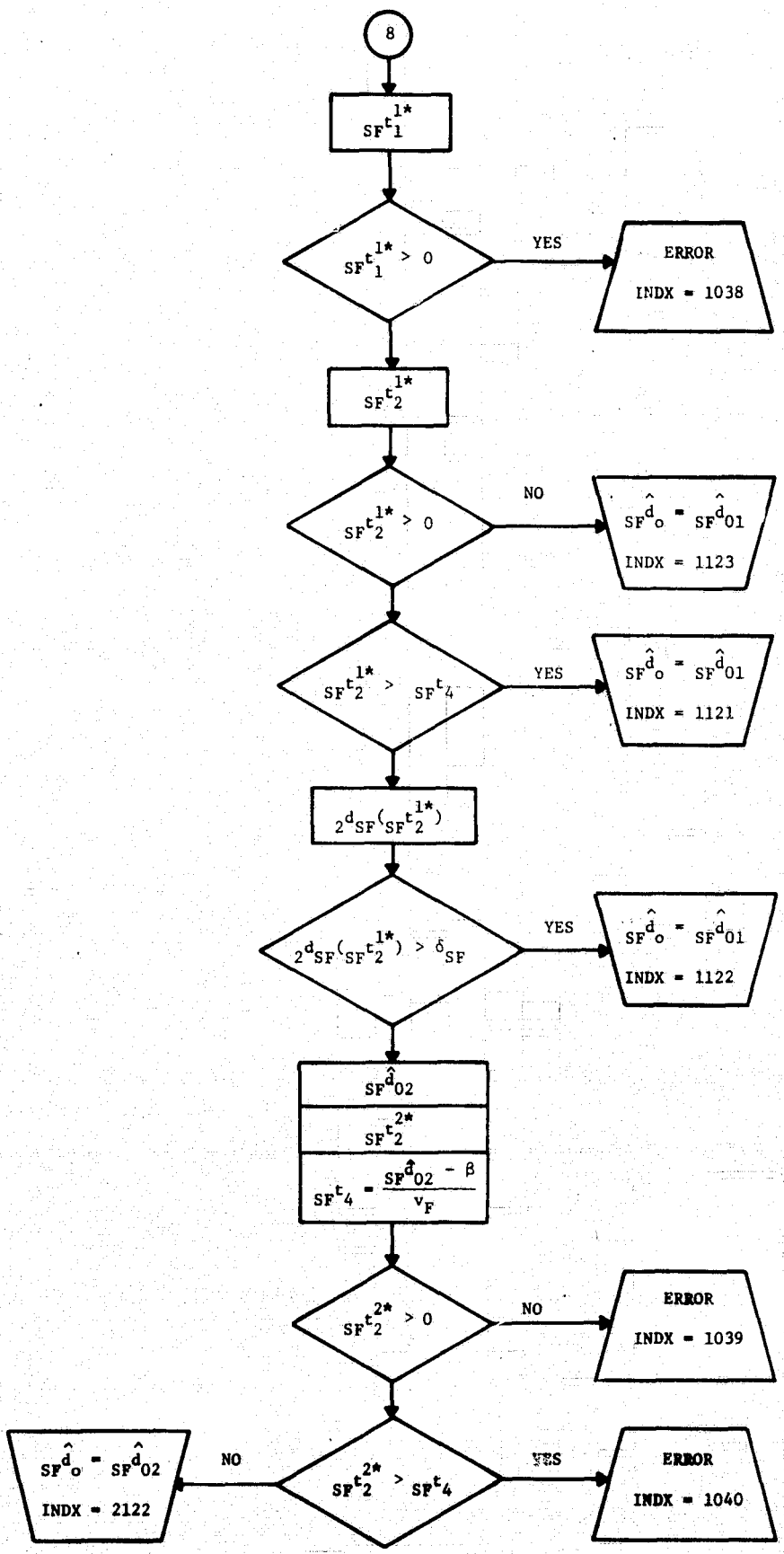
8
$SF^{t}_{1}{}^{1*}$
$SF^{t}_{1}{}^{1*} > 0$
YES
ERROR
INDX = 1038
$SF^{t}_{2}{}^{1*}$
$SF^{t}_{2}{}^{1*} > 0$
NO
$SF^{\hat{d}}_{o} = SF^{\hat{d}}_{01}$
INDX = 1123
$SF^{t}_{2}{}^{1*} > SF^{t}_{4}$
YES
$SF^{\hat{d}}_{o} = SF^{\hat{d}}_{01}$
INDX = 1121
$2^{d}SF(SF^{t}_{2}{}^{1*})$
$2^{d}SF(SF^{t}_{2}{}^{1*}) > \delta_{SF}$
YES
$SF^{\hat{d}}_{o} = SF^{\hat{d}}_{01}$
INDX = 1122
$SF^{\hat{d}}_{02}$
$SF^{t}_{2}{}^{2*}$
$SF^{t}_{4} = \frac{SF^{\hat{d}}_{02} - \beta}{v_F}$
$SF^{t}_{2}{}^{2*} > 0$
NO
ERROR
INDX = 1039
$SF^{t}_{2}{}^{2*} > SF^{t}_{4}$
NO
$SF^{\hat{d}}_{o} = SF^{\hat{d}}_{02}$
INDX = 2122
YES
ERROR
INDX = 1040

Notes:

1. 2', 2" and 2"' are exactly the same as 2 but with changed error indices as follows:

2	2'	2"	2"'
1001	1005	1013	1020
1002	1006	1014	1021
1003	1007	1015	1022
1004	1008	1016	1023

2. See note 1, Appendix A.1, page 136.

3. See note 2, Appendix A.1, page 136.

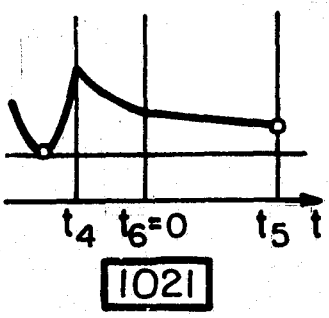

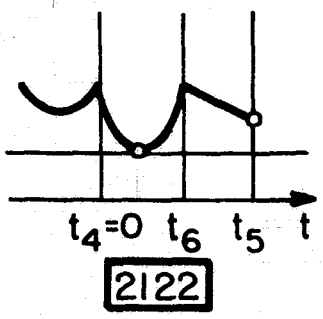

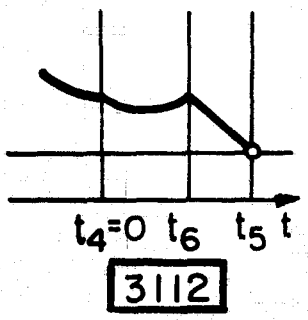

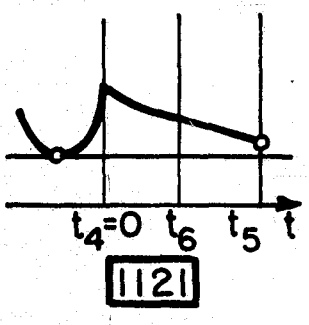

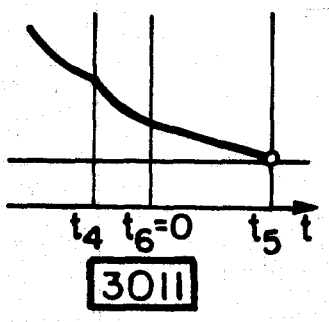

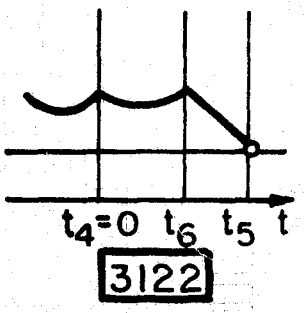

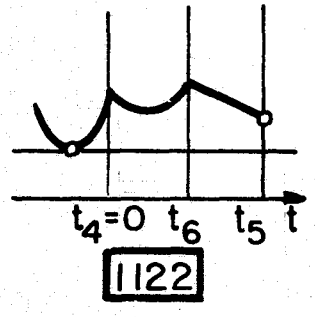

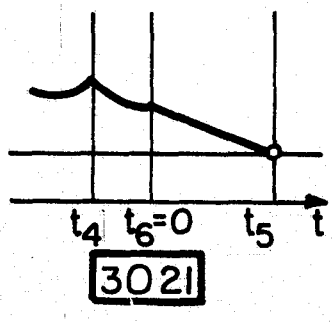

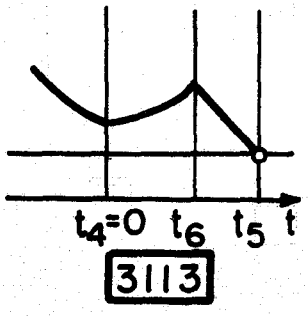

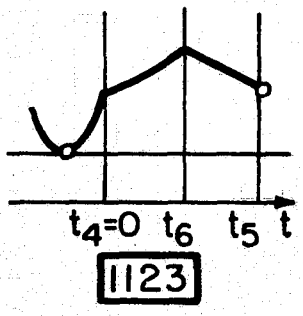

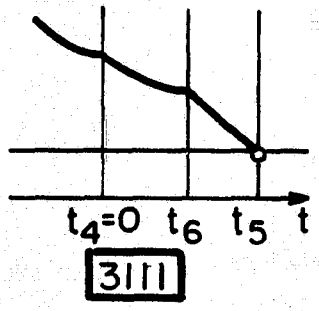

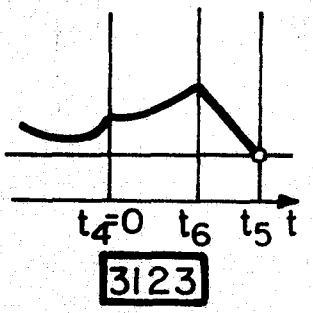

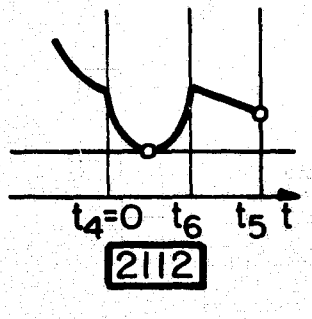

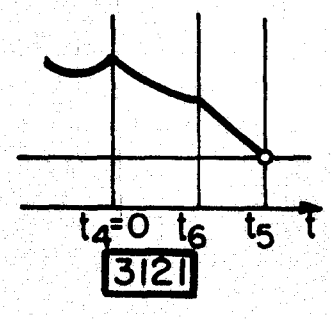

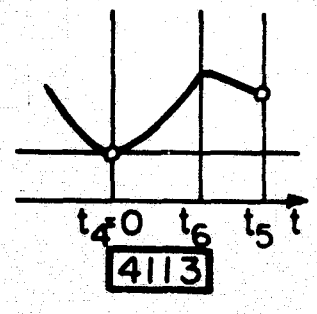

Function $d_{SF}(t)$

B. Program Listing

B.1. List of Variables

All Subroutines

COAS	$\cos \alpha_S$
COAF	$\cos \alpha_F$
COASAF	$\cos(\alpha_S - \alpha_F)$
AMAS	$\mu^2 - 2\mu\cos \alpha_S + 1$
AMAF	$\mu^2 - 2\mu\cos \alpha_F + 1$
AMASAF	$\mu^2 - 2\mu\cos(\alpha_S - \alpha_F) + 1$
AMI	μ
VF	v_F
VS	v_S
GAMAF	γ_F
GAMAS	γ_S
BETA	β
IAFAR	α_F in degrees
IASAR	α_S in degrees
DOSF	$\hat{d}_{o_{SF}}$
DOFS	$\hat{d}_{o_{FS}}$
DOSS	$\hat{d}_{o_{SS}}$
DOFF	$\hat{d}_{o_{FF}}$
INDXFS	INDEX for $d_{FS}(t)$
INDXSF	INDEX for $d_{SF}(t)$
INDXSS	INDEX for $d_{SS}(t)$
INDXFF	INDEX for $d_{FF}(t)$
TSF	t_{SF}
TFS	t_{FS}
TSS	t_{SS}

TFF	t_{FF}
DELTSS	δ_{SS}
DELTFF	δ_{FF}
DELTSF	δ_{SF}
DELTFS	δ_{FS}

Subroutine SDOSF*

DOSF1	${}_{SF}\hat{d}_{01}$
DOSF2	${}_{SF}\hat{d}_{02}$
DOSF3	${}_{SF}\hat{d}_{03}$
DOSF4	${}_{SF}\hat{d}_{04}$
V1S1	${}_{SF}t_1^{1*}$
V2S1	${}_{SF}t_1^{2*}$
V3S1	${}_{SF}t_1^{3*}$
V4S1	${}_{SF}t_1^{4*}$
V1S2	${}_{SF}t_2^{1*}$
V2S2	${}_{SF}t_2^{2*}$
V3S2	${}_{SF}t_2^{3*}$
DV2S1	${}_1d_{SF}({}_{SF}t_1^{2*})$
DV3S1	${}_1d_{SF}({}_{SF}t_1^{3*})$
DV1S2	${}_2d_{SF}({}_{SF}t_2^{1*})$
DV3S2	${}_2d_{SF}({}_{SF}t_2^{3*})$
DV1S3	${}_3d_{SF}({}_{SF}t_3^{1*})$
DV2S3	${}_3d_{SF}({}_{SF}t_3^{2*})$

*Subroutines have names of variables which they compute with letter S as the first letter, e.g., SDOSF is subroutine which computes DOSF.

DV4S3	$_3d_{SF}(_{SF}t_3^{4*})$
DODO3	$_2d_{SF}(0)$ computed using $_{SF}\hat{d}_{03}$

Subroutine DOFS

DOFS1	$_{FS}\hat{d}_{01}$
DOFS2	$_{FS}\hat{d}_{02}$
DOFS4	$_{FS}\hat{d}_{04}$
DOFS5	$_{FS}\hat{d}_{05}$
T1S1	$_{FS}t_1^{1*}$
T2S1	$_{FS}t_1^{2*}$
T4S1	$_{FS}t_1^{4*}$
T5S1	$_{FS}t_1^{5*}$
T1S2	$_{FS}t_2^{1*}$
T2S2	$_{FS}t_2^{2*}$
T4S2	$_{FS}t_2^{4*}$
DT2S1	$_1d_{FS}(_{FS}t_1^{2*})$
DT5S1	$_1d_{FS}(_{FS}t_1^{5*})$
DT1S2	$_2d_{FS}(_{FS}t_2^{1*})$

CAPSF

DOOSF	$_{SF}\hat{d}_o$ (matrix)
DOOFS	$_{FS}\hat{d}_o$ (matrix)
DOOSS	$_{SS}\hat{d}_o$ (vector)
DOOFF	$_{FF}\hat{d}_o$ (vector)
INXSF	INDEX for $d_{SF}(t)$
INXFS	INDEX for $d_{FS}(t)$
INXSS	INDEX for $d_{SS}(t)$
INXFF	INDEX for $d_{FF}(t)$

CAP3 (Similar is for CAP4)

VKT	v_i approach speed in knots (vector)	
GAMA	γ_i (vector)	
P	p_i (vector)	
PP	p_{ij} (matrix)	
DELTA	δ_{ij} (matrix)	
TT	t_{ij} (matrix)	
IALF1	α_1	values producing optimal N configurations
IALF2	α_2	
IALF3	α_3	
CAPAC	optimal N capacities	
CAPMIN	the lowest N capacities	
IALFM1	α_1	values producing the lowest N capacities
IALFM2	α_2	
IALFM3	α_3	

B.2. Subroutines

```
      SUBROUTINE SDOSF
      DIMENSION DELTA(5,5)
      COMMON /SSFFS/
     1COAS,COAF,COASAF,AMAS,AMAF,AMASAF,AMI,VF,GAMAS,GAMAF,BETA,DELTA,
     2IAFAR,IASAR,DOSF,DOFS,DOSS,DOFF,INDXSF,INDXFS,INDXSS,INDXFF,
     3TSF,TFS,TSS,TFF
     4,DELTSS,DELTFF,DELTSF,DELTFS
      COMMON /SF/
     2DOSF1,DOSF2,DOSF3,DOSF4,V1S1,V2S1,V3S1,V4S1,V1S2,V2S2,V3S2,
     3DV2S1,DV3S1,DV1S2,DV3S2,DV1S3,DV2S3,DV4S3,DODO3
      CALL SDOSF3
      PT12=(DOSF3-BETA)/VF
      IF (PT12) 700,700,100
  100 CONTINUE
      CALL SV3S2
      IF (V3S2-PT12) 200,200,105
  105 CONTINUE
      CALL SV3S1
      IF (V3S1) 115,115,110
  110 CONTINUE
      INDXSF=3111
      DOSF=DOSF3
      GO TO 995
  115 CONTINUE
      CALL SDV3S1
      IF (DV3S1-DELTSF) 125,125,120
  120 CONTINUE
      INDXSF=3121
      DOSF=DOSF3
      GO TO 995
  125 CONTINUE
      CALL SDOSF1
      CALL SV1S1
      IF (V1S1) 135,135,130
  130 CONTINUE
      INDXSF=1
      DOSF=0.
      GO TO 995
  135 CONTINUE
      CALL SV1S2
      PT12=(DOSF1-BETA)/VF
      IF (V1S2-PT12) 155,155,140
  140 CONTINUE
      CALL SDV1S3
      IF (DV1S3-DELTSF) 150,150,145
  145 CONTINUE
      INDXSF=1121
      DOSF=DOSF1
```

```
      GO TO 995
  150 CONTINUE
      INDXSF=2
      DOSF=0.
      GO TO 995
  155 CONTINUE
      IF (V1S2) 185,185,160
  160 CONTINUE
      CALL SDV1S2
      IF (DV1S2-DELTSF) 180,180,165
  165 CONTINUE
      CALL SDV1S3
      IF (DV1S3-DELTSF) 175,175,170
  170 CONTINUE
      INDXSF=1122
      DOSF=DOSF1
      GO TO 995
  175 CONTINUE
      INDXSF=3
      DOSF=0.
      GO TO 995
  180 CONTINUE
      INDXSF=4
      DOSF=0.
      GO TO 995
  185 CONTINUE
      INDXSF=50
      DOSF=0.
      GO TO 995
  200 CONTINUE
      IF (V3S2) 400,400,203
  203 CONTINUE
      CALL SDV3S2
      IF (DV3S2-DELTSF) 300,300,205
  205 CONTINUE
      CALL SV3S1
      IF (V3S1) 215,215,210
  210 CONTINUE
      INDXSF=3112
      DOSF=DOSF3
      GO TO 995
  215 CONTINUE
      CALL SDV3S1
      IF (DV3S1-DELTSF) 125,125,220
  220 CONTINUE
      INDXSF=3122
      DOSF=DOSF3
      GO TO 995
```

```
300 CONTINUE
    CALL SDOSF2
    CALL SV2S2
    PT12=(DOSF2-BETA)/VF
    IF (V2S2-PT12) 310,310,305
305 CONTINUE
    INDXSF=9
    DOSF=0.
    GO TO 995
310 CONTINUE
    IF (V2S2) 315,315,320
315 CONTINUE
    INDXSF=10
    DOSF=0.
    GO TO 995
320 CONTINUE
    CALL SV2S1
    IF (V2S1) 340,340,325
325 CONTINUE
    CALL SDV2S3
    IF (DV2S3-DELTSF) 335,335,330
330 CONTINUE
    INDXSF=2112
    DOSF=DOSF2
    GO TO 995
335 CONTINUE
    INDXSF=11
    DOSF=0.
    GO TO 995
340 CONTINUE
    CALL SDV2S1
    IF (DV2S1-DELTSF) 360,360,345
345 CONTINUE
    CALL SDV2S3
    IF (DV2S3-DELTSF) 355,355,350
350 CONTINUE
    INDXSF=2122
    DOSF=DOSF2
    GO TO 995
355 CONTINUE
    INDXSF=12
    DOSF=0.
    GO TO 995
360 CONTINUE
    GO TO 125
400 CONTINUE
    CALL SV3S1
    IF (V3S1) 600,600,405
```

```
405 CONTINUE
    CALL SDOD03
    IF (DOD03-DELTSF) 415,415,410
410 CONTINUE
    INDXSF=3113
    DOSF=DOSF3
    GO TO 995
415 CONTINUE
    CALL SDOSF2
    CALL SV2S2
    PT12=(DOSF2-BETA)/VF
    IF (V2S2-PT12) 425,425,420
420 CONTINUE
    INDXSF=17
    DOSF=0.
    GO TO 995
425 CONTINUE
    IF (V2S2) 500,500,320
500 CONTINUE
    CALL SDOSF1
    CALL SV1S1
    IF (V1S1) 540,540,505
505 CONTINUE
    CALL SDOSF4
    CALL SV4S1
    IF (V4S1) 510,510,515
510 CONTINUE
    INDXSF=24
    DOSF=0.
    GO TO 995
515 CONTINUE
    IF (V4S1) 525,525,520
520 CONTINUE
    INDXSF=25
    DOSF=0.
    GO TO 995
525 CONTINUE
    CALL SDV4S3
    IF (DV4S3-DELTSF) 530,530,535
530 CONTINUE
    INDXSF=26
    DOSF=0.
    GO TO 995
535 CONTINUE
    INDXSF=4113
    DOSF=DOSF4
    GO TO 995
540 CONTINUE
```

```
      CALL SV1S2
      PT12=(DOSF1-BETA)/VF
      IF (V1S2-PT12) 560,560,140
  560 CONTINUE
      IF (V1S2) 570,570,160
  570 CONTINUE
      INDXSF=1123
      DOSF=DOSF1
      GO TO 995
  600 CONTINUE
      CALL SDV3S1
      IF (DV3S1-DELTSF) 610,610,605
  605 CONTINUE
      INDXSF=3123
      DOSF=DOSF3
      GO TO 995
  610 CONTINUE
      CALL SDOSF1
      CALL SV1S1
      IF (V1S1) 620,620,615
  615 CONTINUE
      INDXSF=30
      DOSF=0.
      GO TO 995
  620 CONTINUE
      CALL SV1S2
      IF (V1S2) 625,625,640
  625 CONTINUE
      CALL SDV1S3
      IF (DV1S3-DELTSF) 635,635,630
  630 CONTINUE
      INDXSF=1123
      DOSF=DOSF1
      GO TO 995
  635 CONTINUE
      INDXSF=31
      DOSF=0.
      GO TO 995
  640 CONTINUE
      PT12=(DOSF1-BETA)/VF
      IF (V1S2-PT12) 650,650,645
  645 CONTINUE
      INDXSF=32
      DOSF=0.
      GO TO 995
  650 CONTINUE
      CALL SDOSF2
      CALL SV2S2
```

```
      IF (V2S2) 655,655,660
  655 CONTINUE
      INDXSF=33
      DOSF=0.
      GO TO 995
  660 CONTINUE
      PT12=(DOSF2-BETA)/VF
      IF (V2S2-PT12) 670,670,665
  665 CONTINUE
      INDXSF=34
      DOSF=0.
      GO TO 995
  670 CONTINUE
      CALL SV2S1
      IF (V2S1) 680,680,675
  675 CONTINUE
      INDXSF=35
      DOSF=0.
      GO TO 995
  680 CONTINUE
      CALL SDV2S1
      IF (DV2S1-DELTSF) 685,685,690
  685 CONTINUE
      INDXSF=36
      DOSF=0.
      GO TO 995
  690 CONTINUE
      CALL SDV2S3
      IF (DV2S3-DELTSF) 693,693,696
  693 CONTINUE
      INDXSF=37
      DOSF=0.
      GO TO 995
  696 CONTINUE
      INDXSF=2122
      DOSF=DOSF2
      GO TO 995
  700 CONTINUE
      CALL SV3S1
      PT12=(DOSF3-BETA)/VF
      IF (V3S1-PT12) 710,710,705
  705 CONTINUE
      INDXSF=3011
      DOSF=DOSF3
      GO TO 995
  710 CONTINUE
      CALL SDV3S1
      IF (DV3S1-DELTSF) 720,720,715
```

```
715 CONTINUE
    INDXSF=3021
    DOSF=DOSF3
    GO TO 995
720 CONTINUE
    CALL SDOSF1
    PT12=(DOSF1-BETA)/VF
    IF (PT12) 725,725,800
725 CONTINUE
    INDXSF=1021
    DOSF=DOSF1
    GO TO 995
800 CONTINUE
    CALL SV1S1
    IF (V1S1) 810,810,805
805 CONTINUE
    INDXSF=38
    DOSF=0.
    GO TO 995
810 CONTINUE
    CALL SV1S2
    IF (V1S2) 815,815,820
815 CONTINUE
    INDXSF=1123
    DOSF=DOSF1
    GO TO 995
820 CONTINUE
    PT12=(DOSF1-BETA)/VF
    IF (V1S2-PT12) 830,830,825
825 CONTINUE
    INDXSF=1121
    DOSF=DOSF1
    GO TO 995
830 CONTINUE
    CALL SDV1S2
    IF (DV1S2-DELTSF) 840,840,835
835 CONTINUE
    INDXSF=1122
    DOSF=DOSF1
    GO TO 995
840 CONTINUE
    CALL SDOSF2
    CALL SV2S2
    IF (V2S2) 845,845,850
845 CONTINUE
    INDXSF=39
    DOSF=0.
    GO TO 995
```

```
850 CONTINUE
    PT12=(DOSF2-BETA)/VF
    IF (V2S2-PT12) 860,860,855
855 CONTINUE
    INDXSF=40
    DOSF=0.
    GO TO 995
860 CONTINUE
    INDXSF=2122
    DOSF=DOSF2
    GO TO 995
995 CONTINUE
    RETURN
    END


    SUBROUTINE SDOSF1
    DIMENSION DELTA(5,5)
    COMMON /SSFFS/
   1COAS,COAF,COASAF,AMAS,AMAF,AMASAF,AMI,VF,GAMAS,GAMAF,BETA,DELTA,
   2IAFAR,IASAR,DOSF,DOFS,DOSS,DOFF,INDXSF,INDXFS,INDXSS,INDXFF,
   3TSF,TFS,TSS,TFF
   4,DELTSS,DELTFF,DELTSF,DELTFS
    COMMON /SF/
   2DOSF1,DOSF2,DOSF3,DOSF4,V1S1,V2S1,V3S1,V4S1,V1S2,V2S2,V3S2,
   3DV2S1,DV3S1,DV1S2,DV3S2,DV1S3,DV2S3,DV4S3,DOD03
    ASF1=1.-(1.-AMI*COASAF)**2./AMASAF
    BSF1=-2.*BETA*(1.-COAF+(AMI*COASAF-1.)*(1.-COAF-AMI*
   1(COASAF-COAS))/AMASAF)
    C1SF1=BETA**2.*(2.*(1.-COAF)-(1.-COAF-AMI*(COASAF-COAS))**2/
   1AMASAF)
    CSF1=C1SF1-DELTSF**2
    DETSF1=BSF1**2-4.*ASF1*CSF1
    IF (DETSF1) 10,20,30
 10 CONTINUE
    PRINT 100,IASAR,IAFAR,DETSF1
100 FORMAT (//,*SUBROUTINE SDOSF1,DETERMINANT  NEGATIVE *,3X,
   1*ALFAS =*,I3,3X,*ALFAF =*,I3,3X,*DETSF1 =*,F10.5/)
    GO TO 40
 20 CONTINUE
    DOSF1=-BSF1/(2.*ASF1)
    GO TO 40
 30 CONTINUE
    DO1SF1=(-BSF1-SQRT(DETSF1))/(2.*ASF1)
    DO2SF1=(-BSF1+SQRT(DETSF1))/(2.*ASF1)
    DOSF1=DO2SF1
 40 CONTINUE
    RETURN
```

```
      END

      SUBROUTINE SDOSF2
      DIMENSION DELTA(5,5)
      COMMON /SSFFS/
     1COAS,COAF,COASAF,AMAS,AMAF,AMASAF,AMI,VF,GAMAS,GAMAF,BETA,DELTA,
     2IAFAR,IASAR,DOSF,DOFS,DOSS,DOFF,INDXSF,INDXFS,INDXSS,INDXFF,
     3TSF,TFS,TSS,TFF
     4,DELTSS,DELTFF,DELTSF,DELTFS
      COMMON /SF/
     2DOSF1,DOSF2,DOSF3,DOSF4,V1S1,V2S1,V3S1,V4S1,V1S2,V2S2,V3S2,
     3DV2S1,DV3S1,DV1S2,DV3S2,DV1S3,DV2S3,DV4S3,DODO3
      ASF2=1.-(1.-AMI*COAF)**2./AMAF
      BSF2=-2.*BETA*(1.-COAF-(1.-AMI*COAF)*(1.-COAF)*(1.+AMI)/AMAF)
      C1SF2=BETA**2.*(2.*(1.-COAF)-(1.-COAF)**2.*(1.+AMI)**2./AMAF)
      CSF2=C1SF2-DELTSF**2
      DETSF2=BSF2**2-4.*ASF2*CSF2
      IF  (DETSF2) 10,20,30
   10 CONTINUE
      PRINT 100,IASAR,IAFAR,DETSF2
  100 FORMAT (//,*SUBROUTINE SDOSF2,DETERMINANT  NEGATIVE *,3X,
     1*ALFAS =*,I3,3X,*ALFAF =*,I3,3X,*DETSF2 =*,F10.5/)
      GO TO 40
   20 CONTINUE
      DOSF2=-BSF2/(2.*ASF2)
      GO TO 40
   30 CONTINUE
      DO1SF2=(-BSF2-SQRT(DETSF2))/(2.*ASF2)
      DO2SF2=(-BSF2+SQRT(DETSF2))/(2.*ASF2)
      DOSF2=DO2SF2
   40 CONTINUE
      RETURN
      END

      SUBROUTINE SDOSF3
      DIMENSION DELTA(5,5)
      COMMON /SSFFS/
     1COAS,COAF,COASAF,AMAS,AMAF,AMASAF,AMI,VF,GAMAS,GAMAF,BETA,DELTA,
     2IAFAR,IASAR,DOSF,DOFS,DOSS,DOFF,INDXSF,INDXFS,INDXSS,INDXFF,
     3TSF,TFS,TSS,TFF
     4,DELTSS,DELTFF,DELTSF,DELTFS
      COMMON /SF/
     2DOSF1,DOSF2,DOSF3,DOSF4,V1S1,V2S1,V3S1,V4S1,V1S2,V2S2,V3S2,
     3DV2S1,DV3S1,DV1S2,DV3S2,DV1S3,DV2S3,DV4S3,DODO3
      DOSF3=DELTSF+(1.-AMI)*GAMAS/AMI
      RETURN
```

```
      END


      SUBROUTINE SDOSF4
      DIMENSION DELTA(5,5)
      COMMON /SSFFS/
     1COAS,COAF,COASAF,AMAS,AMAF,AMASAF,AMI,VF,GAMAS,GAMAF,BETA,DELTA,
     2IAFAR,IASAR,DOSF,DOFS,DOSS,DOFF,INDXSF,INDXFS,INDXSS,INDXFF,
     3TSF,TFS,TSS,TFF
     4,DELTSS,DELTFF,DELTSF,DELTFS
      COMMON /SF/
     2DOSF1,DOSF2,DOSF3,DOSF4,V1S1,V2S1,V3S1,V4S1,V1S2,V2S2,V3S2,
     3DV2S1,DV3S1,DV1S2,DV3S2,DV1S3,DV2S3,DV4S3,DODO3
      ASF4=1.
      BSF4=-2.*BETA*(1.-COAF)
      C1SF4=2.*BETA**2.*(1.-COAF)
      CSF4=C1SF4-DELTSF**2
      DETSF4=BSF4**2-4.*ASF4*CSF4
      IF (DETSF4) 10,20,30
   10 CONTINUE
      PRINT 100,IASAR,IAFAR,DETSF4
  100 FORMAT (//,*SUBROUTINE SDOSF4,DETERMINANT  NEGATIVE *,3X,
     1*ALFAS =*,I3,3X,*ALFAF =*,I3,3X,*DETSF4 =*,F10.5/)
      GO TO 40
   20 CONTINUE
      DOSF4=-BSF4/(2.*ASF4)
      GO TO 40
   30 CONTINUE
      DO1SF4=(-BSF4-SQRT(DETSF4))/(2.*ASF4)
      DO2SF4=(-BSF4+SQRT(DETSF4))/(2.*ASF4)
      DOSF4=DO2SF4
   40 CONTINUE
      RETURN
      END


      SUBROUTINE SV1S1
      DIMENSION DELTA(5,5)
      COMMON /SSFFS/
     1COAS,COAF,COASAF,AMAS,AMAF,AMASAF,AMI,VF,GAMAS,GAMAF,BETA,DELTA,
     2IAFAR,IASAR,DOSF,DOFS,DOSS,DOFF,INDXSF,INDXFS,INDXSS,INDXFF,
     3TSF,TFS,TSS,TFF
     4,DELTSS,DELTFF,DELTSF,DELTFS
      COMMON /SF/
     2DOSF1,DOSF2,DOSF3,DOSF4,V1S1,V2S1,V3S1,V4S1,V1S2,V2S2,V3S2,
     3DV2S1,DV3S1,DV1S2,DV3S2,DV1S3,DV2S3,DV4S3,DODO3
      V3S1=-(DOSF1*(AMI*COASAF-1.)+BETA*(1.-COAF-AMI*(COASAF-COAS)))
     1/(AMASAF*VF)
```

```
      RETURN
      END


      SUBROUTINE SV2S1
      DIMENSION DELTA(5,5)
      COMMON /SSFFS/
     1COAS,COAF,COASAF,AMAS,AMAF,AMASAF,AMI,VF,GAMAS,GAMAF,BETA,DELTA,
     2IAFAR,IASAR,DOSF,DOFS,DOSS,DOFF,INDXSF,INDXFS,INDXSS,INDXFF,
     3TSF,TFS,TSS,TFF
     4,DELTSS,DELTFF,DELTSF,DELTFS
      COMMON /SF/
     2DOSF1,DOSF2,DOSF3,DOSF4,V1S1,V2S1,V3S1,V4S1,V1S2,V2S2,V3S2,
     3DV2S1,DV3S1,DV1S2,DV3S2,DV1S3,DV2S3,DV4S3,DODO3
      V2S1=-(DOSF2*(AMI*COASAF-1.)+BETA*(1.-COAF-AMI*(COASAF-COAS)))
     1/(AMASAF*VF)
      RETURN
      END


      SUBROUTINE SV3S1
      DIMENSION DELTA(5,5)
      COMMON /SSFFS/
     1COAS,COAF,COASAF,AMAS,AMAF,AMASAF,AMI,VF,GAMAS,GAMAF,BETA,DELTA,
     2IAFAR,IASAR,DOSF,DOFS,DOSS,DOFF,INDXSF,INDXFS,INDXSS,INDXFF,
     3TSF,TFS,TSS,TFF
     4,DELTSS,DELTFF,DELTSF,DELTFS
      COMMON /SF/
     2DOSF1,DOSF2,DOSF3,DOSF4,V1S1,V2S1,V3S1,V4S1,V1S2,V2S2,V3S2,
     3DV2S1,DV3S1,DV1S2,DV3S2,DV1S3,DV2S3,DV4S3,DODO3
      V3S1=-(DOSF3*(AMI*COASAF-1.)+BETA*(1.-COAF-AMI*(COASAF-COAS)))
     1/(AMASAF*VF)
      RETURN
      END


      SUBROUTINE SV4S1
      DIMENSION DELTA(5,5)
      COMMON /SSFFS/
     1COAS,COAF,COASAF,AMAS,AMAF,AMASAF,AMI,VF,GAMAS,GAMAF,BETA,DELTA,
     2IAFAR,IASAR,DOSF,DOFS,DOSS,DOFF,INDXSF,INDXFS,INDXSS,INDXFF,
     3TSF,TFS,TSS,TFF
     4,DELTSS,DELTFF,DELTSF,DELTFS
      COMMON /SF/
     2DOSF1,DOSF2,DOSF3,DOSF4,V1S1,V2S1,V3S1,V4S1,V1S2,V2S2,V3S2,
     3DV2S1,DV3S1,DV1S2,DV3S2,DV1S3,DV2S3,DV4S3,DODO3
      V4S1=-(DOSF4*(AMI*COASAF-1.)+BETA*(1.-COAF-AMI*(COASAF-COAS)))
     1/(AMASAF*VF)
```

```
      RETURN
      END


      SUBROUTINE SV1S2
      DIMENSION DELTA(5,5)
      COMMON /SSFFS/
     1COAS,COAF,COASAF,AMAS,AMAF,AMASAF,AMI,VF,GAMAS,GAMAF,BETA,DELTA,
     2IAFAR,IASAR,DOSF,DOFS,DOSS,DOFF,INDXSF,INDXFS,INDXSS,INDXFF,
     3TSF,TFS,TSS,TFF
     4,DELTSS,DELTFF,DELTSF,DELTFS
      COMMON /SF/
     2DOSF1,DOSF2,DOSF3,DOSF4,V1S1,V2S1,V3S1,V4S1,V1S2,V2S2,V3S2,
     3DV2S1,DV3S1,DV1S2,DV3S2,DV1S3,DV2S3,DV4S3,DOD03
      V3S2=(DOSF1*(1.-AMI*COAF)-BETA*(1.-COAF)*(1.+AMI))/(AMAF*VF)
      RETURN
      END


      SUBROUTINE SV2S2
      DIMENSION DELTA(5,5)
      COMMON /SSFFS/
     1COAS,COAF,COASAF,AMAS,AMAF,AMASAF,AMI,VF,GAMAS,GAMAF,BETA,DELTA,
     2IAFAR,IASAR,DOSF,DOFS,DOSS,DOFF,INDXSF,INDXFS,INDXSS,INDXFF,
     3TSF,TFS,TSS,TFF
     4,DELTSS,DELTFF,DELTSF,DELTFS
      COMMON /SF/
     2DOSF1,DOSF2,DOSF3,DOSF4,V1S1,V2S1,V3S1,V4S1,V1S2,V2S2,V3S2,
     3DV2S1,DV3S1,DV1S2,DV3S2,DV1S3,DV2S3,DV4S3,DOD03
      V2S2=(DOSF2*(1.-AMI*COAF)-BETA*(1.-COAF)*(1.+AMI))/(AMAF*VF)
      RETURN
      END


      SUBROUTINE SV3S2
      DIMENSION DELTA(5,5)
      COMMON /SSFFS/
     1COAS,COAF,COASAF,AMAS,AMAF,AMASAF,AMI,VF,GAMAS,GAMAF,BETA,DELTA,
     2IAFAR,IASAR,DOSF,DOFS,DOSS,DOFF,INDXSF,INDXFS,INDXSS,INDXFF,
     3TSF,TFS,TSS,TFF
     4,DELTSS,DELTFF,DELTSF,DELTFS
      COMMON /SF/
     2DOSF1,DOSF2,DOSF3,DOSF4,V1S1,V2S1,V3S1,V4S1,V1S2,V2S2,V3S2,
     3DV2S1,DV3S1,DV1S2,DV3S2,DV1S3,DV2S3,DV4S3,DOD03
      V3S2=(DOSF3*(1.-AMI*COAF)-BETA*(1.-COAF)*(1.+AMI))/(AMAF*VF)
      RETURN
      END
```

```
      SUBROUTINE SDV2S1
      DIMENSION DELTA(5,5)
      COMMON /SSFFS/
     1COAS,COAF,COASAF,AMAS,AMAF,AMASAF,AMI,VF,GAMAS,GAMAF,BETA,DELTA,
     2IAFAR,IASAR,DOSF,DOFS,DOSS,DOFF,INDXSF,INDXFS,INDXSS,INDXFF,
     3TSF,TFS,TSS,TFF
     4,DELTSS,DELTFF,DELTSF,DELTFS
      COMMON /SF/
     2DOSF1,DOSF2,DOSF3,DOSF4,V1S1,V2S1,V3S1,V4S1,V1S2,V2S2,V3S2,
     3DV2S1,DV3S1,DV1S2,DV3S2,DV1S3,DV2S3,DV4S3,DODO3
      ASF1=1.-(1.-AMI*COASAF)**2./AMASAF
      BSF1=-2.*BETA*(1.-COAF+(AMI*COASAF-1.)*(1.-COAF-AMI*
     1(COASAF-COAS))/AMASAF)
      C1SF1=BETA**2.*(2.*(1.-COAF)-(1.-COAF-AMI*(COASAF-COAS))**2/
     1AMASAF)
      A=DOSF2**2.*ASF1+DOSF2*BSF1+C1SF1
      IF (A) 10,20,20
   10 CONTINUE
      PRINT 100,IASAR,IAFAR,A
  100 FORMAT (//,*SUBROUTINE SDV2S1,SQ. RUOTE ARGUMENT NEGATIVE *,3X,
     1*ALFAS =*,I3,3X,*ALFAF =*,I3,3X,*SQRT.ARG. =*,F10.5/)
      GO TO 40
   20 CONTINUE
      DV2S1=SQRT(A)
   40 CONTINUE
      RETURN
      END


      SUBROUTINE SDV3S1
      DIMENSION DELTA(5,5)
      COMMON /SSFFS/
     1COAS,COAF,COASAF,AMAS,AMAF,AMASAF,AMI,VF,GAMAS,GAMAF,BETA,DELTA,
     2IAFAR,IASAR,DOSF,DOFS,DOSS,DOFF,INDXSF,INDXFS,INDXSS,INDXFF,
     3TSF,TFS,TSS,TFF
     4,DELTSS,DELTFF,DELTSF,DELTFS
      COMMON /SF/
     2DOSF1,DOSF2,DOSF3,DOSF4,V1S1,V2S1,V3S1,V4S1,V1S2,V2S2,V3S2,
     3DV2S1,DV3S1,DV1S2,DV3S2,DV1S3,DV2S3,DV4S3,DODO3
      ASF1=1.-(1.-AMI*COASAF)**2./AMASAF
      BSF1=-2.*BETA*(1.-COAF+(AMI*COASAF-1.)*(1.-COAF-AMI*
     1(COASAF-COAS))/AMASAF)
      C1SF1=BETA**2.*(2.*(1.-COAF)-(1.-COAF-AMI*(COASAF-COAS))**2/
     1AMASAF)
      A=DOSF3**2.*ASF1+DOSF3*BSF1+C1SF1
      IF (A) 10,20,20
   10 CONTINUE
```

```
      PRINT 100,IASAR,IAFAR,A
  100 FORMAT (//,*SUBROUTINE SDV3S1,SQ. ROUTE ARGUMENT NEGATIVE *,3X,
     1*ALFAS =*,I3,3X,*ALFAF =*,I3,3X,*SQRT.ARG. =*,F10.5/)
      GO TO 40
   20 CONTINUE
      DV3S1=SQRT(A)
   40 CONTINUE
      RETURN
      END


      SUBROUTINE SDV1S2
      DIMENSION DELTA(5,5)
      COMMON /SSFFS/
     1COAS,COAF,COASAF,AMAS,AMAF,AMASAF,AMI,VF,GAMAS,GAMAF,BETA,DELTA,
     2IAFAR,IASAR,DOSF,DOFS,DOSS,DOFF,INDXSF,INDXFS,INDXSS,INDXFF,
     3TSF,TFS,TSS,TFF
     4,DELTSS,DELTFF,DELTSF,DELTFS
      COMMON /SF/
     2DOSF1,DOSF2,DOSF3,DOSF4,V1S1,V2S1,V3S1,V4S1,V1S2,V2S2,V3S2,
     3DV2S1,DV3S1,DV1S2,DV3S2,DV1S3,DV2S3,DV4S3,DODO3
      ASF2=1.-(1.-AMI*COAF)**2./AMAF
      BSF2=-2.*BETA*(1.-COAF-(1.-AMI*COAF)*(1.-COAF)*(1.+AMI)/AMAF)
      C1SF2=BETA**2.*(2.*(1.-COAF)-(1.-COAF)**2.*(1.+AMI)**2./AMAF)
      A=DOSF1**2.*ASF2+DOSF1*BSF2+C1SF1
      IF (A) 10,20,20
   10 CONTINUE
      PRINT 100,IASAR,IAFAR,A
  100 FORMAT (//,*SUBROUTINE SDV1S2,SQ. ROUTE ARGUMENT NEGATIVE *,3X,
     1*ALFAS =*,I3,3X,*ALFAF =*,I3,3X,*SQRT.ARG. =*,F10.5/)
      GO TO 40
   20 CONTINUE
      DV1S2=SQRT(A)
   40 CONTINUE
      RETURN
      END


      SUBROUTINE SDV3S2
      DIMENSION DELTA(5,5)
      COMMON /SSFFS/
     1COAS,COAF,COASAF,AMAS,AMAF,AMASAF,AMI,VF,GAMAS,GAMAF,BETA,DELTA,
     2IAFAR,IASAR,DOSF,DOFS,DOSS,DOFF,INDXSF,INDXFS,INDXSS,INDXFF,
     3TSF,TFS,TSS,TFF
     4,DELTSS,DELTFF,DELTSF,DELTFS
      COMMON /SF/
     2DOSF1,DOSF2,DOSF3,DOSF4,V1S1,V2S1,V3S1,V4S1,V1S2,V2S2,V3S2,
     3DV2S1,DV3S1,DV1S2,DV3S2,DV1S3,DV2S3,DV4S3,DODO3
```

```
      ASF2=1.-(1.-AMI*COAF)**2./AMAF
      BSF2=-2.*BETA*(1.-COAF-(1.-AMI*COAF)*(1.-COAF)*(1.+AMI)/AMAF)
      C1SF2=BETA**2.*(2.*(1.-COAF)-(1.-COAF)**2.*(1.+AMI)**2./AMAF)
      A=DOSF3**2.*ASF2+DOSF3*BSF2+C1SF2
      IF (A) 10,20,20
   10 CONTINUE
      PRINT 100,IASAR,IAFAR,A
  100 FORMAT (//,*SUBROUTINE SDV3S2,SQ. ROUTE ARGUMENT NEGATIVE *,3X,
     1*ALFAS =*,I3,3X,*ALFAF =*,I3,3X,*SQRT.ARG. =*,F10.5/)
      GO TO 40
   20 CONTINUE
      DV3S2=SQRT(A)
   40 CONTINUE
      RETURN
      END


      SUBROUTINE SDV1S3
      DIMENSION DELTA(5,5)
      COMMON /SSFFS/
     1COAS,COAF,COASAF,AMAS,AMAF,AMASAF,AMI,VF,GAMAS,GAMAF,BETA,DELTA,
     2IAFAR,IASAR,DOSF,DOFS,DOSS,DOFF,INDXSF,INDXFS,INDXSS,INDXFF,
     3TSF,TFS,TSS,TFF
     4,DELTSS,DELTFF,DELTSF,DELTFS
      COMMON /SF/
     2DOSF1,DOSF2,DOSF3,DOSF4,V1S1,V2S1,V3S1,V4S1,V1S2,V2S2,V3S2,
     3DV2S1,DV3S1,DV1S2,DV3S2,DV1S3,DV2S3,DV4S3,DODO3
      DV1S3=BETA+(DOSF1-BETA)*AMI-VF*(1.-AMI)*(GAMAS/(AMI*VF)-
     1(DOSF1-BETA)/VF)
      RETURN
      END


      SUBROUTINE SDV2S3
      DIMENSION DELTA(5,5)
      COMMON /SSFFS/
     1COAS,COAF,COASAF,AMAS,AMAF,AMASAF,AMI,VF,GAMAS,GAMAF,BETA,DELTA,
     2IAFAR,IASAR,DOSF,DOFS,DOSS,DOFF,INDXSF,INDXFS,INDXSS,INDXFF,
     3TSF,TFS,TSS,TFF
     4,DELTSS,DELTFF,DELTSF,DELTFS
      COMMON /SF/
     2DOSF1,DOSF2,DOSF3,DOSF4,V1S1,V2S1,V3S1,V4S1,V1S2,V2S2,V3S2,
     3DV2S1,DV3S1,DV1S2,DV3S2,DV1S3,DV2S3,DV4S3,DODO3
      DV2S3=BETA+(DOSF2-BETA)*AMI-VF*(1.-AMI)*(GAMAS/(AMI*VF)-
     1(DOSF2-BETA)/VF)
      RETURN
      END
```

```
      SUBROUTINE SDV4S3
      DIMENSION DELTA(5,5)
      COMMON /SSFFS/
     1COAS,COAF,COASAF,AMAS,AMAF,AMASAF,AMI,VF,GAMAS,GAMAF,BETA,DELTA,
     2IAFAR,IASAR,DOSF,DOFS,DOSS,DOFF,INDXSF,INDXFS,INDXSS,INDXFF,
     3TSF,TFS,TSS,TFF
     4,DELTSS,DELTFF,DELTSF,DELTFS
      COMMON /SF/
     2DOSF1,DOSF2,DOSF3,DOSF4,V1S1,V2S1,V3S1,V4S1,V1S2,V2S2,V3S2,
     3DV2S1,DV3S1,DV1S2,DV3S2,DV1S3,DV2S3,DV4S3,DOD03
      DV4S3=BETA+(DOSF4-BETA)*AMI-VF*(1.-AMI)*(GAMAS/(AMI*VF)-
     1(DOSF4-BETA)/VF)
      RETURN
      END


      SUBROUTINE SDOD03
      DIMENSION DELTA(5,5)
      COMMON /SSFFS/
     1COAS,COAF,COASAF,AMAS,AMAF,AMASAF,AMI,VF,GAMAS,GAMAF,BETA,DELTA,
     2IAFAR,IASAR,DOSF,DOFS,DOSS,DOFF,INDXSF,INDXFS,INDXSS,INDXFF,
     3TSF,TFS,TSS,TFF
     4,DELTSS,DELTFF,DELTSF,DELTFS
      COMMON /SF/
     2DOSF1,DOSF2,DOSF3,DOSF4,V1S1,V2S1,V3S1,V4S1,V1S2,V2S2,V3S2,
     3DV2S1,DV3S1,DV1S2,DV3S2,DV1S3,DV2S3,DV4S3,DOD03
      DOD03=DOSF3**2.-2.*DOSF3*BETA*(1.-COAF)+2.*BETA**2.*(1.-COAF)
      RETURN
      END


      SUBROUTINE SDOFS
      DIMENSION DELTA(5,5)
      COMMON /SSFFS/
     1COAS,COAF,COASAF,AMAS,AMAF,AMASAF,AMI,VF,GAMAS,GAMAF,BETA,DELTA,
     2IAFAR,IASAR,DOSF,DOFS,DOSS,DOFF,INDXSF,INDXFS,INDXSS,INDXFF,
     3TSF,TFS,TSS,TFF
     4,DELTSS,DELTFF,DELTSF,DELTFS
      COMMON /FS/
     1DOFS1,DOFS2,DOFS4,DOFS5,T1S1,T2S1,T4S1,T1S2,T2S2,T4S2,DT2S1,DT1S2
     2,T5S1,DT5S1
      T12=-BETA/VF
      CALL SDOFS1
      CALL ST1S1
      IF (T1S1-T12) 100,100,120
  100 CONTINUE
```

```
      CALL ST1S2
      IF (T1S2-T12) 105,105,110
  105 CONTINUE
      DOFS=DOFS1
      INDXFS=1010
      GO TO 995
  110 CONTINUE
      CALL SDT1S2
      IF (DT1S2-DELTFS) 120,120,115
  115 CONTINUE
      DOFS=DOFS1
      INDXFS=1020
      GO TO 995
  120 CONTINUE
      CALL SDOFS2
      CALL ST2S2
      IF (T2S2-T12) 300,300,125
  125 CONTINUE
      IF (T2S2) 130,130,200
  130 CONTINUE
      CALL ST2S1
      IF (T2S1-T12) 140,140,135
  135 CONTINUE
      DOFS=DOFS2
      INDXFS=2010
      GO TO 995
  140 CONTINUE
      CALL SDT2S1
      IF (DT2S1-DELTFS) 150,150,145
  145 CONTINUE
      DOFS=DOFS2
      INDXFS=2020
      GO TO 995
  150 CONTINUE
      DOFS=0.
      INDXFS=1
      GO TO 995
  200 CONTINUE
      T5=GAMAS/VF
      IF (T2S2-T5) 205,205,240
  205 CONTINUE
      CALL ST2S1
      IF (T2S1-T12) 215,215,210
  210 CONTINUE
      DOFS=DOFS2
      INDXFS=2110
      GO TO 995
  215 CONTINUE
```

```
      CALL SDT2S1
      IF (DT2S1-DELTFS) 225,225,220
  220 CONTINUE
      DOFS=DOFS2
      INDXFS=2120
      GO TO 995
  225 CONTINUE
      DOFS=0.
      INDXFS=2
      GO TO 995
  240 CONTINUE
      CALL SDOFS5
      CALL ST5S1
      IF (T5S1-T12) 250,250,245
  245 CONTINUE
      DOFS=DOFS5
      INDXFS=5110
      GO TO 995
  250 CONTINUE
      CALL SDT5S1
      IF (DT5S1-DELTFS) 260,260,255
  255 CONTINUE
      DOFS=DOFS5
      INDXFS=5120
      GO TO 995
  260 CONTINUE
      CALL SDOFS1
      DOFS=DOFS1
      INDXFS=1030
      GO TO 995
  300 CONTINUE
      CALL SDOFS4
      CALL ST4S1
      CALL ST4S2
      IF (T4S1-T12) 320,320,305
  305 CONTINUE
      IF (T4S2-T12) 310,310,315
  310 CONTINUE
      DOFS=DOFS4
      INDXFS=4000
      GO TO 995
  315 CONTINUE
      DOFS=0.
      INDXFS=3
      GO TO 995
  320 CONTINUE
      IF (T4S2-T12) 325,325,330
  325 CONTINUE
```

```
      DOFS=0.
      INDXFS=4
      GO TO 995
  330 CONTINUE
      DOFS=0.
      INDXFS=5
      GO TO 995
  995 CONTINUE
      RETURN
      END


      SUBROUTINE SDOFS1
      DIMENSION DELTA(5,5)
      COMMON /SSFFS/
     1COAS,COAF,COASAF,AMAS,AMAF,AMASAF,AMI,VF,GAMAS,GAMAF,BETA,DELTA,
     2IAFAR,IASAR,DOSF,DOFS,DOSS,DOFF,INDXSF,INDXFS,INDXSS,INDXFF,
     3TSF,TFS,TSS,TFF
     4,DELTSS,DELTFF,DELTSF,DELTFS
      COMMON /FS/
     1DOFS1,DOFS2,DOFS4,DOFS5,T1S1,T2S1,T4S1,T1S2,T2S2,T4S2,DT2S1,DT1S2
     2,T5S1,DT5S1
      AFS1=1.-(COASAF-AMI)**2/AMASAF
      BFS1=2.*BETA*((COASAF-COAS)-(COASAF-AMI)*((1.-COAF)-AMI*
     1(COASAF-COAS))/AMASAF)
      C1FS1=BETA**2*(2.*(1.-COAF)-((1.-COAF)-AMI*(COASAF-COAS))**2/
     1AMASAF)
      CFS1=C1FS1-DELTFS**2
      DETFS1=BFS1**2-4.*AFS1*CFS1
      IF (DETFS1) 10,20,30
   10 CONTINUE
      PRINT 100,IASAR,IAFAR,DETFS1
  100 FORMAT (//,*SUBROUTINE SDOFS1,DETERMINANT  NEGATIVE *,3X,*ALFAS =*
     1,I3,3X,*ALFAF =*,I3,3X,*DETFS1 =*,F10.5/)
      GO TO 40
   20 CONTINUE
      DOFS1=-BFS1/(2.*AFS1)
      GO TO 40
   30 CONTINUE
      DO1FS1=(-BFS1-SQRT(DETFS1))/(2.*AFS1)
      DO2FS1=(-BFS1+SQRT(DETFS1))/(2.*AFS1)
      DOFS1=DO2FS1
   40 CONTINUE
      RETURN
      END


      SUBROUTINE SDOFS2
```

```
      DIMENSION DELTA(5,5)
      COMMON /SSFFS/
     1COAS,COAF,COASAF,AMAS,AMAF,AMASAF,AMI,VF,GAMAS,GAMAF,BETA,DELTA,
     2IAFAR,IASAR,DOSF,DOFS,DOSS,DOFF,INDXSF,INDXFS,INDXSS,INDXFF,
     3TSF,TFS,TSS,TFF
     4,DELTSS,DELTFF,DELTSF,DELTFS
      COMMON /FS/
     1DOFS1,DOFS2,DOFS4,DOFS5,T1S1,T2S1,T4S1,T1S2,T2S2,T4S2,DT2S1,DT1S2
     2,T5S1,DT5S1
      A=1.-(COAS-AMI)**2/AMAS
      IF (A) 10,10,20
   10 CONTINUE
      PRINT 100,IASAR,IAFAR,A
  100 FORMAT(//,*SUBROUTINE SDOFS2 NEG. ROUTE ARGUMENT NEGATIVE *,3X,
     1*ALFAS =*,I3,3X,*ALFAF =*,I3,3X,*SQRT.ARG. =*,F10.5/)
      GO TO 40
   20 CONTINUE
      DOFS2=DELTFS/SQRT(A)
   40 CONTINUE
      RETURN
      END


      SUBROUTINE SDOFS4
      DIMENSION DELTA(5,5)
      COMMON /SSFFS/
     1COAS,COAF,COASAF,AMAS,AMAF,AMASAF,AMI,VF,GAMAS,GAMAF,BETA,DELTA,
     2IAFAR,IASAR,DOSF,DOFS,DOSS,DOFF,INDXSF,INDXFS,INDXSS,INDXFF,
     3TSF,TFS,TSS,TFF
     4,DELTSS,DELTFF,DELTSF,DELTFS
      COMMON /FS/
     1DOFS1,DOFS2,DOFS4,DOFS5,T1S1,T2S1,T4S1,T1S2,T2S2,T4S2,DT2S1,DT1S2
     2,T5S1,DT5S1
      AFS4=1.
      BFS4=-2.*BETA*(COAS-AMI)
      C1FS4=BETA**2*AMAS
      CFS4=C1FS4-DELTFS**2
      DETFS4=BFS4**2-4.*AFS4*CFS4
      IF (DETFS4) 10,20,30
   10 CONTINUE
      PRINT 100,IASAR,IAFAR,DETFS4
  100 FORMAT(//,*SUBROUTINE SDOFS4,DETERMINANT  NEGATIVE *,3X,*ALFAS =*,
     1I3,3X,*ALFAF =*,I3,3X,*DETFS4 =*,F10.5/)
      GO TO 40
   20 CONTINUE
      DOFS4=-BFS4/(2.*AFS4)
      GO TO 40
   30 CONTINUE
```

```
      DO1FS4=(-BFS4-SQRT(DETFS4))/(2.*AFS4)
      DO2FS4=(-BFS4+SQRT(DETFS4))/(2.*AFS4)
      DOFS4=DO2FS4
   40 CONTINUE
      RETURN
      END


      SUBROUTINE SDOFS5
      DIMENSION DELTA(5,5)
      COMMON /SSFFS/
     1COAS,COAF,COASAF,AMAS,AMAF,AMASAF,AMI,VF,GAMAS,GAMAF,BETA,DELTA,
     2IAFAR,IASAR,DOSF,DOFS,DOSS,DOFF,INDXSF,INDXFS,INDXSS,INDXFF,
     3TSF,TFS,TSS,TFF
     4,DELTSS,DELTFF,DELTSF,DELTFS
      COMMON /FS/
     1DOFS1,DOFS2,DOFS4,DOFS5,T1S1,T2S1,T4S1,T1S2,T2S2,T4S2,DT2S1,DT1S2
     2,T5S1,DT5S1
      AFS5=1.
      BFS5=GAMAS*(COAS-AMI)*2.
      C1FS5=GAMAS**2*AMAS
      CFS5=C1FS5-DELTFS**2
      DETFS5=BFS5**2-4.*CFS5
      IF (DETFS5) 10,20,30
   10 CONTINUE
      PRINT 100,IASAR,IAFAR,DETFS5
  100 FORMAT (//,*SUBROUTINE SDOFS5,DETERMINANT  NEGATIVE *,3X,*ALFAS =*
     1,I3,3X,*ALFAF =*,I3,3X,*DETFS5 =*,F10.5/)
      GO TO 40
   20 CONTINUE
      DOFS5=-BFS5/2.
      GO TO 40
   30 CONTINUE
      DOFS5=(-BFS5+SQRT(DETFS5))/2.
   40 CONTINUE
      RETURN
      END


      SUBROUTINE ST1S1
      DIMENSION DELTA(5,5)
      COMMON /SSFFS/
     1COAS,COAF,COASAF,AMAS,AMAF,AMASAF,AMI,VF,GAMAS,GAMAF,BETA,DELTA,
     2IAFAR,IASAR,DOSF,DOFS,DOSS,DOFF,INDXSF,INDXFS,INDXSS,INDXFF,
     3TSF,TFS,TSS,TFF
     4,DELTSS,DELTFF,DELTSF,DELTFS
      COMMON /FS/
     1DOFS1,DOFS2,DOFS4,DOFS5,T1S1,T2S1,T4S1,T1S2,T2S2,T4S2,DT2S1,DT1S2
```

```
2,T5S1,DT5S1
 T1S1=-(DOFS1*(COASAF-AMI)+BETA*((1.-COAF)-AMI*(COASAF-COAS)))/
1(AMASAF*VF)
 RETURN
 END


 SUBROUTINE ST2S1
 DIMENSION DELTA(5,5)
 COMMON /SSFFS/
1COAS,COAF,COASAF,AMAS,AMAF,AMASAF,AMI,VF,GAMAS,GAMAF,BETA,DELTA,
2IAFAR,IASAR,DOSF,DOFS,DOSS,DOFF,INDXSF,INDXFS,INDXSS,INDXFF,
3TSF,TFS,TSS,TFF
4,DELTSS,DELTFF,DELTSF,DELTFS
 COMMON /FS/
1DOFS1,DOFS2,DOFS4,DOFS5,T1S1,T2S1,T4S1,T1S2,T2S2,T4S2,DT2S1,DT1S2
2,T5S1,DT5S1
 T2S1=-(DOFS2*(COASAF-AMI)+BETA*((1.-COAF)-AMI*(COASAF-COAS)))/
1(AMASAF*VF)
 RETURN
 END


 SUBROUTINE ST4S1
 DIMENSION DELTA(5,5)
 COMMON /SSFFS/
1COAS,COAF,COASAF,AMAS,AMAF,AMASAF,AMI,VF,GAMAS,GAMAF,BETA,DELTA,
2IAFAR,IASAR,DOSF,DOFS,DOSS,DOFF,INDXSF,INDXFS,INDXSS,INDXFF,
3TSF,TFS,TSS,TFF
4,DELTSS,DELTFF,DELTSF,DELTFS
 COMMON /FS/
1DOFS1,DOFS2,DOFS4,DOFS5,T1S1,T2S1,T4S1,T1S2,T2S2,T4S2,DT2S1,DT1S2
2,T5S1,DT5S1
 T4S1=-(DOFS4*(COASAF-AMI)+BETA*((1.-COAF)-AMI*(COASAF-COAS)))/
1(AMASAF*VF)
 RETURN
 END


 SUBROUTINE ST5S1
 DIMENSION DELTA(5,5)
 COMMON /SSFFS/
1COAS,COAF,COASAF,AMAS,AMAF,AMASAF,AMI,VF,GAMAS,GAMAF,BETA,DELTA,
2IAFAR,IASAR,DOSF,DOFS,DOSS,DOFF,INDXSF,INDXFS,INDXSS,INDXFF,
3TSF,TFS,TSS,TFF
4,DELTSS,DELTFF,DELTSF,DELTFS
 COMMON /FS/
1DOFS1,DOFS2,DOFS4,DOFS5,T1S1,T2S1,T4S1,T1S2,T2S2,T4S2,DT2S1,DT1S2
```

```
2,T5S1,DT5S1
 T5S1=-(DOFS5*(COASAF-AMI)+BETA*((1.-COAF)-AMI*(COASAF-COAS)))/
1(AMASAF*VF)
 RETURN
 END


 SUBROUTINE ST1S2
 DIMENSION DELTA(5,5)
 COMMON /SSFFS/
1COAS,COAF,COASAF,AMAS,AMAF,AMASAF,AMI,VF,GAMAS,GAMAF,BETA,DELTA,
2IAFAR,IASAR,DOSF,DOFS,DOSS,DOFF,INDXSF,INDXFS,INDXSS,INDXFF,
3TSF,TFS,TSS,TFF
4,DELTSS,DELTFF,DELTSF,DELTFS
 COMMON /FS/
1DOFS1,DOFS2,DOFS4,DOFS5,T1S1,T2S1,T4S1,T1S2,T2S2,T4S2,DT2S1,DT1S2
2,T5S1,DT5S1
 T1S2=-DOFS1*(COAS-AMI)/(AMAS*VF)
 RETURN
 END


 SUBROUTINE ST2S2
 DIMENSION DELTA(5,5)
 COMMON /SSFFS/
1COAS,COAF,COASAF,AMAS,AMAF,AMASAF,AMI,VF,GAMAS,GAMAF,BETA,DELTA,
2IAFAR,IASAR,DOSF,DOFS,DOSS,DOFF,INDXSF,INDXFS,INDXSS,INDXFF,
3TSF,TFS,TSS,TFF
4,DELTSS,DELTFF,DELTSF,DELTFS
 COMMON /FS/
1DOFS1,DOFS2,DOFS4,DOFS5,T1S1,T2S1,T4S1,T1S2,T2S2,T4S2,DT2S1,DT1S2
2,T5S1,DT5S1
 T2S2=-DOFS2*(COAS-AMI)/(AMAS*VF)
 RETURN
 END


 SUBROUTINE ST4S2
 DIMENSION DELTA(5,5)
 COMMON /SSFFS/
1COAS,COAF,COASAF,AMAS,AMAF,AMASAF,AMI,VF,GAMAS,GAMAF,BETA,DELTA,
2IAFAR,IASAR,DOSF,DOFS,DOSS,DOFF,INDXSF,INDXFS,INDXSS,INDXFF,
3TSF,TFS,TSS,TFF
4,DELTSS,DELTFF,DELTSF,DELTFS
 COMMON /FS/
1DOFS1,DOFS2,DOFS4,DOFS5,T1S1,T2S1,T4S1,T1S2,T2S2,T4S2,DT2S1,DT1S2
2,T5S1,DT5S1
 T4S2=-DOFS4*(COAS-AMI)/(AMAS*VF)
```

```
      RETURN
      END


      SUBROUTINE SDT2S1
      DIMENSION DELTA(5,5)
      COMMON /SSFFS/
     1COAS,COAF,COASAF,AMAS,AMAF,AMASAF,AMI,VF,GAMAS,GAMAF,BETA,DELTA,
     2IAFAR,IASAR,DOSF,DOFS,DOSS,DOFF,INDXSF,INDXFS,INDXSS,INDXFF,
     3TSF,TFS,TSS,TFF
     4,DELTSS,DELTFF,DELTSF,DELTFS
      COMMON /FS/
     1DOFS1,DOFS2,DOFS4,DOFS5,T1S1,T2S1,T4S1,T1S2,T2S2,T4S2,DT2S1,DT1S2
     2,T5S1,DT5S1
      AFS1=1.-(COASAF-AMI)**2/AMASAF
      BFS1=2.*BETA*((COASAF-COAS)-(COASAF-AMI)*((1.-COAF)-AMI*(COASAF-
     1COAS))/AMASAF)
      C1FS1=BETA**2*(2.*(1.-COAF)-((1.-COAF)-AMI*(COASAF-COAS))**2/
     1AMASAF)
      A=DOFS2**2*AFS1+DOFS2*BFS1+C1FS1
      IF (A) 10,20,20
   10 CONTINUE
      PRINT 100,IASAR,IAFAR,A
  100 FORMAT (//,*SUBROUTINE SDT2S1,SQ. ROUTE ARGUMENT NEGATIVE *,3X,
     1*ALFAS =*,I3,3X,*ALFAF =*,I3,3X,*SQRT.ARG. =*,F10.5/)
      GO TO 40
   20 CONTINUE
      DT2S1=SQRT(A)
   40 CONTINUE
      RETURN
      END


      SUBROUTINE SDT5S1
      DIMENSION DELTA(5,5)
      COMMON /SSFFS/
     1COAS,COAF,COASAF,AMAS,AMAF,AMASAF,AMI,VF,GAMAS,GAMAF,BETA,DELTA,
     2IAFAR,IASAR,DOSF,DOFS,DOSS,DOFF,INDXSF,INDXFS,INDXSS,INDXFF,
     3TSF,TFS,TSS,TFF
     4,DELTSS,DELTFF,DELTSF,DELTFS
      COMMON /FS/
     1DOFS1,DOFS2,DOFS4,DOFS5,T1S1,T2S1,T4S1,T1S2,T2S2,T4S2,DT2S1,DT1S2
     2,T5S1,DT5S1
      AFS1=1.-(COASAF-AMI)**2/AMASAF
      BFS1=2.*BETA*((COASAF-COAS)-(COASAF-AMI)*((1.-COAF)-AMI*(COASAF-
     1COAS))/AMASAF)
      C1FS1=BETA**2*(2.*(1.-COAF)-((1.-COAF)-AMI*(COASAF-COAS))**2/
     1AMASAF)
```

```
      A=DOFS5**2*AFS1+DOFS5*BFS1+CIFS1
      IF (A) 10,20,20
   10 CONTINUE
      PRINT 100,IASAR,IAFAR,A
  100 FORMAT (//,*SUBROUTINE SDT5S1,SQ. ROUTE ARGUMENT NEGATIVE *,3X,
     1*ALFAS =*,I3,3X,*ALFAF =*,I3,3X,*SQRT.ARG. =*,F10.5/)
      GO TO 40
   20 CONTINUE
      DT5S1=SQRT(A)
   40 CONTINUE
      RETURN
      END


      SUBROUTINE SDT1S2
      DIMENSION DELTA(5,5)
      COMMON /SSFFS/
     1COAS,COAF,COASAF,AMAS,AMAF,AMASAF,AMI,VF,GAMAS,GAMAF,BETA,DELTA,
     2IAFAR,IASAR,DOSF,DOFS,DOSS,DOFF,INDXSF,INDXFS,INDXSS,INDXFF,
     3TSF,TFS,TSS,TFF
     4,DELTSS,DELTFF,DELTSF,DELTFS
      COMMON /FS/
     1DOFS1,DOFS2,DOFS4,DOFS5,T1S1,T2S1,T4S1,T1S2,T2S2,T4S2,DT2S1,DT1S2
     2,T5S1,DT5S1
      A=1.-(COAS-AMI)**2/AMAS
      IF (A) 10,20,20
   10 CONTINUE
      PRINT 100,IASAR,IAFAR,A
  100 FORMAT(//,*SUBROUTINE SDT1S2,SQ. ROUTE ARGUMENT NEGATIVE *,3X,
     1*ALFAS =*,I3,3X,*ALFAF =*,I3,3X,*SQRT.ARG. =*,F10.5/)
      GO TO 40
   20 CONTINUE
      DT1S2=DOFS1*SQRT(A)
   40 CONTINUE
      RETURN
      END


      SUBROUTINE SDOSS
      DIMENSION DELTA(5,5)
      COMMON /SSFFS/
     1COAS,COAF,COASAF,AMAS,AMAF,AMASAF,AMI,VF,GAMAS,GAMAF,BETA,DELTA,
     2IAFAR,IASAR,DOSF,DOFS,DOSS,DOFF,INDXSF,INDXFS,INDXSS,INDXFF,
     3TSF,TFS,TSS,TFF
     4,DELTSS,DELTFF,DELTSF,DELTFS
      DOSS1=DELTSS/SQRT(.5+.5*COAS)
      T1S1=DOSS1/(2.*AMI*VF)
      T5=GAMAS/(AMI*VF)
```

```
      IF (T1S1-T5) 10,10,110
   10 CONTINUE
      DOSS=DOSS1
      INDXSS=1000
      GO TO 200
  110 CONTINUE
      ASS5=1.
      BSS5=-2.*GAMAS*(1.-COAS)
      C1SS5=2.*GAMAS**2*(1.-COAS)
      CSS5=C1SS5-DELTSS**2
      DETSS5=BSS5**2-4.*CSS5
      DOSS5=(-BSS5+SQRT(DETSS5))/2.
      DOSS=DOSS5
      INDXSS=4000
  200 CONTINUE
      RETURN
      END


      SUBROUTINE SDOFF
      DIMENSION DELTA(5,5)
      COMMON /SSFFS/
     1COAS,COAF,COASAF,AMAS,AMAF,AMASAF,AMI,VF,GAMAS,GAMAF,BETA,DELTA,
     2IAFAR,IASAR,DOSF,DOFS,DOSS,DOFF,INDXSF,INDXFS,INDXSS,INDXFF,
     3TSF,TFS,TSS,TFF
     4,DELTSS,DELTFF,DELTSF,DELTFS
      DOFF1=DELTFF/SQRT(.5+.5*COAF)
      T1S1=DOFF1/(2.*VF)
      T5=GAMAF/VF
      IF (T1S1-T5) 10,10,110
   10 CONTINUE
      DOFF=DOFF1
      INDXFF=1000
      GO TO 200
  110 CONTINUE
      AFF5=1.
      BFF5=-2.*GAMAF*(1.-COAF)
      C1FF5=2.*GAMAF**2*(1.-COAF)
      CFF5=C1FF5-DELTFF**2
      DETFF5=BFF5**2-4.*CFF5
      DOFF5=(-BFF5+SQRT(DETFF5))/2.
      DOFF=DOFF5
      INDXFF=4000
  200 CONTINUE
      RETURN
      END
```

```
      SUBROUTINE DOT
      DIMENSION DELTA(5,5)
      COMMON /SSFFS/
     1COAS,COAF,COASAF,AMAS,AMAF,AMASAF,AMI,VF,GAMAS,GAMAF,BETA,DELTA,
     2IAFAR,IASAR,DOSF,DOFS,DOSS,DOFF,INDXSF,INDXFS,INDXSS,INDXFF,
     3TSF,TFS,TSS,TFF
     4,DELTSS,DELTFF,DELTSF,DELTFS
      TSS=DOSS/(AMI*VF)
      TFF=DOFF/VF
      TSF=(GAMAS+DOSF)/VF-GAMAS/(AMI*VF)
      TFS=(GAMAS+DOFS)/(AMI*VF)-GAMAS/VF
      RETURN
      END
```

B.3. Program CAPSF (Case with two aircraft types)

```
C
C   PROGRAM COMPUTING  CAPSF
C
      PROGRAM CAPSF (INPUT,OUTPUT)
      DIMENSION ISAR(10,19),IFAR(10,19),DOOSF(10,19),INXSF(10,19),
     1DOOFS(10,19),INXFS(10,19),DOOSS(10),INXSS(10),DOOFF(10,19),
     2INXFF(10,19),CAPAC(10,19),
     3DELTA(5,5)
      COMMON /SSFFS/
     1COAS,COAF,COASAF,AMAS,AMAF,AMASAF,AMI,VF,GAMAS,GAMAF,BETA,DELTA,
     2IAFAR,IASAR,DOSF,DOFS,DOSS,DOFF,INDXSF,INDXFS,INDXSS,INDXFF,
     3TSF,TFS,TSS,TFF
     4,DELTSS,DELTFF,DELTSF,DELTFS
C
C   DO LOOP TO REPEAT THE WHOLE PROGRAM WITH NEW INPUT DATA
C
 9999 CONTINUE
C
C   INPUT DATA
C
      PALF=1.57077
      DALF=0.17453
      IPALF=90
      IDALF=10
 3010 FORMAT(2F10.5)
 3015 FORMAT(4F10.5)
      READ 3010,VFKT,VSKT
      READ 3010,GAMAF,GAMAS
      READ 3015,DELTSS,DELTSF,DELTFS,DELTFF
      READ 3010,PF,PS
C
C   INITIAL DATA CONVERSION
C
      VS=VSKT/3600.
      VF=VFKT/3600.
      AMI=VS/VF
      BETA=GAMAF-GAMAS
      PFF=PF*PF
      PSS=PS*PS
      PFS=PS*PF
      PSF=PS*PF
C
C   PRINT INPUT DATA
C
      PRINT 3110,VFKT
 3110 FORMAT(1H1,10X,*VF =*,F7.2/)
      PRINT 3120,VSKT
 3120 FORMAT(11X,*VS =*,F7.2/)
```

```
      PRINT 3130,AMI
 3130 FORMAT(11X,*MI =*,F10.5/)
      PRINT 3140,GAMAF
 3140 FORMAT(8X,*GAMAF =*,F7.2/)
      PRINT 3150,GAMAS
 3150 FORMAT(8X,*GAMAS =*,F7.2/)
      PRINT 3160,BETA
 3160 FORMAT(9X,*BETA =*,F7.2/)
      PRINT 3171,DELTSS
      PRINT 3172,DELTSF
      PRINT 3173,DELTFS
      PRINT 3174,DELTFF
 3171 FORMAT(7X,*DELTSS =*,F7.2/)
 3172 FORMAT(7X,*DELTSF =*,F7.2/)
 3173 FORMAT(7X,*DELTFS =*,F7.2/)
 3174 FORMAT(7X,*DELTFF =*,F7.2/)
      PRINT 3180,PF
      PRINT 3190,PS
 3180 FORMAT(11X,*PF =*,F7.2/)
 3190 FORMAT(11X,*PS =*,F7.2/)
C
C   ANGLE MATRIX GENERATION
C
      DO 999 I=1,10
      EI1=FLOAT(I-1)
      AS=PALF-DALF*EI1
      IASAR=IPALF-IDALF*(I-1)
      DO 998 J=I,19
      IF (I-J) 2120,2110,2120
 2110 CONTINUE
      AF=AS-0.5*DALF
      IAFAR=IASAR-IDALF/2
      GO TO 2130
 2120 CONTINUE
      EJ1=FLOAT(J-1)
      AF=PALF-DALF*EJ1
      IAFAR=IPALF-IDALF*(J-1)
 2130 CONTINUE
      ISAR(I,J)=IASAR
      IFAR(I,J)=IAFAR
C
C   PREPARATION FOR SUBROUTINES
C
      COAS=COS(AS)
      COAF=COS(AF)
      COASAF=COS(AS-AF)
      AMAS=AMI**2.-2.*AMI*COAS+1.
      AMAF=AMI**2.-2.*AMI*COAF+1.
```

```
      AMASAF=AMI**2.-2.*AMI*COASAF+1.
C
C   MAIN PROGRAM
C
      CALL SDOSF
      DOOSF(I,J)=DOSF
      INXSF(I,J)=INDXSF
      CALL SDOFS
      DOOFS(I,J)=DOFS
      INXFS(I,J)=INDXFS
      CALL SDOFF
      DOOFF(I,J)=DOFF
      INXFF(I,J)=INDXFF
      CALL SDOSS
      DOOSS(I)=DOSS
      INXSS(I)=INDXSS
      CALL DOT
      TBAR=TSF*PSF+TFS*PFS+TFF*PFF+TSS*PSS
      CAP=3600./TBAR
      CAPAC(I,J)=CAP
  998 CONTINUE
  999 CONTINUE
C
C   PRINT TABLES
C
      PRINT 4700
 4700 FORMAT(1H1,20X,*CAPSF*////)
      PRINT 4805,(ISAR(I,J),I=1,10)
      DO 4710 J=1,19
      IANGF=100-10*J
      PRINT 4711,IANGF,(CAPAC(I,J),I=1,10)
 4711 FORMAT(I6,4X,10F10.3/)
 4710 CONTINUE
      PRINT 4800
 4800 FORMAT(1H1,20X,*DOSF*////)
      PRINT 4805,(ISAR(I,J),I=1,10)
      DO 4810 J=1,19
      IANGF=100-10*J
      PRINT 4811,IANGF,(DOOSF(I,J),I=1,10)
 4810 CONTINUE
      PRINT 4820
 4820 FORMAT(1H1,20X,*INDXSF*////)
      PRINT 4805,(ISAR(I,J),I=1,10)
      DO 4830 J=1,19
      IANGF=100-10*J
      PRINT 4812,IANGF,(INXSF(I,J),I=1,10)
 4830 CONTINUE
 4805 FORMAT(10X,10I10//)
```

```
4811 FORMAT(I6,4X,10F10.5/)
4812 FORMAT(I6,4X,10I10/)
     PRINT 4840
4840 FORMAT(1H1,20X,*DOFS*////)
     PRINT 4805,(ISAR(I,J),I=1,10)
     DO 4850 J=1,19
     IANGF=100-10*J
     PRINT 4811,IANGF,(DOOFS(I,J),I=1,10)
4850 CONTINUE
     PRINT 4860
4860 FORMAT(1H1,20X,*INDXFS*////)
     PRINT 4805,(ISAR(I,J),I=1,10)
     DO 4870 J=1,19
     IANGF=100-10*J
     PRINT 4812,IANGF,(INXFS(I,J),I=1,10)
4870 CONTINUE
     PRINT 4880
4880 FORMAT(1H1,20X,*DOSS,INDXSS*////)
     PRINT 4805,(ISAR(I,J),I=1,10)
     PRINT 4881,(DOOSS(I),I=1,10)
4881 FORMAT(10X,10F10.5/)
     PRINT 4882,(INXSS(I),I=1,10)
4882 FORMAT(10X,10I10)
     PRINT 4890
4890 FORMAT(1H1,20X,*DOFF*////)
     PRINT 4805,(ISAR(I,J),I=1,10)
     DO 4900 J=1,19
     IANGF=100-10*J
     PRINT 4811,IANGF,(DOOFF(I,J),I=1,10)
4900 CONTINUE
     PRINT 4910
4910 FORMAT(1H1,20X,*INDXFF*////)
     PRINT 4805,(ISAR(I,J),I=1,10)
     DO 4920 J=1,19
     IANGF=100-10*J
     PRINT 4812,IANGF,(INXFF(I,J),I=1,10)
4920 CONTINUE
     GO TO 9999
     STOP
     END
```

B.4. Program CAP3 (Case with three aircraft types)

```
C
C   PROGRAM COMPUTING  CAP3
C
      PROGRAM CAP3(INPUT,OUTPUT)
      DIMENSION VKT(5),GAMA(5),P(5),PP(5,5),DELTA(5,5),TT(5,5),
     1IALF1(50),IALF2(50),IALF3(50),CAPAC(50),CAPMIN(50),
     2IALFM1(50),IALFM2(50),IALFM3(50)
      COMMON /SSFFS/
     1COAS,COAF,COASAF,AMAS,AMAF,AMASAF,AMI,VF,GAMAS,GAMAF,BETA,DELTA,
     2IAFAR,IASAR,DOSF,DOFS,DOSS,DOFF,INDXSF,INDXFS,INDXSS,INDXFF,
     3TSF,TFS,TSS,TFF
     4,DELTSS,DELTFF,DELTSF,DELTFS
C
C   DO LOOP TO REPEAT THE WHOLE PROGRAM WITH NEW INPUT DATA
C
 9999 CONTINUE
C
C   INPUT DATA
C
      M=3
      NM=40
      READ 3010,(VKT(I),I=1,M)
 3010 FORMAT(3F10.5)
      READ 3010,(GAMA(I),I=1,M)
      READ 3010,(P(I),I=1,M)
      READ 3010,((DELTA(I,J),J=1,M),I=1,M)
C
C   PRINT INPUT DATA
C
      PRINT 3111
 3111 FORMAT(1H1,10X,*INPUT DATA*,///)
      DO 3110 I=1,M
      PRINT 3112,I,VKT(I),I,GAMA(I),I,P(I)
 3112 FORMAT(11X,*VKT*,I1,* =*,F7.2,3X,*GAMA*,I1,* =*,F7.2,3X,*P*,I1,
     1* =*,F4.2/)
 3110 CONTINUE
      PRINT 3120
 3120 FORMAT(//,11X,*DELTA MATRIX*//)
      PRINT 3130
 3130 FORMAT(20X,*TRAILING A/C*/)
      PRINT 3131,(J,J=1,M)
 3131 FORMAT(19X,3(I1,9X),/)
      DO 3140 I=1,M
      PRINT 3132,I,(DELTA(I,J),J=1,M)
 3132 FORMAT(9X,I2,3F10.2,/)
 3140 CONTINUE
C
C   INITIAL DATA PREPARATION
```

```
C
      DO 4010 I=1,M
      DO 4009 J=1,M
      PP(I,J)=P(I)*P(J)
 4009 CONTINUE
 4010 CONTINUE
      DO 4020 N=1,NM
      CAPAC(N)=0.
      CAPMIN(N)=9999.
      IALF1(N)=0
      IALF2(N)=0
      IALF3(N)=0
 4020 CONTINUE
      PALF=1.57077
      DALF=0.17453
      IPALF=90
      IDALF=10
C
CC   MAIN PROGRAM
C
C    CASE  A
C
C    ANGLES GENERATION
C
      DO 2495 I1=1,8
      E11=FLOAT(I1-1)
      A1=PALF-DALF*E11
      IA1AR=IPALF-IDALF*(I1-1)
      I1PLS1=I1+1
      DO 2490 I2=I1PLS1,9
      E21=FLOAT(I2-1)
      A2=PALF-DALF*E21
      IA2AR=IPALF-IDALF*(I2-1)
      I2PLS1=I2+1
      DO 2485 I3=I2PLS1,19
      E31=FLOAT(I3-1)
      A3=PALF-DALF*E31
      IA3AR=IPALF-IDALF*(I3-1)
C
CC   AIRCRAFT  1  AND  2
C
      VS=VKT(1)/3600.
      VF=VKT(2)/3600.
      AMI=VS/VF
      GAMAF=GAMA(2)
      GAMAS=GAMA(1)
      BETA=GAMAF-GAMAS
      DELTSS=DELTA(1,1)
```

```
      DELTFF=DELTA(2,2)
      DELTSF=DELTA(1,2)
      DELTFS=DELTA(2,1)
      AS=A1
      AF=A2
      IAFAR=IA2AR
      IASAR=IA1AR
      COAS=COS(AS)
      COAF=COS(AF)
      COASAF=COS(AS-AF)
      AMAS=AMI**2-2.*AMI*COAS+1.
      AMAF=AMI**2-2.*AMI*COAF+1.
      AMASAF=AMI**2-2.*AMI*COASAF+1.
      CALL SDOSF
      CALL SDOFS
      CALL SDOFF
      CALL SDOSS
      CALL DOT
      TT(1,1)=TSS
      TT(1,2)=TSF
      TT(2,1)=TFS
      TT(2,2)=TFF
C
CC  AIRCRAFT  1  AND  3
C
      VS=VKT(1)/3600.
      VF=VKT(3)/3600.
      AMI=VS/VF
      GAMAF=GAMA(3)
      GAMAS=GAMA(1)
      BETA=GAMAF-GAMAS
      DELTSS=DELTA(1,1)
      DELTFF=DELTA(3,3)
      DELTSF=DELTA(1,3)
      DELTFS=DELTA(3,1)
      AS=A1
      AF=A3
      IAFAR=IA3AR
      IASAR=IA1AR
      COAS=COS(AS)
      COAF=COS(AF)
      COASAF=COS(AS-AF)
      AMAS=AMI**2-2.*AMI*COAS+1.
      AMAF=AMI**2-2.*AMI*COAF+1.
      AMASAF=AMI**2-2.*AMI*COASAF+1.
      CALL SDOSF
      CALL SDOFS
      CALL SDOFF
```

```
      CALL SDOSS
      CALL DOT
      TT(1,3)=TSF
      TT(3,1)=TFS
      TT(3,3)=TFF
C
C  AIRCRAFT  2  AND  3
C
      VS=VKT(2)/3600.
      VF=VKT(3)/3600.
      AMI=VS/VF
      GAMAF=GAMA(3)
      GAMAS=GAMA(2)
      BETA=GAMAF-GAMAS
      DELTSS=DELTA(2,2)
      DELTFF=DELTA(3,3)
      DELTSF=DELTA(2,3)
      DELTFS=DELTA(3,2)
      AS=A2
      AF=A3
      IASAR=IA2AR
      IAFAR=IA3AR
      COAS=COS(AS)
      COAF=COS(AF)
      COASAF=COS(AS-AF)
      AMAS=AMI**2-2.*AMI*COAS+1.
      AMAF=AMI**2-2.*AMI*COAF+1.
      AMASAF=AMI**2-2.*AMI*COASAF+1.
      CALL SDOSF
      CALL SDOFS
      CALL SDOFF
      CALL SDOSS
      CALL DOT
      TT(2,3)=TSF
      TT(3,2)=TFS
C
C  MEAN INTERARRIVAL TIME AND CAPACITY
C
      TBAR=0.
      DO 2420 I=1,M
      DO 2410 J=1,M
      TBAR=TBAR+TT(I,J)*PP(I,J)
 2410 CONTINUE
 2420 CONTINUE
      CAP=3600./TBAR
      N=NM
      IF (CAP.LT.CAPAC(N)) GO TO 2470
      DO 2450 NI=1,N
```

```
      IF (CAP-CAPAC(N1)) 2450,2450,2440
 2440 CONTINUE
      NN=N1
      GO TO 2455
 2450 CONTINUE
 2455 CONTINUE
      NMINNN=N-NN
      DO 2460 NOP=1,NMINNN
      N2=N-NOP
      N2P1=N2+1
      CAPAC(N2P1)=CAPAC(N2)
      IALF1(N2P1)=IALF1(N2)
      IALF2(N2P1)=IALF2(N2)
      IALF3(N2P1)=IALF3(N2)
 2460 CONTINUE
      CAPAC(NN)=CAP
      IALF1(NN)=IA1AR
      IALF2(NN)=IA2AR
      IALF3(NN)=IA3AR
 2470 CONTINUE
      N=NM
      IF (CAP.GT.CAPMIN(N)) GO TO 2478
      DO 2474 N1=1,N
      IF (CAP-CAPMIN(N1)) 2472,2474,2474
 2472 NN=N1
      GO TO 2475
 2474 CONTINUE
 2475 CONTINUE
      NMINNN=N-NN
      DO 2476 NOP=1,NMINNN
      N2=N-NOP
      N2P1=N2+1
      CAPMIN(N2P1)=CAPMIN(N2)
      IALFM1(N2P1)=IALFM1(N2)
      IALFM2(N2P1)=IALFM2(N2)
      IALFM3(N2P1)=IALFM3(N2)
 2476 CONTINUE
      CAPMIN(NN)=CAP
      IALFM1(NN)=IA1AR
      IALFM2(NN)=IA2AR
      IALFM3(NN)=IA3AR
 2478 CONTINUE
 2485 CONTINUE
 2490 CONTINUE
 2495 CONTINUE
C
C   MAIN PROGRAM
C
```

```
C  CASE  8
CC
CC  ANGLE GENERATION
C
      DO 2595 I1=1,9
      E11=FLOAT(I1-1)
      A1=PALF-DALF*E11
      IA1AR=IPALF-IDALF*(I1-1)
      I1PLS1=I1+1
      DO 2590 I2=11,19
      E21=FLOAT(I2-1)
      A2=PALF-DALF*E21
      IA2AR=IPALF-IDALF*(I2-1)
      I2MIN1=I2-1
      DO 2585 I3=I1PLS1,I2MIN1
      E31=FLOAT(I3-1)
      A3=PALF-DALF*E31
      IA3AR=IPALF-IDALF*(I3-1)
C
CC  AIRCRAFT  1  AND  2
C
      VS=VKT(1)/3600.
      VF=VKT(2)/3600.
      AMI=VS/VF
      GAMAF=GAMA(2)
      GAMAS=GAMA(1)
      BETA=GAMAF-GAMAS
      DELTSS=DELTA(1,1)
      DELTFF=DELTA(2,2)
      DELTSF=DELTA(1,2)
      DELTFS=DELTA(2,1)
      AS=A1
      AF=A2
      IAFAR=IA2AR
      IASAR=IA1AR
      COAS=COS(AS)
      COAF=COS(AF)
      COASAF=COS(AS-AF)
      AMAS=AMI**2-2.*AMI*COAS+1.
      AMAF=AMI**2-2.*AMI*COAF+1.
      AMASAF=AMI**2-2.*AMI*COASAF+1.
      CALL SDOSF
      CALL SDOFS
      CALL SDOFF
      CALL SDOSS
      CALL DOT
      TT(1,1)=TSS
      TT(1,2)=TSF
```

```
      TT(2,1)=TFS
      TT(2,2)=TFF
C
CC   AIRCRAFT  1  AND  3
C
      VS=VKT(1)/3600.
      VF=VKT(3)/3600.
      AMI=VS/VF
      GAMAF=GAMA(3)
      GAMAS=GAMA(1)
      BETA=GAMAF-GAMAS
      DELTSS=DELTA(1,1)
      DELTFF=DELTA(3,3)
      DELTSF=DELTA(1,3)
      DELTFS=DELTA(3,1)
      AS=A1
      AF=A3
      IAFAR=IA3AR
      IASAR=IA1AR
      COAS=COS(AS)
      COAF=COS(AF)
      COASAF=COS(AS-AF)
      AMAS=AMI**2-2.*AMI*COAS+1.
      AMAF=AMI**2-2.*AMI*COAF+1.
      AMASAF=AMI**2-2.*AMI*COASAF+1.
      CALL SDOSF
      CALL SDOFS
      CALL SDOFF
      CALL SDOSS
      CALL DOT
      TT(1,3)=TSF
      TT(3,1)=TFS
      TT(3,3)=TFF
C
CC   AIRCRAFT  2  AND  3
C
      VS=VKT(2)/3600.
      VF=VKT(3)/3600.
      AMI=VS/VF
      GAMAF=GAMA(3)
      GAMAS=GAMA(2)
      BETA=GAMAF-GAMAS
      DELTSS=DELTA(2,2)
      DELTFF=DELTA(3,3)
      DELTSF=DELTA(2,3)
      DELTFS=DELTA(3,2)
      AS=A2
      AF=A3
```

```
      IASAR=IA2AR
      IAFAR=IA3AR
      COAS=COS(AS)
      COAF=COS(AF)
      COASAF=COS(AS-AF)
      AMAS=AMI**2-2.*AMI*COAS+1.
      AMAF=AMI**2-2.*AMI*COAF+1.
      AMASAF=AMI**2-2.*AMI*COASAF+1.
      CALL SDOSF
      CALL SDOFS
      CALL SDOFF
      CALL SDOSS
      CALL DOT
      TT(2,3)=TSF
      TT(3,2)=TFS
C
C  MEAN INTERARRIVAL TIME
C
      TBAR=0.
      DO 2520 I=1,M
      DO 2510 J=1,M
      TBAR=TBAR+TT(I,J)*PP(I,J)
 2510 CONTINUE
 2520 CONTINUE
      CAP=3600./TBAR
      N=NM
      IF (CAP.LT.CAPAC(N)) GO TO 2570
      DO 2550 N1=1,N
      IF (CAP-CAPAC(N1)) 2550,2550,2540
 2540 CONTINUE
      NN=N1
      GO TO 2555
 2550 CONTINUE
 2555 CONTINUE
      NMINNN=N-NN
      DO 2560 NOP=1,NMINNN
      N2=N-NOP
      N2P1=N2+1
      CAPAC(N2P1)=CAPAC(N2)
      IALF1(N2P1)=IALF1(N2)
      IALF2(N2P1)=IALF2(N2)
      IALF3(N2P1)=IALF3(N2)
 2560 CONTINUE
      CAPAC(NN)=CAP
      IALF1(NN)=IA1AR
      IALF2(NN)=IA2AR
      IALF3(NN)=IA3AR
 2570 CONTINUE
```

```
      N=NM
      IF (CAP.GT.CAPMIN(N)) GO TO 2578
      DO 2574 N1=1,N
      IF (CAP-CAPMIN(N1)) 2572,2574,2574
 2572 NN=N1
      GO TO 2575
 2574 CONTINUE
 2575 CONTINUE
      NMINNN=N-NN
      DO 2576 NOP=1,NMINNN
      N2=N-NOP
      N2P1=N2+1
      CAPMIN(N2P1)=CAPMIN(N2)
      IALFM1(N2P1)=IALFM1(N2)
      IALFM2(N2P1)=IALFM2(N2)
      IALFM3(N2P1)=IALFM3(N2)
 2576 CONTINUE
      CAPMIN(NN)=CAP
      IALFM1(NN)=IA1AR
      IALFM2(NN)=IA2AR
      IALFM3(NN)=IA3AR
 2578 CONTINUE
 2585 CONTINUE
 2590 CONTINUE
 2595 CONTINUE
C
C  PRINTING RESULTS
C
      PRINT 4050
 4050 FORMAT(1H1,///,13X,*MAXIMAL CAPACITY-OPTIMAL ANGLES*,////)
      PRINT 4100
 4100 FORMAT(14X,*CAPACITY*,5X,*ALFA1*,5X,*ALFA2*,5X,*ALFA3*,///)
      DO 4150 NP=1,NM
      PRINT 4151,NP,CAPAC(NP),IALF1(NP),IALF2(NP),IALF3(NP)
 4151 FORMAT(5X,I5,F10.3,3I10)
 4150 CONTINUE
      PRINT 4250
 4250 FORMAT(1H1,///,13X,*MINIMAL CAPACITY-THE WORSE ANGLES*,////)
      PRINT 4100
      DO 4260 NP=1,NM
      PRINT 4151,NP,CAPMIN(NP),IALFM1(NP),IALFM2(NP),IALFM3(NP)
 4260 CONTINUE
      GO TO 9999
      STOP
      END
```

B.5. Program CAP4 (Case with four aircraft types)

```
C
C  PROGRAM COMPUTING  CAP4
C
      PROGRAM CAP4(INPUT,OUTPUT)
      DIMENSION VKT(5),GAMA(5),P(5),PP(5,5),DELTA(5,5),TT(5,5),
     1IALF1(50),IALF2(50),IALF3(50),IALF4(50),CAPAC(50),CAPMIN(50),
     2IALFM1(50),IALFM2(50),IALFM3(50),IALFM4(50)
      COMMON /SSFFS/
     1COAS,COAF,COASAF,AMAS,AMAF,AMASAF,AMI,VF,GAMAS,GAMAF,BETA,DELTA,
     2IAFAR,IASAR,DOSF,DOFS,DOSS,DOFF,INDXSF,INDXFS,INDXSS,INDXFF,
     3TSF,TFS,TSS,TFF
     4,DELTSS,DELTFF,DELTSF,DELTFS
C
C  DO LOOP TO REPEAT THE WHOLE PROGRAM WITH NEW INPUT DATA
C
 9999 CONTINUE
C
C  INPUT DATA
C
      M=4
      NM=40
      READ 3010,(VKT(I),I=1,M)
 3010 FORMAT(4F10.5)
      READ 3010,(GAMA(I),I=1,M)
      READ 3010,(P(I),I=1,M)
      READ 3010,((DELTA(I,J),J=1,M),I=1,M)
C
C  PRINT INPUT DATA
C
      PRINT 3111
 3111 FORMAT(1H1,10X,*INPUT DATA*,///)
      DO 3110 I=1,M
      PRINT 3112,I,VKT(I),I,GAMA(I),I,P(I)
 3112 FORMAT(11X,*VKT*,I1,* =*,F7.2,3X,*GAMA*,I1,* =*,F7.2,3X,*P*,I1,
     1* =*,F4.2/)
 3110 CONTINUE
      PRINT 3120
 3120 FORMAT(//,11X,*DELTA MATRIX*//)
      PRINT 3130
 3130 FORMAT(21X,*TRAILING A/C*//)
      PRINT 3131,(J,J=1,M)
 3131 FORMAT(18X,4(I1,9X),/)
      DO 3140 I=1,M
      PRINT 3132,I,(DELTA(I,J),J=1,M)
 3132 FORMAT(7X,I2,2X,4(F10.2),/)
 3140 CONTINUE
C
C  INITIAL DATA PREPARATION
```

```
C
      DO 4010 I=1,M
      DO 4009 J=1,M
      PP(I,J)=P(I)*P(J)
 4009 CONTINUE
 4010 CONTINUE
      DO 4020 N=1,NM
      CAPAC(N)=0.
      CAPMIN(N)=9999.
      IALF1(N)=0
      IALF2(N)=0
      IALF3(N)=0
      IALF4(N)=0
 4020 CONTINUE
      PALF=1.57077
      DALF=0.17453
      IPALF=90
      IDALF=10
C
C
C  MAIN PROGRAM CASE  A
C
C  ANGLES GENERATION
C
      DO 2195 I1=1,7
      E11=FLOAT(I1-1)
      A1=PALF-DALF*E11
      IA1AR=IPALF-IDALF*(I1-1)
      I1PLS1=I1+1
      DO 2190 I2=I1PLS1,8
      E21=FLOAT(I2-1)
      A2=PALF-DALF*E21
      IA2AR=IPALF-IDALF*(I2-1)
      I2PLS1=I2+1
      DO 2185 I3=I2PLS1,9
      E31=FLOAT(I3-1)
      A3=PALF-DALF*E31
      IA3AR=IPALF-IDALF*(I3-1)
      I3PLS1=I3+1
      DO 2180 I4=I3PLS1,19
      E41=FLOAT(I4-1)
      A4=PALF-DALF*E41
      IA4AR=IPALF-IDALF*(I4-1)
C
C  AIRCRAFT  1  AND  2
C
      VS=VKT(1)/3600.
      VF=VKT(2)/3600.
```

```
      AMI=VS/VF
      GAMAF=GAMA(2)
      GAMAS=GAMA(1)
      BETA=GAMAF-GAMAS
      DELTSS=DELTA(1,1)
      DELTFF=DELTA(2,2)
      DELTSF=DELTA(1,2)
      DELTFS=DELTA(2,1)
      AS=A1
      AF=A2
      IAFAR=IA2AR
      IASAR=IA1AR
      COAS=COS(AS)
      COAF=COS(AF)
      COASAF=COS(AS-AF)
      AMAS=AMI**2-2.*AMI*COAS+1.
      AMAF=AMI**2-2.*AMI*COAF+1.
      AMASAF=AMI**2-2.*AMI*COASAF+1.
      CALL SDOSF
      CALL SDOFS
      CALL SDOFF
      CALL SDOSS
      CALL DOT
      TT(1,1)=TSS
      TT(1,2)=TSF
      TT(2,1)=TFS
      TT(2,2)=TFF
C
CC    AIRCRAFT  1  AND  3
C
      VS=VKT(1)/3600.
      VF=VKT(3)/3600.
      AMI=VS/VF
      GAMAF=GAMA(3)
      GAMAS=GAMA(1)
      BETA=GAMAF-GAMAS
      DELTSS=DELTA(1,1)
      DELTFF=DELTA(3,3)
      DELTSF=DELTA(1,3)
      DELTFS=DELTA(3,1)
      AS=A1
      AF=A3
      IAFAR=IA3AR
      IASAR=IA1AR
      COAS=COS(AS)
      COAF=COS(AF)
      COASAF=COS(AS-AF)
      AMAS=AMI**2-2.*AMI*COAS+1.
```

```
      AMAF=AMI**2-2.*AMI*COAF+1.
      AMASAF=AMI**2-2.*AMI*COASAF+1.
      CALL SDOSF
      CALL SDOFS
      CALL SDOFF
      CALL SDOSS
      CALL DOT
      TT(1,3)=TSF
      TT(3,1)=TFS
      TT(3,3)=TFF
C
C   AIRCRAFT  1  AND  4
C
      VS=VKT(1)/3600.
      VF=VKT(4)/3600.
      AMI=VS/VF
      GAMAF=GAMA(4)
      GAMAS=GAMA(1)
      BETA=GAMAF-GAMAS
      DELTSS=DELTA(1,1)
      DELTFF=DELTA(4,4)
      DELTSF=DELTA(1,4)
      DELTFS=DELTA(4,1)
      AS=A1
      AF=A4
      IAFAR=IA4AR
      IASAR=IA1AR
      COAS=COS(AS)
      COAF=COS(AF)
      COASAF=COS(AS-AF)
      AMAS=AMI**2-2.*AMI*COAS+1.
      AMAF=AMI**2-2.*AMI*COAF+1.
      AMASAF=AMI**2-2.*AMI*COASAF+1.
      CALL SDOSF
      CALL SDOFS
      CALL SDOFF
      CALL SDOSS
      CALL DOT
      TT(1,4)=TSF
      TT(4,1)=TFS
      TT(4,4)=TFF
C
C   AIRCRAFT  2  AND  3
C
      VS=VKT(2)/3600.
      VF=VKT(3)/3600.
      AMI=VS/VF
      GAMAF=GAMA(3)
```

```
      GAMAS=GAMA(2)
      BETA=GAMAF-GAMAS
      DELTSS=DELTA(2,2)
      DELTFF=DELTA(3,3)
      DELTSF=DELTA(2,3)
      DELFS=DELTA(3,2)
      AS=A2
      AF=A3
      IASAR=IA2AR
      IAFAR=IA3AR
      COAS=COS(AS)
      COAF=COS(AF)
      COASAF=COS(AS-AF)
      AMAS=AMI**2-2.*AMI*COAS+1.
      AMAF=AMI**2-2.*AMI*COAF+1.
      AMASAF=AMI**2-2.*AMI*COASAF+1.
      CALL SDOSF
      CALL SDOFS
      CALL SDOFF
      CALL SDOSS
      CALL DOT
      TT(2,3)=TSF
      TT(3,2)=TFS
C
C   AIRCRAFT  2  AND  4
C
      VS=VKT(2)/3600.
      VF=VKT(4)/3600.
      AMI=VS/VF
      GAMAF=GAMA(4)
      GAMAS=GAMA(2)
      BETA=GAMAF-GAMAS
      DELTSS=DELTA(2,2)
      DELTFF=DELTA(4,4)
      DELTSF=DELTA(2,4)
      DELTFS=DELTA(4,2)
      AS=A2
      AF=A4
      IASAR=IA2AR
      IAFAR=IA4AR
      COAS=COS(AS)
      COAF=COS(AF)
      COASAF=COS(AS-AF)
      AMAS=AMI**2-2.*AMI*COAS+1.
      AMAF=AMI**2-2.*AMI*COAF+1.
      AMASAF=AMI**2-2.*AMI*COASAF+1.
      CALL SDOSF
      CALL SDOFS
```

```
      CALL SDOFF
      CALL SDOSS
      CALL DOT
      TT(2,4)=TSF
      TT(4,2)=TFS
C
C   AIRCRAFT  3  AND  4
C
      VS=VKT(3)/3600.
      VF=VKT(4)/3600.
      AMI=VS/VF
      GAMAF=GAMA(4)
      GAMAS=GAMA(3)
      BETA=GAMAF-GAMAS
      DELTSS=DELTA(3,3)
      DELTFF=DELTA(4,4)
      DELTSF=DELTA(3,4)
      DELTFS=DELTA(4,3)
      AS=A3
      AF=A4
      IASAR=IA3AR
      IAFAR=IA4AR
      COAS=COS(AS)
      COAF=COS(AF)
      COASAF=COS(AS-AF)
      AMAS=AMI**2-2.*AMI*COAS+1.
      AMAF=AMI**2-2.*AMI*COAF+1.
      AMASAF=AMI**2-2.*AMI*COASAF+1.
      CALL SDOSF
      CALL SDOFS
      CALL SDOFF
      CALL SDOSS
      CALL DOT
      TT(3,4)=TSF
      TT(4,3)=TFS
C
C   MEAN INTERARRIVAL TIME
C
      TBAR=0.
      DO 2120 I=1,M
      DO 2110 J=1,M
      TBAR=TBAR+TT(I,J)*PP(I,J)
 2110 CONTINUE
 2120 CONTINUE
      CAP=3600./TBAR
      N=NM
      IF (CAP.LT.CAPAC(N)) GO TO 2170
      DO 2150 N1=1,N
```

```
      IF (CAP-CAPAC(N1)) 2150,2150,2140
 2140 CONTINUE
      NN=N1
      GO TO 2155
 2150 CONTINUE
 2155 CONTINUE
      NMINNN=N-NN
      DO 2160 NOP=1,NMINNN
      N2=N-NOP
      N2P1=N2+1
      CAPAC(N2P1)=CAPAC(N2)
      CAPAC(N2P1)=CAPAC(N2)
      IALF1(N2P1)=IALF1(N2)
      IALF2(N2P1)=IALF2(N2)
      IALF3(N2P1)=IALF3(N2)
      IALF4(N2P1)=IALF4(N2)
 2160 CONTINUE
      CAPAC(NN)=CAP
      IALF1(NN)=IA1AR
      IALF2(NN)=IA2AR
      IALF3(NN)=IA3AR
      IALF4(NN)=IA4AR
 2170 CONTINUE
      N=NM
      IF (CAP.GT.CAPMIN(N)) GO TO 2178
      DO 2174 N1=1,N
      IF (CAP-CAPMIN(N1)) 2172,2174,2174
 2172 NN=N1
      GO TO 2175
 2174 CONTINUE
 2175 CONTINUE
      NMINNN=N-NN
      DO 2176 NOP=1,NMINNN
      N2=N-NOP
      N2P1=N2+1
      CAPMIN(N2P1)=CAPMIN(N2)
      IALFM1(N2P1)=IALFM1(N2)
      IALFM2(N2P1)=IALFM2(N2)
      IALFM3(N2P1)=IALFM3(N2)
      IALFM4(N2P1)=IALFM4(N2)
 2176 CONTINUE
      CAPMIN(NN)=CAP
      IALFM1(NN)=IA1AR
      IALFM2(NN)=IA2AR
      IALFM3(NN)=IA3AR
      IALFM4(NN)=IA4AR
 2178 CONTINUE
 2180 CONTINUE
```

```
 2185 CONTINUE
 2190 CONTINUE
 2195 CONTINUE
C
C
C   MAIN PROGRAM CASE  8
C
C   ANGLES GENERATION
C
      DO 2295 I1=1,8
      E11=FLOAT(I1-1)
      A1=PALF-DALF*E11
      IA1AR=IPALF-IDALF*(I1-1)
      I1PLS1=I1+1
      DO 2290 I2=I1PLS1,9
      E21=FLOAT(I2-1)
      A2=PALF-DALF*E21
      IA2AR=IPALF-IDALF*(I2-1)
      I2PLS1=I2+1
      DO 2285 I3=11,19
      E31=FLOAT(I3-1)
      A3=PALF-DALF*E31
      IA3AR=IPALF-IDALF*(I3-1)
      I3MIN1=I3-1
      DO 2280 I4=I2PLS1,I3MIN1
      E41=FLOAT(I4-1)
      A4=PALF-DALF*E41
      IA4AR=IPALF-IDALF*(I4-1)
C
C   AIRCRAFT  1  AND  2
C
      VS=VKT(1)/3600.
      VF=VKT(2)/3600.
      AMI=VS/VF
      GAMAF=GAMA(2)
      GAMAS=GAMA(1)
      BETA=GAMAF-GAMAS
      DELTSS=DELTA(1,1)
      DELTFF=DELTA(2,2)
      DELTSF=DELTA(1,2)
      DELTFS=DELTA(2,1)
      AS=A1
      AF=A2
      IAFAR=IA2AR
      IASAR=IA1AR
      COAS=COS(AS)
      COAF=COS(AF)
      COASAF=COS(AS-AF)
```

```
      AMAS=AMI**2-2.*AMI*COAS+1.
      AMAF=AMI**2-2.*AMI*COAF+1.
      AMASAF=AMI**2-2.*AMI*COASAF+1.
      CALL SDOSF
      CALL SDOFS
      CALL SDOFF
      CALL SDOSS
      CALL DOT
      TT(1,1)=TSS
      TT(1,2)=TSF
      TT(2,1)=TFS
      TT(2,2)=TFF
C
C     AIRCRAFT  1  AND  3
C
      VS=VKT(1)/3600.
      VF=VKT(3)/3600.
      AMI=VS/VF
      GAMAF=GAMA(3)
      GAMAS=GAMA(1)
      BETA=GAMAF-GAMAS
      DELTSS=DELTA(1,1)
      DELTFF=DELTA(3,3)
      DELTSF=DELTA(1,3)
      DELTFS=DELTA(3,1)
      AS=A1
      AF=A3
      IAFAR=IA3AR
      IASAR=IA1AR
      COAS=COS(AS)
      COAF=COS(AF)
      COASAF=COS(AS-AF)
      AMAS=AMI**2-2.*AMI*COAS+1.
      AMAF=AMI**2-2.*AMI*COAF+1.
      AMASAF=AMI**2-2.*AMI*COASAF+1.
      CALL SDOSF
      CALL SDOFS
      CALL SDOFF
      CALL SDOSS
      CALL DOT
      TT(1,3)=TSF
      TT(3,1)=TFS
      TT(3,3)=TFF
C
C     AIRCRAFT  1  AND  4
C
      VS=VKT(1)/3600.
      VF=VKT(4)/3600.
```

```
      AMI=VS/VF
      GAMAF=GAMA(4)
      GAMAS=GAMA(1)
      BETA=GAMAF-GAMAS
      DELTSS=DELTA(1,1)
      DELTFF=DELTA(4,4)
      DELTSF=DELTA(1,4)
      DELTFS=DELTA(4,1)
      AS=A1
      AF=A4
      IAFAR=IA4AR
      IASAR=IA1AR
      COAS=COS(AS)
      COAF=COS(AF)
      COASAF=COS(AS-AF)
      AMAS=AMI**2-2.*AMI*COAS+1.
      AMAF=AMI**2-2.*AMI*COAF+1.
      AMASAF=AMI**2-2.*AMI*COASAF+1.
      CALL SDOSF
      CALL SDOFS
      CALL SDOFF
      CALL SDOSS
      CALL DOT
      TT(1,4)=TSF
      TT(4,1)=TFS
      TT(4,4)=TFF
C
C   AIRCRAFT  2  AND  3
C
      VS=VKT(2)/3600.
      VF=VKT(3)/3600.
      AMI=VS/VF
      GAMAF=GAMA(3)
      GAMAS=GAMA(2)
      BETA=GAMAF-GAMAS
      DELTSS=DELTA(2,2)
      DELTFF=DELTA(3,3)
      DELTSF=DELTA(2,3)
      DELFS=DELTA(3,2)
      AS=A2
      AF=A3
      IASAR=IA2AR
      IAFAR=IA3AR
      COAS=COS(AS)
      COAF=COS(AF)
      COASAF=COS(AS-AF)
      AMAS=AMI**2-2.*AMI*COAS+1.
      AMAF=AMI**2-2.*AMI*COAF+1.
```

```
      AMASAF=AMI**2-2.*AMI*COASAF+1.
      CALL SDOSF
      CALL SDOFS
      CALL SDOFF
      CALL SDOSS
      CALL DOT
      TT(2,3)=TSF
      TT(3,2)=TFS
C
CC  AIRCRAFT  2  AND  4
C
      VS=VKT(2)/3600.
      VF=VKT(4)/3600.
      AMI=VS/VF
      GAMAF=GAMA(4)
      GAMAS=GAMA(2)
      BETA=GAMAF-GAMAS
      DELTSS=DELTA(2,2)
      DELTFF=DELTA(4,4)
      DELTSF=DELTA(2,4)
      DELTFS=DELTA(4,2)
      AS=A2
      AF=A4
      IASAR=IA2AR
      IAFAR=IA4AR
      COAS=COS(AS)
      COAF=COS(AF)
      COASAF=COS(AS-AF)
      AMAS=AMI**2-2.*AMI*COAS+1.
      AMAF=AMI**2-2.*AMI*COAF+1.
      AMASAF=AMI**2-2.*AMI*COASAF+1.
      CALL SDOSF
      CALL SDOFS
      CALL SDOFF
      CALL SDOSS
      CALL DOT
      TT(2,4)=TSF
      TT(4,2)=TFS
C
CC  AIRCRAFT  3  AND  4
C
      VS=VKT(3)/3600.
      VF=VKT(4)/3600.
      AMI=VS/VF
      GAMAF=GAMA(4)
      GAMAS=GAMA(3)
      BETA=GAMAF-GAMAS
      DELTSS=DELTA(3,3)
```

```
      DELTFF=DELTA(4,4)
      DELTSF=DELTA(3,4)
      DELTFS=DELTA(4,3)
      AS=A3
      AF=A4
      IASAR=IA3AR
      IAFAR=IA4AR
      COAS=COS(AS)
      COAF=COS(AF)
      COASAF=COS(AS-AF)
      AMAS=AMI**2-2.*AMI*COAS+1.
      AMAF=AMI**2-2.*AMI*COAF+1.
      AMASAF=AMI**2-2.*AMI*COASAF+1.
      CALL SDOSF
      CALL SDOFS
      CALL SDOFF
      CALL SDOSS
      CALL DOT
      TT(3,4)=TSF
      TT(4,3)=TFS
C
C   MEAN INTERARRIVAL TIME
C
      TBAR=0.
      DO 2220 I=1,M
      DO 2210 J=1,M
      TBAR=TBAR+TT(I,J)*PP(I,J)
 2210 CONTINUE
 2220 CONTINUE
      CAP=3600./TBAR
      N=NM
      IF (CAP.LT.CAPAC(N)) GO TO 2270
      DO 2250 N1=1,N
      IF (CAP-CAPAC(N1)) 2250,2250,2240
 2240 CONTINUE
      NN=N1
      GO TO 2255
 2250 CONTINUE
 2255 CONTINUE
      NMINNN=N-NN
      DO 2260 NOP=1,NMINNN
      N2=N-NOP
      N2P1=N2+1
      CAPAC(N2P1)=CAPAC(N2)
      IALF1(N2P1)=IALF1(N2)
      IALF2(N2P1)=IALF2(N2)
      IALF3(N2P1)=IALF3(N2)
      IALF4(N2P1)=IALF4(N2)
```

```
 2260 CONTINUE
      CAPAC(NN)=CAP
      IALF1(NN)=IA1AR
      IALF2(NN)=IA2AR
      IALF3(NN)=IA3AR
      IALF4(NN)=IA4AR
 2270 CONTINUE
      N=NM
      IF (CAP.GT.CAPMIN(N)) GO TO 2278
      DO 2274 N1=1,N
      IF (CAP-CAPMIN(N1)) 2272,2274,2274
 2272 NN=N1
      GO TO 2275
 2274 CONTINUE
 2275 CONTINUE
      NMINNN=N-NN
      DO 2276 NOP=1,NMINNN
      N2=N-NOP
      N2P1=N2+1
      CAPMIN(N2P1)=CAPMIN(N2)
      IALFM1(N2P1)=IALFM1(N2)
      IALFM2(N2P1)=IALFM2(N2)
      IALFM3(N2P1)=IALFM3(N2)
      IALFM4(N2P1)=IALFM4(N2)
 2276 CONTINUE
      CAPMIN(NN)=CAP
      IALFM1(NN)=IA1AR
      IALFM2(NN)=IA2AR
      IALFM3(NN)=IA3AR
      IALFM4(NN)=IA4AR
 2278 CONTINUE
 2280 CONTINUE
 2285 CONTINUE
 2290 CONTINUE
 2295 CONTINUE
C
C
C  MAIN PROGRAM CASE  C
C
C  ANGLES GENERATION
C
      DO 2395 I1=1,8
      E11=FLOAT(I1-1)
      A1=PALF-DALF*E11
      IA1AR=IPALF-IDALF*(I1-1)
      I1PLS1=I1+1
      DO 2390 I2=1,19
      E21=FLOAT(I2-1)
```

```
      A2=PALF-DALF*E21
      IA2AR=IPALF-IDALF*(I2-1)
      I2MIN1=I2-1
      DO 2385 I3=I1PLS1,9
      E31=FLOAT(I3-1)
      A3=PALF-DALF*E31
      IA3AR=IPALF-IDALF*(I3-1)
      I3PLS1=I3+1
      DO 2380 I4=I3PLS1,I2MIN1
      E41=FLOAT(I4-1)
      A4=PALF-DALF*E41
      IA4AR=IPALF-IDALF*(I4-1)
C
C   AIRCRAFT  1  AND  2
C
      VS=VKT(1)/3600.
      VF=VKT(2)/3600.
      AMI=VS/VF
      GAMAF=GAMA(2)
      GAMAS=GAMA(1)
      BETA=GAMAF-GAMAS
      DELTSS=DELTA(1,1)
      DELTFF=DELTA(2,2)
      DELTSF=DELTA(1,2)
      DELTFS=DELTA(2,1)
      AS=A1
      AF=A2
      IAFAR=IA2AR
      IASAR=IA1AR
      COAS=COS(AS)
      COAF=COS(AF)
      COASAF=COS(AS-AF)
      AMAS=AMI**2-2.*AMI*COAS+1.
      AMAF=AMI**2-2.*AMI*COAF+1.
      AMASAF=AMI**2-2.*AMI*COASAF+1.
      CALL SDOSF
      CALL SDOFS
      CALL SDOFF
      CALL SDOSS
      CALL DOT
      TT(1,1)=TSS
      TT(1,2)=TSF
      TT(2,1)=TFS
      TT(2,2)=TFF
C
C   AIRCRAFT  1  AND  3
C
      VS=VKT(1)/3600.
```

```
      VF=VKT(3)/3600.
      AMI=VS/VF
      GAMAF=GAMA(3)
      GAMAS=GAMA(1)
      BETA=GAMAF-GAMAS
      DELTSS=DELTA(1,1)
      DELTFF=DELTA(3,3)
      DELTSF=DELTA(1,3)
      DELTFS=DELTA(3,1)
      AS=A1
      AF=A3
      IAFAR=IA3AR
      IASAR=IA1AR
      COAS=COS(AS)
      COAF=COS(AF)
      COASAF=COS(AS-AF)
      AMAS=AMI**2-2.*AMI*COAS+1.
      AMAF=AMI**2-2.*AMI*COAF+1.
      AMASAF=AMI**2-2.*AMI*COASAF+1.
      CALL SDOSF
      CALL SDOFS
      CALL SDOFF
      CALL SDOSS
      CALL DOT
      TT(1,3)=TSF
      TT(3,1)=TFS
      TT(3,3)=TFF
C
C   AIRCRAFT  1  AND  4
C
      VS=VKT(1)/3600.
      VF=VKT(4)/3600.
      AMI=VS/VF
      GAMAF=GAMA(4)
      GAMAS=GAMA(1)
      BETA=GAMAF-GAMAS
      DELTSS=DELTA(1,1)
      DELTFF=DELTA(4,4)
      DELTSF=DELTA(1,4)
      DELTFS=DELTA(4,1)
      AS=A1
      AF=A4
      IAFAR=IA4AR
      IASAR=IA1AR
      COAS=COS(AS)
      COAF=COS(AF)
      COASAF=COS(AS-AF)
      AMAS=AMI**2-2.*AMI*COAS+1.
```

```
      AMAF=AMI**2-2.*AMI*COAF+1.
      AMASAF=AMI**2-2.*AMI*COASAF+1.
      CALL SDOSF
      CALL SDOFS
      CALL SDOFF
      CALL SDOSS
      CALL DOT
      TT(1,4)=TSF
      TT(4,1)=TFS
      TT(4,4)=TFF
C
C  AIRCRAFT  2  AND  3
C
      VS=VKT(2)/3600.
      VF=VKT(3)/3600.
      AMI=VS/VF
      GAMAF=GAMA(3)
      GAMAS=GAMA(2)
      BETA=GAMAF-GAMAS
      DELTSS=DELTA(2,2)
      DELTFF=DELTA(3,3)
      DELTSF=DELTA(2,3)
      DELFS=DELTA(3,2)
      AS=A2
      AF=A3
      IASAR=IA2AR
      IAFAR=IA3AR
      COAS=COS(AS)
      COAF=COS(AF)
      COASAF=COS(AS-AF)
      AMAS=AMI**2-2.*AMI*COAS+1.
      AMAF=AMI**2-2.*AMI*COAF+1.
      AMASAF=AMI**2-2.*AMI*COASAF+1.
      CALL SDOSF
      CALL SDOFS
      CALL SDOFF
      CALL SDOSS
      CALL DOT
      TT(2,3)=TSF
      TT(3,2)=TFS
C
C  AIRCRAFT  2  AND  4
C
      VS=VKT(2)/3600.
      VF=VKT(4)/3600.
      AMI=VS/VF
      GAMAF=GAMA(4)
      GAMAS=GAMA(2)
```

```
      BETA=GAMAF-GAMAS
      DELTSS=DELTA(2,2)
      DELTFF=DELTA(4,4)
      DELTSF=DELTA(2,4)
      DELTFS=DELTA(4,2)
      AS=A2
      AF=A4
      IASAR=IA2AR
      IAFAR=IA4AR
      COAS=COS(AS)
      COAF=COS(AF)
      COASAF=COS(AS-AF)
      AMAS=AMI**2-2.*AMI*COAS+1.
      AMAF=AMI**2-2.*AMI*COAF+1.
      AMASAF=AMI**2-2.*AMI*COASAF+1.
      CALL SDOSF
      CALL SDOFS
      CALL SDOFF
      CALL SDOSS
      CALL DOT
      TT(2,4)=TSF
      TT(4,2)=TFS
C
CC   AIRCRAFT  3  AND  4
C
      VS=VKT(3)/3600.
      VF=VKT(4)/3600.
      AMI=VS/VF
      GAMAF=GAMA(4)
      GAMAS=GAMA(3)
      BETA=GAMAF-GAMAS
      DELTSS=DELTA(3,3)
      DELTFF=DELTA(4,4)
      DELTSF=DELTA(3,4)
      DELTFS=DELTA(4,3)
      AS=A3
      AF=A4
      IASAR=IA3AR
      IAFAR=IA4AR
      COAS=COS(AS)
      COAF=COS(AF)
      COASAF=COS(AS-AF)
      AMAS=AMI**2-2.*AMI*COAS+1.
      AMAF=AMI**2-2.*AMI*COAF+1.
      AMASAF=AMI**2-2.*AMI*COASAF+1.
      CALL SDOSF
      CALL SDOFS
      CALL SDOFF
```

```
      CALL SDOSS
      CALL DOT
      TT(3,4)=TSF
      TT(4,3)=TFS
C
C  MEAN INTERARRIVAL TIME
C
      TBAR=0.
      DO 2320 I=1,M
      DO 2310 J=1,M
      TBAR=TBAR+TT(I,J)*PP(I,J)
 2310 CONTINUE
 2320 CONTINUE
      CAP=3600./TBAR
      N=NM
      IF (CAP.LT.CAPAC(N)) GO TO 2370
      DO 2350 N1=1,N
      IF (CAP-CAPAC(N1)) 2350,2350,2340
 2340 CONTINUE
      NN=N1
      GO TO 2355
 2350 CONTINUE
 2355 CONTINUE
      NMINNN=N-NN
      DO 2360 NOP=1,NMINNN
      N2=N-NOP
      N2P1=N2+1
      CAPAC(N2P1)=CAPAC(N2)
      IALF1(N2P1)=IALF1(N2)
      IALF2(N2P1)=IALF2(N2)
      IALF3(N2P1)=IALF3(N2)
      IALF4(N2P1)=IALF4(N2)
 2360 CONTINUE
      CAPAC(NN)=CAP
      IALF1(NN)=IA1AR
      IALF2(NN)=IA2AR
      IALF3(NN)=IA3AR
      IALF4(NN)=IA4AR
 2370 CONTINUE
      N=NM
      IF (CAP.GT.CAPMIN(N)) GO TO 2378
      DO 2374 N1=1,N
      IF (CAP-CAPMIN(N1)) 2372,2374,2374
 2372 NN=N1
      GO TO 2375
 2374 CONTINUE
 2375 CONTINUE
      NMINNN=N-NN
```

```
      DO 2376 NOP=1,NMINNN
      N2=N-NOP
      N2P1=N2+1
      CAPMIN(N2P1)=CAPMIN(N2)
      IALFM1(N2P1)=IALFM1(N2)
      IALFM2(N2P1)=IALFM2(N2)
      IALFM3(N2P1)=IALFM3(N2)
      IALFM4(N2P1)=IALFM4(N2)
 2376 CONTINUE
      CAPMIN(NN)=CAP
      IALFM1(NN)=IA1AR
      IALFM2(NN)=IA2AR
      IALFM3(NN)=IA3AR
      IALFM4(NN)=IA4AR
 2378 CONTINUE
 2380 CONTINUE
 2385 CONTINUE
 2390 CONTINUE
 2395 CONTINUE
C
CC
C  MAIN PROGRAM CASE  D
CC
C  ANGLES GENERATION
C
      DO 2495 I1=1,9
      E11=FLOAT(I1-1)
      A1=PALF-DALF*E11
      IA1AR=IPALF-IDALF*(I1-1)
      I1PLS1=I1+1
      DO 2490 I2=12,19
      E21=FLOAT(I2-1)
      A2=PALF-DALF*E21
      IA2AR=IPALF-IDALF*(I2-1)
      I2MIN1=I2-1
      DO 2485 I3=11,I2MIN1
      E31=FLOAT(I3-1)
      A3=PALF-DALF*E31
      IA3AR=IPALF-IDALF*( 3-1)
      I3MIN1=I3-1
      DO 2480 I4=I1PLS1,I3MIN1
      E41=FLOAT(I4-1)
      A4=PALF-DALF*E41
      IA4AR=IPALF-IDALF*(I4-1)
C
CC  AIRCRAFT  1  AND  2
C
      VS=VKT(1)/3600.
```

```
      VF=VKT(2)/3600.
      AMI=VS/VF
      GAMAF=GAMA(2)
      GAMAS=GAMA(1)
      BETA=GAMAF-GAMAS
      DELTSS=DELTA(1,1)
      DELTFF=DELTA(2,2)
      DELTSF=DELTA(1,2)
      DELTFS=DELTA(2,1)
      AS=A1
      AF=A2
      IAFAR=IA2AR
      IASAR=IA1AR
      COAS=COS(AS)
      COAF=COS(AF)
      COASAF=COS(AS-AF)
      AMAS=AMI**2-2.*AMI*COAS+1.
      AMAF=AMI**2-2.*AMI*COAF+1.
      AMASAF=AMI**2-2.*AMI*COASAF+1.
      CALL SDOSF
      CALL SDOFS
      CALL SDOFF
      CALL SDOSS
      CALL DOT
      TT(1,1)=TSS
      TT(1,2)=TSF
      TT(2,1)=TFS
      TT(2,2)=TFF
C
CC   AIRCRAFT  1  AND  3
C
      VS=VKT(1)/3600.
      VF=VKT(3)/3600.
      AMI=VS/VF
      GAMAF=GAMA(3)
      GAMAS=GAMA(1)
      BETA=GAMAF-GAMAS
      DELTSS=DELTA(1,1)
      DELTFF=DELTA(3,3)
      DELTSF=DELTA(1,3)
      DELTFS=DELTA(3,1)
      AS=A1
      AF=A3
      IAFAR=IA3AR
      IASAR=IA1AR
      COAS=COS(AS)
      COAF=COS(AF)
      COASAF=COS(AS-AF)
```

```
      AMAS=AMI**2-2.*AMI*COAS+1.
      AMAF=AMI**2-2.*AMI*COAF+1.
      AMASAF=AMI**2-2.*AMI*COASAF+1.
      CALL SDOSF
      CALL SDOFS
      CALL SDOFF
      CALL SDOSS
      CALL DOT
      TT(1,3)=TSF
      TT(3,1)=TFS
      TT(3,3)=TFF
C
CC    AIRCRAFT  1  AND  4
C
      VS=VKT(1)/3600.
      VF=VKT(4)/3600.
      AMI=VS/VF
      GAMAF=GAMA(4)
      GAMAS=GAMA(1)
      BETA=GAMAF-GAMAS
      DELTSS=DELTA(1,1)
      DELTFF=DELTA(4,4)
      DELTSF=DELTA(1,4)
      DELTFS=DELTA(4,1)
      AS=A1
      AF=A4
      IAFAR=IA4AR
      IASAR=IA1AR
      COAS=COS(AS)
      COAF=COS(AF)
      COASAF=COS(AS-AF)
      AMAS=AMI**2-2.*AMI*COAS+1.
      AMAF=AMI**2-2.*AMI*COAF+1.
      AMASAF=AMI**2-2.*AMI*COASAF+1.
      CALL SDOSF
      CALL SDOFS
      CALL SDOFF
      CALL SDOSS
      CALL DOT
      TT(1,4)=TSF
      TT(4,1)=TFS
      TT(4,4)=TFF
C
CC    AIRCRAFT  2  AND  3
C
      VS=VKT(2)/3600.
      VF=VKT(3)/3600.
      AMI=VS/VF
```

```
      GAMAF=GAMA(3)
      GAMAS=GAMA(2)
      BETA=GAMAF-GAMAS
      DELTSS=DELTA(2,2)
      DELTFF=DELTA(3,3)
      DELTSF=DELTA(2,3)
      DELFS=DELTA(3,2)
      AS=A2
      AF=A3
      IASAR=IA2AR
      IAFAR=IA3AR
      COAS=COS(AS)
      COAF=COS(AF)
      COASAF=COS(AS-AF)
      AMAS=AMI**2-2.*AMI*COAS+1.
      AMAF=AMI**2-2.*AMI*COAF+1.
      AMASAF=AMI**2-2.*AMI*COASAF+1.
      CALL SDOSF
      CALL SDOFS
      CALL SDOFF
      CALL SDOSS
      CALL DOT
      TT(2,3)=TSF
      TT(3,2)=TFS
C
CC   AIRCRAFT  2  AND  4
C
      VS=VKT(2)/3600.
      VF=VKT(4)/3600.
      AMI=VS/VF
      GAMAF=GAMA(4)
      GAMAS=GAMA(2)
      BETA=GAMAF-GAMAS
      DELTSS=DELTA(2,2)
      DELTFF=DELTA(4,4)
      DELTSF=DELTA(2,4)
      DELTFS=DELTA(4,2)
      AS=A2
      AF=A4
      IASAR=IA2AR
      IAFAR=IA4AR
      COAS=COS(AS)
      COAF=COS(AF)
      COASAF=COS(AS-AF)
      AMAS=AMI**2-2.*AMI*COAS+1.
      AMAF=AMI**2-2.*AMI*COAF+1.
      AMASAF=AMI**2-2.*AMI*COASAF+1.
      CALL SDOSF
```

```
      CALL SDOFS
      CALL SDOFF
      CALL SDOSS
      CALL DOT
      TT(2,4)=TSF
      TT(4,2)=TFS
C
CC   AIRCRAFT  3  AND  4
C
      VS=VKT(3)/3600.
      VF=VKT(4)/3600.
      AMI=VS/VF
      GAMAF=GAMA(4)
      GAMAS=GAMA(3)
      BETA=GAMAF-GAMAS
      DELTSS=DELTA(3,3)
      DELTFF=DELTA(4,4)
      DELTSF=DELTA(3,4)
      DELTFS=DELTA(4,3)
      AS=A3
      AF=A4
      IASAR=IA3AR
      IAFAR=IA4AR
      COAS=COS(AS)
      COAF=COS(AF)
      COASAF=COS(AS-AF)
      AMAS=AMI**2-2.*AMI*COAS+1.
      AMAF=AMI**2-2.*AMI*COAF+1.
      AMASAF=AMI**2-2.*AMI*COASAF+1.
      CALL SDOSF
      CALL SDOFS
      CALL SDOFF
      CALL SDOSS
      CALL DOT
      TT(3,4)=TSF
      TT(4,3)=TFS
C
CC   MEAN INTERARRIVAL TIME
C
      TBAR=0.
      DO 2420 I=1,M
      DO 2410 J=1,M
      TBAR=TBAR+TT(I,J)*PP(I,J)
 2410 CONTINUE
 2420 CONTINUE
      CAP=3600./TBAR
      N=NM
      IF (CAP.LT.CAPAC(N)) GO TO 2470
```

```
      DO 2450 N1=1,N
      IF (CAP-CAPAC(N1)) 2450,2450,2440
 2440 CONTINUE
      NN=N1
      GO TO 2455
 2450 CONTINUE
 2455 CONTINUE
      NMIN1=N-1
      NMINNN=N-NN
      DO 2460 NOP=1,NMINNN
      N2=N-NOP
      CAPAC(N2P1)=CAPAC(N2)
      IALF1(N2P1)=IALF1(N2)
      IALF2(N2P1)=IALF2(N2)
      IALF3(N2P1)=IALF3(N2)
      IALF4(N2P1)=IALF4(N2)
 2460 CONTINUE
      CAPAC(NN)=CAP
      IALF1(NN)=IA1AR
      IALF2(NN)=IA2AR
      IALF3(NN)=IA3AR
      IALF4(NN)=IA4AR
 2470 CONTINUE
      N=NM
      IF (CAP.GT.CAPMIN(N)) GO TO 2478
      DO 2474 N1=1,N
      IF (CAP-CAPMIN(N1)) 2472,2474,2474
 2472 NN=N1
      GO TO 2475
 2474 CONTINUE
 2475 CONTINUE
      NMINNN=N-NN
      DO 2476 NOP=1,NMINNN
      N2=N-NOP
      N2P1=N2+1
      CAPMIN(N2P1)=CAPMIN(N2)
      IALFM1(N2P1)=IALFM1(N2)
      IALFM2(N2P1)=IALFM2(N2)
      IALFM3(N2P1)=IALFM3(N2)
      IALFM4(N2P1)=IALFM4(N2)
 2476 CONTINUE
      CAPMIN(NN)=CAP
      IALFM1(NN)=IA1AR
      IALFM2(NN)=IA2AR
      IALFM3(NN)=IA3AR
      IALFM4(NN)=IA4AR
 2478 CONTINUE
 2480 CONTINUE
```

```
 2485 CONTINUE
 2490 CONTINUE
 2495 CONTINUE
C
C
C  PRINTING RESULTS
C
      PRINT 4050
 4050 FORMAT(1H1,///,13X,*MAXIMAL CAPACITY-OPTIMAL ANGLES*,////)
      PRINT 4100
 4100 FORMAT(14X,*CAPACITY*,5X,*ALFA1*,5X,*ALFA2*,5X,*ALFA3*,
     15X,*ALFA4*,///)
      DO 4150 NP=1,NM
      PRINT 4151,NP,CAPAC(NP),IALF1(NP),IALF2(NP),IALF3(NP),IALF4(NP)
 4151 FORMAT(5X,I5,F10.3,4I10)
 4150 CONTINUE
      PRINT 4250
 4250 FORMAT(1H1,///,13X,*MINIMAL CAPACITY-THE WORSE ANGLES*,////)
      PRINT 4100
      DO 4260 NP=1,NM
      PRINT 4151,NP,CAPMIN(NP),IALFM1(NP),IALFM2(NP),IALFM3(NP),
     1IALFM4(NP)
 4260 CONTINUE
      GO TO 9999
      STOP
      END
```

C. Example outputs

C.1. Example of CAPSF output (ILS case)

```
    VF = 150.00
    VS = 140.00
    MI =    .93333
 GAMAF =   6.00
 GAMAS =   6.00
  BETA =   0.
DELTSS =   3.00
DELTSF =   3.00
DELTFS =   3.00
DELTFF =   3.00
    PF =    .60
    PS =    .40
```

CAPSF

	90	80	70	60	50	40	30	20	10	0
90	35.215	-I	-I	-I	-I	-I	-I	-I	-I	-I
80	36.000	37.996	-I	-I	-I	-I	-I	-I	-I	-I
70	37.384	38.705	40.054	-I	-I	-I	-I	-I	-I	-I
60	38.539	39.944	41.108	41.608	-I	-I	-I	-I	-I	-I
50	39.482	40.958	42.183	43.189	42.730	-I	-I	-I	-I	-I
40	39.950	41.462	42.718	43.749	44.581	43.432	-I	-I	-I	-I
30	40.285	41.823	43.101	44.151	44.998	45.553	43.954	-I	-I	-I
20	40.518	42.074	43.368	44.432	45.290	45.957	46.061	44.306	-I	-I
10	40.556	42.223	43.526	44.597	45.462	46.134	46.616	46.385	44.493	-I
0	40.701	42.272	43.578	44.652	45.519	46.193	46.676	46.924	46.530	44.519
-10	40.656	42.223	43.526	44.597	45.462	46.134	46.616	46.866	B 46.951	46.499
-20	40.518	42.074	43.368	44.432	45.290	45.957	46.435	46.683	46.770	46.797
-30	40.285	41.823	43.101	44.151	44.998	45.657	46.129	46.374	46.459	46.488
-40	39.950	41.462	42.718	43.749	44.581	B' 45.227	45.690	45.930	46.014	46.042
-50	39.482	40.958	42.183	43.189	43.999	44.628	45.079	45.313	45.394	45.421
-60	38.539	39.944	41.108	B'' 42.062	42.331	43.427	43.853	44.075	44.152	44.178
-70	37.384	38.705	39.797	40.691	41.409	41.966	42.365	42.571	42.643	42.667
-80	36.000	B''' 37.223	38.232	39.057	39.718	40.231	40.596	40.786	40.852	40.874
-90	34.364	35.476	36.392	37.138	37.735	38.198	38.527	38.698	38.757	38.777

DOSE

	90	80	70	60	50	40	30	20	10	0
90	4.21728	-1	-1	-1	-1	-1	-1	-1	-1	-1
80	4.05947	3.92039	-1	-1	-1	-1	-1	-1	-1	-1
70	3.79769	3.79769	3.68948	-1	-1	-1	-1	-1	-1	-1
60	3.59420	3.59420	3.59420	3.51060	-1	-1	-1	-1	-1	-1
50	3.43770	3.43770	3.43770	3.43770	3.42857	-1	-1	-1	-1	-1
40	3.42857	3.42857	3.42857	3.42857	3.42857	3.42857	-1	-1	-1	-1
30	3.42857	3.42857	3.42857	3.42857	3.42857	3.42857	3.42857	-1	-1	-1
20	3.42857	3.42857	3.42857	3.42857	3.42857	3.42857	3.42857	3.42857	-1	-1
10	3.42857	3.42857	3.42857	3.42857	3.42857	3.42857	3.42857	3.42857	3.42857	-1
0	3.42857	3.42857	3.42857	3.42857	3.42857	3.42857	3.42857	3.42857	3.42857	3.42857
-10	3.42857	3.42857	3.42857	3.42857	3.42857	3.42857	3.42857	3.42857	3.42857	3.42857
-20	3.42857	3.42857	3.42857	3.42857	3.42857	3.42857	3.42857	3.42857	3.42857	3.42857
-30	3.42857	3.42857	3.42857	3.42857	3.42857	3.42857	3.42857	3.42857	3.42857	3.42857
-40	3.42857	3.42857	3.42857	3.42857	3.42857	3.42857	3.42857	3.42857	3.42857	3.42857
-50	3.43770	3.43770	3.43770	3.43770	3.43770	3.43770	3.43770	3.43770	3.43770	3.43770
-60	3.59420	3.59420	3.59420	3.59420	3.59420	3.59420	3.59420	3.59420	3.59420	3.59420
-70	3.79769	3.79769	3.79769	3.79769	3.79769	3.79769	3.79769	3.79769	3.79769	3.79769
-80	4.05947	4.05947	4.05947	4.05947	4.05947	4.05947	4.05947	4.05947	4.05947	4.05947
-90	4.39672	4.39672	4.39672	4.39672	4.39672	4.39672	4.39672	4.39672	4.39672	4.39672

INDXSF

	90	80	70	60	50	40	30	20	10	0
90	2112	R	R	R	R	R	R	R	R	R
80	2112	2112	R	R	R	R	R	R	R	R
70	2112	2112	2112	R	R	R	R	R	R	R
60	2112	2112	2112	2112	R	R	R	R	R	R
50	2112	2112	2112	2112	3112	R	R	R	R	R
40	3112	3112	3112	3112	3112	3112	R	R	R	R
30	3112	3112	3112	3112	3112	3112	3112	R	R	R
20	3111	3111	3111	3111	3111	3111	3111	3111	R	R
10	3111	3111	3111	3111	3111	3111	3111	3111	3111	R
0	3111	3111	3111	3111	3111	3111	3111	3111	3111	3111
-10	3111	3111	3111	3111	3111	3111	3111	3111	3111	3111
-20	3111	3111	3111	3111	3111	3111	3111	3111	3111	3111
-30	3112	3112	3112	3112	3112	3112	3112	3112	3112	3112
-40	3112	3112	3112	3112	3112	3112	3112	3112	3112	3112
-50	2112	2112	2112	2112	2112	2112	2112	2112	2112	2112
-60	2112	2112	2112	2112	2112	2112	2112	2112	2112	2112
-70	2112	2112	2112	2112	2112	2112	2112	2112	2112	2112
-80	2112	2112	2112	2112	2112	2112	2112	2112	2112	2112
-90	2112	2112	2112	2112	2112	2112	2112	2112	2112	2112

DOFS

	90	80	70	60	50	40	30	20	10	0
90	4.10360	-1	-1	-1	-1	-1	-1	-1	-1	-1
80	4.10360	3.78884	-1	-1	-1	-1	-1	-1	-1	-1
70	4.10360	3.78884	3.69892	-1	-1	-1	-1	-1	-1	-1
60	4.10360	3.78884	3.54451	3.69892	-1	-1	-1	-1	-1	-1
50	4.10360	3.78884	3.54451	3.35458	3.69892	-1	-1	-1	-1	-1
40	4.10360	3.78884	3.54451	3.35458	3.20852	3.69892	-1	-1	-1	-1
30	4.10360	3.78884	3.54451	3.35458	3.20852	3.12904	3.69892	-1	-1	-1
20	4.10360	3.78884	3.54451	3.35458	3.20852	3.09993	3.12904	3.69892	-1	-1
10	4.10360	3.78884	3.54451	3.35458	3.20852	3.09993	3.02706	3.12904	3.69892	-1
0	4.10360	3.78884	3.54451	3.35458	3.20852	3.09993	3.02706	3.00052	3.12904	3.69892
-10	4.10360	3.78884	3.54451	3.35458	3.20852	3.09993	3.02706	3.00000	3.00052	3.12904
-20	4.10360	3.78884	3.54451	3.35458	3.20852	3.09993	3.02706	3.00000	3.00000	3.00052
-30	4.10360	3.78884	3.54451	3.35458	3.20852	3.09993	3.02706	3.00000	3.00000	3.00000
-40	4.10360	3.78884	3.54451	3.35458	3.20852	3.09993	3.02706	3.00000	3.00000	3.00000
-50	4.10360	3.78884	3.54451	3.35458	3.20852	3.09993	3.02706	3.00000	3.00000	3.00000
-60	4.10360	3.78884	3.54451	3.35458	3.20852	3.09993	3.02706	3.00000	3.00000	3.00000
-70	4.10360	3.78884	3.54451	3.35458	3.20852	3.09993	3.02706	3.00000	3.00000	3.00000
-80	4.10360	3.78884	3.54451	3.35458	3.20852	3.09993	3.02706	3.00000	3.00000	3.00000
-90	4.10360	3.78884	3.54451	3.35458	3.20852	3.09993	3.02706	3.00000	3.00000	3.00000

INDXFS

	90	80	70	60	50	40	30	20	10	0
90	2120	R	R	R	R	R	R	R	R	R
80	2120	2120	R	R	R	R	R	R	R	R
70	2120	2120	1020	R	R	R	R	R	R	R
60	2110	2120	2120	1020	R	R	R	R	R	R
50	2110	2110	2120	2120	1020	R	R	R	R	R
40	2110	2110	2110	2120	2120	1020	R	R	R	R
30	2110	2110	2110	2110	2120	1020	1020	R	R	R
20	2110	2110	2110	2110	2110	2120	1020	1010	R	R
10	2110	2110	2110	2110	2110	2110	2120	1010	1010	R
0	2110	2110	2110	2110	2110	2110	2110	1010	1010	1010
-10	2110	2110	2110	2110	2110	2110	2110	4000	1010	1010
-20	2110	2110	2110	2110	2110	2110	2110	4000	4000	1010
-30	2110	2110	2110	2110	2110	2110	2110	4000	4000	4000
-40	2110	2110	2110	2110	2110	2110	2110	4000	4000	4000
-50	2110	2110	2110	2110	2110	2110	2110	4000	4000	4000
-60	2110	2110	2110	2110	2110	2110	2110	4000	4000	4000
-70	2110	2110	2110	2110	2110	2110	2110	4000	4000	4000
-80	2110	2110	2110	2110	2110	2110	2110	4000	4000	4000
-90	2110	2110	2110	2110	2110	2110	2110	4000	4000	4000

DOSS,INDXSS

90	80	70	60	50	40	30	20	10	0
4.24258	3.91618	3.66230	3.46408	3.31012	3.19253	3.10582	3.04628	3.01146	3.00000
1000	1000	1000	1000	1000	1000	1000	1000	1000	1000

DOFF

	90	80	70	60	50	40	30	20	10	0
90	4.06898	-1	-1	-1	-1	-1	-1	-1	-1	-1
80	3.91618	3.78139	-1	-1	-1	-1	-1	-1	-1	-1
70	3.66230	3.66230	3.55705	-1	-1	-1	-1	-1	-1	-1
60	3.46408	3.46408	3.46408	3.38213	-1	-1	-1	-1	-1	-1
50	3.31012	3.31012	3.31012	3.31012	3.24717	-1	-1	-1	-1	-1
40	3.19253	3.19253	3.19253	3.19253	3.19253	3.14558	-1	-1	-1	-1
30	3.10582	3.10582	3.10582	3.10582	3.10582	3.10582	3.07284	-1	-1	-1
20	3.04628	3.04628	3.04628	3.04628	3.04628	3.04628	3.04628	3.02589	-1	-1
10	3.01146	3.01146	3.01146	3.01146	3.01146	3.01146	3.01146	3.01146	3.00286	-1
0	3.00000	3.00000	3.00000	3.00000	3.00000	3.00000	3.00000	3.00000	3.00000	3.00286
-10	3.01146	3.01146	3.01146	3.01146	3.01146	3.01146	3.01146	3.01146	3.01146	3.01146
-20	3.04628	3.04628	3.04628	3.04628	3.04628	3.04628	3.04628	3.04628	3.04628	3.04628
-30	3.10582	3.10582	3.10582	3.10582	3.10582	3.10582	3.10582	3.10582	3.10582	3.10582
-40	3.19253	3.19253	3.19253	3.19253	3.19253	3.19253	3.19253	3.19253	3.19253	3.19253
-50	3.31012	3.31012	3.31012	3.31012	3.31012	3.31012	3.31012	3.31012	3.31012	3.31012
-60	3.46408	3.46408	3.46408	3.46408	3.46408	3.46408	3.46408	3.46408	3.46408	3.46408
-70	3.66230	3.66230	3.66230	3.66230	3.66230	3.66230	3.66230	3.66230	3.66230	3.66230
-80	3.91618	3.91618	3.91618	3.91618	3.91618	3.91618	3.91618	3.91618	3.91618	3.91618
-90	4.24258	4.24258	4.24258	4.24258	4.24258	4.24258	4.24258	4.24258	4.24258	4.24258

INDXFF

	90	80	70	60	50	40	30	20	10	0
90	1000	R	R	R	R	R	R	R	R	R
80	1000	1000	R	R	R	R	R	R	R	R
70	1000	1000	1000	R	R	R	R	R	R	R
60	1000	1000	1000	1000	R	R	R	R	R	R
50	1000	1000	1000	1000	1000	R	R	R	R	R
40	1000	1000	1000	1000	1000	1000	R	R	R	R
30	1000	1000	1000	1000	1000	1000	1000	R	R	R
20	1000	1000	1000	1000	1000	1000	1000	1000	R	R
10	1000	1000	1000	1000	1000	1000	1000	1000	1000	R
0	1000	1000	1000	1000	1000	1000	1000	1000	1000	1000
-10	1000	1000	1000	1000	1000	1000	1000	1000	1000	1000
-20	1000	1000	1000	1000	1000	1000	1000	1000	1000	1000
-30	1000	1000	1000	1000	1000	1000	1000	1000	1000	1000
-40	1000	1000	1000	1000	1000	1000	1000	1000	1000	1000
-50	1000	1000	1000	1000	1000	1000	1000	1000	1000	1000
-60	1000	1000	1000	1000	1000	1000	1000	1000	1000	1000
-70	1000	1000	1000	1000	1000	1000	1000	1000	1000	1000
-80	1000	1000	1000	1000	1000	1000	1000	1000	1000	1000
-90	1000	1000	1000	1000	1000	1000	1000	1000	1000	1000

C.2. Example of CAPSF output (MLS case)

VF = 150.00
VS = 140.00
MI = .93333
GAMAF = 4.00
GAMAS = 4.00
BETA = 0.
DELTSS = 3.00
DELTSF = 3.00
DELTFS = 3.00
DELTFF = 3.00
PF = .60
PS = .40

CAPSF

	90	80	70	60	50	40	30	20	10	0
90	35.215	-I	-I	-I	-I	-I	-I	-I	-I	-I
80	36.000	37.996	-I	-I	-I	-I	-I	-I	-I	-I
70	37.384	38.705	40.054	-I	-I	-I	-I	-I	-I	-I
60	38.539	39.944	41.108	41.608	-I	-I	-I	-I	-I	-I
50	39.482	40.958	42.183	43.189	42.887	-I	-I	-I	-I	-I
40	40.226	41.759	43.033	44.080	44.925	43.867	-I	-I	-I	-I
30	40.659	42.226	43.530	44.601	45.466	46.032	44.400	-I	-I	-I
20	40.897	42.483	43.802	44.888	45.763	46.445	46.551	44.759	-I	-I
10	41.037	42.634	43.963	45.057	45.939	46.626	47.118	46.882	44.951	-I
0	41.084	42.684	44.016	45.112	45.997	46.686	47.179	47.433	47.030	44.977
-10	41.037	42.634	43.963	45.057	45.939	46.626	47.118	47.373	A 47.461	46.998
-20	40.897	42.483	43.802	44.888	45.763	46.445	46.933	47.186	47.275	47.301
-30	40.659	42.226	43.530	44.601	45.466	46.138	46.620	46.870	46.958	46.987
-40	40.226	41.759	43.033	44.080	44.925	A' 45.581	46.051	46.295	46.381	46.409
-50	39.482	40.958	42.183	43.189	43.999	44.628	45.079	45.313	45.394	45.421
-60	38.539	39.944	41.108	A'' 42.062	42.831	43.427	43.853	44.075	44.152	44.178
-70	37.384	38.705	39.797	40.691	41.409	41.966	42.365	42.571	42.643	42.667
-80	36.000	A''' 37.223	38.232	39.057	39.718	40.231	40.596	40.786	40.852	40.874
-90	34.364	35.476	36.392	37.138	37.735	38.198	38.527	38.698	38.757	38.777

DOSF

	90	80	70	60	50	40	30	20	10	0
90	4.21728	-1	-1	-1	-1	-1	-1	-1	-1	-1
80	4.05947	3.92039	-1	-1	-1	-1	-1	-1	-1	-1
70	3.79769	3.79769	3.68948	-1	-1	-1	-1	-1	-1	-1
60	3.59420	3.59420	3.59420	3.51060	-1	-1	-1	-1	-1	-1
50	3.43770	3.43770	3.43770	3.43770	3.37477	-1	-1	-1	-1	-1
40	3.32135	3.32135	3.32135	3.32135	3.32135	3.28571	-1	-1	-1	-1
30	3.28571	3.28571	3.28571	3.28571	3.28571	3.28571	3.28571	-1	-1	-1
20	3.28571	3.28571	3.28571	3.28571	3.28571	3.28571	3.28571	3.28571	-1	-1
10	3.28571	3.28571	3.28571	3.28571	3.28571	3.28571	3.28571	3.28571	3.28571	-1
0	3.28571	3.28571	3.28571	3.28571	3.28571	3.28571	3.28571	3.28571	3.28571	3.28571
-10	3.28571	3.28571	3.28571	3.28571	3.28571	3.28571	3.28571	3.28571	3.28571	3.28571
-20	3.28571	3.28571	3.28571	3.28571	3.28571	3.28571	3.28571	3.28571	3.28571	3.28571
-30	3.28571	3.28571	3.28571	3.28571	3.28571	3.28571	3.28571	3.28571	3.28571	3.28571
-40	3.32135	3.32135	3.32135	3.32135	3.32135	3.32135	3.32135	3.32135	3.32135	3.32135
-50	3.43770	3.43770	3.43770	3.43770	3.43770	3.43770	3.43770	3.43770	3.43770	3.43770
-60	3.59420	3.59420	3.59420	3.59420	3.59420	3.59420	3.59420	3.59420	3.59420	3.59420
-70	3.79769	3.79769	3.79769	3.79769	3.79769	3.79769	3.79769	3.79769	3.79769	3.79769
-80	4.05947	4.05947	4.05947	4.05947	4.05947	4.05947	4.05947	4.05947	4.05947	4.05947
-90	4.39672	4.39672	4.39672	4.39672	4.39672	4.39672	4.39672	4.39672	4.39672	4.39672

INDXSF

	90	80	70	60	50	40	30	20	10	0
90	2112	R	R	R	R	R	R	R	R	R
80	2112	2112	R	R	R	R	R	R	R	R
70	2112	2112	2112	R	R	R	R	R	R	R
60	2112	2112	2112	2112	R	R	R	R	R	R
50	2112	2112	2112	2112	2112	R	R	R	R	R
40	2112	2112	2112	2112	2112	3112	R	R	R	R
30	3112	3112	3112	3112	3112	3112	3112	R	R	R
20	3111	3111	3111	3111	3111	3111	3111	3111	R	R
10	3111	3111	3111	3111	3111	3111	3111	3111	3111	R
0	3111	3111	3111	3111	3111	3111	3111	3111	3111	3111
-10	3111	3111	3111	3111	3111	3111	3111	3111	3111	3111
-20	3111	3111	3111	3111	3111	3111	3111	3111	3111	3111
-30	3112	3112	3112	3112	3112	3112	3112	3112	3112	3112
-40	2112	2112	2112	2112	2112	2112	2112	2112	2112	2112
-50	2112	2112	2112	2112	2112	2112	2112	2112	2112	2112
-60	2112	2112	2112	2112	2112	2112	2112	2112	2112	2112
-70	2112	2112	2112	2112	2112	2112	2112	2112	2112	2112
-80	2112	2112	2112	2112	2112	2112	2112	2112	2112	2112
-90	2112	2112	2112	2112	2112	2112	2112	2112	2112	2112

DOFS

	90	80	70	60	50	40	30	20	10	0
90	4.10360	-1	-1	-1	-1	-1	-1	-1	-1	-1
80	4.10360	3.78884	-1	-1	-1	-1	-1	-1	-1	-1
70	4.10360	3.78884	3.69892	-1	-1	-1	-1	-1	-1	-1
60	4.10360	3.78884	3.54451	3.69892	-1	-1	-1	-1	-1	-1
50	4.10360	3.78884	3.54451	3.35458	3.69892	-1	-1	-1	-1	-1
40	4.10360	3.78884	3.54451	3.35458	3.20852	3.69892	-1	-1	-1	-1
30	4.10360	3.78884	3.54451	3.35458	3.20852	3.12904	3.69892	-1	-1	-1
20	4.10360	3.78884	3.54451	3.35458	3.20852	3.09993	3.12904	3.69892	-1	-1
10	4.10360	3.78884	3.54451	3.35458	3.20852	3.09993	3.02706	3.12904	3.69892	-1
0	4.10360	3.78884	3.54451	3.35458	3.20852	3.09993	3.02706	3.00052	3.12904	3.69892
-10	4.10360	3.78884	3.54451	3.35458	3.20852	3.09993	3.02706	3.00000	3.00052	3.12904
-20	4.10360	3.78884	3.54451	3.35458	3.20852	3.09993	3.02706	3.00000	3.00000	3.00052
-30	4.10360	3.78884	3.54451	3.35458	3.20852	3.09993	3.02706	3.00000	3.00000	3.00000
-40	4.10360	3.78884	3.54451	3.35458	3.20852	3.09993	3.02706	3.00000	3.00000	3.00000
-50	4.10360	3.78884	3.54451	3.35458	3.20852	3.09993	3.02706	3.00000	3.00000	3.00000
-60	4.10360	3.78884	3.54451	3.35458	3.20852	3.09993	3.02706	3.00000	3.00000	3.00000
-70	4.10360	3.78884	3.54451	3.35458	3.20852	3.09993	3.02706	3.00000	3.00000	3.00000
-80	4.10360	3.78884	3.54451	3.35458	3.20852	3.09993	3.02706	3.00000	3.00000	3.00000
-90	4.10360	3.78884	3.54451	3.35458	3.20852	3.09993	3.02706	3.00000	3.00000	3.00000

INDXFS

	90	80	70	60	50	40	30	20	10	0
90	2120	R	R	R	R	R	R	R	R	R
80	2120	2120	R	R	R	R	R	R	R	R
70	2120	2120	1020	R	R	R	R	R	R	R
60	2110	2120	2120	1020	R	R	R	R	R	R
50	2110	2110	2120	2120	1020	R	R	R	R	R
40	2110	2110	2110	2120	2120	1020	R	R	R	R
30	2110	2110	2110	2110	2120	1020	1020	R	R	R
20	2110	2110	2110	2110	2110	2120	1020	1010	R	R
10	2110	2110	2110	2110	2110	2110	2120	1010	1010	R
0	2110	2110	2110	2110	2110	2110	2110	1010	1010	1010
-10	2110	2110	2110	2110	2110	2110	2110	4000	1010	1010
-20	2110	2110	2110	2110	2110	2110	2110	4000	4000	1010
-30	2110	2110	2110	2110	2110	2110	2110	4000	4000	4000
-40	2110	2110	2110	2110	2110	2110	2110	4000	4000	4000
-50	2110	2110	2110	2110	2110	2110	2110	4000	4000	4000
-60	2110	2110	2110	2110	2110	2110	2110	4000	4000	4000
-70	2110	2110	2110	2110	2110	2110	2110	4000	4000	4000
-80	2110	2110	2110	2110	2110	2110	2110	4000	4000	4000
-90	2110	2110	2110	2110	2110	2110	2110	4000	4000	4000

DOSS, INDXSS

90	80	70	60	50	40	30	20	10	0
4.24258	3.91618	3.66230	3.46408	3.31012	3.19253	3.10582	3.04628	3.01146	3.00000
1000	1000	1000	1000	1000	1000	1000	1000	1000	1000

DOFF

	90	80	70	60	50	40	30	20	10	0
90	4.06898	-1	-1	-1	-1	-1	-1	-1	-1	-1
80	3.91618	3.78139	-1	-1	-1	-1	-1	-1	-1	-1
70	3.66230	3.66230	3.55705	-1	-1	-1	-1	-1	-1	-1
60	3.46408	3.46408	3.46408	3.38213	-1	-1	-1	-1	-1	-1
50	3.31012	3.31012	3.31012	3.31012	3.24717	-1	-1	-1	-1	-1
40	3.19253	3.19253	3.19253	3.19253	3.19253	3.14559	-1	-1	-1	-1
30	3.10582	3.10582	3.10582	3.10582	3.10582	3.10582	3.07284	-1	-1	-1
20	3.04628	3.04628	3.04628	3.04628	3.04628	3.04628	3.04628	3.02589	-1	-1
10	3.01146	3.01146	3.01146	3.01146	3.01146	3.01146	3.01146	3.01146	3.00286	-1
0	3.00000	3.00000	3.00000	3.00000	3.00000	3.00000	3.00000	3.00000	3.00000	3.00286
-10	3.01146	3.01146	3.01146	3.01146	3.01146	3.01146	3.01146	3.01146	3.01146	3.01146
-20	3.04628	3.04628	3.04628	3.04628	3.04628	3.04628	3.04628	3.04628	3.04628	3.04628
-30	3.10582	3.10582	3.10582	3.10582	3.10582	3.10582	3.10582	3.10582	3.10582	3.10582
-40	3.19253	3.19253	3.19253	3.19253	3.19253	3.19253	3.19253	3.19253	3.19253	3.19253
-50	3.31012	3.31012	3.31012	3.31012	3.31012	3.31012	3.31012	3.31012	3.31012	3.31012
-60	3.46408	3.46408	3.46408	3.46408	3.46408	3.46408	3.46408	3.46408	3.46408	3.46408
-70	3.66230	3.66230	3.66230	3.66230	3.66230	3.66230	3.66230	3.66230	3.66230	3.66230
-80	3.91618	3.91618	3.91618	3.91618	3.91618	3.91618	3.91618	3.91618	3.91618	3.91618
-90	4.24258	4.24258	4.24258	4.24258	4.24258	4.24258	4.24258	4.24258	4.24258	4.24258

INDXFF

	90	80	70	60	50	40	30	20	10	0
90	1000	R	R	R	R	R	R	R	R	R
80	1000	1000	R	R	R	R	R	R	R	R
70	1000	1000	1000	R	R	R	R	R	R	R
60	1000	1000	1000	1000	R	R	R	R	R	R
50	1000	1000	1000	1000	1000	R	R	R	R	R
40	1000	1000	1000	1000	1000	1000	R	R	R	R
30	1000	1000	1000	1000	1000	1000	1000	R	R	R
20	1000	1000	1000	1000	1000	1000	1000	1000	R	R
10	1000	1000	1000	1000	1000	1000	1000	1000	1000	R
0	1000	1000	1000	1000	1000	1000	1000	1000	1000	1000
-10	1000	1000	1000	1000	1000	1000	1000	1000	1000	1000
-20	1000	1000	1000	1000	1000	1000	1000	1000	1000	1000
-30	1000	1000	1000	1000	1000	1000	1000	1000	1000	1000
-40	1000	1000	1000	1000	1000	1000	1000	1000	1000	1000
-50	1000	1000	1000	1000	1000	1000	1000	1000	1000	1000
-60	1000	1000	1000	1000	1000	1000	1000	1000	1000	1000
-70	1000	1000	1000	1000	1000	1000	1000	1000	1000	1000
-80	1000	1000	1000	1000	1000	1000	1000	1000	1000	1000
-90	1000	1000	1000	1000	1000	1000	1000	1000	1000	1000

C.3. Example of CAP4 output (MLS case)

INPUT DATA

VKT1 =	100.00	GAMA1 =	2.00	P1 =	.20
VKT2 =	120.00	GAMA2 =	2.00	P2 =	.20
VKT3 =	140.00	GAMA3 =	4.00	P3 =	.40
VKT4 =	150.00	GAMA4 =	4.00	P4 =	.20

DELTA MATRIX

TRAILING A/C

	1	2	3	4
1	3.00	3.00	3.00	3.00
2	3.00	3.00	3.00	3.00
3	3.00	3.00	3.00	3.00
4	3.00	3.00	3.00	3.00

MAXIMAL CAPACITY-OPTIMAL ANGLES

	CAPACITY	ALFA1	ALFA2	ALFA3	ALFA4
1	39.887	40	-30	10	-10
2	39.887	40	-30	-10	10
3	39.824	40	-30	20	-10
4	39.822	40	-30	-20	0
5	39.782	50	-30	-10	10
6	39.775	40	-30	-10	0
7	39.750	50	30	-10	10
8	39.743	50	-30	-10	30
9	39.724	50	-30	20	0
10	39.719	50	-30	20	-10
11	39.718	50	-30	-20	0
12	39.707	40	-30	20	10
13	39.705	40	-40	10	-10
14	39.604	40	-20	10	0
15	39.701	40	-30	-20	-10
16	39.691	40	-40	-10	20
17	39.686	50	30	20	0
18	39.682	50	30	20	-10
19	39.671	50	-30	10	0
20	39.671	50	-30	-10	0
21	39.666	40	-40	10	-30
22	39.656	40	-20	20	0
23	39.649	40	-30	10	-20
24	39.647	40	-40	20	0
25	39.644	50	30	10	-40
26	39.643	40	-40	20	-10
27	39.642	50	30	20	-30
28	39.639	50	30	10	0
29	39.639	50	30	-10	0
30	39.629	40	-40	20	-20
31	39.607	30	-30	-20	0
32	39.604	40	-40	20	-30
33	39.603	50	-30	20	10
34	39.601	50	-40	10	-10
35	39.593	50	-30	-20	-10
36	39.595	40	-40	-10	0
37	39.538	50	-30	30	10
38	39.588	50	-30	30	-10
39	39.587	50	-40	10	-20
40	39.587	50	-40	-10	20

MINIMAL CAPACITY-THE WORST ANGLES

	CAPACITY	ALFA1	ALFA2	ALFA3	ALFA4
1	32.284	90	80	-90	-80
2	32.574	90	-90	80	-80
3	32.574	90	-90	-80	80
4	32.588	90	80	-90	70
5	32.588	90	80	-90	-70
6	32.719	90	10	-90	-80
7	32.741	90	70	-90	-80
8	32.810	90	80	-90	60
9	32.810	90	80	-90	-60
10	32.883	90	-90	80	70
11	32.883	90	-90	80	-70
12	32.883	90	-90	-80	70
13	32.883	90	-90	-80	-70
14	32.944	90	80	-90	50
15	32.944	90	80	-90	-50
16	33.031	90	10	-90	-70
17	33.046	90	80	-90	40
18	33.046	90	80	-90	-40
19	33.053	90	70	-90	-70
20	33.072	90	60	-90	-80
21	33.092	90	80	-90	30
22	33.092	90	80	-90	-30
23	33.109	90	-90	80	60
24	33.109	90	-90	80	-60
25	33.109	90	-90	-80	60
26	33.109	90	-90	-80	-60
27	33.109	90	80	-90	20
28	33.109	90	80	-90	-20
29	33.120	90	80	-90	10
30	33.120	90	80	-90	-10
31	33.123	90	80	-90	0
32	33.156	90	-90	70	-80
33	33.156	90	-90	-70	80
34	33.185	80	70	-90	-80
35	33.197	90	10	-90	0
36	33.246	90	-90	80	50
37	33.246	90	-90	-80	50
38	33.246	90	-90	80	-50
39	33.246	90	-90	-80	-50
40	33.259	90	10	-90	-60